STUDIES ON THE PATHOGENESIS OF CHARCOT OSTEOARTHROPATHY

Petrova, Nina Lyubenova

Awarding institution:
King's College London

STUDIES ON THE PATHOGENESIS OF CHARCOT OSTEOARTHROPATHY

Presented for the degree of Doctor of Philosophy to King's College London

Nina Petrova

Acknowledgements

There are many people that I would like to thank. Without their support this work would not have been possible.

Firstly, I warmly thank my supervisors, Professor Michael Edmonds, Professor Catherine Shanahan and Professor Alan McGregor – it has been an honour and privilege to work with you. I thank them for their continued support, guidance and encouragement. I valued their time, energy and effort.

Special thanks to Mike Edmonds for all those early morning and late evening discussions of results, abstracts, papers and grant applications – I always found these meetings very inspiring; To Cathy Shanahan, who kindly supported my laboratory work; for her constructive feedback and most of all for all those challenging questions during the lab meetings, which helped me broaden my perspective; To Prof McGregor, who always reminded me to keep my focus.

I also owe a lot to my colleagues from the Diabetic Foot Clinic: for their friendship and moral support; to all colleagues from the lab who helped me find my way in tissue culture; to Tracy Dew from the Department of Clinical Biochemistry for helping me analyse my ELISA assays.

I am indebted to Dr Afsie Sabokbar and Dr Guillaume Mabilleau from University of Oxford with whom I carried out the pilot work on osteoclasts; special thanks to Guillaume, for teaching me patiently how to generate osteoclasts.

I am very grateful to Dr Peter Petrov, Imperial College London with whom I devised and optimised the method to measure the surface profile of resorbed bone discs; To Professor Neil Alford for his support to use the Thin Film Technology Laboratory.

I am really grateful to all patients who took part in my studies and donated their time and samples.

My research was funded by Diabetes UK and the Diabetes Research and Wellness Foundation and without their support this work would not have been possible.

Lastly and most importantly;

To my husband and son, who never complained that I was late or busy at work, who consoled me and fully trusted me and reminded me that there is life outside the PhD;

To my mother and late father, who taught me always to aim high and excel with my work and to my sister for continued encouragement and support.

Abstract

The rapid bone destruction of the acute Charcot foot is well documented. Osteoclasts are the principal cells responsible for bone resorption but their activation and function in Charcot osteoarthropathy remain unresolved.

I hypothesised that aberrantly activated osteoclasts play a key role in the pathological bone destruction of the acute Charcot foot. I studied the role of receptor activator of nuclear factor-kβ ligand (RANKL), as an osteoclastic activator in Charcot osteoarthropathy. I also assessed the role of the proinflammatory cytokines tumour necrosis factor-α (TNF-α) and interleukin-6 (IL-6) on osteoclastic activity by using neutralising antibodies (anti-TNF-α and anti-IL-6).

I introduced for the first time in the field of Charcot osteoarthropathy a well-established osteoclast culture assay together with a novel method to quantitate resorption on bone discs, namely surface profilometry.

I demonstrated the usefulness of these methods as novel techniques to investigate osteoclastic activity in Charcot osteoarthropathy. My studies revealed that in the presence of macrophage-colony stimulating factor (M-CSF), a survival factor, and RANKL, osteoclastic precursors derived from patients with acute Charcot osteoarthropathy exhibited increased resorbing activity. This activity was attenuated by osteoprotegerin (OPG), a decoy receptor for RANKL, confirming the role of RANKL as an osteoclast activator. The addition of anti-TNF-α to M-CSF+RANKL-treated cultures led to a significant reduction in the area of resorption (at and below surface) of resorbed bone discs and reversed the aberrant erosion profile. The addition of anti-IL-6 to M-CSF+RANKL-treated cultures resulted only in reduction of the area of resorption at the surface.

My observations shed light on the pathogenesis of increased osteoclastic activity in acute Charcot osteoarthropathy and have pointed out several possible cellular targets that may be important for planning future therapies in this devastating condition.

Abbreviations

2D	Two-dimensional
3D	Three-dimensional
BMD	Bone mineral density
CATK	Cathepsin K
CD	Cluster of differentiation
CDUK	Charcot disease in the United Kingdom
CGRP	Calcitonin gene-related peptide
CT	Computer tomography
CTX	C-terminal telopeptide
DAPI	4', 6'-diamidino-2-pheylindoledihydrochoride
DMSO	Dimethyl sulfoxide
DPX	Distrene, plasticiser, xylene
EDTA	Ethylenediaminetetraacetic acid
ELISA	Enzyme-linked immunosorbent assay
F-18 FDG PET/CT	Fluorine-18 Fluorodeoxyglucose positron emission tomography–computed tomography
FBS	Foetal bovine serum
FITC	Fluorescein isothiocyanate
HIV	Human immunodeficiency virus
IL	Interleukin

IL-6R	Il-6 receptor
LIGHT	LIGHT homologous to lymphotoxins exhibiting inducible expression and competing with herpes simplex virus glycoprotein D for herpes virus entry mediator (HVEM), a receptor expressed by T lymphocytes
M-CSF	Macrophage-colony stimulating factor
MRI	Magnetic resonance imaging
MSC	Microbiological safety cabinet
OPG	Osteoprotegerin
PBMCs	Peripheral blood mononuclear cells
PBS	Phosphate buffered saline
PET-CT	Positron emission tomography–computed tomography
RANK	Receptor activator of nuclear factor-kβ
RANKL	Receptor activator of nuclear factor-kβ ligand
rpm	Rounds per minute
RT	Room temperature
STIR	Short tau inversion recovery
TNF-α	Tumour necrosis factor α
TRAP	Tartrate-resistant acid phosphatase
α-MEM	α-minimum essential medium

Contents

List of Figures

List of Tables

Chapter 1 Charcot osteoarthropathy in diabetes

1.1 Introduction

Charcot osteoarthropathy is one of the most challenging foot complications in diabetes in the 21st century. Its pathogenesis is not fully understood and its management is at best symptomatic. Common predisposing and precipitating factors include neuropathy and increased mechanical forces, fracture and bone resorption, trauma and inflammation.

The frequent presentation of vascular calcification and increased osteoclastic activity in patients with diabetic neuropathy has brought attention to a novel cytokine pathway receptor activator of nuclear factor-kβ (RANK) ligand (RANKL)/ osteoprotegerin (OPG) which is known to mediate both processes. Although there is now evidence to confirm the role of RANKL as a mediator of vascular calcification in Charcot osteoarthropathy (Ndip, Williams et al. 2011), its role as an osteoclastic activator is unknown. Furthermore, bone resorption in Charcot osteoarthropathy may be modulated by inflammation via proinflammatory cytokines (Jeffcoate, Game et al. 2005). Cytokines of particular interest include tumour necrosis factor-α (TNF-α) and interleukin-6 (IL-6) as their concentrations are raised in the sera of patients presenting with acute active disease (Petrova, Dew et al. 2015), (Uccioli, Sinistro et al. 2010) but their role as osteoclastogenic modulators is unknown.

My main hypothesis is that aberrantly activated osteoclasts play a key role in the pathological bone destruction of the acute Charcot foot and my main objective was to study the cellular mechanism of increased osteoclastic activity, and in particular the role of RANKL, TNF-α and IL-6. I have explored osteclastogenesis using a classical resorption pit assay to generate functional human osteoclasts *in vitro* together with a novel technique to quantitate resorption on bone discs using surface profilometry. Both

methods have been used for the first time in the field of Charcot osteoarthropathy and have been proposed by the author.

The introduction of this thesis aims to inform the reader of how existing predisposing and precipitating factors known to trigger Charcot osteoarthropathy can modulate these cytokine pathways and argue a case for pathological osteoclast activation within this paradigm.

1.2 The Charcot foot in diabetes

Neuropathic bone and joint disease bears the name of the French neurologist, Jean Marie Charcot, who initially reported this condition in tabes dorsalis in 1868. The association with diabetes was described by Jordan in 1936 and in the 21st century Charcot joints are most frequently seen in patients with diabetes.

The true incidence of Charcot osteoarthropathy in diabetes is unknown, as there are no large epidemiological studies. Sinha *et al* cited a prevalence of 1:680 of people with diabetes developing this condition (Sinha, Munichoodappa et al. 1972). The acute active osteoarthropathy usually presents unilaterally. Involvement of the contralateral foot is not uncommon and has been noted to occur in up to 39 % of the cases (Sanders and Frykberg 2001).

Although considered a rare complication of diabetes, Charcot osteoarthropathy is quite often overlooked. Evidence of radiological changes associated with Charcot osteoarthropathy has been reported in up to 10% of patients with diabetes and neuropathy (Cavanagh, Young et al. 1994). Recent advances in imaging modalities have facilitated the diagnosis at an earlier stage when the conventional radiographs are normal and this may be also linked with the considerable underreporting of this condition (Rogers, Frykberg et al. 2011). Thus Charcot osteoarthropathy could be much more common than previously thought.

Charcot osteoarthropathy is associated with significant morbidity (Fabrin, Larsen et al. 2000). A novel data mining approach has identified more than 100 associations with a significant temporal relationship to the development of Charcot foot (Munson, Wrobel et al. 2014). Patients with this condition require considerable long-term support and their prognosis is poor. In a summary of 15 published reports, there were 11 deaths in 301 patients in a 2.5 year follow up, partial or complete foot amputation occurred in 20/301, whereas 83/301 patients had mobility limitations (Sinacore and Withrington 1999) leading to the characterisation of patients with Charcot osteoarthropathy as "frail patients with fragile feet" (Fabrin, Larsen et al. 2000). Thus an improved understanding of the pathogenesis of Charcot osteoarthropathy is essential as these patients have reduced quality of life and even increased mortality (Dhawan, Spratt et al. 2005), (Gazis, Pound et al. 2004), (van Baal, Hubbard et al. 2010).

Charcot osteoarthropathy typically affects the joints of the foot and ankle in diabetes. Rare presentations include osteoarthropathy of the knee or wrist (Petrova and Edmonds 2008). Charcot osteoarthropathy affects both type 1 and type 2 diabetes. Patients with type 1 diabetes present at a younger age when they are in their fourth or fifth decades whereas in type 2 diabetes, it occurs during their sixth and seventh decades (Petrova, Foster et al. 2004). Duration of diabetes is significantly longer in type 1 diabetes compared to type 2 diabetes and in some cases Charcot osteoarthropathy may be the initial manifestation of previously unrecognised type 2 diabetes (Petrova, Foster et al. 2004), (Pedersen, Madsen et al. 1993). A relative preponderance of type 1 diabetes compared with type 2 diabetes has been recorded (Petrova, Foster et al. 2004) and recently, it was shown that the odds ratio of a patient with type 1 diabetes to develop Charcot osteoarthropathy is 3.9 times greater that the odds ratio of a patient with type 2 diabetes (Ross, Mendicino et al. 2013).

1.2.1 Theories on the pathogenesis of Charcot osteoarthropathy in diabetes

Two fundamental theories have been put forward to explain the aetiopathogenesis of this condition.

The first, formulated by Charcot himself, also known as the French theory, or the "neuro-trophic theory", suggests that the bone and joint changes seen in tabes dorsalis are a result of a spinal cord lesion. He believed that the impaired nutritive trophic regulation alters the sympathetic tone, leading to vasodilation and increased blood flow. Charcot also highlighted the importance of inflammation. He postulated that hyperaemia (inflammation) due to abnormal neurovascular control leads to increased bone resorption and osteopenia ultimately resulting in bone and joint destruction.

The second theory, also known as the German theory or the "neuro-traumatic theory" was proposed by Volkman and Virchow. They attributed the joint destruction to external trauma and repetitive stress, which is quite often unperceived by the patient due to loss of proprioception and pain sensation. The patient continues to traumatise the bones and soft tissue. This can lead to joint swelling and ligament stretching, resulting in joint laxity (Lee, Blume et al. 2003). Ultimately, the inflammatory response to injury leads to hyperaemia, soft tissue swelling and bone and joint destruction.

The pathways to bone and joint destruction according to both theories are presented schematically below (Figure 1-1).

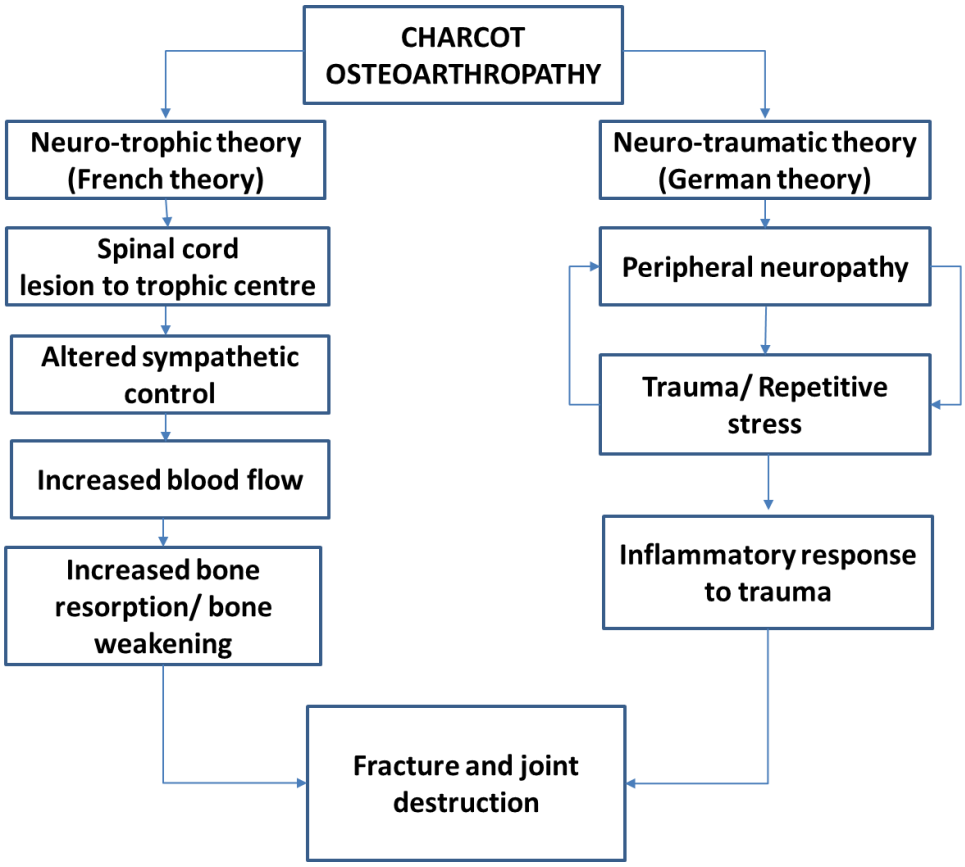

Figure 1-1 Pathways of development of Charcot osteoarthropathy: neuro-trophic and neuro-traumatic theories

1.2.2 Classification and presentation

The evolution of the Charcot foot was documented by Eichenholtz in 1966. In his monograph “Charcot joints” he described a cohort of 68 patients in whom Charcot joints were associated with diabetes (n=12), syphilis (n=34), alcoholism (n=4), syringomyelia (n=3) and leprosy (n=1), (Chantelau and Grutzner 2014). Based on the X-rays, he summarised the changes into three stages: (1) development, (2) coalescence and (3) reconstruction and reconstitution (Table 1-1).

Table 1-1 Eichenholtz's description of the natural course of the Charcot joint (radiological features and foot presentation)

Stages	Radiological features	Foot presentation (appearance)
Stage of development	Debris Fragmentation Disruption Dislocations	Redness Swelling Warmth Bounding pulses
Stage of coalescence	Sclerosis Absorption of fine debris Fusion of most large fragments	No redness Reduced swelling No warmth
Stage of reconstruction and reconstitution	Lessened sclerosis Rounding of major fragments Attempts at reformation of joint architecture	Ultimate foot deformity Rocker bottom deformity Medial convexity Ankle subluxation

The anatomical sites of bone and joint involvement have been classified into five patterns (Sanders and Frykberg's classification), (Table 1-2).

Table 1-2 Sanders and Frykberg's anatomical classification

Pattern	Bone and joint involvement
Pattern I	Metatarsal/ phalangeal joints
Pattern II	Metatarsal/ tarsal joints (Lisfranc joints)
Pattern III	Midtarsal joints (Chopart joints)
Pattern IV	Ankle and subtalar joint
Pattern V	Calcaneum

Data from a web-based survey of 288 new cases of acute Charcot foot registered from 76 different centres in the UK and Ireland within 20 months reported that the majority of lesions were in the mid-foot and hind foot and the distribution of the lesions is presented schematically (Figure 1-2), (Game, Catlow et al. 2012).

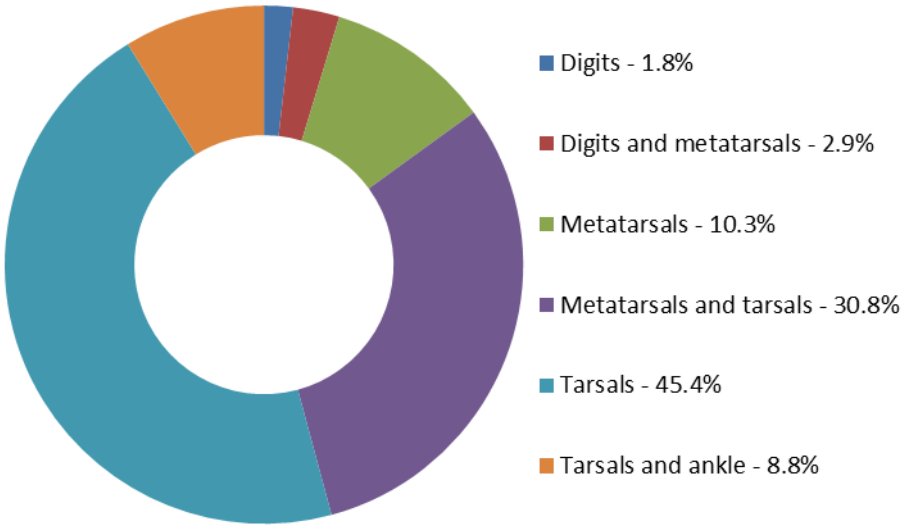

Figure 1-2 Charcot disease in the UK (CDUK) study: distribution of lesions

The Charcot foot is usually characterised by a unilateral redness and swelling following minor trauma which may remain unnoticed by the patient, (Figure 1-3A). Patients may present early in the acute active phase with normal X-ray or later when there may be already existing deformity and typical radiological changes of bone and joint destruction, (Figure 1-3B, C), (Petrova and Edmonds 2008).

(A) (B) (C)

Figure 1-3 Clinical and radiological presentation of acute Charcot osteoarthropathy in diabetes.
Acutely inflamed and swollen foot (A) with classical radiographic features of Charcot osteoarthropathy. The anterior-posterior view (B) shows increased space between the first and second metatarsal bases associated with severe metatarsal/ tarsal dislocation on the lateral view with rocker bottom foot deformity (C)

The X-ray negative stage is now well recognised, and it is often referred to Stage 0, or sometimes called “the incipient Charcot foot” (Yu and Hudson 2002), (Chantelau 2005). Imaging modalities including technetium diphosphonate bone scan, magnetic resonance imaging (MRI) and positron emission tomography–computed tomography (PET-CT) scanning have enabled the detection of early signs of inflammation and underlying bone damage before overt bone and joint destruction has occurred (Rogers, Frykberg et al. 2011), (Chantelau and Poll 2006), (Ruotolo, Di Pietro et al. 2013). Recognition and management at this stage could arrest disease activity and prevent foot deformity (Chantelau 2005).

This X-ray negative / MRI positive stage of inflammatory bone marrow oedema has been included into the recently proposed modified classification of Charcot osteoarthropathy (Chantelau and Grutzner 2014) in addition to the Eichenholtz’s stages I-III.

The acute active osteoarthropathy is divided into a low severity stage (grade 0) or high severity stage (grade 1) according to the absence or presence of cortical fracture (Chantelau and Grutzner 2014).

Grade 0 is characterised by mild inflammation, soft tissue oedema, normal X-ray but abnormal MRI scan showing evidence of microfracture, bone marrow oedema and bone bruising (Figure 1-4), (Chantelau and Grutzner 2014).

Grade 1 is characterised by severe inflammation, soft tissue oedema, abnormal X-ray with macrofractures and abnormal MRI scan showing evidence of macrofracture, bone marrow oedema and bone bruising (Figure 1-4), (Chantelau and Grutzner 2014).

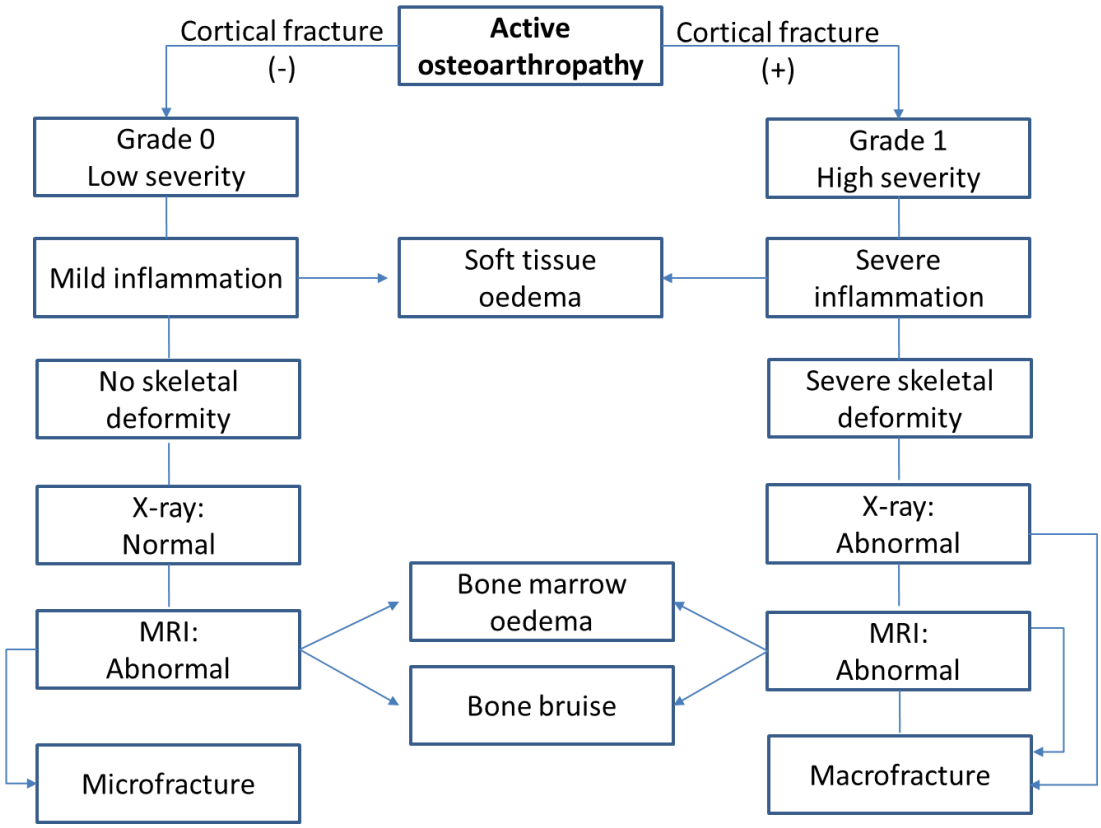

Figure 1-4 Categories of Charcot osteoarthropathy based on MRI scan (active osteoarthropathy)

Once the inflammation has resolved, the osteoarthropathy is deemed inactive. In both categories (grade 0 and grade 1), there is no evidence of inflammation both clinically and on MRI scan (absence of significant bone marrow oedema), (Figure 1-5). However, in grade 1 the foot has progressed to severe deformity and there is a

radiological evidence of healed macrofractures. In contrast, in grade 0, there is no deformity and the X-ray remains normal (Figure 1-5), (Chantelau and Grutzner 2014).

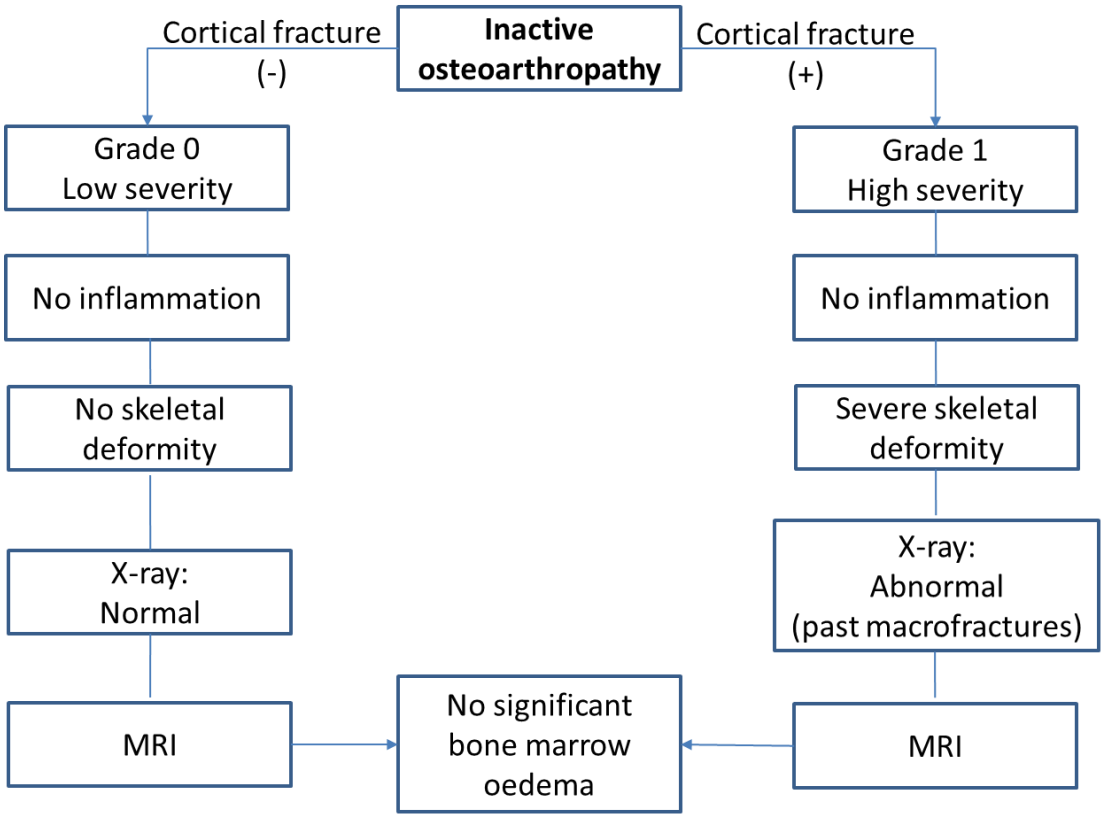

Figure 1-5 Categories of Charcot osteoarthropathy based on MRI scan (inactive osteoarthropathy)

Early recognition of Charcot osteoarthropathy when the X-ray is normal is extremely important (Petrova and Edmonds 2008), (Chantelau 2005) and this has been emphasised in the recent task force document (Rogers, Frykberg et al. 2011). If not recognised and managed at this stage, extensive irreversible bone and joint destruction can occur (Chantelau 2005) associated with severe foot deformity (Figure 1-3 B, C), leading to ulceration and possible amputation (Rogers, Frykberg et al. 2011).

1.2.3 Management of Charcot osteoathropathy

Current standard of care includes casting immobilisation until the inflammation subsides, the fractures heal and the deformity stabilises (Petrova and Edmonds 2008), (Petrova and Edmonds 2013). Patients require close follow up to monitor reduction of inflammation (infrared skin thermometry) and healing of fractures (Rogers, Frykberg et al. 2011). Anti-resorptive therapies including bisphosphonates and calcitonin have been used with some success as an adjunct to standard therapy (Petrova and Edmonds 2013) although according to others evidence to support their use is weak (Richard, Almasri et al. 2012). Thus an improved understanding of the mechanisms involved in the process of rapid bone destruction is essential for improved management of this condition (Petrova and Edmonds 2013), (Jeffcoate 2005).

1.3 Predisposing and precipitating factors

Well established predisposing and precipitating factors of Charcot osteoarthropathy include neuropathy and increased mechanical forces, bone resorption and fractures, trauma and inflammation.

1.3.1 Neuropathy

Diabetic neuropathy is a common complication of diabetes and affects almost 20% of the patients (Boulton, Vinik et al. 2005). It is associated not only with the development of foot ulceration but also with Charcot osteoarthropathy. In fact, neuropathy is the common denominator for all conditions that present with Charcot joints including tabes dorsalis, syringomyelia, leprosy, congenital sensory, familial amyloid neuropathy and toxic polyneuropathies, such as alcohol and human immunodeficiency virus (HIV) -induced (Shibuya, La Fontaine et al. 2008), (Young, Neiderer et al. 2012).

The presence of nerve damage is a required feature for the development of the characteristic bone and joint damage and involves either the spinal cord or the peripheral

nerves (Mabilleau and Edmonds 2010). Early experimental models have demonstrated that bone and joint destruction occur shortly after sectioning of the posterior nerve root (Mabilleau and Edmonds 2010). However, dogs, in whom, a combination of gangliotomy and transection of the cruciate ligament was carried out, developed more severe bone destruction compared to dogs subjected to gangliotomy alone. Thus the importance of peripheral neuropathy in association with trauma in the pathogenesis of this condition is established.

Standard tests to detect nerve damage demonstrate a variable degree of impairment in patients with Charcot osteoarthropathy. Numbness of the extremity is one of the most frequently reported symptoms although it is not always easy to quantify it by testing fine touch (Meyer 1992). Abnormal vibration sensation to 128 cycle/sec tuning fork was noted in 93% of patients with Charcot osteoarthropathy- 70% had diminished sensation and in 20% it was absent (Meyer 1992). Decreased ankle jerks were noted in 25% and were absent in 30% (Meyer 1992).

Nerve damage in Charcot osteoarthropathy could affect the large myelinated fibres (A α), the small myelinated fibres (A δ) and the unmyelinated fibres (C-fibres). In a study, which reported the presence of a global neuropathy in patients with Charcot osteoarthropathy, there was impaired sensation to hot and cold (small fibre neuropathy) and also reduced vibration threshold (large fibre neuropathy) when compared to controls (Young, Marshall et al. 1995). This study also demonstrated that nerve conduction velocity was similar between the Charcot and non-Charcot foot suggesting that the foot involvement was precipitated by the site of trauma (Young, Marshall et al. 1995). A further study of patients presenting with unilateral Charcot osteoarthropathy demonstrated that pinprick, light touch and temperature sensations were not significantly different between the affected and non-affected foot (Valabhji, Marshall et al. 2012). However, the level of attenuation of vibration sensation was more proximal in the affected compared with the unaffected limb, suggesting that an asymmetrical attenuation

of vibration sensation may predict the side that will develop a Charcot joint (Valabhji, Marshall et al. 2012).

Patients also exhibit abnormal pain sensation. A recent cross-sectional study demonstrated that perception thresholds for cutaneous pressure pain (using calibrated von-Frey-hairs with sharp non-injuring tip) but not for deep pressure pain (using Algometer II) were significantly elevated in patients with chronic Charcot feet (Chantelau, Wienemann et al. 2012). Although this study has shown the presence of diminished nociceptive C-fibre function at the skin level, it is not clear why musculoskeletal pressure pain perception threshold was preserved in Charcot osteoarthropathy and also in patients with diabetic neuropathy (Chantelau, Wienemann et al. 2012).

In our observations we reported that sensory perception threshold to hot and cold was significantly raised in the non-Charcot foot of type 1 and type 2 patients with osteoarthropathy compared with type 1 and type 2 control patients (Petrova, Foster et al. 2005) Vibration perception threshold was also raised in the non-Charcot foot in both type 1 and type 2 diabetes compared with controls, but only reached statistical significance in type 2 diabetes (Petrova, Foster et al. 2005).

Abnormal threshold to pain, hot and cold stimuli suggest that there may be a selective small fibre sensory loss associated with the development of Charcot osteoarthropathy (Stevens, Edmonds et al. 1992), predominantly in type 1 diabetes. A similar dissociation with impaired pain and temperature thresholds (small fibres) but preserved light touch and vibration (large fibres) has been noted in Charcot joints associated with syringomyelia (Miller 2001). However, other reports stress the importance of both small and large fibre global neuropathy in association with osteoarthropathy in both type 1 and type 2 diabetes (Young, Marshall et al. 1995). However, the role of neuropathy in the pathogenesis of Charcot osteoarthropathy is universal although further studies are needed to determine the specific neurological deficit in this devastating condition.

1.3.2 Trauma

Patients with diabetic neuropathy have limited joint mobility, increased plantar pressures and abnormal gait allowing them to frequently traumatise their feet (Mueller, Zou et al. 2008), (Katoulis, Ebdon-Parry et al. 1997), (Wrobel and Najafi 2010). In a recent cohort of 288 cases of Charcot foot, a third of patients recalled a particular episode of preceding trauma (Game, Catlow et al. 2012), whilst in others, the development of Charcot osteoarthropathy has been noted short after foot surgery or after an episode of foot ulcer of infection (Game, Catlow et al. 2012). However, in the majority of cases, trauma is trivial and is quite often unperceived by the patient due to the underlying neuropathy.

Recent studies of the physiology of the cholinergic anti-inflammatory pathway indicate that the nervous system via the inflammatory reflex of the vagus nerve can control cytokine release in response to trauma (Tracey 2007). Afferent signals carried in the vagus nerve can activate an efferent response that inhibits cytokine release and this is called the cholinergic anti-inflammatory pathway. It is mediated primarily by nicotinic acetylcholine receptor on tissue macrophages and leads to decreased production of proinflammatory cytokines and thus prevents tissue injury (Wang, Yu et al. 2003).

A similar pathway may exist to protect the bone and joint tissue. It is well documented that both sympathetic and sensory nerve fibres are present in periosteum and bone (Hill and Elde 1991), (Hohmann, Elde et al. 1986) , (Konttinen, Imai et al. 1996) and form dense parallel networks around blood vessels adjacent to bone trabeculae, in close contact to bone cells (Goto, Yamaza et al. 1998), (Hara-Irie, Amizuka et al. 1996), (Serre, Farlay et al. 1999). Experimental and clinical studies have shown increasing evidence for a neural control of bone development, growth, turnover and repair (Cherruau, Facchinetti et al. 1999), (Edoff, Hellman et al. 1997), (Hill, Turner et al. 1991), (Hukkanen, Konttinen et al. 1995), (Li, Ahmad et al. 2001), (Ramnemark, Nyberg et al. 1999).

In the limb without neuropathy the intact nerve supply and cholinergic anti-inflammatory pathway may be protective and the consequences of trauma are limited and do not progress to bone and joint damage (Mabilleau and Edmonds 2010), (Schaper, Huijberts et al. 2008). In the Charcot limb, trauma results in exaggerated inflammation due to the loss of the sensory neuropeptide and the cholinergic anti-inflammatory pathway (Mabilleau and Edmonds 2010), (Schaper, Huijberts et al. 2008). This leads to osteolysis and pathological bone and joint damage.

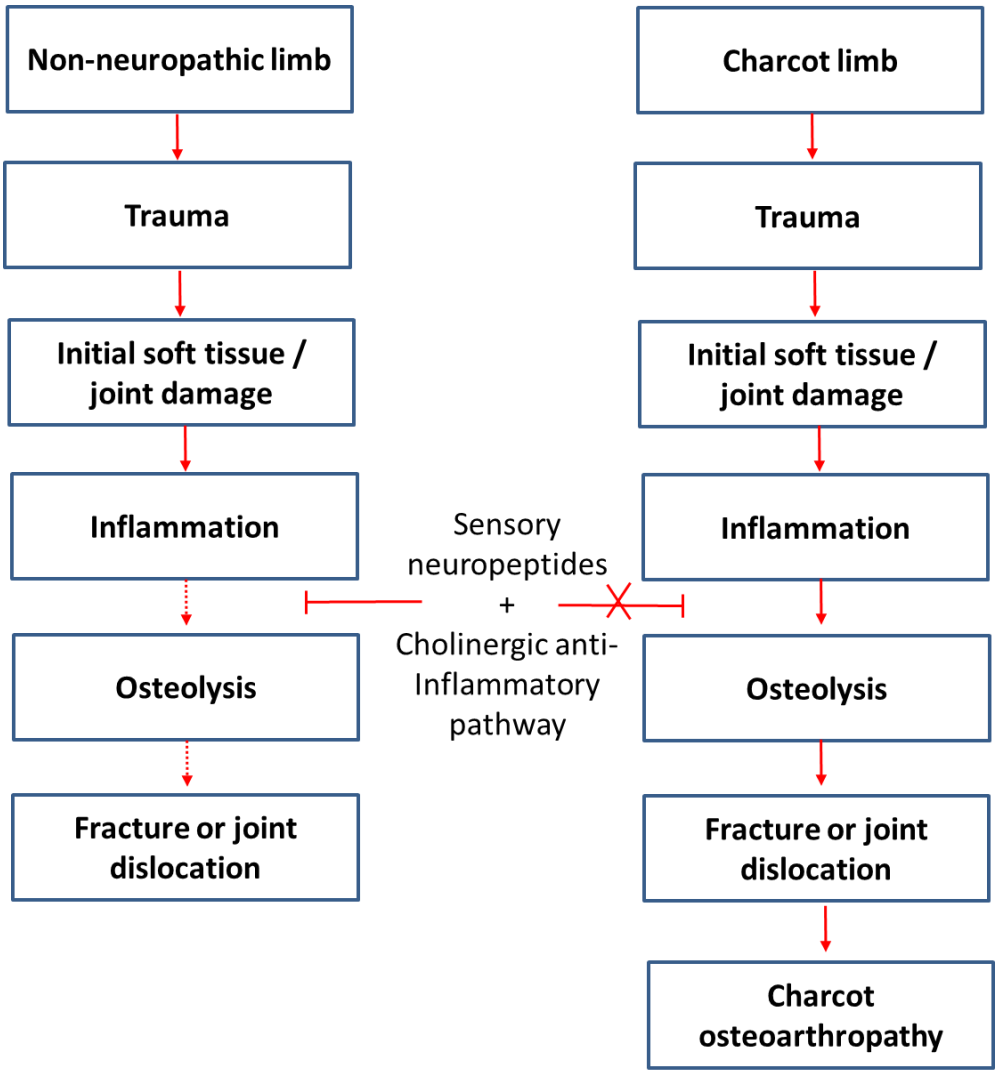

Figure 1-6 The role of neuropathy in Charcot osteoarthropathy
(Adapted from Mabilleau G, Edmonds ME: Role of neuropathy on fracture healing in Charcot neuro-osteoarthropathy. J Musculoskelet Neuronal Interact 2010;10: 84-91)

1.3.3 Bone resorption and fractures

Trauma on the background of neuropathy also leads to fracture and the importance of fracture as a trigger event for the development of Charcot osteoarthropathy is well recognised (Young, Marshall et al. 1995), (Johnson 1967), (Cundy, Edmonds et al. 1985).

Fractures are often juxta- articular and can cause the joint to become unstable and subjected to abnormal stress which will result in erosion of bone and cartilage. Early observations of Charcot joints in diabetes have reported that “fractures are the earliest sign of impending joint derangement and neurorthropathy” (El-Khoury and Kathol 1980). Fractures of significant magnitude were responsible for initiating joint changes in the majority of the 118 cases of Charcot foot reported by Johnson (Johnson 1967). In this classical review, he clearly demonstrated that fractures are the harbinger of the Charcot foot (Johnson 1967). These fractures are not painful because of the underlying peripheral neuropathy and the patient, who is unaware of the condition, is able to tolerate walking. Eventually, a stage with multiple fractures, bony fragmentation and loss of normal foot architecture develops i.e. the Charcot foot.

“Bone weakness”, as an underlying cause for these pathological fractures was proposed by Charcot himself. Several investigations have explored whether this condition is a “late sequela of osteoporosis” in diabetic neuropathy (Childs, Armstrong et al. 1998).

Using radiographic morphometry as a method of assessing bone mass, Cundy demonstrated diminished cortical bone mass in both hands and feet in patients with severe neuropathy (Cundy, Edmonds et al. 1985). This study also showed that metatarsal fractures were strongly associated with the subsequent development of Charcot osteoarthropathy (Cundy, Edmonds et al. 1985). In a further study, a fracture pattern of Charcot osteoarthropathy, which was more frequently seen in the ankle and forefoot, was associated with a reduced bone mineral density (BMD) of the femoral neck of the contralateral limb, whilst a dislocation pattern was associated with a normal BMD

(Herbst, Jones et al. 2004). Furthermore, the odds ratio for patients with osteopenia to develop fracture pattern opposed to dislocation pattern was 9.5, confirming the role of reduced BMD.

In Charcot osteoarthropathy osteopenia more frequently affects the peripheral rather than the axial skeleton. A study, which reported data on BMD measurements at several sites, showed reduced stiffness in the calcaneum of the Charcot and non-Charcot foot (Bem, Jirkovska et al. 2010). In addition, BMD in the femoral neck but not in the lumbar spine was reduced in Charcot patients compared with controls. In patients with acute Charcot osteoarthropathy, BMD in calcaneum of the affected Charcot foot was significantly lower compared with the BMD at the lumbar spine and the femoral neck (Bem, Jirkovska et al. 2010). In another series, patients with Charcot osteoarthropathy had a significantly reduced BMD in the lower limbs but relatively preserved BMD in the spine when compared with patients with diabetic neuropathy, (Young, Marshall et al. 1995). A further study confirmed that the reduction of BMD was limited to the affected foot and does not affect BMD of the spine and hip (Christensen, Bulow et al. 2010). These studies indicate that in the acute Charcot foot there is a focal reduction in BMD which could be a result of the destructive nature of the osteoarthropathy and could be modulated by local factors. Nevertheless there may be an underlying reduction in BMD, present in both feet that predisposes to fracture.

The association between diabetes and osteopenia in Charcot osteoarthropathy is more marked in type 1 rather than in type 2 diabetes (Petrova, Foster et al. 2005). Evidence of a pre-existing osteopenia was more frequently noted in Type 1 diabetes (Petrova, Foster et al. 2005). This reduction in BMD may be associated with neuropathy, which can lead to osteopenia not only in the calcaneum but also in femoral neck and distal limb (Rix, Andreassen et al. 1999). Moreover, there was a correlation between BMD of the lower limb and nerve conduction velocity, which is a further evidence to support the association between BMD and neuropathy (Young, Marshall et al. 1995).

Despite these discrepancies of the presence of osteopenia in type 1 and type 2 diabetes, the risk of fracture is increased in both presentations. Fractures in type 1 diabetes are more frequently associated with reduced BMD and are often spontaneous. History of trauma is rarely reported and in the majority of cases, fractures develop during normal daily activities (Kathol, el-Khoury et al. 1991). In type 2 diabetes, fractures result from alteration of weight bearing and load in the foot (Clasen 2000). Obesity in diabetic patients with neuropathy could lead to increased loading of the foot, although no relationship between elevated body mass index and acute Charcot osteoarthropathy was found in a recent case control study (Ross, Mendicino et al. 2013). However, mechanical pressures are significantly elevated in patients with neuropathy and the highest peak plantar pressures were reported in patients with Charcot osteoarthropathy in the affected and also in the contralateral foot (Armstrong and Lavery 1998). Patients with type 2 diabetes have increased risk of fractures that is mainly attributed to the increased risk of falling (Hofbauer, Brueck et al. 2007). Patients who report falls have multiple risk factors including neuropathy, impaired balance, advanced age, and a history of coronary disease (Schwartz, Hillier et al. 2002).

1.3.4 Inflammation

Inflammation has been long recognised as an important feature of the acute Charcot foot. Charcot himself pointed out its importance and postulated that hyperaemia (inflammation) due to abnormal neurovascular control results in bone and joint destruction. Clinical signs of the underlying inflammation are swelling and warmth. Although evidence of soft tissue inflammation can be noted on foot and ankle radiographs, in patients presenting at stage 0, radiographs may be normal (Yu and Hudson 2002). However, at this stage a triphasic disphosphonate bone scan shows increased uptake in all three phases namely blood flow, early blood pooling and delayed bony phase (Figure 1-7).

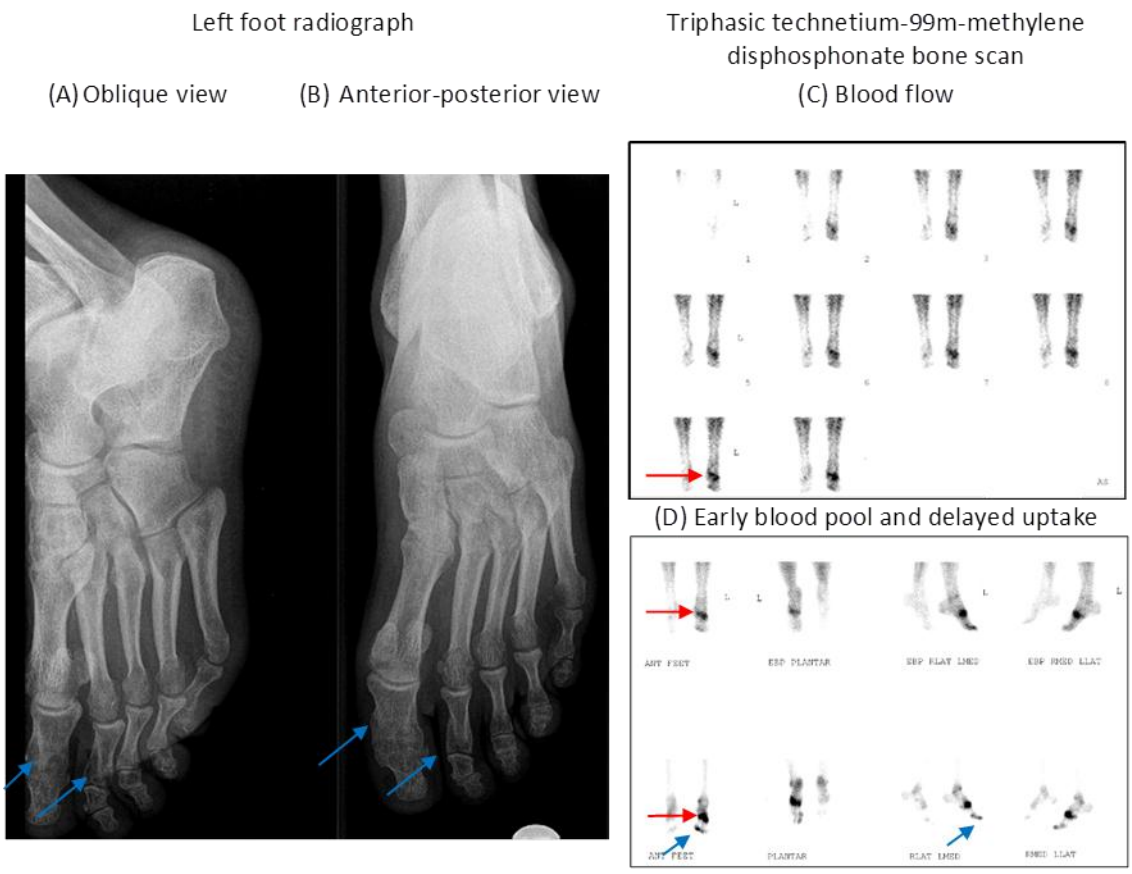

Figure 1-7 Foot radiograph and a triphasic technetium-99m-methylene disphosphonate bone scan of a patient presenting with a hot swollen left foot;
Normal alignment of the mid-foot with no bone and joint damage of the tarsometatarsal joints noted on the oblique (A) and anterior-posterior view (B) of the left foot radiograph.
The bone scan shows an asymmetrical blood flow (left foot > right foot) with acute inflammation in the left foot together with a focal increased uptake in the mid-foot (blood flow and early blood pool images), (red arrows), (A, B); increased bone turnover associated with a mid-foot lesion at the delayed uptake image (red arrow), (B).
In addition, there is radiological evidence of healed fractures of the 1st and 2nd toes (blue arrows), associated with increased bone turnover noted only at the delayed uptake images of the bone scan (blue arrows).

A normal foot radiograph does not rule out Charcot osteoarthropathy and further imaging can reveal the extent of pathology. The MRI scan of the same patient revealed subchondral bone marrow oedema and enhancement at the 2nd and 3rd tarsometatarsal joint noted on the T1, (Figure 1-8A), short tau inversion recovery (STIR) sequence with fat suppression (Figure 1-8B) and also after gadolinium, (Figure 1-8C).

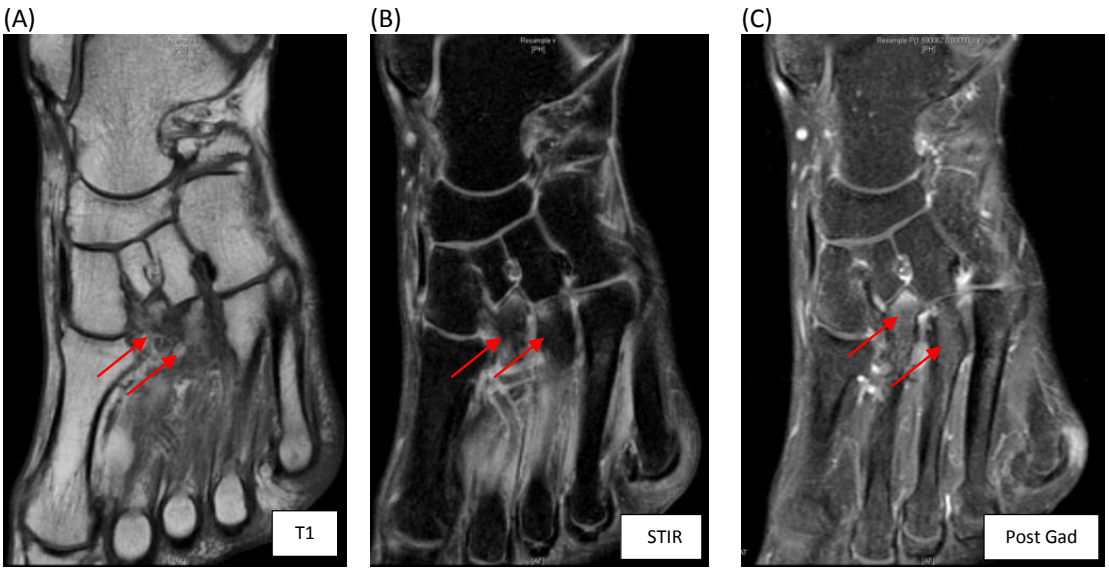

Figure 1-8 Magnetic resonance imaging of a patient presenting at Stage 0 Charcot osteoarthropathy.
Abnormal MRI scan showing subchondral oedema with enhancement (red arrows) noted at the 2nd and 3rd tarsometatarsal joints on the T1 (A), STIR sequence with fat suppression (B) and post gadolinium (Post Gad), (C).

At presentation, the affected foot is usually more than 2°C warmer compared with the non-affected foot (Armstrong, Todd et al. 1997), (McCrory, Morag et al. 1998). During the treatment phase, there is a gradual cooling (on average 0.022±0.0005°C per day or 2.1°C for every 100 days), (McCrory, Morag et al. 1998). In addition to skin foot temperatures, quantitative bone scanning techniques have been also used to assess healing and a strong correlation between temperature difference and the ratio of isotope uptake has been reported (McGill, Molyneaux et al. 2000). More recently, dynamic MRI scans have been used to quantitate inflammation at presentation and also on follow up (Zampa, Bargellini et al. 2011). There was a strong agreement between clinical and MRI findings in definite lesion healing**,** which was associated with a significant reduction of the contrast medium uptake rate in all patients with improved clinical findings (Zampa, Bargellini et al. 2011).

Foot inflammation and swelling characterise the acute active phase (Eichenholtz stage I) and subside in the stage of coalescence (Eichenholtz stage II). Foot swelling and skin foot temperatures are traditionally monitored within the course of the disease to

assess healing (Armstrong and Lavery 1997). Recently, using Fluorine-18 Fluorodeoxyglucose (F-18 FDG) PET/CT it was shown that an inflammatory state may precede bone damage in patients presenting with Charcot osteoarthropathy (Pickwell, van Kroonenburgh et al. 2011).

A further study noted increased blood flow associated with weakened but not absent venoarteriolar sympathetic axon reflex in Charcot patients and suggested that hyperaemia is more likely to be secondary to local inflammatory response to trauma (Christensen, Simonsen et al. 2011). The acute inflammatory response to trauma in acute Charcot osteoarthropathy is local as it is not usually associated with a rise in systemic markers of inflammation (Petrova, Moniz et al. 2007). Furthermore, inflammation is closely linked to bone and joint destruction and a recent immunohistochemistry of surgical specimens from Charcot patients has shown that bone resorption takes place in inflammatory environment with increased expression of proinflammatory cytokines (IL-1, IL-6 and TNF-α), (Baumhauer, O'Keefe et al. 2006).

The role of cytokines as modulators of bone resorption has become central to a recent theory comprising well established characteristic factors (neuropathy - abnormal loading – trauma – increased force – dislocation/ fracture) and possible cellular pathways that could be involved (Jeffcoate, Game et al. 2005), (Figure 1-9).

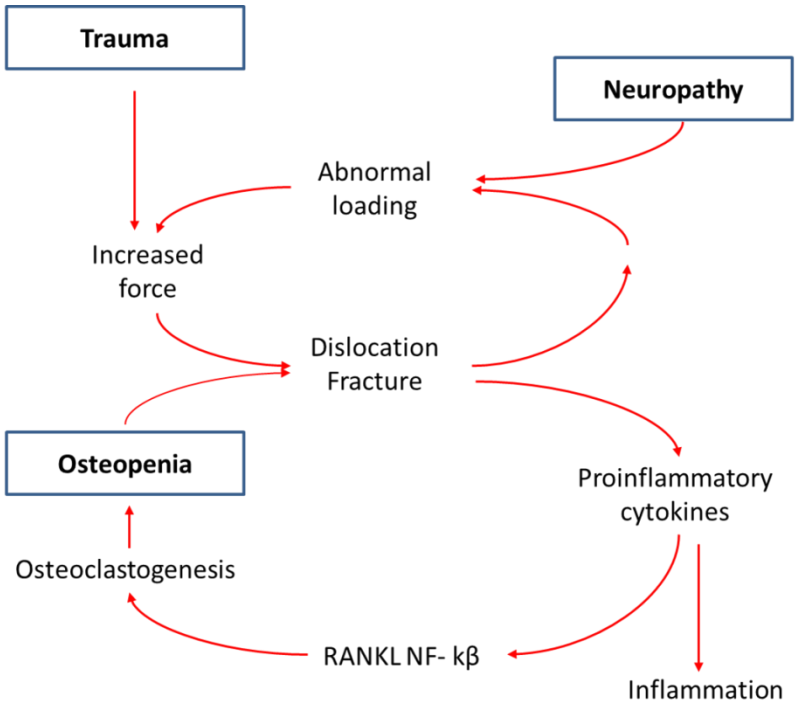

Figure 1-9 The role of the proinflammatory cytokines in the cause of acute Charcot foot in diabetes
(Adapted from Jeffcoate WJ, Game F, Cavanagh PR: The role of proinflammatory cytokines in the cause of neuropathic osteoarthropathy (acute Charcot foot) in diabetes. Lancet 2005;366: 2058-2061)

1.4 Recent theory in the pathogenesis of Charcot osteoarthropathy

Recently, attention has been drawn towards two cellular pathways as possible drivers of the rapid bone destruction that occurs in the diabetic neuropathic foot (Jeffcoate, Game et al. 2005). These include uncontrolled release of proinflammatory cytokines (IL-1, IL-6, and TNF-α) and the osteoclastic activator RANKL. The latter mediates medial arterial calcification in Charcot osteoarthropathy (Ndip, Williams et al. 2011). RANKL is also the key mediator of osteoclast formation and activation, although its role as an osteoclastogenic factor in Charcot osteoarthropathy is unknown. It has been hypothesised that proinflammatory cytokines can up-regulate RANKL and thereby osteoclastic activity (Jeffcoate, Game et al. 2005), (Figure 1-9).

1.5 Osteoclastic activity in acute Charcot osteoarthropathy

Clinical studies have confirmed that the acute active stage of Charcot osteoarthropathy is associated with increased osteoclastic activity. Serum concentrations of bone resorption markers are raised in patients with Charcot osteoarthropathy (Gough, Abraha et al. 1997), (Piaggesi, Rizzo et al. 2002) and there is evidence of osteopenia of the acute Charcot foot in both type 1 and type 2 diabetes (Petrova, Foster et al. 2005), (Jirkovska, Kasalicky et al. 2001).

The cellular mechanisms of this increased function are unknown and recently I hypothesised that the severe bone and joint destruction of the acute Charcot foot was driven by aberrantly activated osteoclasts.

1.5.1 Osteoclastogenesis and the role of RANKL

Osteoclasts have been shown to be the principal cell type responsible for bone resorption (Teitelbaum 2000). These tissue specific multi-nucleated cells are derived by differentiation of monocyte/ macrophage precursor cells at or near the bone surface (Boyle, Simonet et al. 2003). Osteoclastic precursors circulate in the blood in the monocytic fraction (Fujikawa, Quinn et al. 1996). Subtypes of monocytes which express the cluster of differentiation (CD) markers CD14, CD11b and CD61 exhibit 90-, 30- and 20-fold higher osteoclast formation capacity in contrast to CD15+ and CD169+ monocytes which can hardly generate osteoclasts (Husheem, Nyman et al. 2005). Two cytokines are both necessary and sufficient for osteoclastogenesis: RANKL, and macrophage-colony stimulating factor (M-CSF), (Figure 1-10).

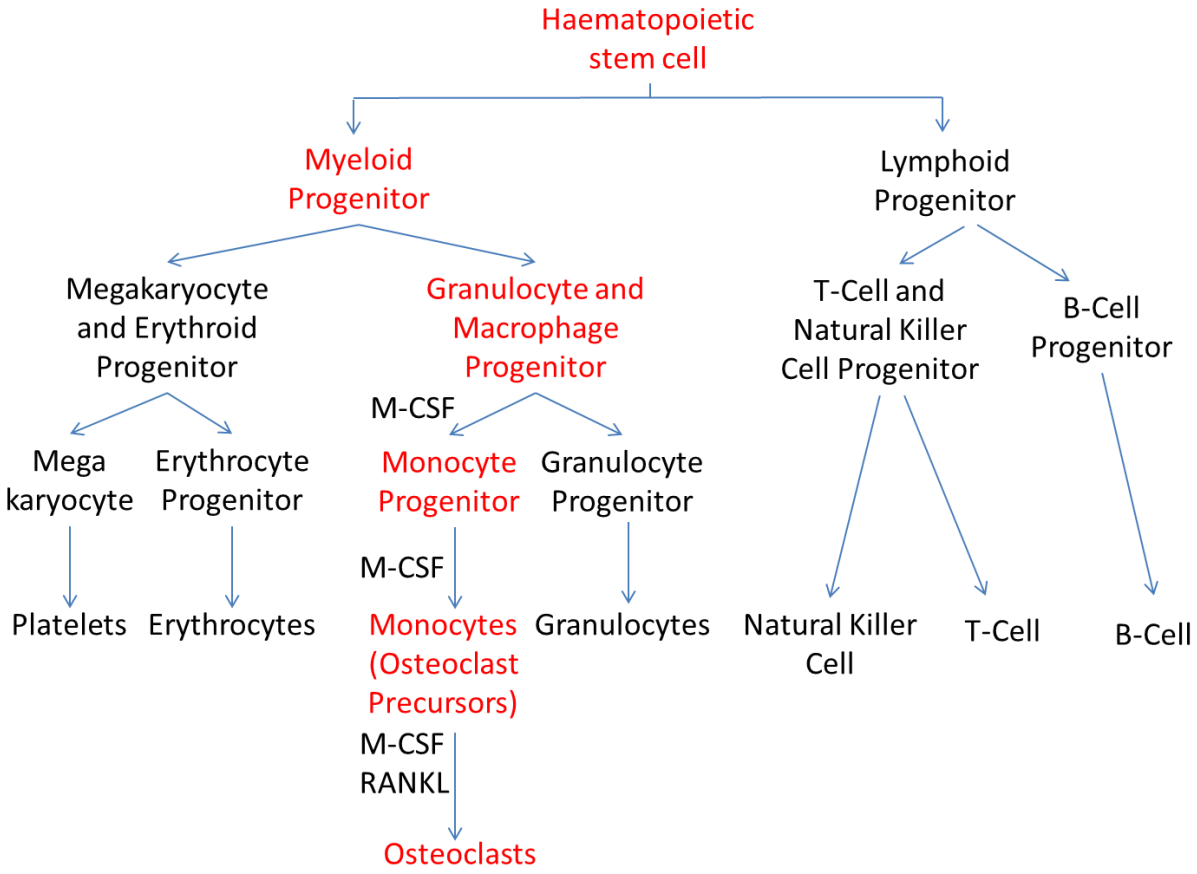

Figure 1-10 Haematopoiesis from multi-potent stem cell

RANKL, a cytokine from the TNF-ligand superfamily is expressed on a variety of cell types (bone forming osteoblasts, T lymphocytes, dendritic cells, endothelial cells and fibroblasts). RANKL binds to its target RANK, expressed on mononuclear osteoclastic precursors, induces NF-kβ signalling, resulting in NF-kβ translocation to the nucleus and drives osteoclastogenesis (Boyce and Xing 2008). RANKL has been shown to stimulate the fusion of pre-osteoclasts, the attachment of the osteoclasts to bone and it is also an important factor for their activation and survival (Kostenuik 2005). M-CSF, a hematopoietic growth factor, is an essential cytokine required for proliferation and survival of mononuclear cells and it acts via its receptor c-fms (Yasuda, Shima et al. 1998).

In the presence of RANKL and M-CSF osteoclast precursors undergo various stages of proliferation, fusion and differentiation before they become fully functionally active, mature osteoclasts (Figure 1-11).

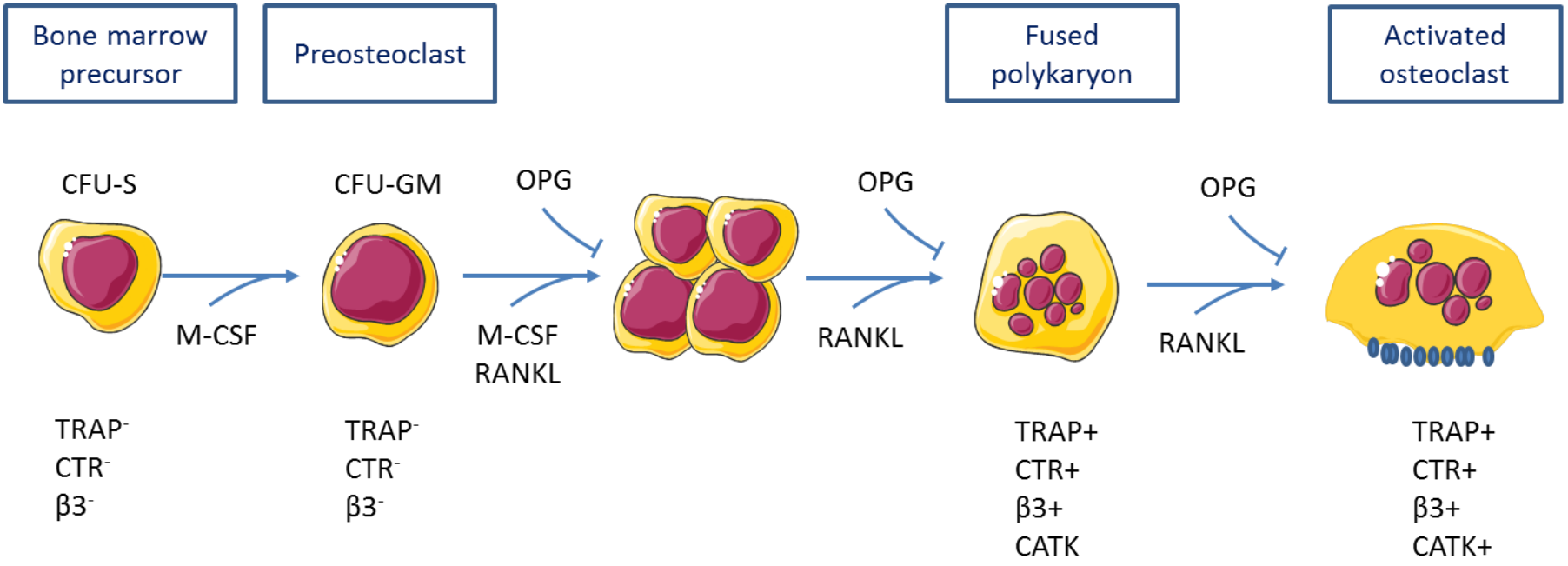

Figure 1-11 Schematic diagram of osteoclastogenesis.

Haematopoietic precursor cells differentiate into mature osteoclasts in the presence of M-CSF and RANKL after cell fusion of multiple (10-20) individual mononuclear cells. The process is regulated by OPG which acts as a decoy receptor for RANKL. In contact with bone, the multi-nuclear osteoclast undergoes cytodifferentiation and activation; Adapted from Boyle WJ, Simonet WS, Lacey DL: Osteoclast differentiation and activation. Nature 2003; 423(6937): 337-342 .

These large multi-nucleated cells express a series of osteoclast markers, including tartrate-resistant acid phosphatase (TRAP), cathepsin K, calcitonin receptor and β_3-intergrin (Boyle, Simonet et al. 2003), (Henriksen, Bollerslev et al. 2011). To degrade mineralised matrix, these cells have a unique cytoskeleton. In contact with bone, they form ruffled membrane and actin rings, characteristic of actively resorbing osteoclasts (Teitelbaum 2007). RANKL stimulates osteoclast activation by inducing secretion of protons and lytic enzymes into a sealed resorption zone formed between the basal surface of the osteoclast and the bone surface, (Figure 1-12), (Boyle, Simonet et al. 2003). The secreted protons in the resorption lacuna activate TRAP and cathepsin K which are essential for the degradation of bone mineral and collagen matrix (Boyle, Simonet et al. 2003). The resorbed material is then removed by uptake and transcytosis through the osteoclasts, (Figure 1-12). After completing the resorption, osteoclasts undergo apoptosis or migrate and perform a further round of resorption.

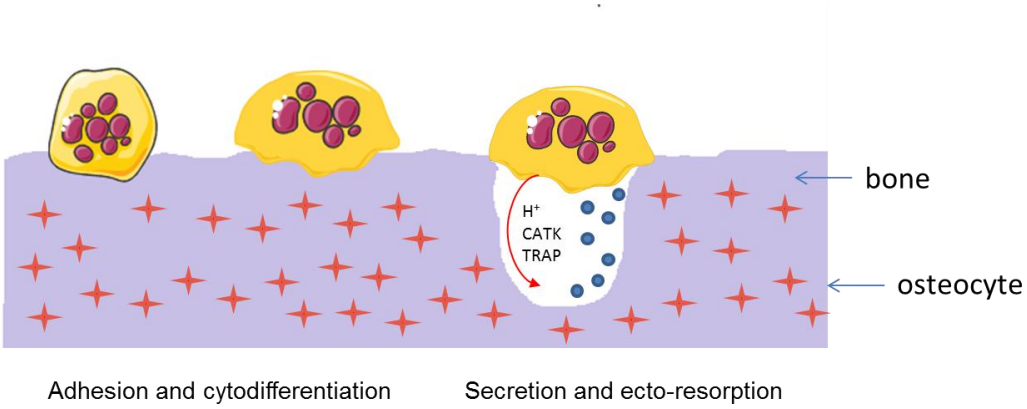

Figure 1-12 Schematic diagram of activation of bone resorption
Multi-nucleated osteoclasts adhere to bone and undergo cytodifferentiation by forming a ruffled membrane. RANKL stimulates osteoclast activation by inducing secretion of protons, cathepsin K (CATK) and TRAP into the resorption lacuna. The degraded bone mineral and collagen are removed by uptake and transcytosis through the osteoclasts.

The effects of RANKL are physiologically counterbalanced by osteoprotegerin (OPG). The latter is a TNF receptor superfamily member glycoprotein acting as a soluble decoy receptor for RANKL. It is secreted by a variety of cells including stromal cells, B

lymphocytes and dendritic cells. OPG blocks the interaction between RANKL-RANK thereby counteracting the osteoclatogenic activity (Boyce and Xing 2008). OPG and RANKL are important for osteoclast regulation. The balance between RANKL and OPG determines osteoclast functions. Expression of RANKL and OPG is coordinated to regulate bone resorption and density and acts negatively to control the activation state of RANK on osteoclasts.

In addition to bone, this signalling pathway also plays a role in vascular calcification. The first evidence to suggest this association comes from animal knock-out studies. Transgenic mice overexpressing OPG develop osteopetrosis (Simonet, Lacey et al. 1997) and conversely, OPG knockout mice develop severe osteoporosis (Bucay, Sarosi et al. 1998). These mice also develop arterial calcification of the aorta, which is also mediated via this signalling pathway. There is evidence that calcified arteries of OPG knockout mice mice express RANKL and RANK, proteins not normally present in non-calcified arteries (Min, Morony et al. 2000). Similarly, a study in atherosclerotic human arteries has shown the presence of OPG and RANKL in advanced calcified lesions (Dhore, Cleutjens et al. 2001). It is well known that there is a high clinical prevalence and coincidence of arterial calcification and cardiovascular disease in patients with osteoporosis and such association has been noted in patients with diabetes (Petrova and Shanahan 2014). This common presentation of vascular calcification and pathological osteolysis in diabetic neuropathy has led to a hypothesis that both processes could be a result of RANKL up-regulation (Jeffcoate 2004)

1.5.2 RANKL/OPG signalling pathway as a mediator of vascular calcification in diabetes

The first evidence to suggest the association between vascular calcification and neuropathy in diabetes comes from clinical observations (Edmonds, Morrison et al. 1982). Foot and ankle radiographs of diabetic foot patients showed typical "pipe-stem or tramline" appearance of continuous parallel lines of calcification of foot and leg

arteries (Edmonds, Morrison et al. 1982). Histological examination of the peripheral artery specimens from diabetic patients with neuropathy revealed medial calcification, characterised by the presence of calcified elastic fibres in the mildly affected arteries, to extensive calcium deposits and areas of true bone formation in the advanced lesions (Shanahan, Cary et al. 1999).

The association between diabetic neuropathy and vascular calcification extends to neuropathy-related complications including foot ulceration, osteomyelitis and Charcot osteoarthropathy. Vascular calcification in peripheral arteries was reported in 54% of patients presenting with uncomplicated foot ulcer and in 66% of patients with osteomyelitis (Sharma, Scammell et al. 2010). Charcot osteoarthropathy, is a condition in which vascular calcification is particularly common (Sharma, Scammell et al. 2010) and in some cohorts, it has been observed in up to 90% of cases (Sinha, Munichoodappa et al. 1972). There is evidence to suggest that the RANKL/OPG signalling pathway is up-regulated in patients with Charcot osteoarthropathy who exhibit elevated serum levels of RANKL, OPG and RANKL/OPG ratio (Ndip, Williams et al. 2011). Furthermore high serum OPG is significantly associated with the presence of vascular calcification in foot and leg arteries in neuropathic patients (Edmonds, Korzon-Burakowska et al. 2009).

In the vasculature histological examination of tibial peripheral artery specimens from Charcot patients, undergoing surgery has identified positive RANKL staining in both medial and intimal calcified areas, which were not present in non-calcified areas or in specimens from control subjects (Ndip, Williams et al. 2011). Moreover, vascular smooth muscle cells from Charcot patients treated with RANKL showed a greater capacity to mineralise and this increased osteoblastic differentiation was inhibited by OPG, confirming the role of RANKL in the process of calcification (Ndip, Williams et al. 2011). In bone, evidence from a pilot *in vitro study* has shown that newly formed osteoclasts, derived from patients with Charcot osteoarthropathy, exhibit extensive resorbing activity in the presence of M-CSF and RANKL, a response which is attenuated by OPG

(Mabilleau, Petrova et al. 2008). Thus in the vessel wall, progenitor cells differentiate into osteoblast-like cells, depositing mineralised matrix, whereas in bone, the enhanced osteoclastic activation results in osteolysis and severe bone damage (Alexander 2009).

Hence RANKL and OPG are identified as key players in the pathogenesis of both vascular calcification and bone loss in Charcot osteoarthropathy. Factors that can upregulate RANKL in diabetes are neuropathy and inflammation.

1.5.3 Neuropathy and RANKL

It is possible that upregulation of RANKL could be triggered by the loss of nerve-derived peptides, e.g. calcitonin gene-related peptide (CGRP), (Jeffcoate 2004). The latter is a neuropeptide that acts as a neurotransmitter in small fibres (C-fibres), (Pittenger and Vinik 2003). Local innervation plays a modulating role in bone growth, repair and remodelling. The terminal structure of the osseous CGRP-containing nerves directly contact osteoblasts, osteoclasts, and the periosteal lining cells, and are a source of local CGRP, which can act as a local modulator of bone metabolism. CGRP increases osteoblastic cyclic adenosine monophosphate via its action on bone specific CGRP receptors (Bjurholm, Kreicbergs et al. 1992) thus stimulating osteogenesis (Bernard and Shih 1990). Osseous CGRP-containing fibres are also involved in pathologic events in bone. The density of CGRP fibres is increased near sites of post-fracture osteogenesis (healing callus) and is decreased at the stumps of non-union (Santavirta, Konttinen et al. 1992). Evidence from bone marrow macrophage cultures has shown that CGRP inhibits RANKL induced NF-κB activation, down-regulates osteoclastic genes like TRAP and cathepsin K and decreases the number of TRAP-positive cells and RANKL-mediated bone resorption (Wang, Shi et al. 2010).

Thus CGRP deficiency in small fibre neuropathy may lead to impaired osteogenesis and delayed fracture healing, and also increased RANKL-mediated osteoclastic activity leading to Charcot osteoarthropathy.

1.5.4 Inflammation and RANKL

Trauma on the background of neuropathy may trigger an exaggerated cytokine response with release of proinflammatory cytokines (Jeffcoate, Game et al. 2005). In such pathological conditions with excessive activation of the immune system, osteoclastic activity becomes deregulated due to increased production of pro-inflammatory cytokines by activated T-cells. In neuropathy, it is possible that there is a misbalance between the production of pro-osteoclastogenic cytokines (IL-1β, IL-6, IL-8, IL-11, IL-17 and TNF-α) and anti-osteoclastogenic mediators (IL-4, IL-10, IL-13, IL-18, Interferon-γ and Interferon-β), (Zupan, Jeras et al. 2013). It has been recently shown that blood monocytes from patients with acute Charcot osteoarthropathy spontaneously produced detectable amounts of TNF-α, IL-1β, IL-6 but not IL-4 and IL-10 (Uccioli, Sinistro et al. 2010). When stimulated with lipopolysaccharide, monocytes from Charcot patients had enhanced production of TNF-α, IL-1β, IL-6 but less IL-4 and IL-10 compared with monocytes from diabetic control and healthy control subjects (Uccioli, Sinistro et al. 2010). In patients with acute Charcot osteoarthropathy, the concentrations of TNF-α and IL-6 in the serum were raised (Petrova, Dew et al. 2015) although their role in osteoclastogenesis is unknown.

The proinflammatory cytokines can target osteoclasts directly or indirectly by modulating the RANKL/OPG signalling pathway. TNF-α enhances expression of RANKL by stromal cells and also experimental work has demonstrated synergism in their action on osteoclastic precursors (Lam, Takeshita et al. 2000), (Kobayashi, Takahashi et al. 2000), (Fuller, Murphy et al. 2002). IL-6 enhances RANKL and OPG expression but also directly stimulates osteoclast differentiation (Zupan, Jeras et al. 2013), (Kudo, Sabokbar et al. 2003). In addition to trauma, bone fracture itself triggers a coordinated healing cytokine response with induction of pro-inflammatory cytokines, including IL-1 and TNF-α. RANKL is also increased in fracture healing (Kon, Cho et al. 2001).

Thus it is important to study RANKL-mediated osteoclastic activity and its interaction with inflammation to achieve a better understanding of the pathogenesis of this condition.

1.6 Hypothesis and proposed work

I have hypothesised that aberrantly activated osteoclasts play a key role in the pathological bone destruction that is seen in the acute Charcot foot.

My main objectives are:

1. To assess the role of RANKL as an osteoclastic activator in patients with acute Charcot osteoarthropathy
2. To assess the role of TNF-α on RANKL-mediated osteoclastic activity in patients with acute Charcot osteoarthropathy by using neutralising antibodies to TNF-α (anti-TNF-α)
3. To assess the role of IL-6 on RANKL-mediated osteoclastic activity in patients with acute Charcot osteoarthropathy by using neutralising antibodies to IL-6 (anti-IL-6)

To achieve these goals, I introduced for the first time in the field of Charcot osteoarthropathy, a well-established osteoclast culture assay. The technique to generate functional human osteoclasts from peripheral blood monocytes (PBMCs), (Sabokbar and Athanasou 2003) in the presence of M-CSF and soluble RANKL has been validated as a useful tool to determine the cellular mechanisms involved in the process of osteoclast formation and resorption in physiological and pathological conditions. This technique has been used in a variety of conditions including rheumatoid arthritis and psoriatic arthritis but such studies have not been carried out in Charcot osteoarthropathy. A detailed description of the osteoclast culture assay is presented in Chapter 2.

In addition to this *in vitro* assay, I introduced a novel method to quantitate resorption on bone discs, namely surface profilometry. This technique provided a new perspective

for measuring osteoclastic activity and was used to evaluate erosion patterns and pit parameters of resorbed bone discs under different culture treatments. Details on surface profilometry and applied methodology are described in Chapter 3.

Using traditional osteoclastic culture assays (as described in Chapter 2) together with surface profilometry (as described in Chapter 3), I studied osteoclastogenesis in patients with Charcot osteoarthropathy, diabetic patients and healthy control subjects.

My experimental work falls into three parts.

Experimental cultures with M-CSF+RANKL with and without the addition of OPG (Chapter 4)

Experimental cultures with M-CSF+RANKL+anti-TNF-α with and without the addition of OPG (Chapter 5)

Experimental cultures with M-CSF+RANKL+anti-IL-6 with and without the addition of OPG (Chapter 6)

Chapters 4, 5 and 6 provide information on the study groups, methods, statistical analyses, results and relevant discussion.

Chapter 7 summarises the main conclusions and future perspectives of the proposed work.

1.7 Expected outcome

It is hoped that these studies will elucidate the cellular mechanisms of increased osteoclastic activity in acute Charcot osteoarthropathy. A better understanding of the mechanisms leading to severe bone and joint destruction of the acute Charcot foot could become a basis for pharmacological intervention with new therapies and improved management of this condition.

Chapter 2 Generation of functional human osteoclasts *in vitro*

2.1 Introduction

The breakthrough discovery of RANKL in 1998, which was identified as osteoblast produced ligand promoting osteoclast differentiation, has facilitated the establishment of an *in vitro* system to generate bone-resorbing osteoclasts without the need of co-culture of osteoblasts or stromal cells and haematopoietic cells (Susa, Luong-Nguyen et al. 2004), (Marino, Logan et al. 2014).

This chapter describes the technique to generate functional human osteoclasts *in vitro* from peripheral blood mononuclear cells (PBMCs). It explains in detail the methodology of cell isolation, culture set up and long-term cell culture maintenance. The different culture conditions and cell treatments are described. The main staining protocols, together with illustrations of each technique, are presented. For each section, detailed information on the required consumables, preparation of stock solutions and storage is provided.

2.2 Collection of blood samples

Blood samples from patients and controls were obtained by venepucture of the anticubital vein following standard sterile procedure. All samples were taken in the Diabetic Foot Clinic at King's College Hospital. Blood was taken into four 10 ml ethylenediaminetetraacetic acid (EDTA) tubes (BD Vacutainer - K2E 18.0 mg, Ref 367525) for each subject. Blood samples were stored overnight at 4 °C and processed on the next day within 24 hours of collection. All subjects had been informed verbally for the purpose of the study and had been given a patient information sheet. All subjects had agreed to take part in the study and signed a written informed consent.

2.3 Cell culture

Cell culture work was set up and carried out in Professor Shanahan's laboratory in James Black Centre, King's College London. All cell culture experiments were carried out in the microbiological safety cabinet (MSC) under appropriate aseptic conditions and health and safety requirements.

A list of the osteoclast culture specific consumables, manufacturers and instructions for the preparation of stock solutions and storage is presented in the table below (Table 2-1).

Table 2-1 Osteoclast culture assay consumables

Consumables	Manufacturer	Preparation	Storage
α-minimum essential medium (α MEM)	Lonza, Wokingham, UK	Ready to use	4°C
Penicillin / Streptomycin	Sigma- Aldrich Ltd, Poole, UK	aliquot in 5 ml	-20°C
L-Glutamine	Sigma- Aldrich Ltd, Poole, UK	aliquot in 5 ml	-20°C
Foetal bovine serum (FBS)	Lonza Ltd, Wokingham, UK	aliquot in 50 ml	-20°C
Phosphate buffered saline (PBS)	Sigma- Aldrich Ltd, Poole, UK	Ready to use	4°C
Trypan blue solution in PBS (0.4%)	Sigma- Aldrich Ltd, Poole, UK	Ready to use	RT*
Bovine bone discs in 70% ethanol	Immunodiagnostics Systems, Boldon, UK	Mark one side of the bone disc with F	4°C
Recombinant human M-CSF 25 µg	R&D Systems Europe Ltd, Abingdon, UK	Add 25 ml of osteoclast medium to vial; mix and aliquot	-20°C
Recombinant human sRANKL10 µg	PeproTech EC Ltd London, UK	Add 1 ml of osteoclast medium to vial, mix and aliquot	-20°C
Recombinant human OPG 25 µg	R&D Systems Europe, Ltd, Abingdon, UK	Add 5 ml of osteoclast medium to vial; mix and aliquot	-20°C
Anti-human TNF-α antibody 1mg (anti-TNF-α)	R&D Systems Europe, Ltd, Abingdon, UK	Add 1 ml of PBS to vial; mix and aliquot	-20°C
Anti-human IL-6 neutralising antibody 1 mg (anti-IL6)	R&D Systems Europe, Ltd, Abingdon, UK	Add 1 ml of PBS to vial; mix and aliquot	-20°C
Osteoclast culture medium		500 ml α-MEM + 5ml Penicillin (50 U/ml) /Streptomycin (50 µg/ml) + 5ml L-Glutamine (2mM)+ 50 ml FBS (10%); Use within 6 weeks	4°C

***RT - room temperature**

2.3.1 Cell isolation

Peripheral blood mononuclear cells (PBMCs) were isolated from whole blood and cultured on plastic for 17 days in 24-well plates to assess osteoclast formation and on bovine bone discs set up in 96-well plates to assess osteoclast resorption.

Blood was diluted with α-minimal essential medium (α-MEM) in 1:1 (i.e. 20 ml of blood was diluted in 20 ml of α-MEM). After mixing well, the diluted blood was layered over an equivalent volume of histopaque (20 ml of diluted blood layered over 20 ml of histopaque). The automatic pipette was set at the lowest flow to avoid the mixing of the two layers. Samples were centrifugated into a temperature controlled centrifuge (4°C, 2300 rounds per minute (rpm) for 25 minute). After the gradient centrifugation, the following layers from top to bottom were noted: haemolysed blood, PBMC interface, histopaque and red blood cells. The PBMC interface layer was gently aspirated and transferred into a universal containing 5 ml of plain α-MEM. Cells were washed with 20 ml of α-MEM (final volume) and centrifuged at 4°C, 1500 rpm for 15 minutes. After the centrifugation, the cell pellet was noted at the conic bottom of the universal. The supernatant was discarded. The pellet was resuspended in 2 ml of α-MEM and cells were washed with 20 ml of α-MEM (final volume). After a second round of centrifugation (1500 rpm, 4°C for 15 minutes), the pellet was resuspended in 2 ml of osteoclast culture medium (α-MEM, supplemented with Penicillin 50 U/ml / Streptomycin (50 µg/ml), L-Glutamine (2mM) and 10% heat-inactivated FBS.

A schematic approach of the cell isolation is presented (Figure 2-1).

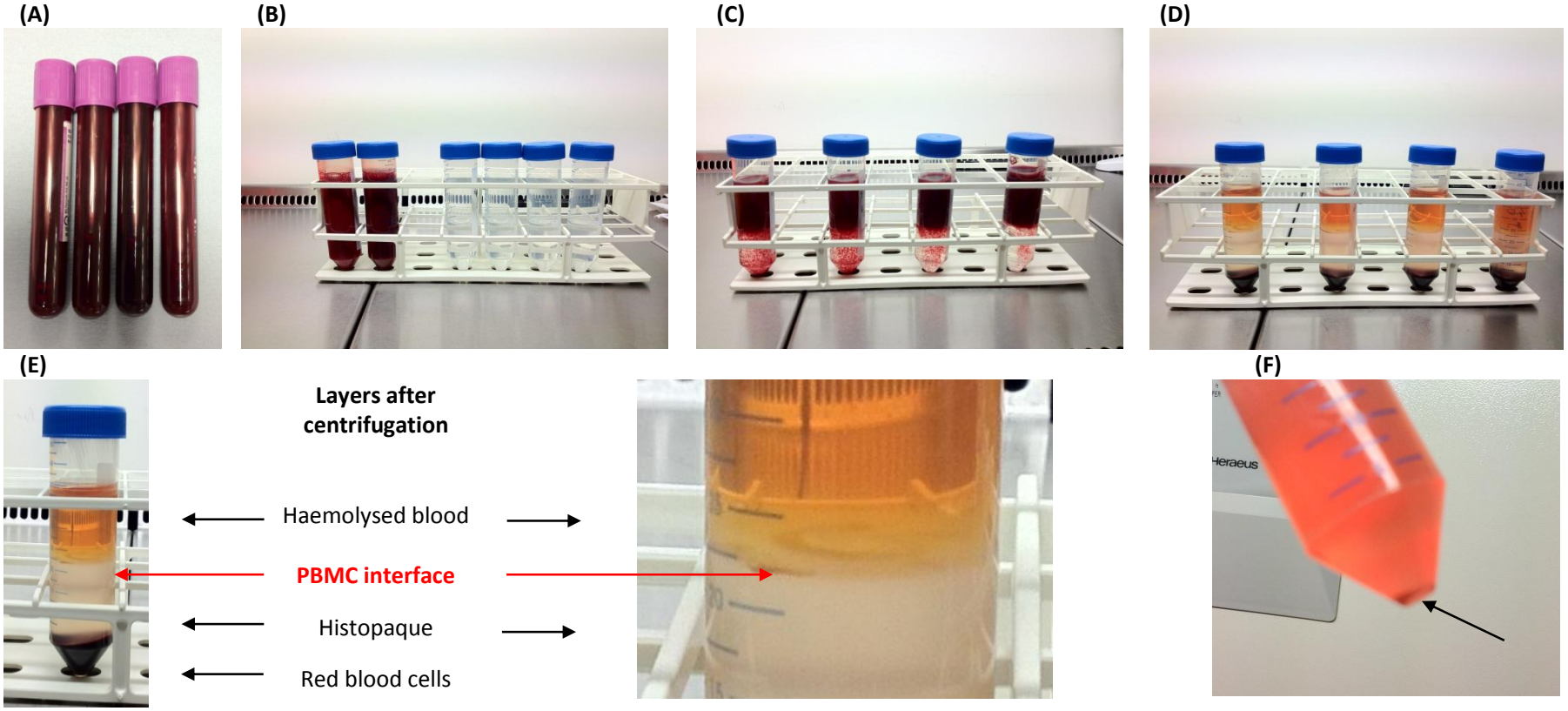

Figure 2-1 Isolation of PBMCs from whole blood

(A) Blood sample collected in EDTA blood tubes; (B) Blood diluted in α-MEM, (1:1); (C) Diluted blood layered over histopaque (1:1); (D) Samples after centrifugation (25 minutes, 4°C, 2300 rpm); (E) The arrows denote the layers after centrifugation; The PBMC interface (red arrow) was removed and transferred into a universal containing α-MEM; Cells were washed twice in α-MEM and centrifugated (15 minutes, 4°C, 1500 rpm); (F) Black arrow denotes the PBMC pellet after the second round of centrifugation.

Cells were counted using haemocytometer. Initially, 10 µl of cell suspension was mixed with 10 µl of 0.4% trypan blue solution on parafilm in the MSC. The chamber of the haemocytometer was loaded with 10 µl of diluted sample. Cells were counted at X100 magnification under light microscopy. The cell concentration was calculated and $2x10^6$ cells were cultured on plastic (24-well plates) and $5x10^5$ cells were cultured on bovine bone discs in the 96-well plates in duplicate to assess osteoclast formation and resorption respectively. After the addition of the cell suspension to the required wells, all plates were incubated at 37°C, 5% CO_2 for 2 hours.

The appropriate number of 24-well and 96-well plates/ subject was set up in advance. For 24-well plates, 1 ml of osteoclast culture medium was added to each well. For 96-well plates, one bovine bone disc together with 250 µl of osteoclast culture medium was added. Initially, the appropriate number of bone discs was removed from the vial and placed in a sterile Petri dish to dry in the MSC. One side of the bovine bone discs was marked with F with a pencil tip sterilised in 70% ethanol. Using sterile forceps, one disc with the F-side face down was placed into a 96-well (1 disc/ well), followed by the addition of 100 µl of osteoclast culture medium. The prepared plates were stored in the incubator (at 37 °C; 5% CO_2). Prior to the addition of the cell suspension to the 96-wells, the plate base was examined to check whether all bovine bone discs were in the wells with the “F-side”, facing down to ensure that cells are cultured on the non-marked side.

Parallel cultures to assess osteoclast formation on plastic and osteoclast resorption on bovine discs were set up for each subject.

2.3.2 Culture set up

After 2 hours incubation at 37°C, plate wells and bovine bone discs were washed to remove non-adherent cells and then maintained in osteoclast culture medium, under 7 main culture treatment conditions (Figure 2-2).

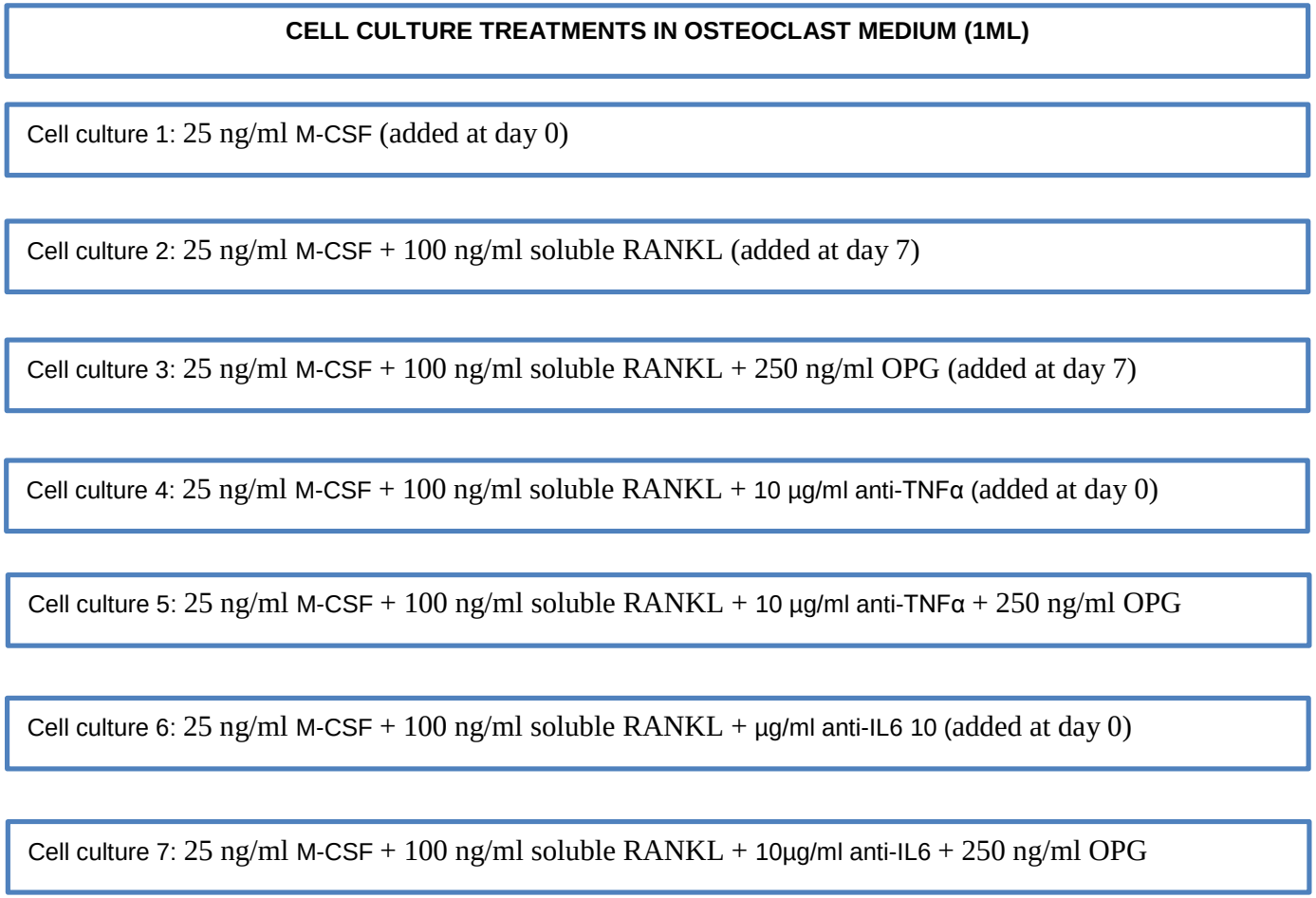

Figure 2-2 Cell culture treatments

The appropriate volume of osteoclast culture medium was initially pre-warmed at 37° and then supplemented with the appropriate volume from the stock solutions of the required treatment agents. Example of the preparation of cell culture treatment 2 at day 7 is presented below (2-A)

2-A

$$Cell\ culture\ treatment\ 2\ =$$

$$(25\mu l\ \ MCSF\ + 10\ \mu L\ RANKL\ + 965\ \mu l\ of\ osteoclast\ meduim) x\ Number\ of\ wells$$

Culture medium was refreshed every 3-4 days. Initially, it was aspirated from the well and then 1 ml of fresh culture medium, supplemented with the appropriate cytokines was added to each well from the 24-well plate and 250 µl were added to each well from the 96-well plate. A summary of the cell culture is presented (Figure 2-3).

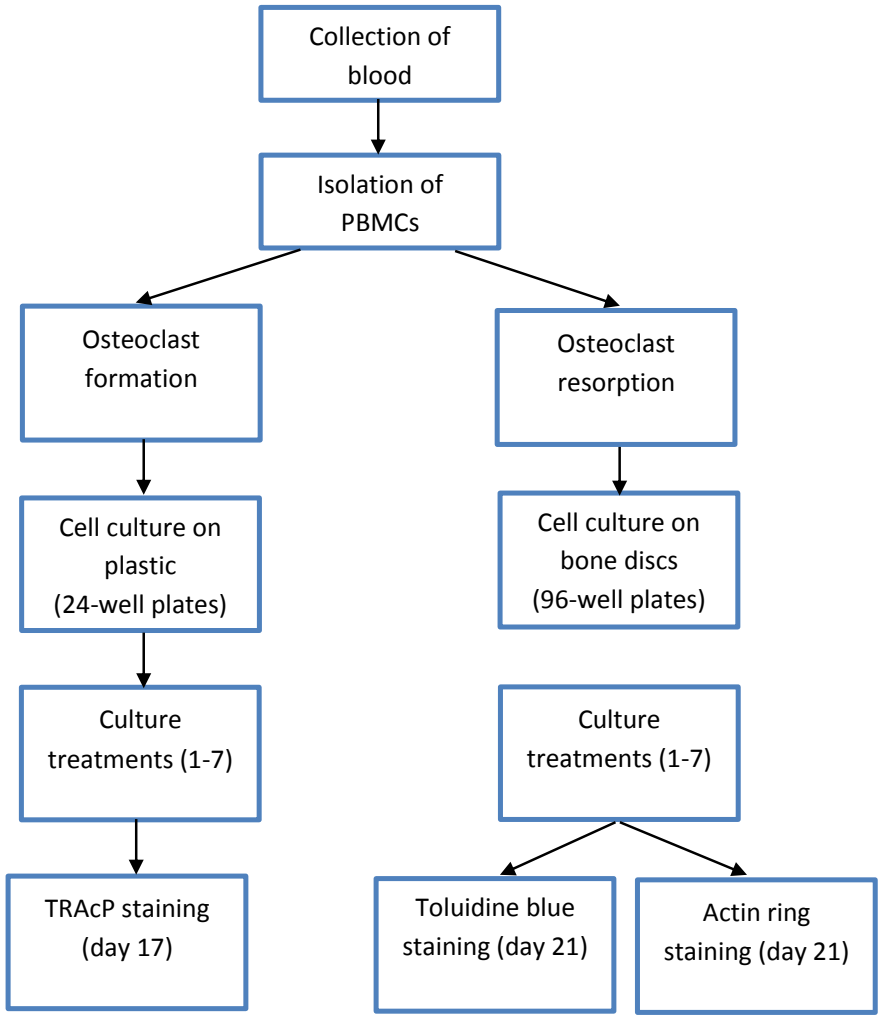

Figure 2-3 Summary of cell culture experiment

2.3.3 Characterisation of osteoclast cultures

Osteoclast formation was assessed at day 17 after tartrate-resistant acid phosphatase (TRAP) staining of the 24-wells. The functional ability of newly-generated osteoclasts to carry out resorption was assessed on bovine bone discs assessed at day 21. Resorption pits were identified after toluidine blue staining of bovine bone discs. Actin ring formation on bovine bone discs, as a marker of actively resorbing osteoclasts, was identified after FitC- phalloidin staining.

2.3.3.1 TRAP staining

List of chemicals and preparation of the solutions required for TRAP staining is provided (Table 2-2). Initially, cells were washed with PBS and fixed with 10% formalin for 10 minutes. The fixative was discarded and the cells were washed three times with PBS. The staining solution was added (solution A: solution B - in ratio 1:1) and plates were incubated in the dark at 37°C for 2±0.5 hours. The principle of TRAP staining is based on the simultaneous coupling reaction using naphtol AS-BI-phosphate as substrate and fast violet B as the diazonium salt which results in the formation of insoluble deposits. After 1.5 hours of incubation, the staining was checked every 30 minutes and once all wells showed evidence of purple colouring, the staining solution was removed and each well was washed three times with PBS, followed by 30 minutes incubation in 0.4% sodium fluoride solution. Finally, plates were washed twice with PBS and once with distilled water and were left to dry at RT overnight. Stained plates were kept at 4°C in the dark for long-term storage and further investigation.

Table 2-2 TRAP staining assay consumables

Consumables	Manufacturer	Preparation	Storage
Acetic acid	Sigma- Aldrich Ltd, Poole, UK	0.2 M Acetic acid solution =0.353 ml of acetic acid + 30 ml of PBS	RT
Sodium acetate	Sigma- Aldrich Ltd, Poole, UK	0.2 M Sodium acetate solution = 1.64g of sodium acetate + 40ml of PBS	RT
Tartaric acid	Sigma- Aldrich Ltd, Poole, UK	Used to prepare acetate-tartrate buffer	RT
Naphtol AS-BI Phosphate	Sigma- Aldrich Ltd, Poole, UK	Used in solution A	-20°C
Fast violet B salt	Sigma- Aldrich Ltd, Poole, UK	Used in solution B	4°C
Dimethyl sulfoxide (DMSO)	Sigma- Aldrich Ltd, Poole, UK	Ready to use	RT
Sodium fluoride	Sigma- Aldrich Ltd, Poole, UK	Sodium fluoride solution = 0.4g sodium fluoride +100 ml PBS	RT
Acetate-tartrate buffer		14.8 ml Acetic acid solution + 35.2 ml Sodium acetate solution + 50 ml Distilled water Add 0.194g of tartaric acid to every 100 ml of buffer and adjust to pH 5.	RT
Solution A		10 mg naphtol AS-BI phosphate + 0.5 ml DMSO + 15ml acetate-tartrate buffer (pH 5); aliquot and freeze	-20°C
Solution B		20 mg fast violet B + 0.5ml DMSO + 15 ml acetate tartrate buffer (pH 5); aliquot and freeze	-20°C

Osteoclast formation was assessed using light microscopy. TRAP-positive cells with more than 3 nuclei were identified as osteoclasts (Figure 2-4A). The total number of cells which was counted in four fields at X40 times magnification was recorded for each well (Figure 2-4B). Cells were cultured in duplicate and the mean number of cells per cell culture condition was calculated and was taken for the purpose of the analysis.

(A)

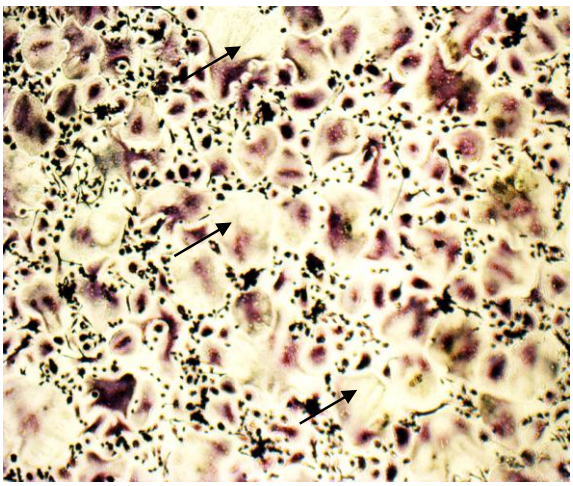

(B)

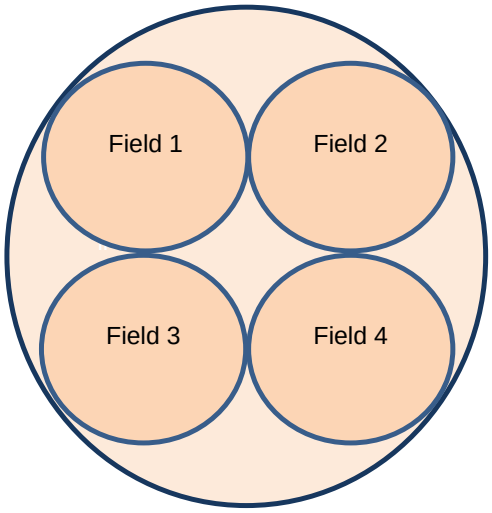

Figure 2-4 Cell counting after TRAP staining
Newly-formed TRAP-positive multi-nucleated cells in M-CSF+RANKL-treated cultures as viewed under light microscopy; The image was taken at X100 magnification; The black arrows denote some of the TRAP-positive multi-nucleated cells (A); Schematic presentation of a 24-well (B); TRAP-positive cells with more than three nuclei were counted in fields 1 to 4 and recorded for each well. All experiments were carried out in duplicate and the mean number of cells per cell culture condition was calculated.

2.3.3.2 Bovine bone disc staining

Bovine bone discs were stained after 21 days of culture. A list of chemicals and the preparation of the solutions required for toluidine blue staining and actin ring formation on bovine bone discs is provided (Table 2-3).

Table 2-3 List of consumables for bovine bone disc staining

Consumables	Manufacturer	Preparation	Storage
Toluidine blue	Sigma- Aldrich Ltd, Poole, UK	1% Toluidine blue solution =1g toluidine blue + 100 ml of distilled water; adjust to pH 5	RT
Ammonium hydroxide	Sigma- Aldrich Ltd, Poole, UK	1 mol Ammonium hydroxide solution = 20 ml of 5mol Ammonium hydroxide solution + 80 ml distilled water)	RT
DPX Mountant for histology	Sigma- Aldrich Ltd, Poole, UK	Ready to use	RT
FITC-Phalloidin -0.1mg	Sigma- Aldrich Ltd, Poole, UK	Inject with a syringe 1ml of DMSO in vial, aliquot and freeze; FITC-Phalloidin staining solution (1:100)= 200µl of FitC-phalloidin in DMSO solution + 20 ml of PBS	-20°C in the dark
Triton X	Sigma- Aldrich Ltd, Poole, UK	10% Triton X solution= 10 ml of Triton X +100 ml distilled water Prior immunofluorescent staining, prepare 0.1% Triton solution for cell permeabilisation	RT
Vectashield Mounting medium with DAPI	Vector Laboratories, Peterborough, UK	Ready to use	4°C in the dark

2.3.3.2.1 Toluidine blue staining:

The bovine bone discs were transferred in 24-well plates, in wells containing one molar ammonium hydroxide solution and were incubated overnight. On the next day, the ammonium hydroxide solution was aspirated and the bone discs were rinsed twice with distilled water. To remove any adherent cells, each well which was containing bone discs in distilled water, was sonicated (Branson Sonifier 150) three times for 15 seconds. Bone slices were incubated with 1% toluidine blue solution for 5 minutes. Excess staining was removed by washing with distilled water. After air-drying, the bovine bone discs were mounted onto a glass slide using DPX mountant for histology. A drop of the mounting agent was dispensed on the glass slide and each disc was mounted with the F-side facing the glass side. The glue was left to dry for 2 hours. All glass slides were clearly marked and stored for further examination.

Resorption pits were identified by light microscopy (Optem, USA). Images were captured using Motic Image Software and saved in JPEG format (Figure 2-5).

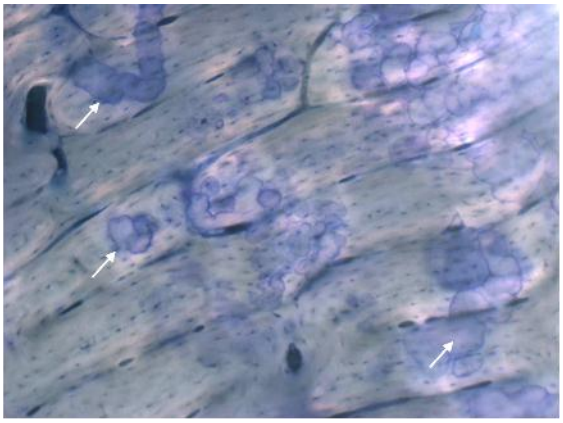

Figure 2-5 Resorption pits on bovine bone discs after toluidine blue staining.
The white arrows denote some of the pits. The process of resorption exposes collagen fibres in the bone, and these fibres are revealed after toluidine blue staining

The captured images were analysed with Adobe Photoshop CS software (Figure 2-6). The resorption pits stained with toluidine blue were identified (Figure 2-6A); (Image

1) and were highlighted with the black brush (Figure 2-6B) and the processed image (Image 2) was saved in a JPEG format. Image 1 was reopened and the total disc surface was changed to white and the border was changed to black (Figure 2-6C) and the processed image (image 3) was saved in a JPEG format.

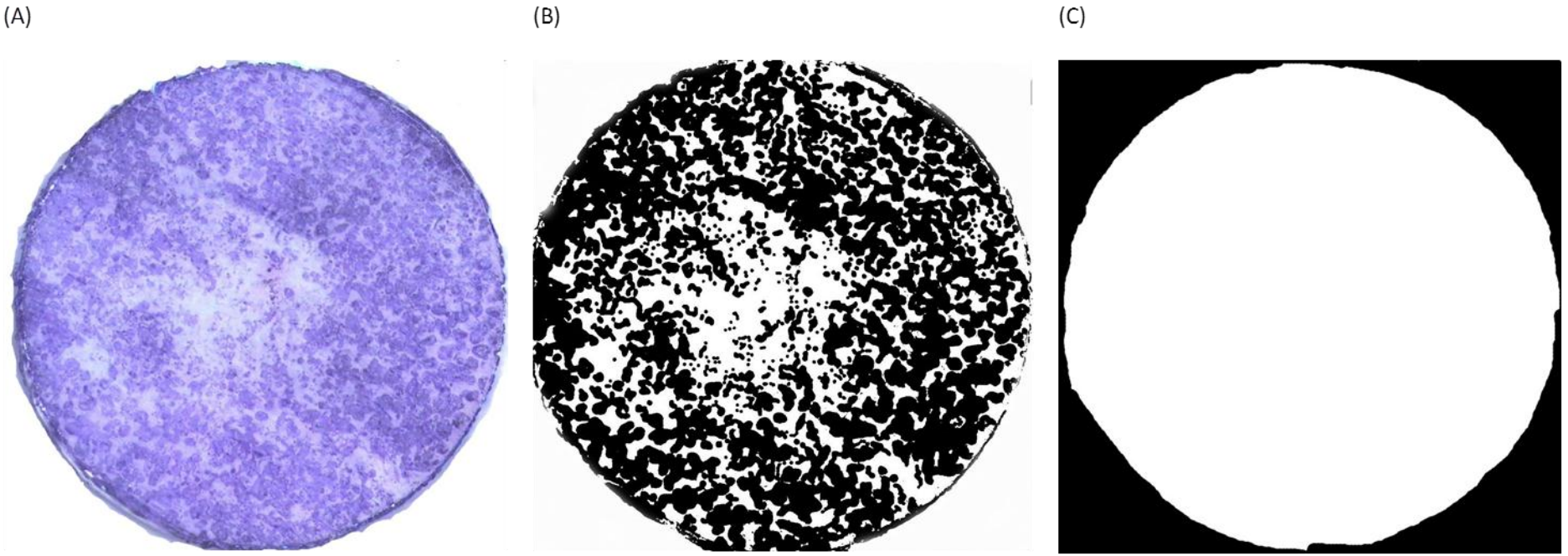

Figure 2-6 Image analysis with Adobe Photoshop CS
Image of a bovine bone disc after toluidine blue staining, (image 1); The resorption pits are stained in blue (A); The pits were highlighted with the black brush in Adobe Photoshop, (image 2), (B); The total disc area was highlighted in white, (image 3), (C).

The number of black pixels representing the area of the pits (image 2) and the number of white pixels representing the total disc area (image 3) were calculated using Image J software. The extent of eroded surface on each bovine bone disc was calculated as a percentage (2-B).

2-B Area of resorption

$$Area\ of\ resorption\ on\ bovine\ bone\ discs\ (\%) = \frac{Number\ of\ black\ pixels}{Number\ of\ white\ pixels} x\ 100$$

Each experiment was carried out in duplicate and the mean area of resorption was calculated for each culture treatment/ subject.

2.3.3.2.2 Immuno-fluorescent staining for actin ring formation on bovine bone discs

Additional bovine bone discs were stained with FitC-phalloidin and mounted with vectashield mounting medium with DAPI for the assessment of actin ring formation, a marker of actively resorbing osteoclasts.

After 21 days in culture, bovine bone discs were rinsed with PBS and fixed with 10% formalin for 10 minutes at room temperature. After fixation, bone discs were washed three times with PBS and cells were permeabilised with 0.1% Triton-X solution for 15 minutes. The discs were washed three times with PBS and were incubated in FitC-phalloidin for 1 hour at room temperature in the dark. After the incubation, discs were washed three times with PBS and mounted on glass slides. To mount each bone disc on a glass slide, initially a drop of Vectashield mounting medium for fluorescence with 4', 6'-Diamidino-2-Pheylindoledihydrochoride (DAPI) was dispensed on the slide with the supplied drop dispenser pipet (each drop was approximately 25 µl). Then the bone disc was immersed into the mounting medium and a glass coverslip was placed on

the top of the disc. The disc was immersed with the F-side facing the glass slide and cells facing the glass coverslip. All slides were wrapped in foil to protect the discs from photobleaching and were kept at 4°C. Actin ring formation was assessed after imaging with immunofluorescence microscope (Olympus IX81). Bone discs were examined in the dark at X100 magnification for the presence of actin ring positive multi-nucleated cells. A merged image from both FITC and DAPI channels was captured using Volocity (Perkin Elmer, USA) software. The protocol to capture the merged image from both channels was devised by Daniel Soong. Images were exported from Volocity as TIFF files for further analysis (Figure 2-7).

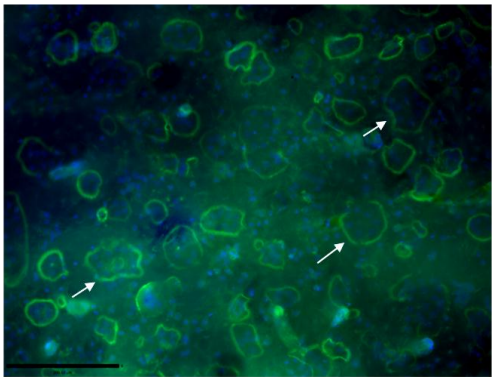

Figure 2-7 Immunofluorescent staining of bovine bone disc for the detection of actin ring positive multi-nucleated cells
Actin filaments stained in green (FITC channel); nuclei stained in blue (DAPI channel). Scale bar - 200µm. White arrows denote some of the multi-nucleated actin ring positive cells on a bone disc in M-CSF+ RANKL-treated culture

2.3.4 Dose adjustments of cytokines

For all *in vitro* experiments, cytokines were used in doses which were previously shown to be sufficient to maintain proliferation and survival of monocytes (25 ng/ ml M-CSF), induce osteoclastogenesis (100 ng/ml RANKL), inhibit RANK-RANKL interaction (250 ng/ml OPG) and inhibit IL-6 modulation on osteoclastic precursors (10 µg/ml anti-IL-6), (Mabilleau, Petrova et al. 2008), (Axmann, Bohm et al. 2009).

To determine the inhibitory dose of anti-TNF-α on osteoclastic resorption, a pilot experiment was set up in 3 Charcot patients and 3 healthy control subjects and the dose response to anti-TNF-α treatment (10 µl/ml and 20 µl/ml anti-TNF-α respectively) on osteoclast formation on cell culture plates and bone resorption on bovine bone discs was assessed. It has been shown that TNF-α targets two membrane receptors on osteoclastic precursors- TNF-α receptor 1 (p55r) and 2 (p75r). The osteoclastogenic properties of TNF-α are mediated by p55r whereas p75 is anti-osteoclastogenic (Teitelbaum 2007).

The addition of 10µl/ml and 20µl/ml of anti-TNF-α to M-CSF+RANKL treatment did not lead to a significant difference in the mean number of TRAP-positive multi-nucleated cells in Charcot patients and healthy control subjects (Table 2-4).

Table 2-4 Number of TRAP-positive multi-nucleated cells in M-CSF+RANKL-treated cultures and after the addition of 10 and 20 µl/ml anti-TNF-α respectively in Charcot patients and healthy control subjects

Number of TRAP-positive multi-nucleated cells	M-CSF+RANKL	M-CSF+RANKL+ anti-TNF-α (10µl/ml)	M-CSF+RANKL+ anti-TNF-α (20µl/ml)	p-value
Charcot (n=3)	185±53	158±43	182±46	>0.05
Control (n=3)	95±16	100±14	114±19	>0.05

Data expressed as mean±SEM; Data assessed with ANOVA-test. Levels of significance are presented in the table.
Non-significant difference in the mean number of TRAP-positive multi-nucleated cells in M-CSF+RANKL-treated cultures compared with cultures supplemented with 10 and 20 µl/ml anti-TNF-α respectively in Charcot patients (p>0.05) and healthy control subjects (p>0.05).

In contrast to osteoclast formation, the addition of anti-TNF-α led to a significant dose-dependent reduction of the area of bone resorption on bovine bone discs only in Charcot patients, but not in healthy control subjects, in whom the area of bone resorption on bovine bone discs remained unchanged (Table 2-5).

Table 2-5 Area of resorption on bovine bone discs in M-CSF+RANKL-treated cultures and after the addition of 10 and 20 µl/ml anti-TNF-α respectively in Charcot patients and healthy control subjects.

Area of resorption on bovine bone discs (%)	M-CSF+RANKL	M-CSF+RANKL+ anti-TNF-α (10µl/ml)	M-CSF+RANKL+ anti-TNF-α (20µl/ml)	p-value
Charcot (n=3)	47±5.7	33±5.1	23±9.9	<0.05
Control (n=3)	20±4.1	15±3.2	18±2.7	>0.05

Data expressed as mean±SEM; Data assessed with ANOVA-test. Levels of significance are presented in the table.
Significant reduction in the area of resorption on bovine bone discs as assessed by image analysis in M-CSF+RANKL-treated cultures compared with cultures supplemented with 10 and 20 µl/ml anti-TNF-α respectively in Charcot patients ($p<0.05$) but not in healthy control subjects ($p>0.05$)

In Charcot patients, paired t-test showed that the area of bone resorption was significantly greater in M-CSF+RANKL-treated cultures compared with cultures treated with M-CSF+RANKL+anti-TNF-α (10µl/ml), ($p<0.05$) and also with cultures treated with M-CSF+RANKL+anti-TNF-α (20µl/ml), ($p<0.05$), (Table 2-6). Although the area of bone resorption after the addition of 20µl/ml of anti-TNF-α was smaller compared to cultures treated with 10µl/ml of anti-TNF-α, this difference was not significant (Table 2-6).

Table 2-6 Comparison of the area of bone resorption in M-CSF+RANKL-treated cultures and after the addition of 10 and 20 µl/ml anti-TNF-α respectively in Charcot patients and healthy control subjects.

	P1-value Charcot	P2-value Control
M-CSF+RANKL vs M-CSF+RANKL+anti-TNF-α (10µl/ml)	<0.05	>0.05
M-CSF+RANKL vs M-CSF+RANKL+anti-TNF-α (20µl/ml)	<0.05	>0.05
M-CSF+RANKL+anti-TNF-α (10µl/ml) vs M-CSF+RANKL +anti-TNF-α (20µl/ml)	>0.05	>0.05

Data assessed with paired t-test. Levels of significance are presented; P1-values indicate differences between the different culture treatments in Charcot patients; P2-values indicate differences between the different culture treatments in healthy control subjects; Significant reduction in the area of resorption on bovine bone discs between M-CSF+RANKL- and M-CSF+RANKL+anti-TNF-α-(10µl/ml)-treated cultures and also between M-CSF+RANKL- and M-CSF+RANKL+anti-TNF-α (20µl/ml)- treated cultures in Charcot patients (P1<0.05 for both pairwise comparisons) but not in healthy control subjects (P2>0.05 for both pairwise comparisons). Non-significant difference in the area of resorption on bovine bone discs in M-CSF+RANKL+anti-TNF-α-(10µl/ml) and M-CSF+RANKL- and M-CSF+RANKL+anti-TNF-α-(20µl/ml)-treated cultures in Charcot patients (P1>0.05) and healthy control subjects (P2>0.05)

This experiment demonstrated that 10 µl/ml anti-TNF-α is sufficient to block TNF-α mediated osteoclastic activity in Charcot patients. As a result of this preliminary observation, all experiments were carried out with the standard inhibitory dose of anti-TNF-α (10 µl/ml), in agreement with previous studies, (Cope, Londei et al. 1994).

2.3.5 Detection of C-telopeptide fragments of collagen type I in culture supernatant

During bone resorption *in vitro*, C-telopeptide degradation products from type I collagen are released in culture supernatant and could be detected with an enzyme-linked immunosorbent assay (ELISA), (Immunodiagnostics System, Boldon, UK.

CrossLaps enzyme-immunoassay was used to detect C-telopeptide fragments of collagen type I generated during osteoclastic bone resorption *in vitro*. The inter-assay

coefficient of variation is 6.3% and the intra-assay coefficient of variation is 3.6% with a measuring range between 0.44 nM and 112.7 nM crosslaps.

For this experiment, cell culture supernatants from various culture treatments were collected at day 21 and stored at -80°C until analysed. The assay was carried out following the manufacturer's instructions.

Culture supernatants and assay controls (cell culture medium control, cell control and bone slice control) were thawed. All solutions were equilibrated at room temperature. The standards were prepared in the recommended solutions. The antibody solution was prepared by mixing biotinylated antibody, peroxidase conjugated antibody and incubation buffer in 1:1:100. All specimens were initially pre-diluted with the standard diluent prior testing in 1:5 and then 50µl of the diluted samples was pipetted in the microplate, followed by the addition of 150 µl of the antibody solution. The plate was sealed and incubated for 120 minutes at room temperature on a mixing apparatus (300 rpm). After five washing cycles with diluted washing buffer (washing buffer in distilled water 1:50), the chromogenic substrate solution was pipetted in each well and the plate was sealed and incubated for 15 minutes in the dark at room temperature on the mixing apparatus (300 rpm). The colour reaction was stopped with sulphuric acid and the absorbance was measured within 2 hours at 450 nm using TECAN Genios Pro Multifunction Microplate Reader. The results were calculated using Multi Calc 2000 software in collaboration with Tracy Dew from the Department of Biochemistry at King's College Hospital. The programme was used to draw the best fitting standard curve and to determine the crosslaps concentration of the control sample, culture medium control, cell control and bone slice control and each of the test specimens by interpolation on the curve. To calculate the true concentration, all values were multiplied by 5 to correct for the pre-dilution of all controls and samples (1 in 5). The results for the bone cell culture supernatants were corrected for the medium, cell and bone slice background effect. All samples were analysed in triplicates and the mean value was calculated for the purpose of the analysis.

2.4 Conclusion

I successfully set up the traditional osteoclast resorption assay in Professor Shanahan's laboratory and I employed this technique to study osteoclast formation and resorption in patients with acute Charcot osteoarthropathy, diabetic patients and healthy control subjects.

This technique was used for the first time in the field of Charcot osteoarthropathy and in a pilot study we have confirmed its usefulness as a robust technique to study the process of osteoclast formation and resorption in this devastating condition (Mabilleau, Petrova et al. 2008).

Chapter 3 Surface profilometry as a novel method to measure erosion profile of resorbed bovine bone discs

3.1 Introduction

Although the assay to generate functional human osteoclasts is widely used to assess osteoclastic activity, measurement of the percentage area which is resorbed by image analysis has its limitations, as this present technique does not provide information on depth and shape of erosions. Thus measurement of the erosion profile could be a useful technique to describe the resorptive capacity of newly formed osteoclasts *in vitro* as it may provide more information on how osteoclasts exert their resorbing activity. To address this need, I devised a novel method to measure the surface roughness of resorbed bovine bone discs. This chapter describes the use of a Dektak 150 Surface Profiler (Veeco, New York, USA) in the assessment of resorbed bovine discs by newly generated osteoclasts. The general principles of contact surface profilometry and the devised methodology used to characterise the resorption pits on bovine bone discs generated under various cell culture treatments are discussed. This technique was developed in collaboration with Dr Peter Petrov from Department of Materials, Imperial College London with whom I optimised the sample measurement technique. All surface profile measurements were carried out by Nina Petrova in the Thin Film Technology Laboratory, Imperial College London.

3.2 Surface profilometry

3.2.1 Main types and application

Profilometry is a technique which was developed to measure the surface's profile in order to quantify its roughness. It measures surface variations as a function of

position. There are two main types: non-contact optic profilometry which uses light and contact profilometry which uses stylus based technology. Both modalities have a wide range of applications and are commonly used in general and materials sciences.

Recently, an optical surface profiler has been applied to measure the eroded amount of bone on dentine slices by newly generated osteoclasts *in vitro* (Pascaretti-Grizon, Mabilleau et al. 2011). This non-contact method used light interferometry to produce three-dimensional (3D) topography maps of the sample surface. However, this technique had its limitation as the 3D reconstruction images did not provide a true representation of the resorption lacuna which made it difficult to compare images between bone slices and culture treatments.

To overcome this limitation, I hypothesised that contact profilometry could provide useful information on the shape and size of the eroded surface of bone slices. This technique uses a stylus which is dragged across a pre-set length of surface for a specified distance and contact force. In general, a profilometer can measure small vertical surface variations ranging in height from 10 nanometres to 1 millimetre. The height position of the stylus generates an analogue signal. This signal is converted into a digital signal, which is stored, analysed and displayed graphically. To investigate the usefulness of this technique in the assessment of resorbed bovine bone discs by newly generated osteoclasts, I measured the surface profile of discs with a Dektak 150 Surface Profiler (Veeco, New York, USA).

3.2.2 Dektak 150 Surface Profiler

Dektak 150 Surface Profiler is a two-dimensional (2D) contact surface profiler. It is fitted with a stylus which has a radius of 2.5 µm. The lateral resolution is limited by the tip shape. The display range of the data extends from 20 nm to 65.5 µm with a vertical resolution of approximately 0.5 nm. The manually controlled XY stage allows the correct positioning of the sample under the stylus. The stylus is then lowered close to the

sample. The sample surface can be examined with the camera integrated with the profiler (Figure 3-1).

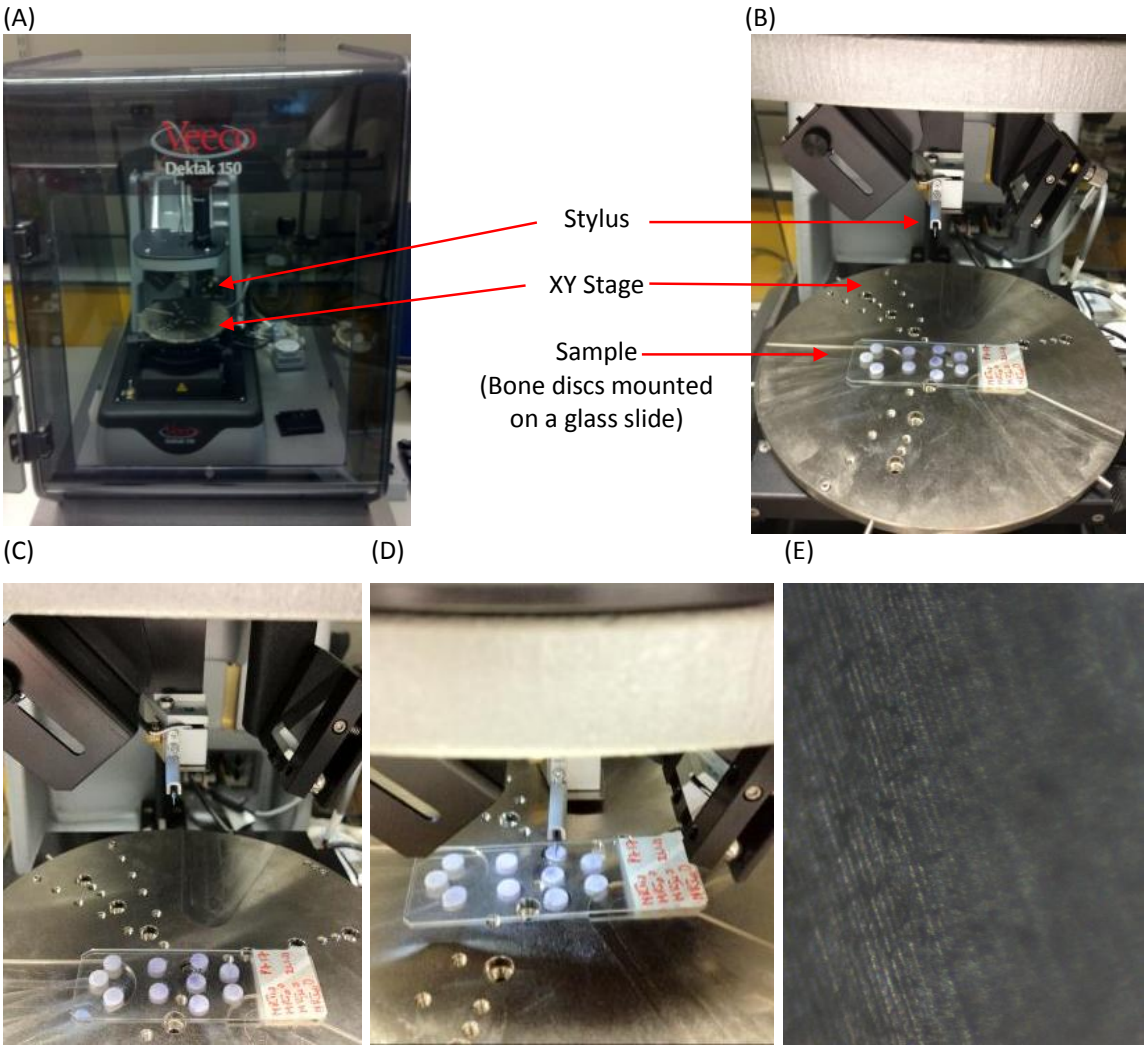

Figure 3-1 Dektak 150 Surface Profiler
The red arrows denote the stylus (A, B), the XY-stage (A, B) and the sample (B). Prior to the surface measurement, the sample is positioned under the lifted stylus (C). The stylus is then lowered close to the sample (D). The motorised XY-stage is used for fine adjustment of the sample position. The sample surface can be visualised with the integrated camera. Typical appearance of the surface of a non-resorbed bone disc observed with the camera of the profiler (E)

Prior to each measurement, the scan parameters were programmed. The stylus is then dragged along the surface of the sample. After the completion of each scan, the measured surface profile is graphically presented. The software allows the levelling of

the data to compensate for the tilt of the sample. Data is recorded in excel file format which allows the reconstruction of the graphs and comparisons between measurements and conditions.

3.3 Roughness of bovine bone discs measured by Dektak 150 Surface Profiler

To assess the roughness of the bovine bone discs, prior to being used in cell culture, the following negative controls were set up.

1. Non-stained air-dried bovine bone discs (Negative control 1)

Bovine bone discs in 70% ethanol were removed from the vial and air dried in a Petri dish in the MSC. One side of the disc was marked with F. Each disc was then mounted with DPX mountant for histology with the F-side facing the glass slide.

2. Toluidine blue stained bovine bone discs (Negative control 2)

Air-dried bovine bone discs, marked with F (as above), were stained with toluidine blue. Initially, bone discs were incubated overnight with 1 molar ammonium hydroxide solution and rinsed twice with distilled water and sonicated for 15 seconds. Bone slices were incubated with 1% toluidine blue solution for 5 minutes. Excess staining was removed by washing with distilled water. After air-drying, the bovine bone discs were mounted onto a glass slide.

3. Bovine bone discs incubated in osteoclast medium and stained with toluidine blue after 21 days in culture (Negative control 3)

Air-dried bovine bone discs, marked with F (as above), were placed in 24 well plates in 1ml osteoclastic culture medium, and supplemented with M-CSF. Discs were incubated for 21 days at 37°C and 5% CO_2. Culture medium was refreshed every 3-4 days. At day 21, bone discs were stained with 1% toluidine blue (as above- negative control 2).

These negative controls were set up to ensure that the various stages of the cell culture protocol (air-drying, incubation, sonication and disc staining) would not affect the roughness of the bovine bone discs and not lead to bending or damaging the discs. For each experiment, 3 to 4 discs were set up and mounted on glass slide with DPX (Distrene, Plasticiser, Xylene) histology mountant.

Initially, the surface of each disc was examined with the integrated camera (Figure 3-2).

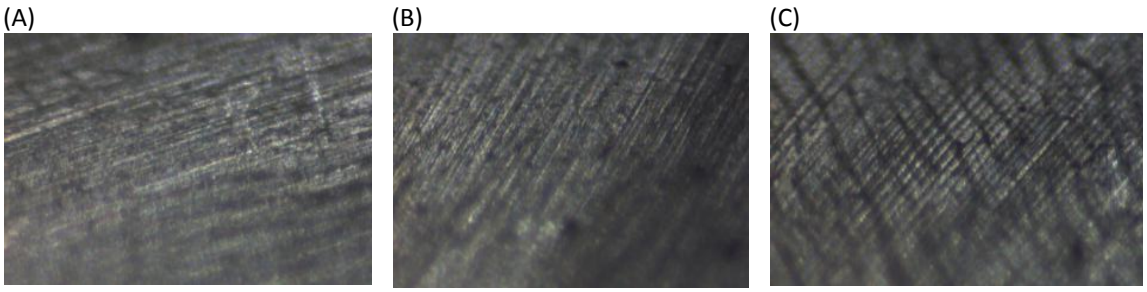

Figure 3-2 Typical appearance of the surface of a bovine bone disc as viewed with the integrated camera of the Dektak 150 Surface Profiler
(A) Non-stained air-dried bone disc (negative control 1); (B) Toluidine blue stained bovine bone disc (negative control 2); (C) Bovine bone disc incubated in osteoclast medium and stained with toluidine blue after 21 days in culture (negative control 3). All images were taken with the integrated camera of the profiler

The surface appearance was similar between the three types of negative controls (Figure 3-2). To assess the roughness of the surface, five scans per bone disc/ condition were carried out. Scan parameters are shown on the table below (Table 3-1).

Table 3-1 Dektak Surface Profile scan settings

Scan Parameters for surface profilometry	
Stylus Radius	2.5 µm
Length	1000.0 µm
Duration	60 sec
Force	3.00 mg
Resolution	0.056 µm/sample
Measurement Range	65.5 µm
Profile	Hills and Valleys

After each measurement, the Veeco software reproduced the surface step heights which were measured by the stylus and an example of the graphical representation of the measured surface profile of a bovine bone disc (negative control 1) is presented (Figure 3-3A). To compensate for the tilt of the mounted disc, the software was used to level the measurement (Figure 3-3B). The data was recorded in an excel format file for further analysis (Figure 3-3C). It was noted that the disc surface was smooth with an average roughness of ±1 µm, after the conversion of the Y-axis values from a nanometre to a micrometre scale (Figure 3-3D).

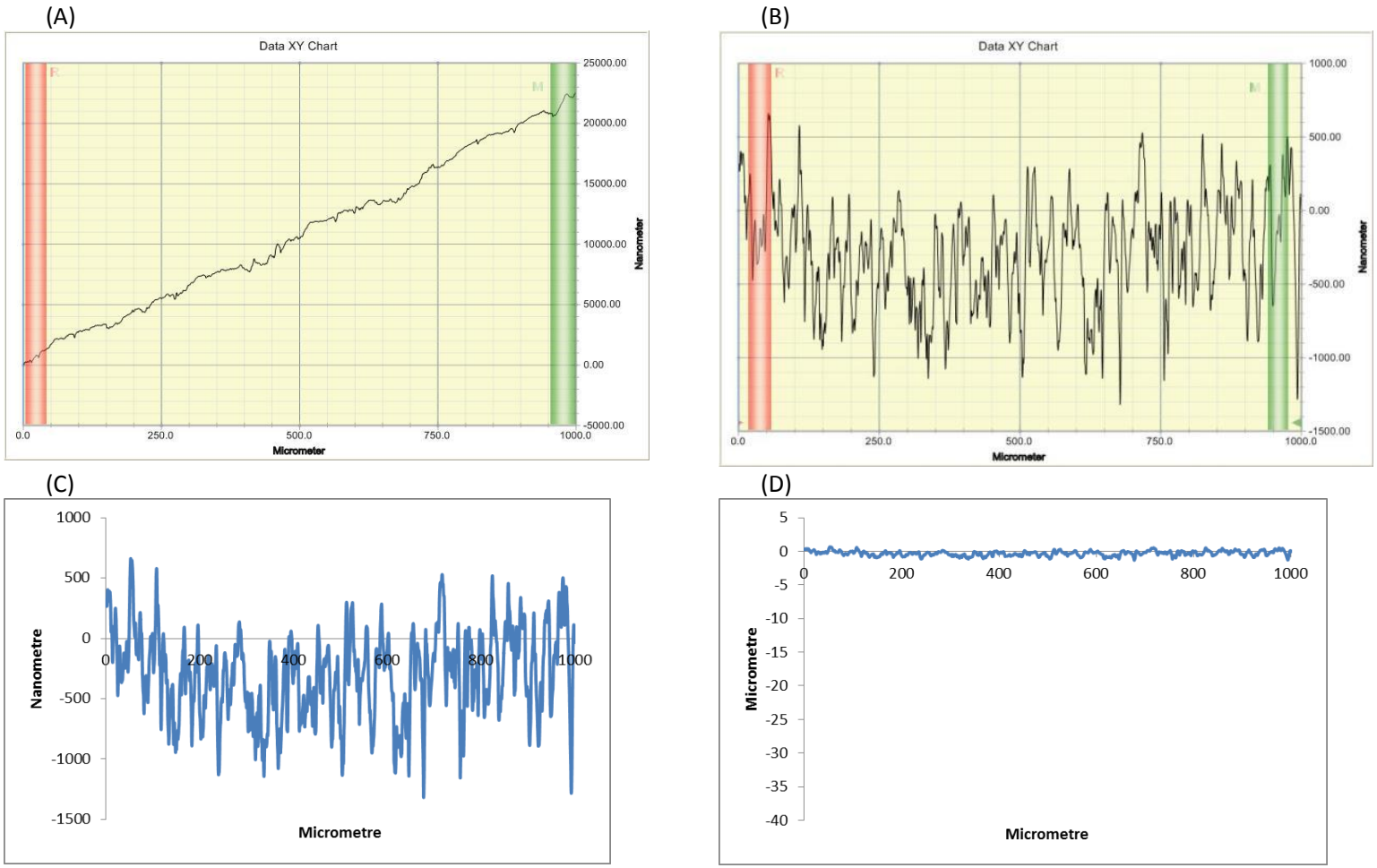

Figure 3-3 Graphical representation of the surface profile of a bone disc measured with Dektak 150 Surface Profiler
Surface profile of the bovine bone disc (negative control 1) before levelling (A) and after levelling (B) reproduced with the Veeco software. The same surface profile reconstructed with Excel program before (C) and after (D) conversion of the Y –axis values from a nanometre scale to a micrometre scale.

A typical example of the surface profile measurements of three non-stained air-dried bovine bone discs (negative control 1) is presented (Figure 3-4A). There was no difference in the surface profile of the three bovine bone discs and the average roughness of their surface was ± 1.0 µm (Figure 3-4B).

(A) (B)

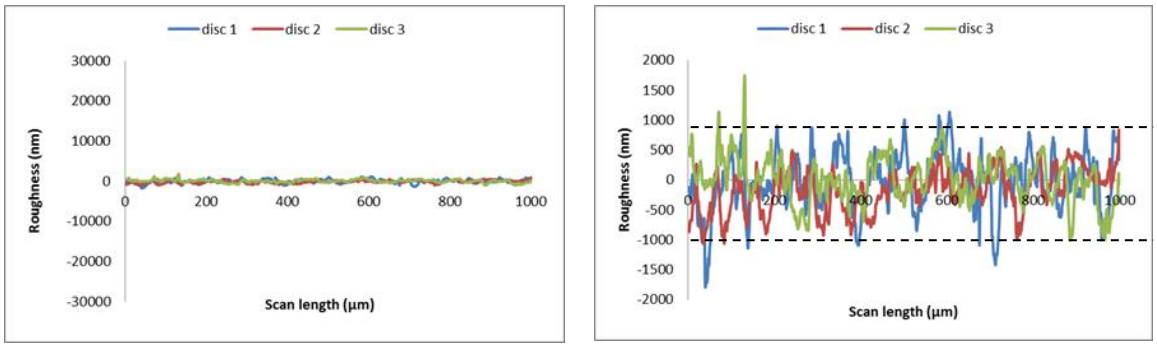

Figure 3-4 Surface profile of non-stained air-dried bovine bone discs
(A) Comparison of the surface profiles of bone discs 1, 2 and 3 (negative control 1).
(B) The graph shows that the average surface roughness of the three discs was ±1000 nm (± 1µm)

Moreover, there was no difference in the surface roughness of the three different types of controls (non-stained air-dried bovine discs; toluidine blue stained bovine bone discs and bovine bone discs incubated in osteoclast medium and stained with toluidine blue). The average surface roughness for all types of negative controls was ±1 µm.

These observations indicated that the surface of the bovine bone discs was smooth and was not affected by the various stages of cell culture and staining protocol. These preliminary observations confirmed my hypothesis that the contact surface profilometry with Dektak 150 Surface Profiler could be a useful tool in the assessment of surface profile of resorbed bone discs.

3.4 Surface profile of resorbed bovine bone discs

I then hypothesised that contact surface profilometry with Dektak 150 Surface Profile could detect differences in the erosion patterns of resorbed bone discs under different culture conditions. For this experiment, PBMCs, isolated from a healthy control subject and a Charcot patient, were cultured on bovine bone discs for 21 days following the protocol, described in Chapter 2. Cells were treated with M-CSF (culture 1) and with M-CSF+RANKL (culture 2). These two culture conditions were chosen to assess the roughness of the bovine bone discs in the absence of resorption (M-CSF-treated cultures) and in the presence of resorption (M-CSF + RANKL-treated cultures). Thus culture 1 served as a negative control and culture 2 served as a positive control.

Initially, the surface of each disc was examined with the camera integrated with the profiler (Figure 3-5). The appearance of the surface of the bone discs from culture 1 (M-CSF treatment) in both control subject and Charcot patient was unremarkable (Figure 3-5A and B) and was similar to the appearance of the negative control bovine discs (Figure 3-2). In contrast, the surface of the bone discs from culture 2 (M-CSF+RANKL treatment) showed multiple dark areas of resorbed bone (pits) surrounded by grey areas of unresorbed bone in both control subject and Charcot patient (Figure 3-5 C and D).

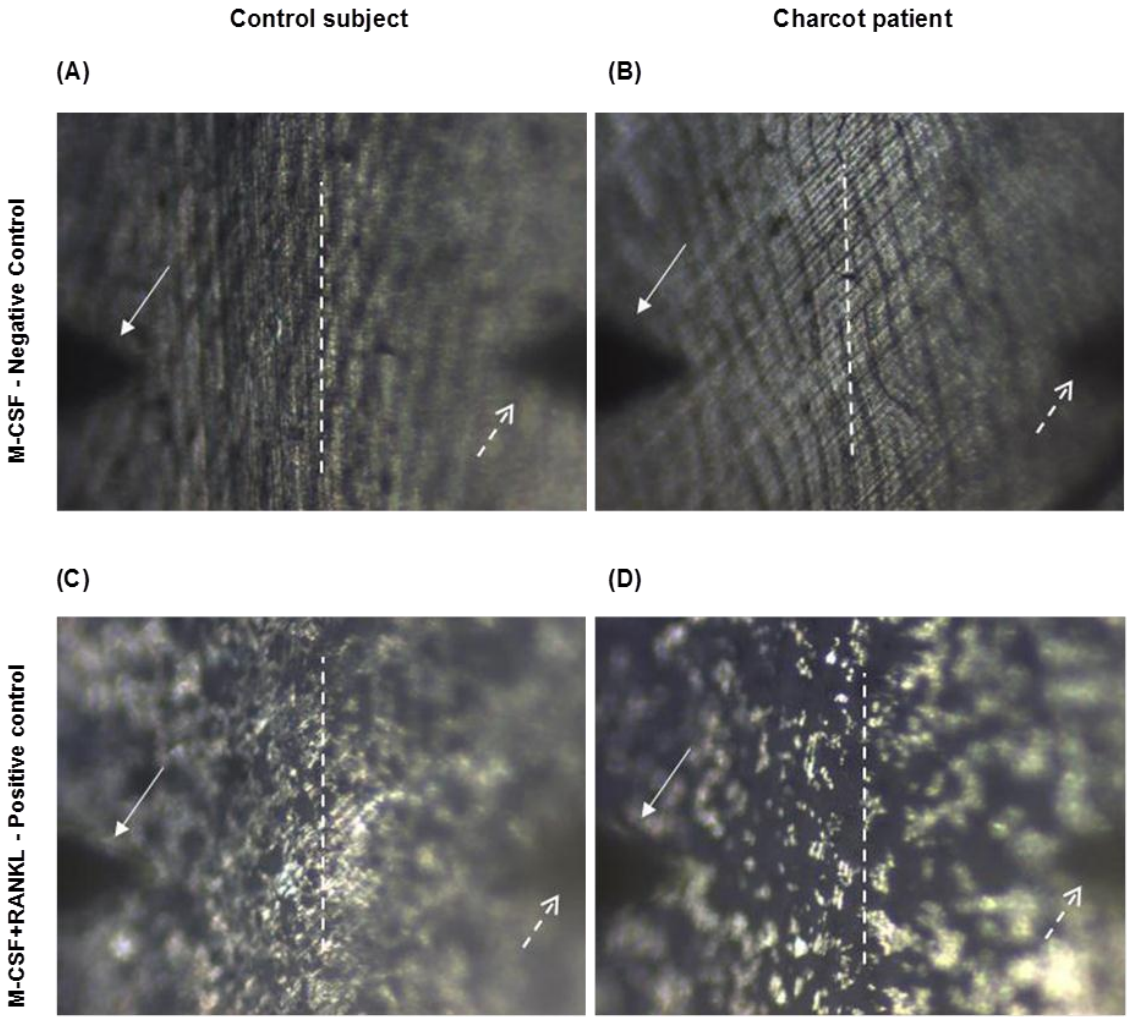

Figure 3-5 Appearance of the bovine bone disc surface as viewed during machine operation.
Images were taken with the integrated camera of the profiler prior to surface measurement. The stylus is lifted above the surface of the sample. (White arrow denotes the stylus; white dash arrow denotes the stylus shadow; white dash line denotes the scan line). The edges of the images appear out of focus due to the acquisition set-up of the camera supplied with a mirror positioned at a 45° angle in respect to the sample plane. Typical appearance of bovine bone discs observed with the integrated camera in M-CSF treated cultures and in M-CSF+RANKL-treated cultures in a control subject (A, C) and in a Charcot patient (B, D) respectively. No erosions were noted in M-CSF-treated cultures in the control subject (A) and the Charcot patient (B) in contrast to numerous erosions in M-CSF+RANKL-treated cultures, as seen in both control subject (C) and Charcot patient (D). Erosions appeared as dark areas surrounded by grey areas of unresorbed bone (C, D).

After each scan, the Veeco software graphically reproduced the measured erosion profile (Figure 3-6). In order to compensate for the tilt of the mounted disc (Figure 3-6A), the profiler software was used to level the measurement and to set the unresorbed bovine surface as the zero level (Figure 3-6B and C).

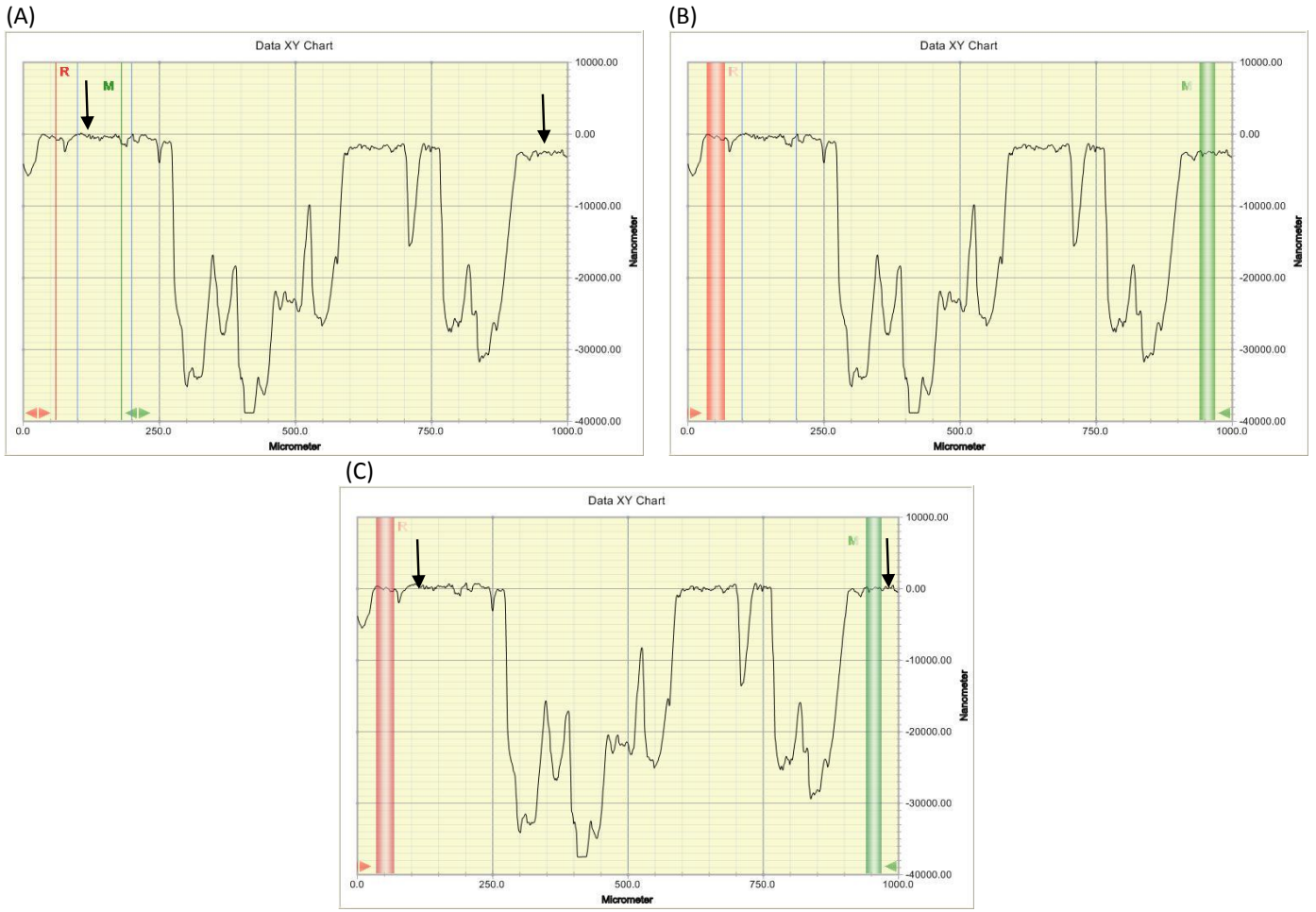

Figure 3-6 Graphical representation of the surface profile of a resorbed bone disc using Veeco software
Cells were isolated from a Charcot patient and treated with M-CSF+RANKL for 21 days. (A) The black arrows denote the tilt of the disc surface (B) The Veeco software was used to correct the tilt of the disc surface (C) The black arrows denote the levelled surface after the correction of the tilt.

Live observation during machine operation showed that the surface profile of bone discs from culture 1 (M-CSF-treated cultures) was unremarkable in both control subject (Figure 3-7A) and Charcot patient (Figure 3-7B). In contrast to the smooth surface of bone discs from culture 1, multiple erosions were detected on the surface of bone discs from culture 2. The stylus followed the pattern of the eroded surface and graphically showed the step heights of the disc surface and typical examples of surface profiles in M-CSF+RANKL-treated cultures in a control subject (Figure 3-7A) and a Charcot patient (Figure 3-7B) are presented.

The erosion profile of the bovine discs from culture 1 (M-CSF-treated culture) in both control subject and Charcot patient appeared as an almost straight line and showed a roughness of ±1 µm (Figure 3-7A and B) similar to the roughness of the negative control bovine discs (Figure 3-4). In contrast, the erosion profile measurement of bovine bone discs from cultures 2 (M-CSF+RANKL-treated cultures) showed multiple pits with various shapes and dimensions in control subject (Figure 3-7A) and Charcot patient (Figure 3-7B).

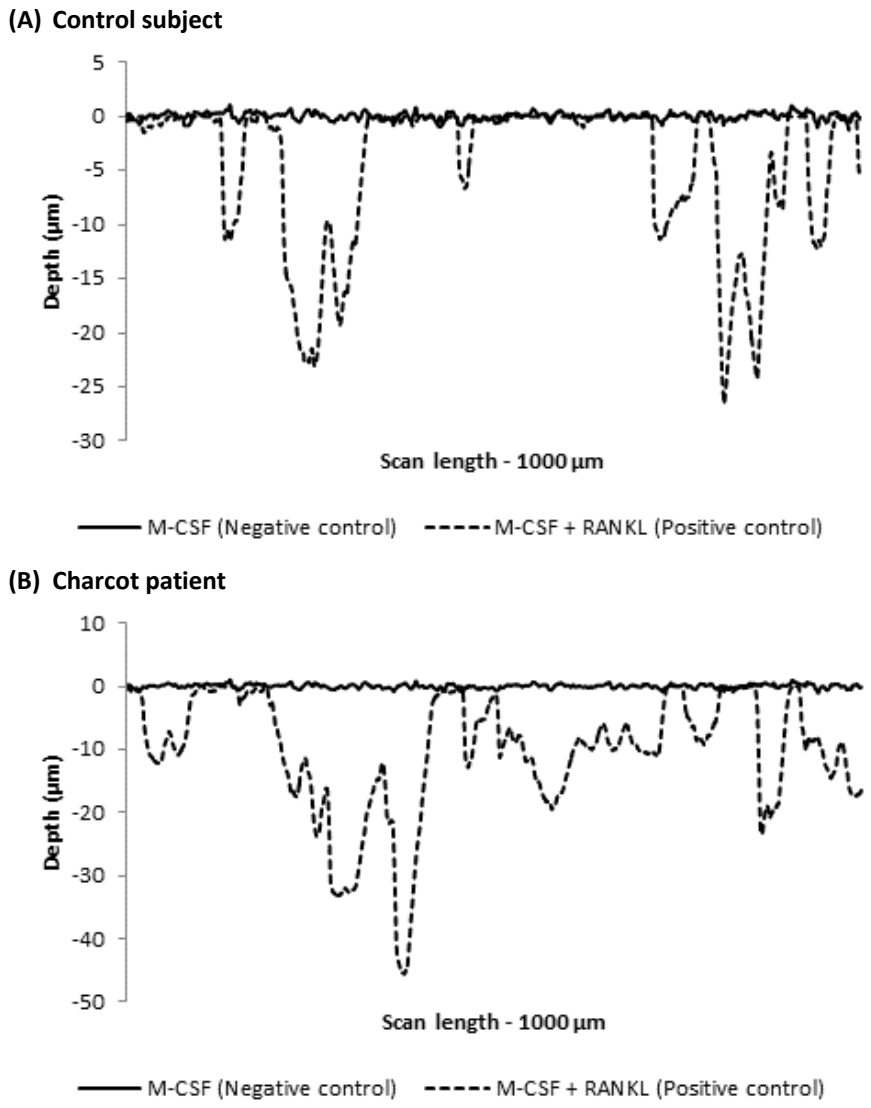

Figure 3-7 Surface profile of resorbed bone discs in a control subject and in a Charcot patient
Erosion profile of bovine bone discs in M-CSF-treated cultures (solid line) and M-CSF+RANKL-treated cultures (dash line) in a control subject (A) and a Charcot patient (B) after surface profilomery.

In order to set up the unresorbed bone at the zero level, the starting point of each measurement was pre-set away from a randomly selected eroded area. To facilitate the graph analysis, (Figure 3-8A), all Y-axis values which were above 0 were changed to 0 for the purpose of the analysis, (Figure 3-8B).

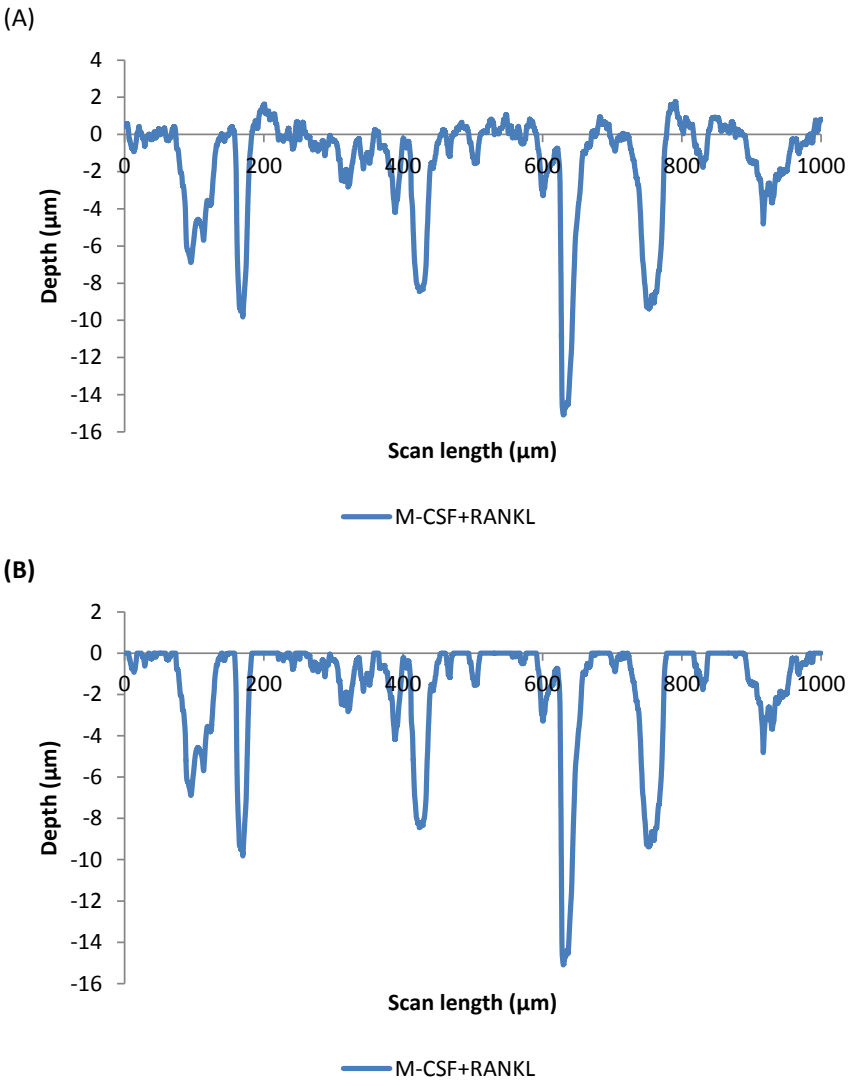

Figure 3-8 Graphical representation of the surface profile of bone disc using Excel software
(A) The graph has been reconstructed with excel.
(B) The same graph after correction of the Y-axis values (Y-axis values above 0 were changed to 0).

Each surface profile measurement had a unique graphical presentation. To analyse the graphs so as to allow comparisons, the area of resorption under the surface and pit morphology were quantitated.

3.4.1 Area of resorption under the surface

The area of resorption under the surface was measured using Origin Pro 8.6 software. The Y-axis values were converted from a nanometre to a micrometre scale. (The Y-axis values were divided by 1000). The graphs were then reconstructed with Origin Pro 8.6 software (Figure 3-9A) and the data was integrated to calculate the resorbed area under surface (μm^2), (Figure 3-9B).

(A)

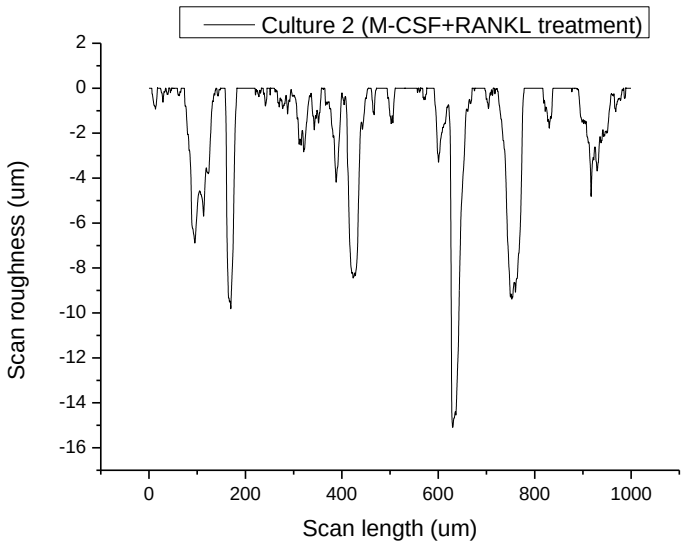

(B)

Results log

x1 = 0

x2 = 999.9

i1 = 1

i2 = 18000

AREA = -1619.6738205

y0 = -15.09297

x0 = 629.9

dx = 603.38416279856

Figure 3-9 Graphical representation of the surface profile of bone disc using Origin software
(A) The graph was integrated
(B) Results' output

The output was multiplied by (-1) to change the sign from a negative to a positive value, as shown on the equation below, (3-A).

3-A

$$\boldsymbol{Area} = (\mathbf{-1619.6738205}) \times (\mathbf{-1})$$

The calculated area was presented as a product (3-B).

3-B

$$Area = 1.6 \times 10^3 \mu m^2$$

3.4.2 Pit morphology

The reconstruction of the measured surface profile with the excel software showed that the pits can be classified into three main categories according to their shape. The following classification was devised.

- Uni-dented pits: defined as erosion with one dent starting from and finishing at the level of the unresorbed surface
- Bi-dented pits: defined as an erosion with two clearly defined dents starting from and finishing at the level of the unresorbed surface
- Multi-dented pits: defined as erosion with three or more clearly defined dents starting from and finishing at the level of the unresorbed surface.

The excel software also allowed the precise measurement of the pit dimensions. The following parameters were measured for each pit:

- Width at the surface (μm)- the distance between the beginning and the end of each pit measured at the surface level
- Full-Width Half-Maximum (FWHM), where the width was measured at the half of the maximum depth.
- Maximum depth (μm) – the distance from the surface level to the maximum depth of the uni-dented pit; the distance from the surface level to the maximum depth of the deeper or the deepest dent of the bi-dented or multi-dented pits respectively

Examples of pits according to their shape together with the measured parameters are presented for a control subject (Figure 3-10A) and a Charcot patient (Figure 3-10B).

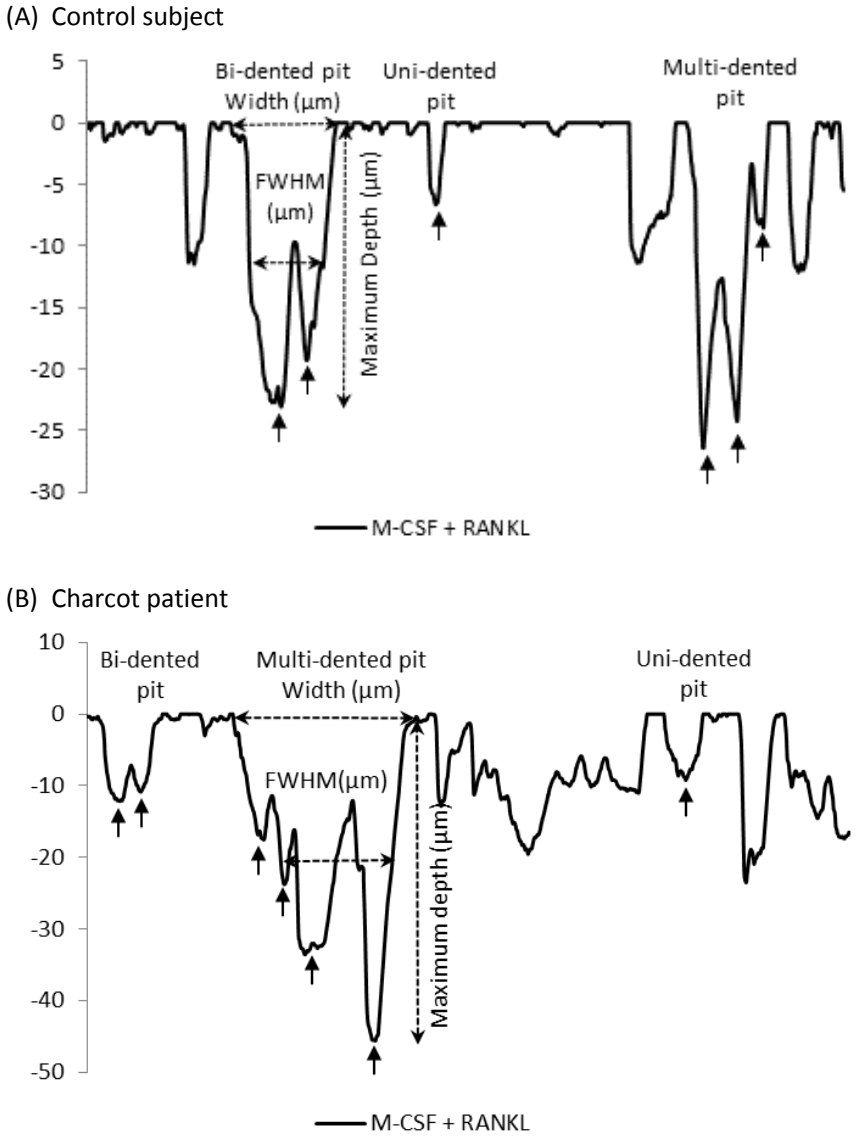

Figure 3-10 Example of pits in M-CSF+RANKL-treated cultures in a control subject and a Charcot patient
Examples of uni-dented, bi-dented and multi-dented pits together with an illustration of the dents (solid line arrow) and pit parameters (width at the surface; FWHM and maximum depth: dash arrow) are shown for a control subject (A) and a Charcot patient (B).

Comparison of the erosion profile measurements of resorbed bone discs from a control subject and a Charcot patient revealed a different pattern of resorption. In M-CSF+RANKL-treated cultures, the area of resorption under the surface of resorbed bone discs was greater in a Charcot patient compared with the area of resorption in control subject (Figure 3-11). Furthermore, the pit morphology was different. Pits appeared deeper and wider in the Charcot patient compared with the control subject.

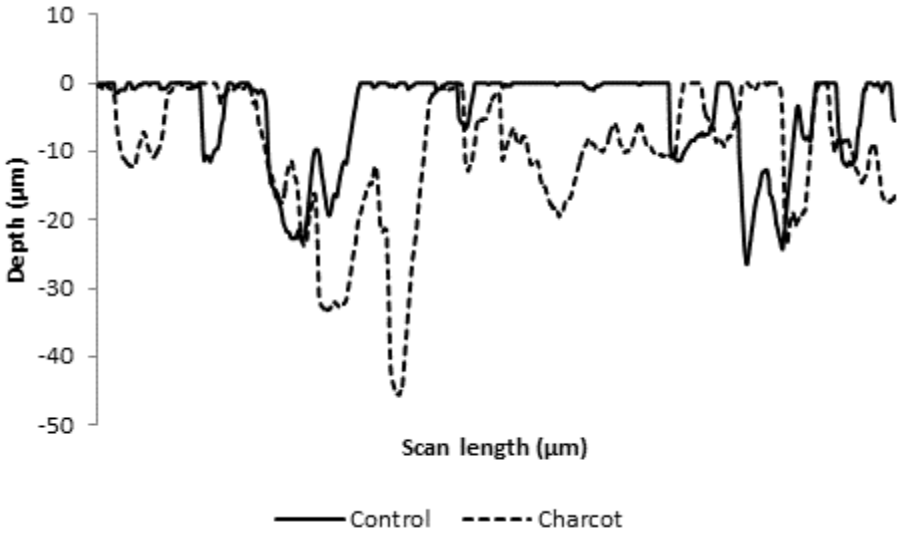

Figure 3-11 Comparison of erosion profile of resorbed bone discs in a control subject and in a Charcot patient in M-CSF+RANKL-treated cultures

These original observations indicated that surface profile measurements could provide additional information on how osteoclasts generated from control subjects and Charcot patients resorb bone. The devised parameters (area of resorption under the surface together, pit measurements including width, depth and FWHM) could be useful to assess the differences in the resorption pattern of osteoclasts derived from Charcot patients and control subjects.

3.5 Conclusion

I applied surface profilometry for the first time and proposed its usefulness as a novel method to assess bone resorption on bone discs cultured *in vitro*. This novel technique could provide a new perspective for measuring osteoclastic activity and may be used to evaluate erosion patterns and parameters (width, FWHM and depth) in a variety of conditions associated with increased osteoclastic activity. Furthermore, it could be applied to compare the erosion profile of resorbed discs cultured in various treatments.

Chapter 4 RANKL-mediated osteoclastic activation in acute Charcot osteoarthropathy

4.1 Introduction

The rapid bone destruction that occurs in the acute Charcot foot is well documented. However, the exact cellular mechanisms contributing to the pathogenesis of this condition are not fully understood. Osteoclasts are the principal cell type responsible for bone resorption but, their activation and function in Charcot osteoarthropathy remain unresolved.

I hypothesised that aberrantly activated osteoclasts play a key role in the pathological bone destruction that occurs in the acute Charcot foot. Osteoclastogenesis is regulated by RANKL, which acts via its receptor RANK, expressed on osteoclastic precursors and osteoclasts. This chapter describes my experiments exploring the role of RANKL in osteoclastic activity in acute Charcot osteoarthropathy. I used a recently established *in vitro* resorption assay to generate functional human osteoclasts from PBMCs. In addition, I employed surface profilometry, as a novel method to assess bone resorption on bovine bone discs. Both techniques have been used for the first time in the field of Charcot osteoarthropathy.

4.2 Research design and methods

Samples from peripheral blood were obtained from 10 consecutive patients with recent onset of acute Charcot osteoarthropathy, 8 diabetic patients with no history of Charcot osteoarthropathy and 9 healthy control subjects. All patients with Charcot osteoarthropathy presented with a unilateral red hot swollen foot and radiological evidence of acute Charcot fractures, demonstrated on plain foot and ankle radiographs (Petrova and Edmonds 2008, Rogers, Frykberg et al. 2011). All participants had intact

feet and had no features of foot infection or sepsis. The study was approved by the Outer West London Research Ethics Committee and was carried out in accordance with institutional guidelines and the Declaration of Helsinki with all patients and control subjects signing written informed consent.

4.2.1 Isolation and culture of peripheral blood mononuclear cells (PBMCs)

The PBMCs were isolated from whole blood as described in Chapter 2 and cultured on plastic to assess osteoclast formation and on bovine bone discs to assess osteoclast resorption. After 17 days in culture, 24-well plates were stained for tartrate-resistant acid phosphatase (TRAP). Plates were viewed by light microscopy and TRAP-positive cells with three or more nuclei were counted as osteoclasts. The bone discs were stained with toluidine blue after 14 and 21 days in culture. Resorption pits were identified by light microscopy. The extent of eroded surface on each bovine bone disc was determined using image analysis and expressed as the percentage of surface area resorbed. Additional bovine bone discs were stained with FitC-phalloidin and mounted with Vectashield mounting medium with DAPI, as described in chapter 2, for the assessment of actin ring formation, a marker of actively resorbing osteoclasts.

4.2.2 Surface profilometry

The erosion profile of resorbed bone discs was measured by the Dektak 150 Surface Profiler (Veeco, New York, USA), as described in Chapter 3. The stylus was dragged across the surface of the sample in hills and valleys mode with ten scans per subject carried out at random sites on each of the two discs. Each measurement had the following scan parameters (stylus force - 3.00 mg, scan length - 1000 µm, scan duration - 60 seconds, vertical measurement range - 65.5 µm, scan resolution - 0.056 µm/scan). On average, 75 pits per condition/ per subject were analysed and the median area of disc erosion was calculated in μm^2 using Origin Pro 8.6 software. According to their

shape, pits were defined as uni-dented, bi-dented and multi-dented. Each pit was characterised by the following parameters: width at the surface (µm), full-width–half-maximum (FWHM), (µm) and maximum depth (µm). The median width, depth, and FWHM for the uni-dented, bi-dented, and multi-dented pits were calculated for each subject.

4.2.3 Rationale for the study

To ascertain that RANKL is a major osteoclastic activator in patients with Charcot osteoarthropathy, the following cell culture treatments were set up in each group:

Control cultures:

Culture 1: M-CSF-treated cultures

M-CSF is a survival factor for PBMCs and 25 ng/ml Human M-CSF (R&D Systems Europe) was added at day 0. This cytokine is not an osteoclastogenic factor and therefore culture 1 served as a negative control.

Culture 2: M-CSF+RANKL- treated cultures

RANKL is a classical osteoclastogenic factor and it was added to the cultures at day 7 (25 ng/ml M-CSF + 100 ng/ml human soluble RANKL (RANKL, Peprotech UK), at a concentration known to facilitate differentiation of osteoclast precursors to active bone-resorbing osteoclasts *in vitro*, (Mabilleau, Petrova et al. 2008). This culture served as positive control.

Experimental culture:

Culture 3: M-CSF+RANKL+OPG-treated cultures

Excess concentration of OPG was added to M-CSF+RANKL treated cultures at day 7 (25 ng/ml M-CSF + 100 ng/ml RANKL + 250 ng/ml human OPG (R&D Systems Europe), (Mabilleau, Petrova et al. 2008). This culture served as test culture aiming to

investigate the role of RANKL. The rationale for this approach was that if osteoclastogenesis is mediated through RANK–RANKL interaction, addition of excess concentration of OPG would abolish the process of osteoclast differentiation and activation. A schematic summary of the experiment is presented (Figure 4-1).

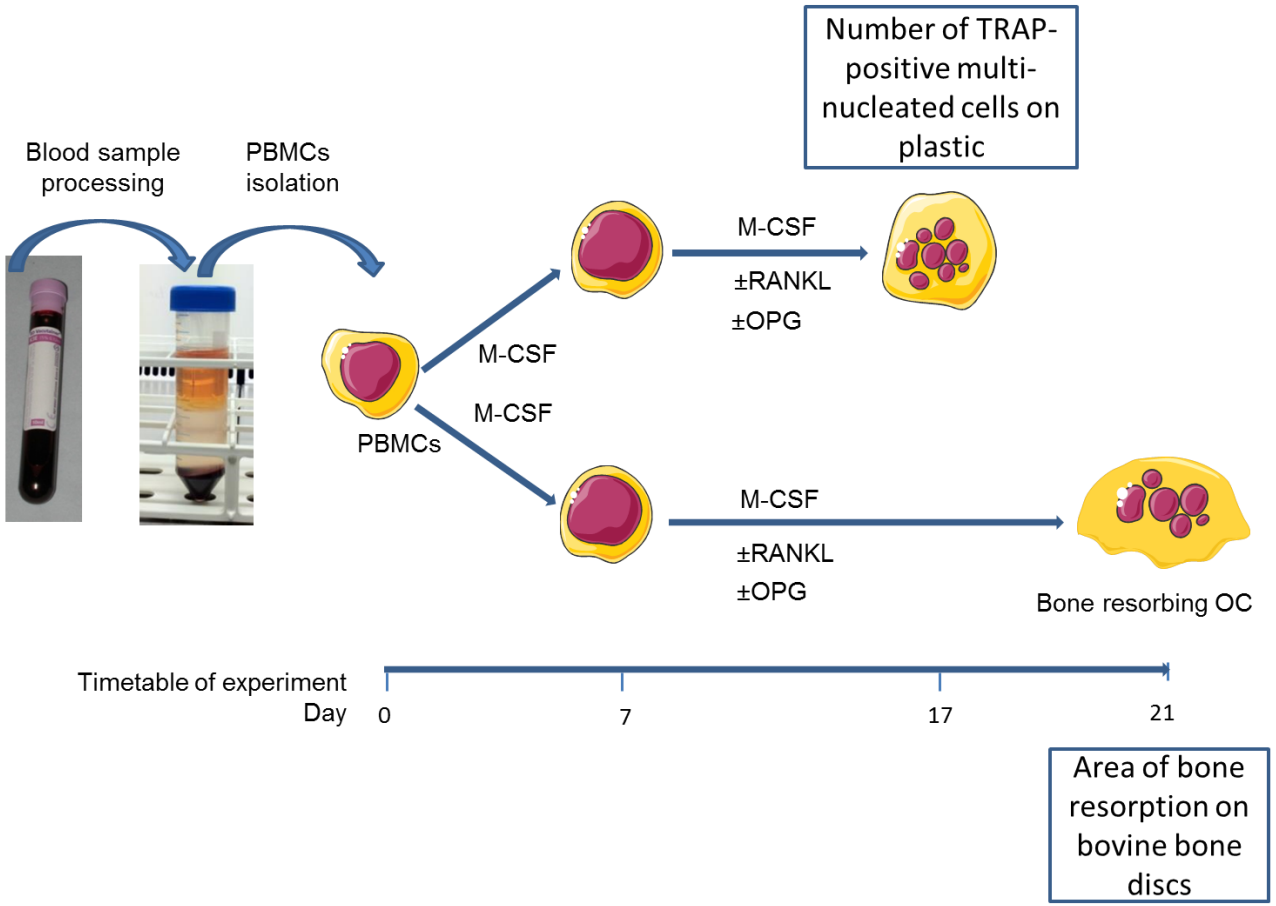

Figure 4-1 Summary of experiment
Blood samples were processed and PBMCs were isolated and cultured in the presence of M-CSF; M-CSF+RANKL; M-CSF+RANKL+OPG on plastic cell culture plates and on bovine bone discs for the assessment of osteoclast formation (number of TRAP-positive multi-nucleated cells at day 17) and bone resorption (area of bone resorption at day 21, as assessed by image analysis)

4.3 Statistical analyses

Data were analysed with Predictive Analytics Software 18 statistical package and expressed as median [25th-75th percentile]. Differences between study groups and culture treatments were analysed using the non-parametric Mann–Whitney U test (two groups) or Kruskal-Wallis test (three groups), as appropriate. Chi-square test was used for categorical variables. Differences were considered significant at $p<0.05$.

4.4 Results

4.4.1 Demographical features

Patients with acute Charcot osteoarthropathy were matched for age, gender, type and duration of diabetes with the diabetic patients and for age and gender with the healthy control subjects. The age, gender distribution, type and duration of diabetes were not significantly different between the Charcot patients and diabetic patients nor were the age and gender distribution between the Charcot patients and healthy control subjects (Table 4-1).

Table 4-1 Demographic features of the study patients

	Charcot	Diabetes	Control
Age (years)	57 [53-64]	60 [55-66]	45 [42-48]
Gender (male: female)	6:4	4:4	5:4
Type 1: Type 2 diabetes	4:6	2:6	-
Duration of diabetes (years)	17 [8-29]	10 [9-26]	-

Data expressed as median [25^{th}-75^{th} percentile]; Data assessed with Mann-Whitney U test. Non-significant difference in age, gender distribution, type and duration of diabetes (Charcot patients versus diabetic patients) and age and gender (Charcot patients versus healthy control subjects), ($p>0.05$ for all pairwise comparisons).

4.4.2 Osteoclast formation on plastic in M-CSF-, M-CSF+RANKL- and M-CSF+RANKL+OPG-treated cultures

Observation of the cell culture plates with light microscopy showed no difference in osteoclast formation in M-CSF-treated cultures between the three groups.

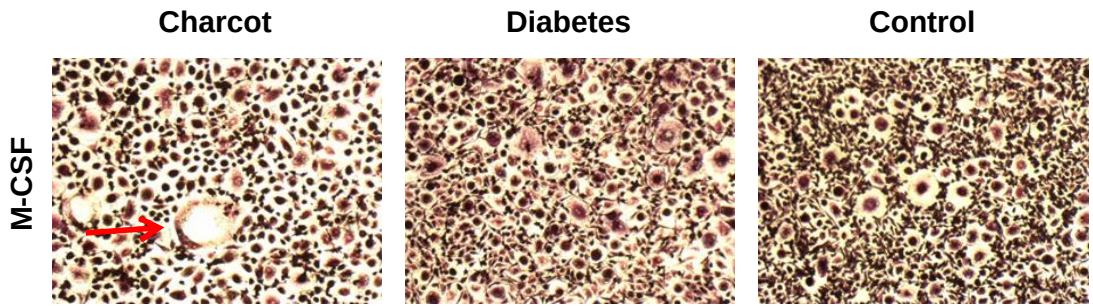

Figure 4-2 Osteoclast formation in M-CSF-treated cultures (light microscopy)
TRAP staining revealed presence of isolated multi-nucleated cells (red arrow) formed on plastic; (original magnification X100). The red arrow denotes a multi-nucleated TRAP-positive cell in M-CSF-treated culture in a Charcot patient.

The median number of TRAP-positive multi-nucleated cells in Charcot patients was not significantly different from the median number of TRAP-positive multi-nucleated cells in diabetic patients and healthy control subjects in M-CSF-treated cultures ($p>0.05$). Furthermore, there was no significant difference in the median number of TRAP-positive multi-nucleated cells in all pairwise comparisons in M-CSF-treated cultures, (Figure 4-3).

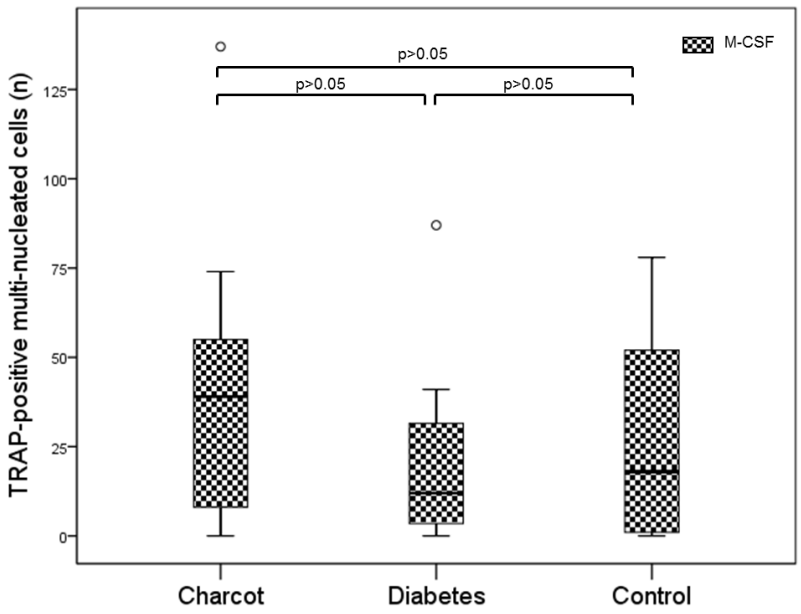

Figure 4-3 Osteoclast formation in M-CSF-treated cultures in Charcot patients, diabetic patients and healthy control subjects.
Significance assessed by Mann-Whitney U test. Levels of significance are demonstrated on the graph. The data is presented as a box and whisker plot, constructed with the Predictive Analytics Software 18 statistical package. The plot represents the median (black horizontal line), the 25th and 75th percentile (the width of the box) and the range. The outliers are marked with open dots.
Non-significant difference in osteoclast formation in M-CSF-treated cultures in Charcot patients versus diabetic patients; Charcot patients versus healthy control subjects and diabetic patients versus healthy control subjects, p>0.05 for all pairwise comparisons.

The addition of RANKL to M-CSF-treated cultures resulted in a significant increase in the median number of TRAP-positive multi-nucleated cells in all study groups, as expected. The number of TRAP-positive multi-nucleated cells increased from 35 [12-64] to 144 [94-225] in Charcot patients ($p<0.01$), from 12 [3.5-31.5] to 142 [69-198] in diabetic patients ($p<0.01$) and from 18 [1-52] to 82 [71-141] in healthy control subjects ($p<0.01$), (Figure 4-4).

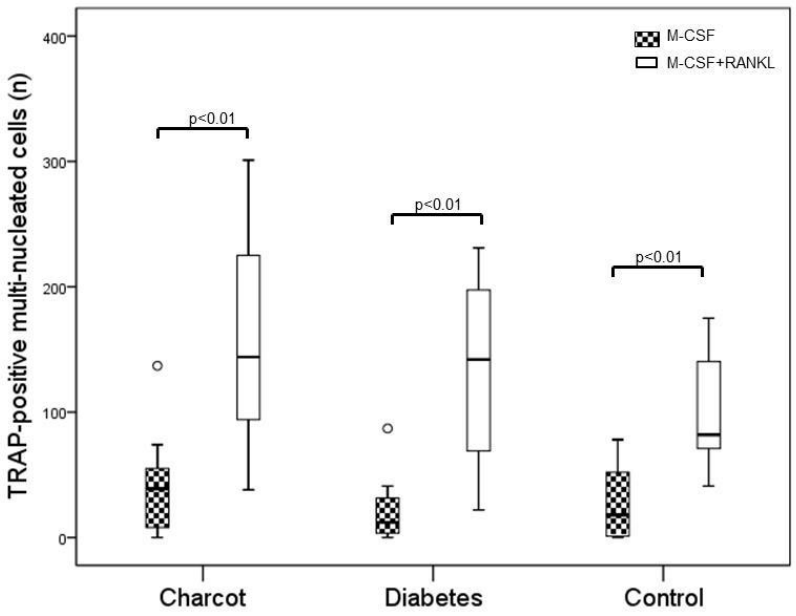

Figure 4-4 Comparison of the number of TRAP-positive multi-nucleated cells in Charcot patients, diabetic patients and healthy control subjects in M-CSF-treated cultures and in M-CSF+RANKL-treated cultures.
Significance assessed by Mann-Whitney U test. Levels of significance are demonstrated on the graph. Significant increase in the median number of TRAP-positive multi-nucleated cells in Charcot patients ($p<0.01$), diabetic patients ($p<0.01$) and healthy control subjects ($p<0.01$) in M-CSF-treated cultures compared with M-CSF+RANKL-treated cultures.

The response to RANKL was not significantly different between the three groups and representative images of newly formed TRAP-positive multi-nucleated cells in a Charcot patient, diabetic patient and healthy control subject are presented below (Figure 4-5).

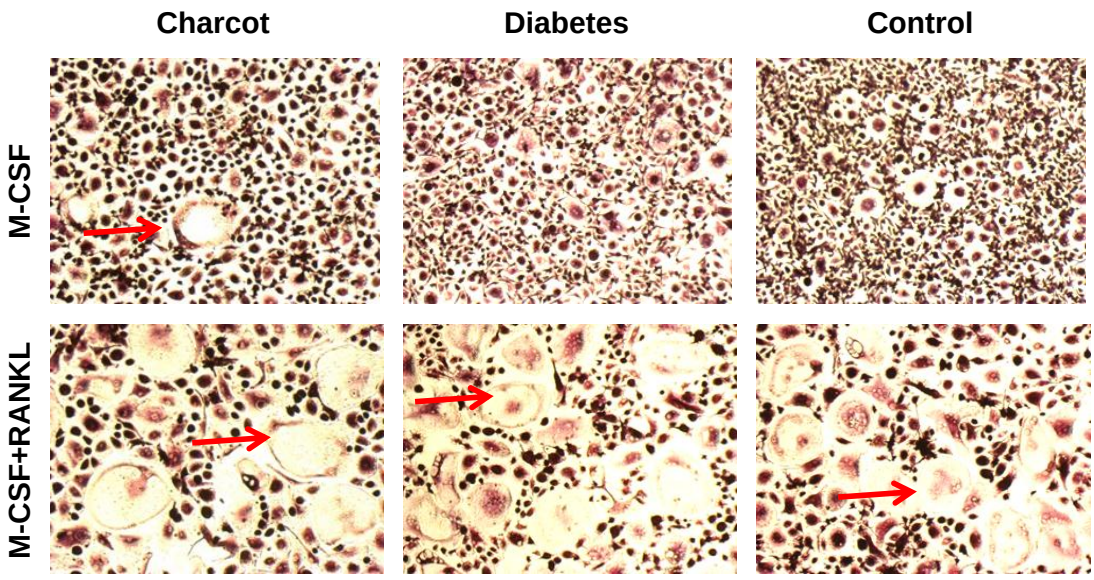

Figure 4-5 Osteoclast formation in M-CSF-treated cultures and M-CSF+RANKL-treated cultures (light microscopy)
Representative images of TRAP-positive multi-nucleated cells formed on plastic in Charcot patient, diabetic patient and healthy control subject; (original magnification X100). The red arrows denote some of the TRAP-positive multi-nucleated cells.

The median number of TRAP-positive multi-nucleated cells in Charcot patients was not significantly different from the median number of TRAP-positive multi-nucleated cells in diabetic patients and healthy control subjects in M-CSF+RANKL-treated culture ($p>0.05$). Furthermore, there was no difference in the median number of TRAP-positive multi-nucleated cells in all pairwise comparisons in M-CSF+RANKL-treated cultures, ($p>0.05$ for all pairwise comparisons), (Figure 4-6).

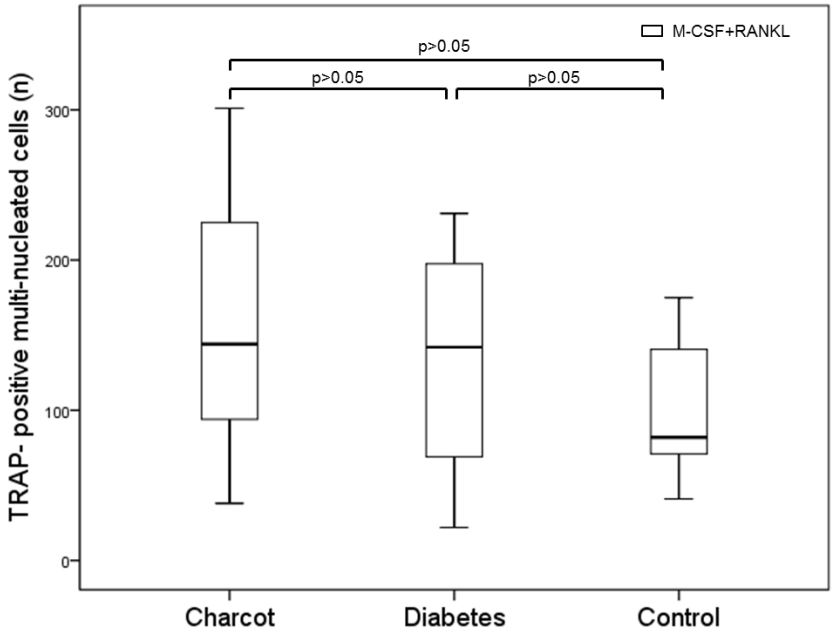

Figure 4-6 Osteoclast formation in M-CSF+RANKL-treated cultures in Charcot patients, diabetic patients and healthy control subjects.
Significance assessed by Mann-Whitney U test. Levels of significance are demonstrated on the graph. Non-significant difference in osteoclast formation in M-CSF+RANKL-treated cultures in Charcot patients versus diabetic patients; Charcot patients versus healthy control subjects and diabetic patients versus healthy control subjects. (p>0.05 for all pairwise comparisons)

The addition of an excess concentration of OPG to M-CSF+RANKL-treated cultures led to a significant reduction in the number of TRAP-positive multi-nucleated cells in Charcot patients ($p<0.01$), diabetic patients ($p<0.01$) and healthy control subjects ($p<0.01$), (Figure 4-7).

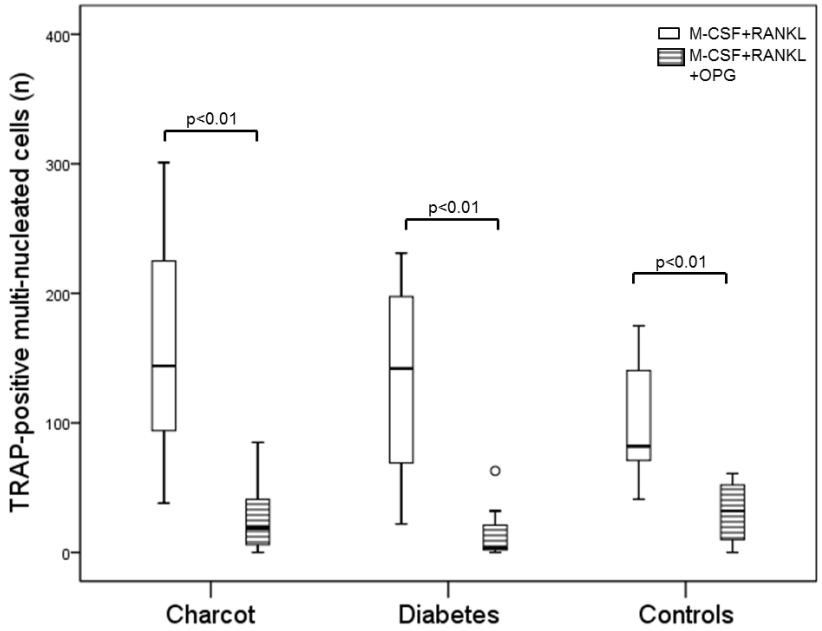

Figure 4-7 Comparison of the number of TRAP-positive multi-nucleated cells in Charcot patients, diabetic patients and healthy control subjects in M-CSF+RANKL-treated cultures and in M-CSF+RANKL+OPG-treated cultures.
Significance assessed by Mann-Whitney U test. Levels of significance are demonstrated on the graph. Significant reduction in the median number of TRAP-positive multi-nucleated cells in Charcot patients (p<0.01), diabetic patients (p<0.01) and healthy control subjects (p<0.01) in M-CSF+RANKL-treated cultures compared with M-CSF+RANKL+OPG-treated cultures.

Observation under light microscopy revealed the presence of isolated multi-nucleated TRAP-positive cells in all study groups (Figure 4-8).

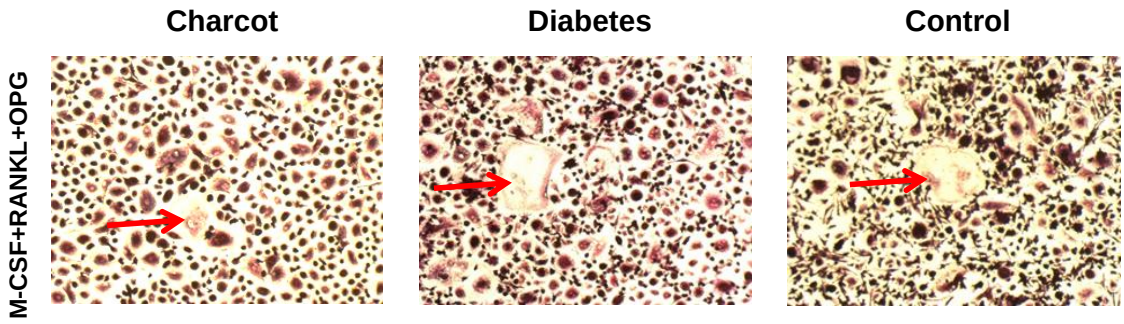

Figure 4-8 Osteoclast formation in M-CSF+RANKL+OPG-treated cultures (light microscopy)
TRAP staining revealed the presence of isolated multi-nucleated cells (red arrow) formed on plastic; (original magnification X100). The red arrows denote multi-nucleated TRAP-positive cells in M-CSF+RANKL+OPG-treated culture in a Charcot patient, diabetic patient and healthy control subject.

The number of TRAP-positive multi-nucleated cells after the addition OPG was not significantly different between Charcot patients, diabetic patients and healthy control subjects, ($p>0.05$). Furthermore, there was no significant difference in the median number of TRAP-positive cells in all pairwise comparisons in M-CSF+RANKL+OPG-treated cultures, (Figure 4-9).

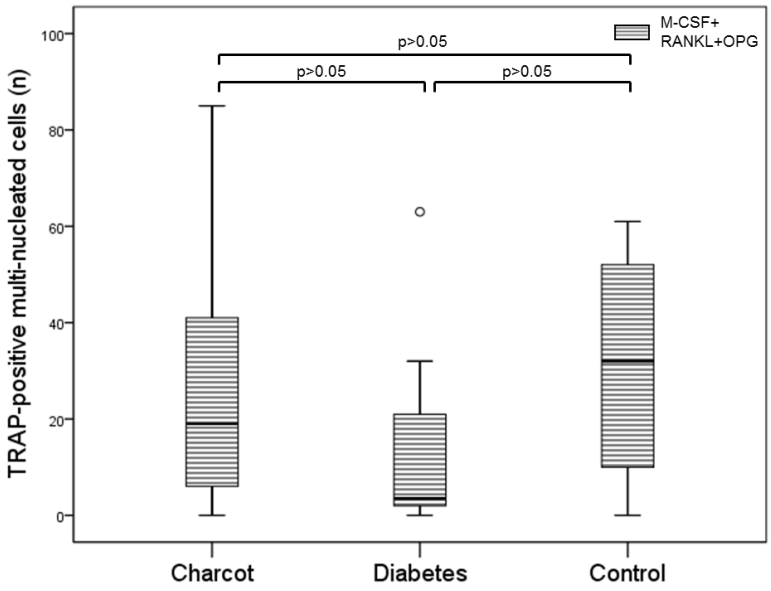

Figure 4-9 Osteoclast formation in M-CSF+RANKL+OPG-treated cultures in Charcot patients, diabetic patients and healthy control subjects.
Significance assessed by Mann-Whitney U test. Levels of significance are demonstrated on the graph. Non-significant difference in osteoclast formation in M-CSF+RANKL+OPG-treated cultures in Charcot patients versus diabetic patients; Charcot patients versus healthy control subjects and diabetic patients versus healthy control subjects, $p>0.05$ for all pairwise comparisons.

4.4.3 Osteoclast formation on bovine bone discs in M-CSF-, M-CSF+RANKL- and M-CSF+RANKL+OPG-treated cultures

To differentiate between resorbing osteoclasts and TRAP-positive macrophage polykaryons, bone discs cultured with M-CSF, M-CSF+RANKL and M-CSF+RANKL+OPG were set up for 21 days in 4 Charcot patients and 4 healthy control subjects. Bone discs were assessed with immunofluorescent microscopy for actin ring formation, a marker of actively resorbing osteoclasts.

There was no actin ring formation in M-CSF-treated cultures in both Charcot patients and healthy control subjects (Figure 4-10 A, B), in contrast to the numerous actin ring positive cells noted after the addition of RANKL in both study groups, (Figure 4-10C, D). This suggested that M-CSF in the absence of RANKL did not trigger differentiation of bone resorbing osteoclasts. Actin ring positive cells were present only in M-CSF+RANKL-treated cultures, indicating a role of RANKL in osteoclastic activity. The absence of actin ring positive cells after the addition of OPG both in Charcot patients and healthy control subjects confirmed that the osteoclastogenic response was mediated by RANKL, (Figure 4-10E, F).

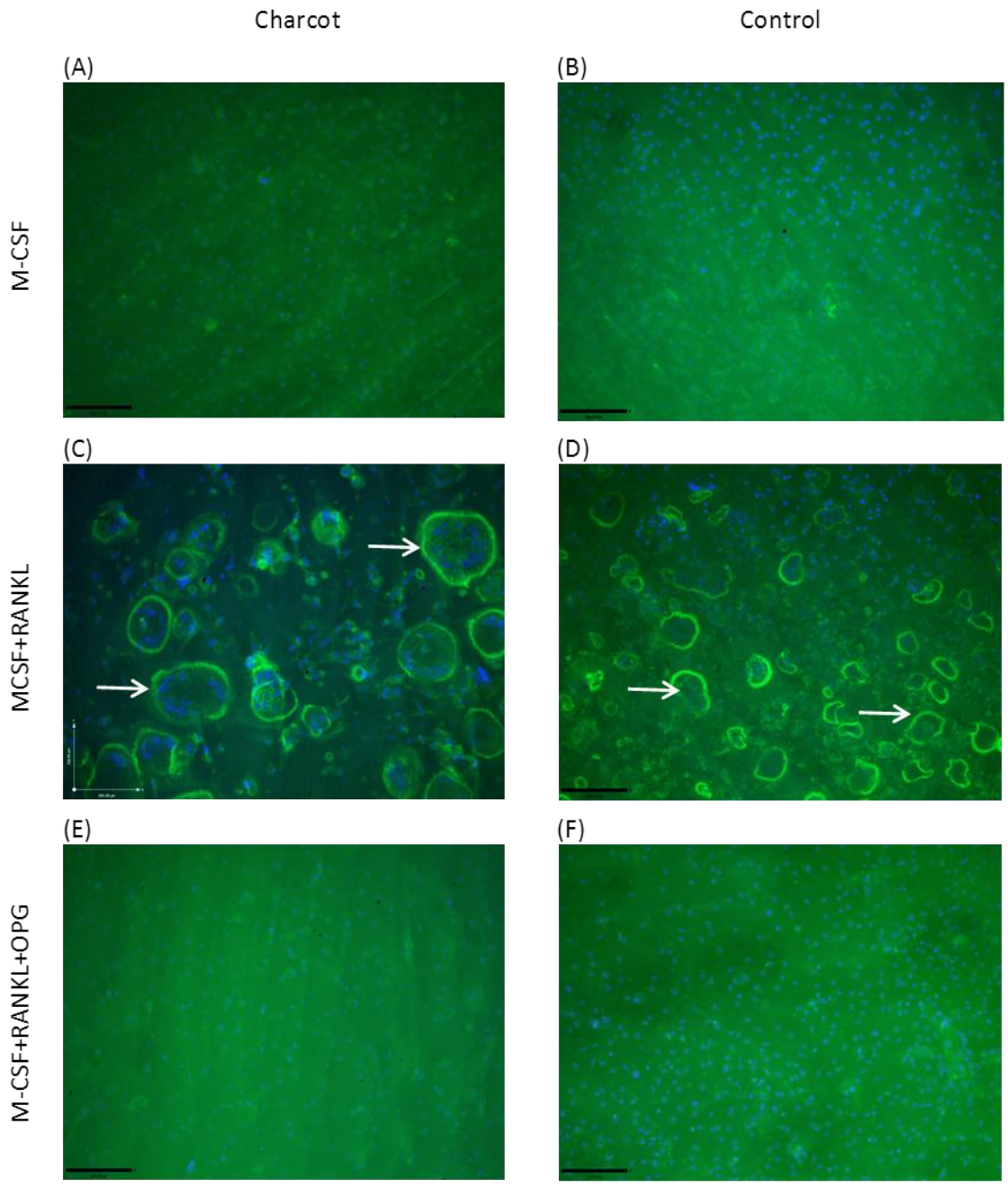

Figure 4-10 Immunofluorescent images of bovine bone discs in M-CSF-, M-CSF+RANKL and M-CSF+RANKL+OPG-treated cultures

Representative images of bovine bone discs which were stained with FitC- phalloidin and mounted with vectashield with DAPI mounting medium for visualisation of actin rings and nuclei in M-CSF-, M-CSF+RANKL- and M-CSF+RANKL+OPG-treated cultures in a Charcot patient (A, C, E) and a healthy control subject (B, D, F). No actin ring formation was observed in both groups in M-CSF-treated cultures (A, B). Multi-nucleated actin ring positive cells were noted in M-CSF+RANKL-treated cultures in both Charcot patient (C) and healthy control subject (D); The white arrows denote some of the multinucleated actin-ring positive cells. Blue staining denotes the nuclei; green staining denotes the actin rings. The addition of OPG led to an inhibition of actin ring formation in both Charcot patient (E) and in healthy control subject (F). (Olympus IX81; magnification, X100; scale bar - 200µm)

4.4.4 Osteoclast resorption on bovine bone discs in M-CSF-; M-CSF+RANKL- and M-CSF+RANKL+OPG-treated cultures

The functional ability of newly formed osteoclasts to resorb bone was assessed on bovine bone discs after toluidine blue staining.

Observation of the surface of the bovine bone discs with light microscopy (magnification X40) showed no evidence of pit formation in M-CSF-treated cultures in all study groups (Figure 4-11).

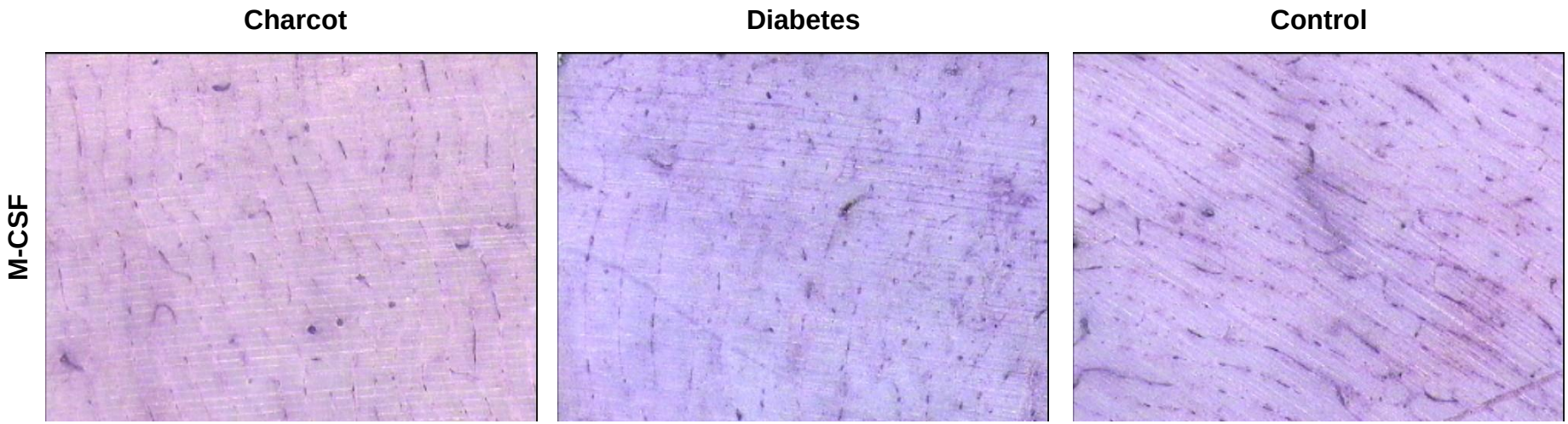

Figure 4-11 Representative images of bovine bone discs in M-CSF-treated cultures in a Charcot patient, diabetic patient and healthy control subject (light microscopy).
No pit formation was noted in all study groups after toluidine blue staining (magnification X40).

At higher magnification (X70), minute isolated pits were noted on bovine bone discs in cultures from Charcot patients (n=1), diabetic patients (n=3) and healthy control subjects (n=1), (Figure 4-12).

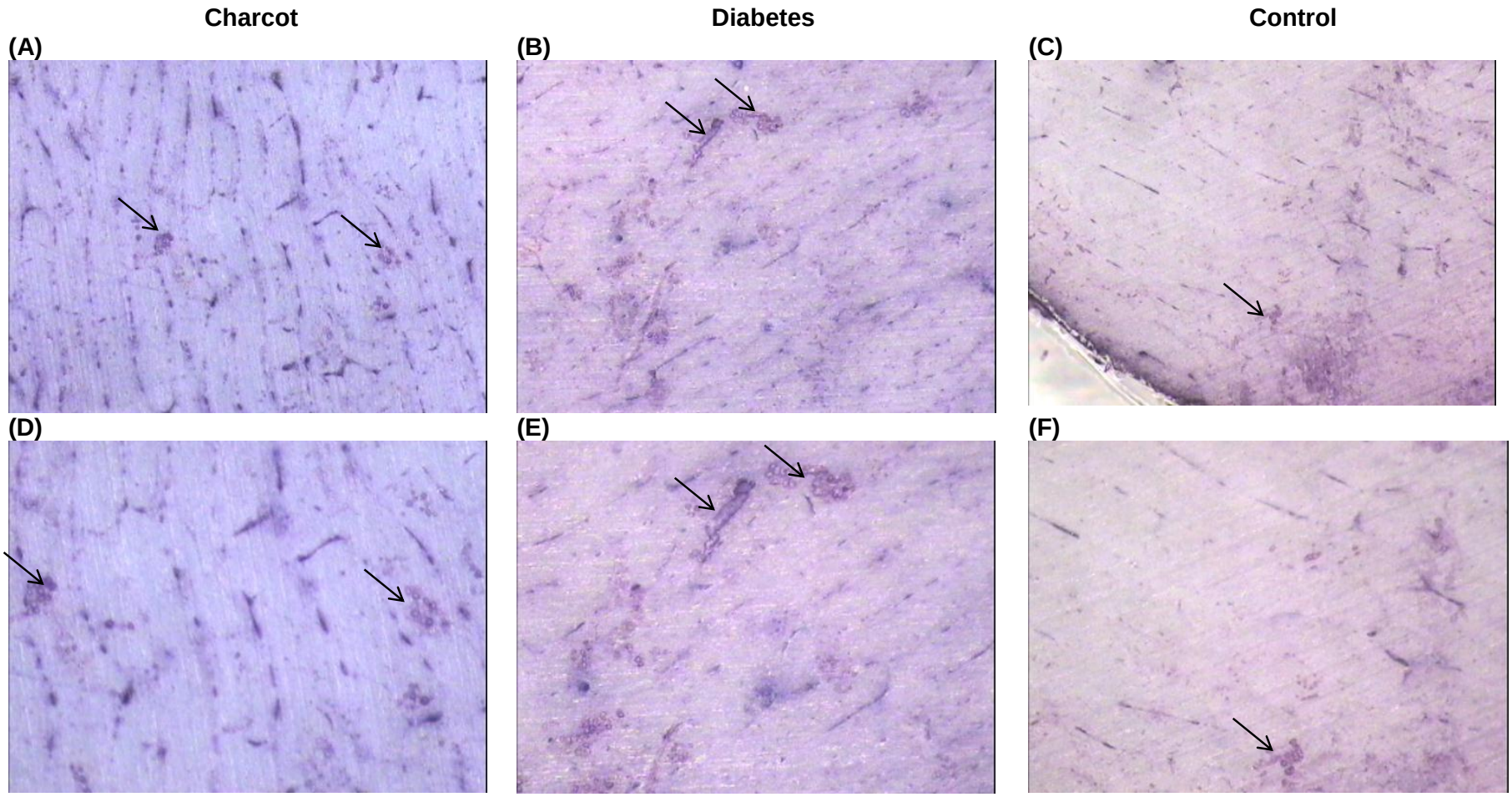

Figure 4-12 Minute isolated resorption pits in M-CSF-treated cultures in a Charcot patient, diabetic patient and healthy control subject (light microscopy). The black arrows denote the isolated minute pits at X40 (A,B,C) and at X70 magnification (D,E,F).

Due to the limited nature of these isolated findings, observed only at X70 magnification, it was not possible to quantitate them by image analysis. Therefore, the percentage area resorbed on bovine bone discs was not measured. Instead, a chi-squared test comparing the distribution (presence/ absence of minute pits on bovine bone discs) in Charcot patients, diabetic patients and healthy control subjects was carried out. There was no difference in the distribution according to the presence/ absence of minute pits in M-CSF-treated cultures between the three study groups ($p>0.05$), (Table 4-2).

Table 4-2 Comparison of distribution according to presence of minute isolated resorption pits in M-CSF-treated cultures in Charcot patients, diabetic patients and healthy control subjects.

Minute pits in M-CSF-treated cultures	Charcot	Diabetes	Control	P-value
Present : absent	1: 9	3: 5	1: 8	>0.05

Chi-square test. P-value indicates the difference between Charcot patients, diabetic patients and healthy control subjects.
Non-significant difference according to presence: absence of minute isolated resorption pits in M-CSF-treated cultures between Charcot patients, diabetic patients and healthy control subjects ($p>0.05$)

In contrast to M-CSF-treated cultures, after the addition of RANKL, numerous pits were noted in all study groups and typical examples of resorbed bone discs in a Charcot patient, diabetic patient and healthy control subject are presented below (Figure 4-13).

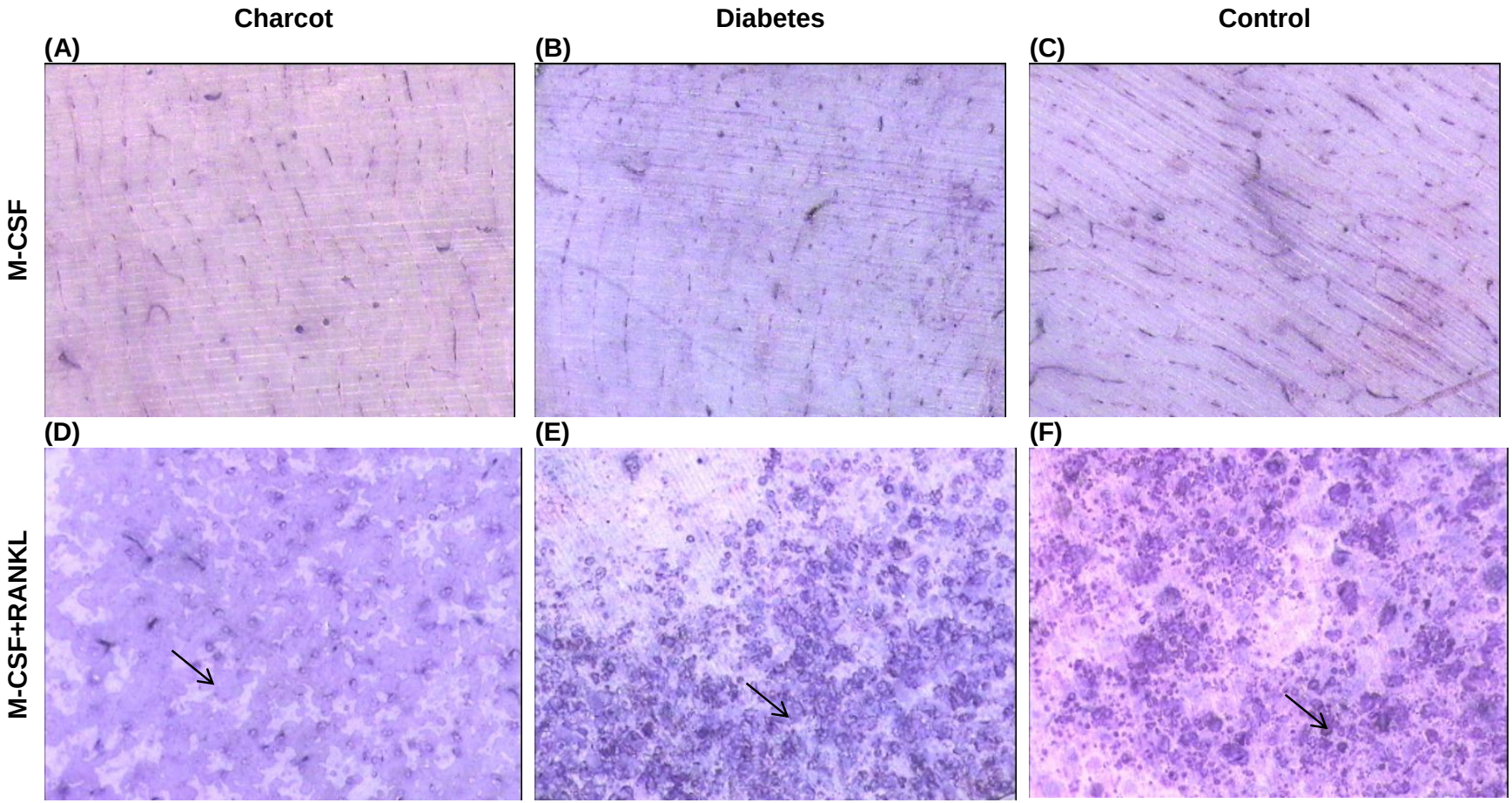

Figure 4-13 Toluidine blue staining of resorbed bovine bone discs in M-CSF-treated cultures and in M-CSF+RANKL-treated cultures (light microscopy) There was no pit formation in M-CSF -treated cultures in a Charcot patient (A), diabetic patient (B) and healthy control subject (C). The addition of RANKL led to extensive resorption noted in all study groups. The black arrows denote some of the pits in the M-CSF+RANKL-treated cultures in a Charcot patient (D), diabetic patient (E) and healthy control subject (F), (magnification x40)

Visualisation of the bovine bone discs revealed that the newly formed osteoclasts isolated from patients with acute Charcot osteoarthropathy exhibited increased resorbing activity in M-CSF+RANKL-treated cultures compared with osteoclasts generated from diabetic patients and healthy control subjects. The total area of the resorbed surface measured by light microscopy was significantly different between Charcot patients (39% [33-46], diabetic patients 16% [8-23] and healthy control subjects 21% [15-26], resulting in a 2.4 fold increase in Charcot patients compared with diabetic patients ($p<0.01$), and a 1.9 fold increase in Charcot patients compared with healthy control subjects ($p<0.01$), (Figure 4-14). The area of resorption at the surface was similar between diabetic patients and healthy control subjects ($p>0.05$), (Figure 4-14).

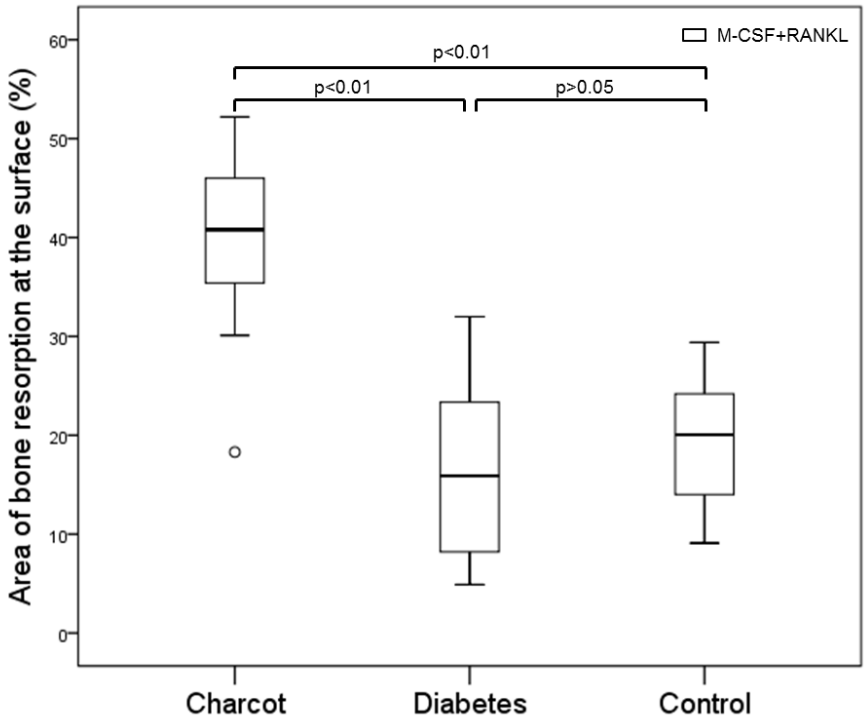

Figure 4-14 Osteoclast resorption on bovine bone discs in Charcot patients, diabetic patients and healthy control subjects in M-CSF+RANKL-treated cultures as assessed by image analysis after toluidine blue staining
Significance assessed by Mann-Whitney U test. Levels of significance are demonstrated on the graph. Significant increase in the area of bone resorption on bovine bone discs in M-CSF+RANKL-treated cultures between Charcot patients and diabetic patients ($p<0.01$) and Charcot patients and healthy control subjects ($p<0.01$). Non-significant difference was noted between diabetic patients and healthy control subjects, ($p>0.05$).

The addition of OPG led to an almost complete inhibition of bone resorption on bovine bone discs in Charcot patients, diabetic patients and healthy control subjects (Figure 4-15).

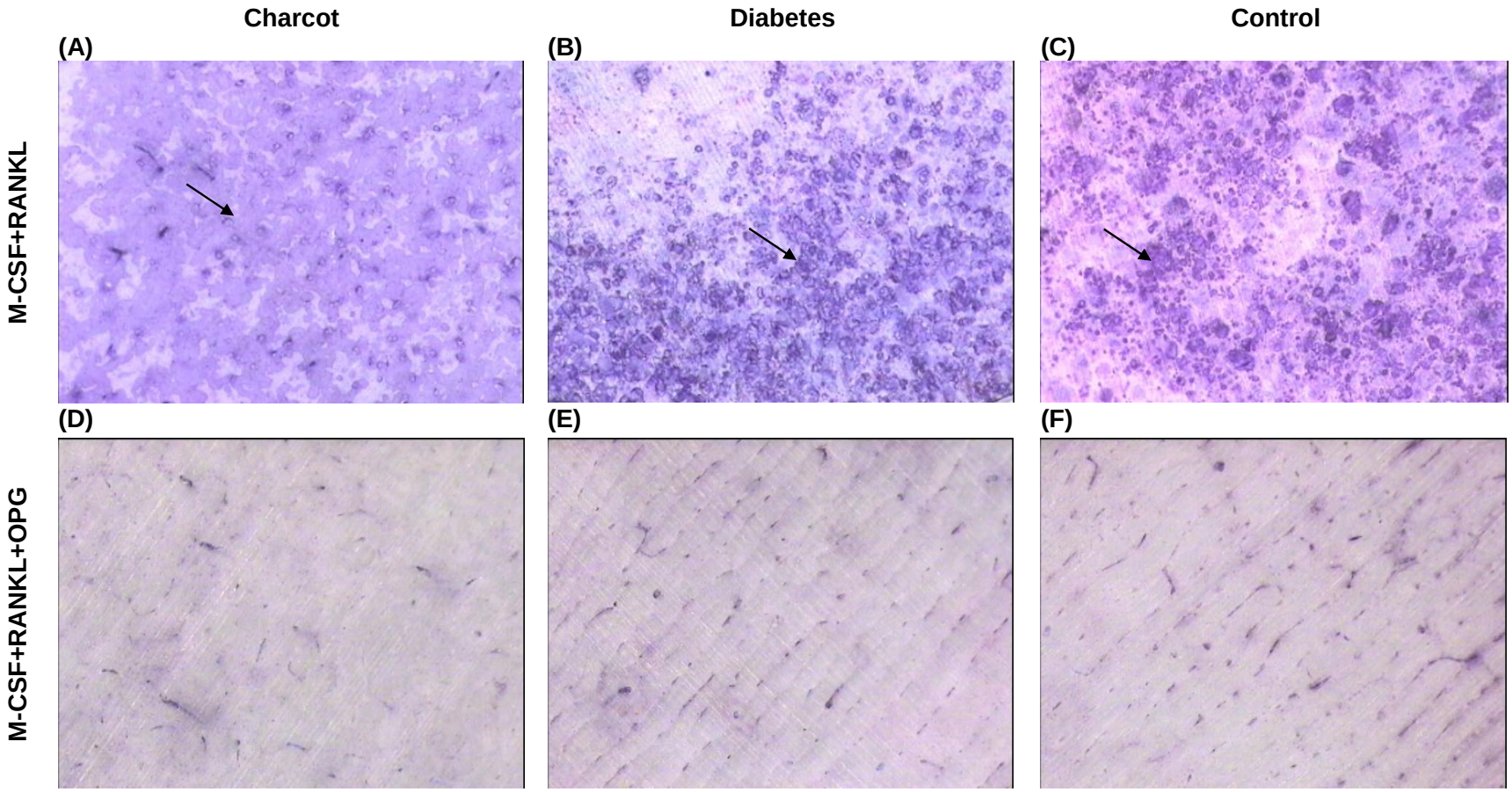

Figure 4-15 Toluidine blue staining of resorbed bovine bone discs in M-CSF+RANKL-treated cultures and in M-CSF+RANKL+OPG-treated cultures (light microscopy)

The addition of OPG inhibited the extensive bone resorption noted in M-CSF+RANKL-treated cultures in all study groups (A, B, C); The black arrows denote some of the pits in the M-CSF+RANKL-treated cultures in a Charcot patient (A), diabetic patient (B) and healthy control subject (C). There was no pit formation in M-CSF+RANKL+OPG-treated cultures in a Charcot patient (D), diabetic patient (D) and healthy control subject (F), (magnification x40)

Non-significant isolated minute pits were noted at higher magnification in 4 subjects (2 Charcot patients, 1 diabetic patient and 1 healthy control subject), (Figure 4-16), but the distribution within the groups according to the presence or absence of pits was not significantly different (p>0.05), (Table 4-3).

Table 4-3 Comparison of distribution according to presence of minute resorption pits in M-CSF+RANKL+OPG treated cultures in Charcot patients, diabetic patients and healthy control subjects.

Minute pits in M-CSF+ RANKL+ OPG treated cultures	Charcot	Diabetes	Control	P-value
Present: absent	2: 8	1: 7	1: 8	>0.05

Chi-square test. P-value indicates the difference between Charcot patients, diabetic patients and healthy control subjects.
Non-significant difference according to presence: absence of minute isolated resorption pits in M-CSF+RANKL+OPG-treated cultures between Charcot patients, diabetic patients and healthy control subjects (p>0.05)

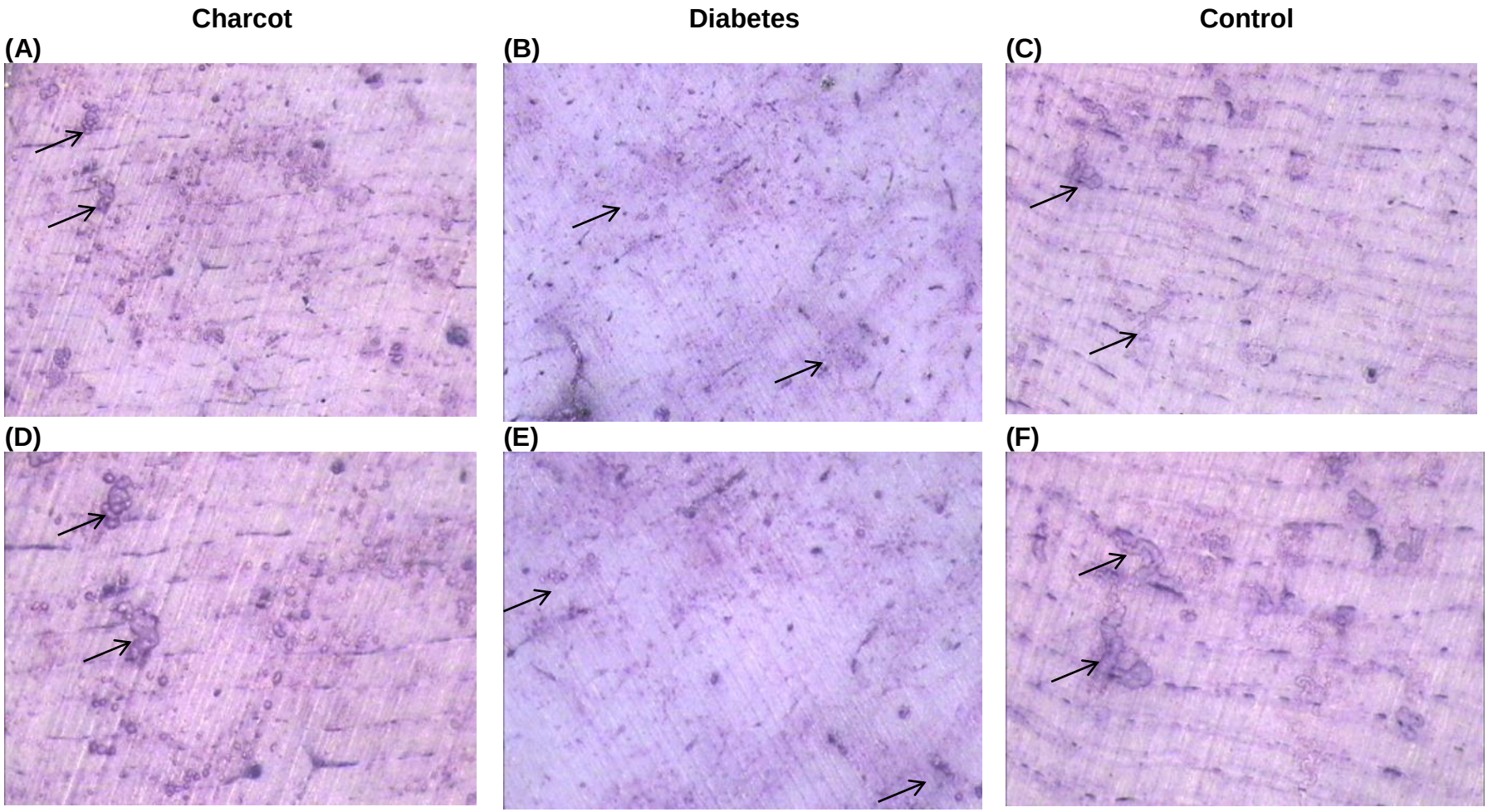

Figure 4-16 Minute isolated resorption pits in M-CSF+RANKL+OPG-treated cultures in a Charcot patient, diabetic patient and healthy control subject (light microscopy).
The black arrows denote the isolated minute pits at X40 (A,B,C) and at X70 magnification (D,E,F).

4.4.5 Pit morphology on bovine bone discs in M-CSF+RANKL-treated cultures in Charcot patients, diabetic patients and healthy control cultures

Visualisation of the bovine bone discs at day 21 at higher magnification (X200) showed that there was a remarkable difference in the morphology of the pits between Charcot patients and control groups. In diabetic patients and healthy control subjects, the resorption events more commonly appeared as discrete round pits, sometimes separated from each other, sometimes in clusters (Figure 4-17), whereas those in Charcot patients tended to be elongated, appearing as continuous grooves described previously as lacunae or trenches, (Figure 4-17), (Soe and Delaisse 2010).

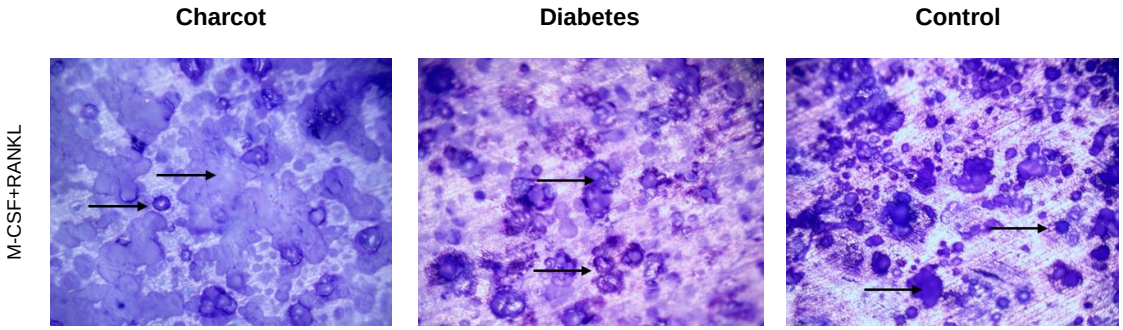

Figure 4-17 Representative images of resorbed bovine bone discs in M-CSF+RANKL-treated cultures at higher magnification (light microscopy)
Resorbed bovine bone discs after toluidine blue staining in M-CSF+RANKL-treated cultures in a Charcot patient, diabetic patient and healthy control subject (magnification X 200). The arrows denote some of the resorption pits.

The observed differences in the pit morphology between Charcot patients, diabetic patients and healthy control subjects have not been noted previously and required further studies. I hypothesised that osteoclasts from Charcot patients have increased osteoclastic potential and can carry out extensive resorption not only at the surface but also under the surface of bovine bone discs. To explore this hypothesis I employed surface profilometry to characterise the morphological appearance and profile of resorption pits on bovine bone discs in various culture conditions in Charcot patients, diabetic patients and healthy control subjects.

4.4.6 Surface profile measurements in M-CSF-, M-CSF+RANKL- and M-CSF+RANKL+OPG-treated cultures

Observation of the surface of bone discs in M-CSF-treated cultures and also after the addition of OPG with the integrated camera of the profiler was unremarkable in the three study groups. In contrast, numerous pits were noted in M-CSF+RANKL-treated cultures. These dark areas surrounded by grey areas of unresorbed bone corresponded to the toluidine blue stained resorption pits as viewed under light microscopy (Figure 4-18).

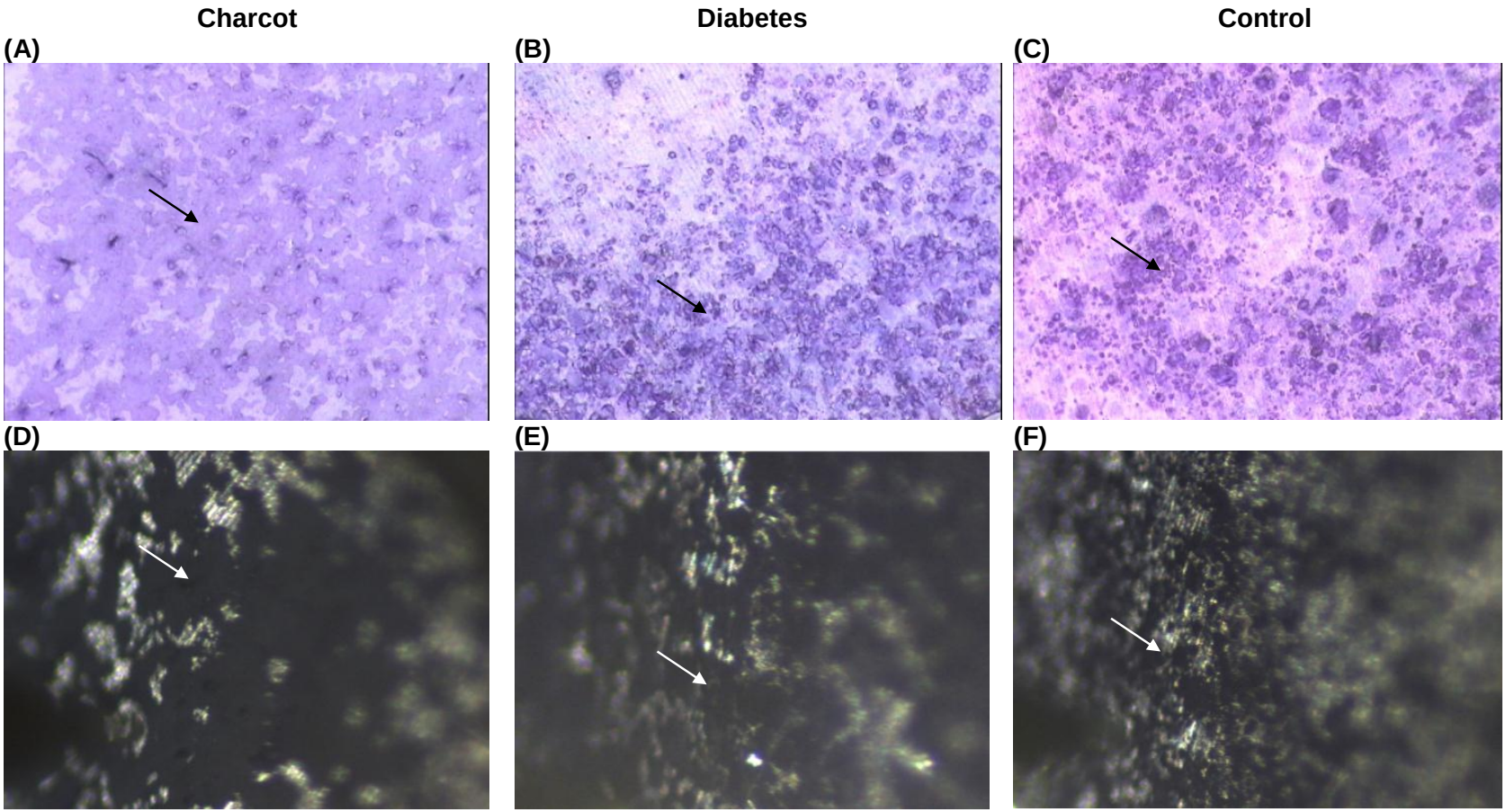

Figure 4-18 Resorbed bovine bone discs in M-CSF+RANKL-treated cultures after toluidine blue staining and as viewed with the integrated camera of the profiler.

The black arrows denote some of the pits after toluidine blue staining and the white arrows denote some of the pits as viewed with the integrated camera of the profiler in a Charcot patient (A, D), diabetic patient (B, E) and healthy control subject (C, F) respectively.

The surface profile measurements of randomly selected areas in MCSF-treated cultures appeared as almost straight line in Charcot patients, diabetic patients and healthy control subjects (blue line, Figure 4-19 A, B, C respectively). In contrast, erosion profile measurements of resorbed bone discs in M-CSF+RANKL-treated cultures revealed multi-shaped erosions in all study groups and typical examples are presented (red line, Figure 4-19 A, B, C).

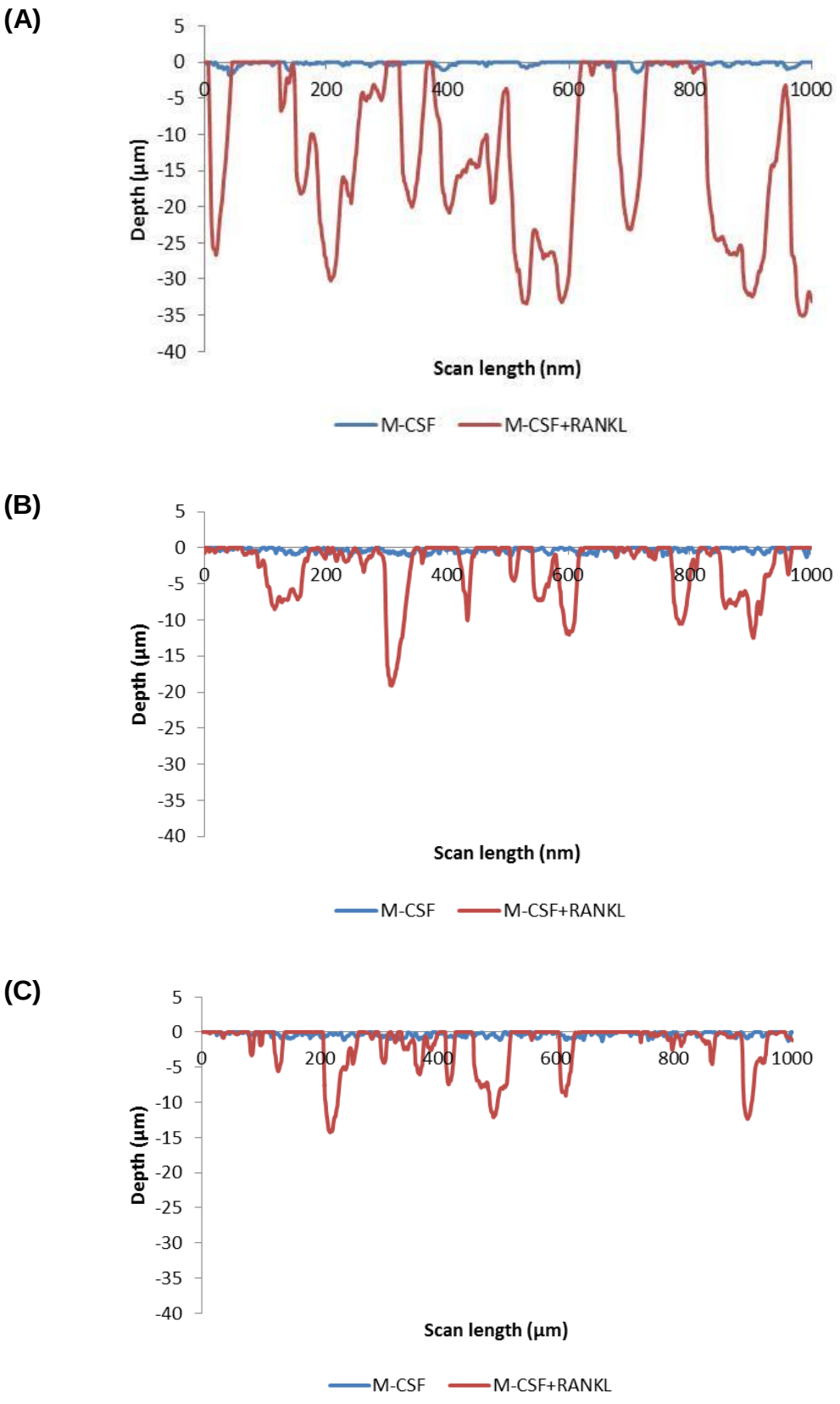

Figure 4-19 Representative surface profiles of bovine bone discs in M-CSF-treated cultures and in M-CSF+RANKL-treated cultures.

Surface profilometry revealed multi-shaped erosions in M-CSF+RANKL-treated cultures (red line) in a Charcot patient (A), diabetic patient (B) and healthy control subject (C). This is in contrast to M-CSF-treated cultures (blue line), where the erosion profile appeared as almost straight line cultures in a Charcot patient (A), diabetic patient (B) and healthy control subject (C).

The addition of OPG reversed the multi-shaped resorption pits noted in M-CSF+RANKL cultures and the erosion profile in M-CSF+RANKL+OPG-treated cultures appeared as almost a straight line in all study groups (Figure 4-20).

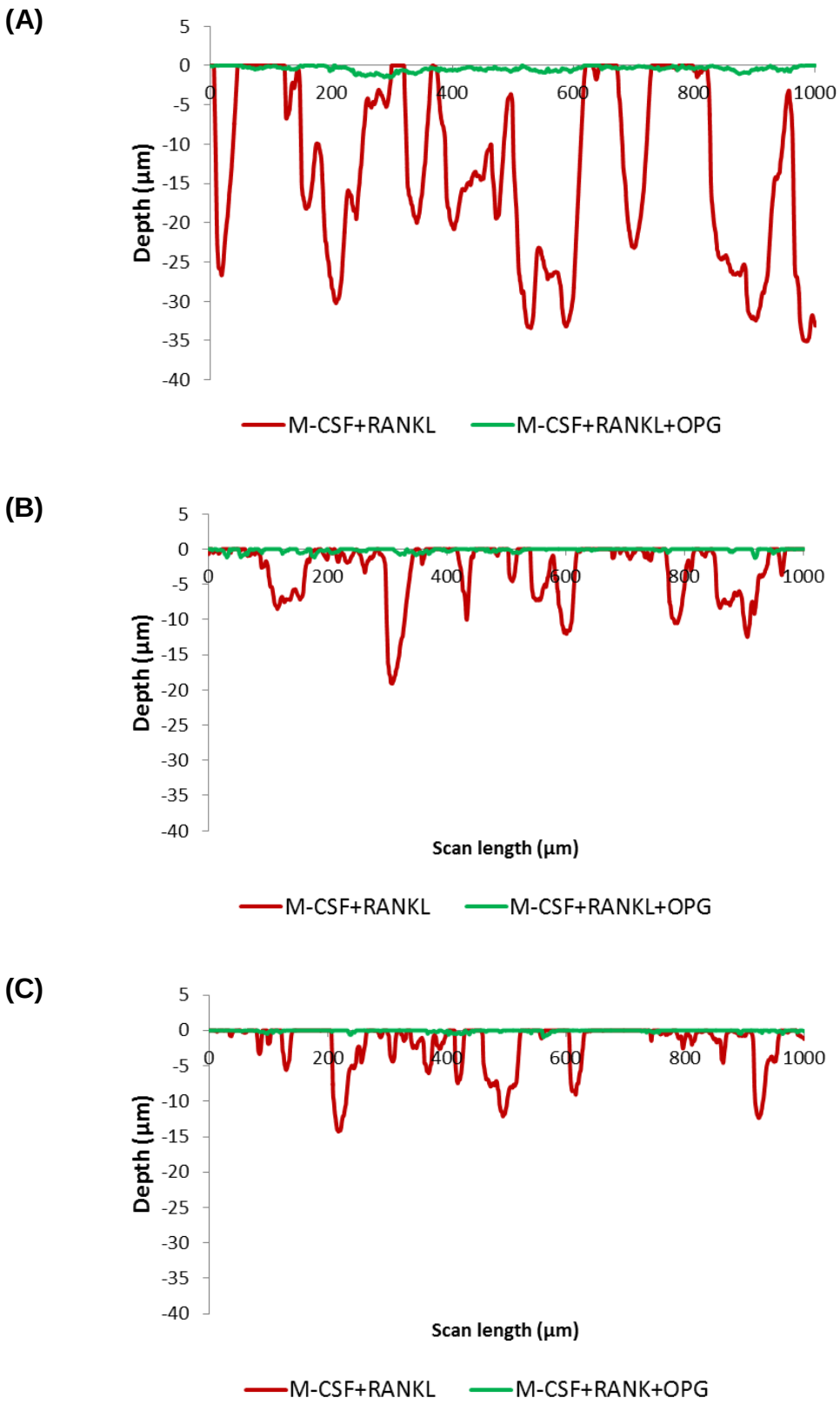

Figure 4-20 Representative surface profiles of bovine bone discs in M-CSF+RANKL-treated cultures and in M-CSF+RANKL+OPG-treated cultures.
The multi-shaped erosions in M-CSF+RANKL-treated cultures (red line) in a Charcot patient (A), diabetic patient (B) and healthy control subject (C) were reversed after the addition of OPG (green line) in all study groups. The erosion profile in M-CSF+RANKL+OPG-treated cultures appeared as almost straight line cultures in a Charcot patient (A), diabetic patient (B) and healthy control subject (C).

Comparison of the erosion profile of resorbed bovine bone discs in M-CSF+RANKL-treated cultures showed a marked difference between the three groups. The erosions appeared greater and deeper in Charcot patients compared to erosions in diabetic patients and healthy controls (Figure 4-21).

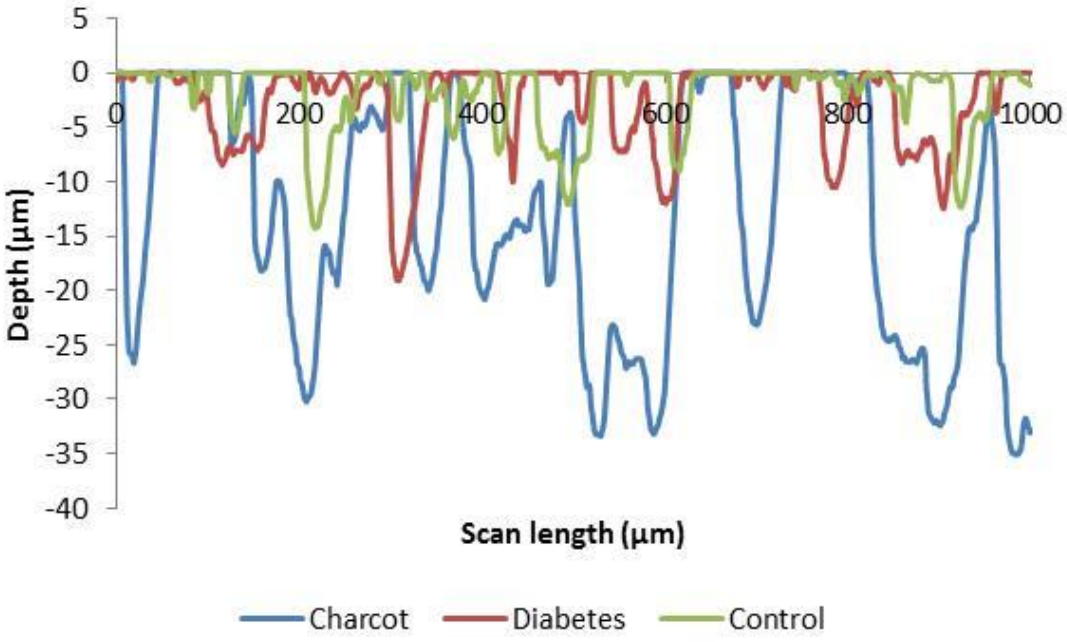

Figure 4-21 Comparison of surface profile measurements between Charcot patient, diabetic patient and healthy control subject in M-CSF+RANKL treated cultures.
The surface profile measurements of resorbed bone discs in M-CSF+RANKL-treated cultures revealed that pits were larger and deeper in a Charcot patient (blue line) compared with pits in a diabetic patient (red line) and healthy control subject (green line).

The area of resorption under the surface after surface profilometry was significantly greater in Charcot patients compared with diabetic patients and healthy control subjects ($p<0.05$). Furthermore, in the pairwise comparisons the area of resorption under the surface was also significantly greater in Charcot patients compared with diabetic patients ($p<0.01$) and also in Charcot patients compared with healthy control subjects ($p<0.01$), (Figure 4-22). Interestingly, the area of resorption under the surface was significantly greater in diabetic patients compared with healthy control subjects ($p<0.05$), (Figure 4-22).

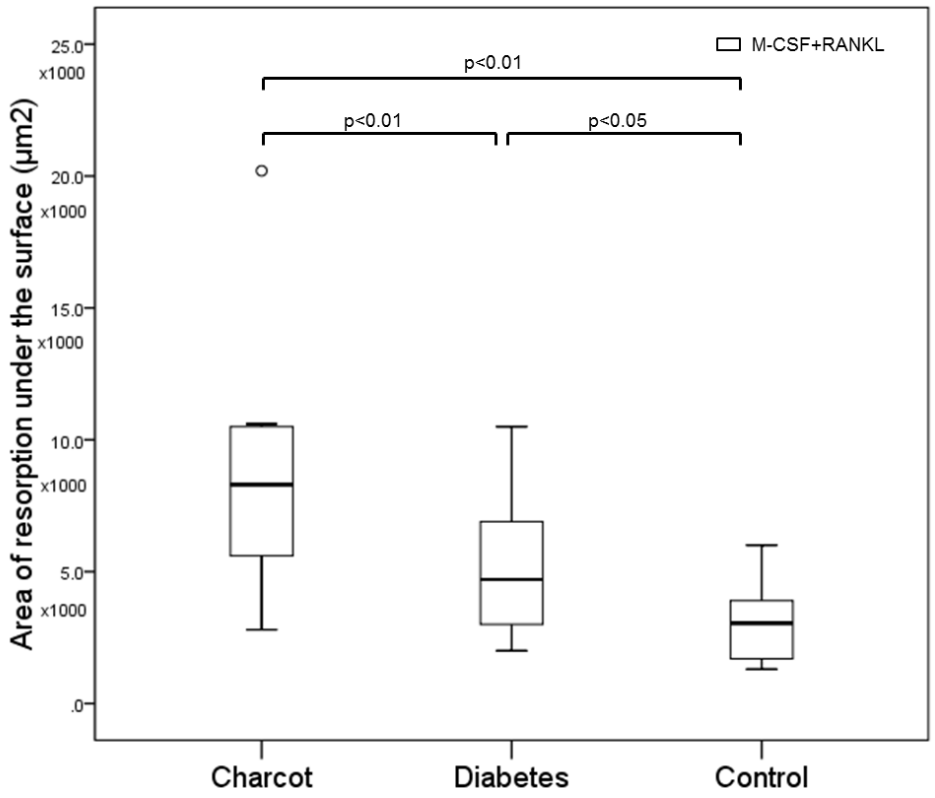

Figure 4-22 Osteoclast resorption on bovine bone discs in Charcot patients, diabetic patients and healthy control subjects in M-CSF+RANKL-treated cultures as assessed by surface profilometry;
Significance assessed by Mann-Whitney U test, Levels of significance are demonstrated on the graph. Significant increase in the area of bone resorption under the surface on bovine bone discs in M-CSF+RANKL-treated cultures between Charcot patients and diabetic patients (p<0.01) and Charcot patients and healthy control subjects (p<0.01). Non-significant difference was noted between diabetic patients and healthy control subjects, (p>0.05).

4.4.7 Pit morphology in M-CSF+RANKL-treated cultures

To assess in more detail the differences in resorption under the surface, I next assessed pit morphology. In M-CSF+RANKL-treated cultures, pit parameters were different between Charcot patients, diabetic patients and healthy control subjects. Uni-dented-pits were significantly wider (median FWHM, $p<0.05$) and deeper (median depth, $p<0.05$) in Charcot patients compared with those in diabetic patients and healthy control subjects. Although the bi-dented pits were not significantly different between the three groups, the multi-dented pits were significantly wider (median width, $p<0.05$) and deeper

(median depth, p<0.05) in Charcot patients compared with the multi-dented in diabetic patients and healthy control subjects, (Table 4-4)

Table 4-4 Measurements of uni-, bi- and multi-dented pits in M-CSF+RANKL-treated cultures in Charcot patients, diabetic patients and healthy control subjects

Pits	Parameter	Charcot	Diabetes	Control	p-value
Uni-dented	Width (µm)	57 [52-61]	48 [43-56]	39 [37-49]	>0.05
	FWHM (µm)	27 [24-30]	20 [18-23]	18 [17-21]	<0.05
	Depth (µm)	11 [9-13]	7 [4-9]	6 [4.3-7.2]	<0.05
Bi-dented	Width (µm)	88 [82-95]	91 [72-106]	74 [69-81]	>0.05
	FWHM (µm)	50 [44-54]	49 [38-60]	39 [34-41]	>0.05
	Depth (µm)	15 [11-19]	14 [10-19]	12 [9-14]	>0.05
Multi-dented	Width (µm)	180 [161-215]	154 [131-210]	119 [108-128]	<0.05
	FWHM (µm)	110 [100-130]	86 [71-143]	70 [58-78]	>0.05
	Depth (µm)	22 [19-28]	24 [19-27]	13 [12-15]	<0.05

Data expressed as median [25^{th}-75^{th} percentile] and analysed by the Kruskal-Wallis test; P-values indicate differences between Charcot patients, diabetic patients and healthy control subjects
Significant increase in the FWHM and depth of the uni-dented pits and also in the width and depth of the multi-dented pits in Charcot patients compared with diabetic patients and healthy control subjects (p<0.05 for all comparisons); Non-significant difference in the width of the uni-dented pits as well as in the width, FWHM and depth of the bi-dented pits and FWHM of the multi-dented pits (p>0.05 for all comparisons)

Data on pairwise comparisons of pit parameters (width, FWHM and depth) is presented below (Table 4-5).

Table 4-5 Pairwise comparisons of pit parameters (width, FWHM and depth) in M-CSF+RANKL-treated cultures

Pits	Parameter	Charcot versus Diabetes (P1-value)	Charcot versus Control (P2-value)	Diabetes versus control (P3-value)
Uni-dented	Width (µm)	>0.05	<0.05	>0.05
	FWHM (µm)	<0.05	<0.01	>0.05
	Depth (µm)	<0.05	<0.01	>0.05
Bi-dented	Width (µm)	>0.05	<0.05	>0.05
	FWHM (µm)	>0.05	<0.05	>0.05
	Depth (µm)	>0.05	>0.05	>0.05
Multi-dented	Width (µm)	>0.05	<0.01	<0.05
	FWHM (µm)	>0.05	<0.01	>0.05
	Depth (µm)	>0.05	<0.05	<0.01

Data is analysed with Mann-Whitney U test; Levels of significance are presented; P1-values indicate differences between Charcot patients and diabetic patients; P2-values indicate differences between Charcot patients and healthy control subjects and P3-values indicate differences between diabetic patients and healthy control subjects.
Significant increase in FWHM and depth of uni-dented pits in M-CSF+RANKL-treated cultures between Charcot patients and diabetic patients (P1<0.05 for both comparisons). Non-significant difference in the depth of uni-dented pits and also in the width, FWHM and depth of the bi-dented and multi-dented pits between Charcot patients and diabetic patients. (P1>0.05 for all comparisons)
Significant increase in the width (P2<0.05), FWHM (P2<0.01) and depth (P2<0.01) of uni-dented pits, in the width (P2<0.05) and FWHM (P2<0.05) of bi-dented pits and also in the width (P2<0.01), FWHM (P2<0.01) and depth (P2<0.05) of multi-dented pits in M-CSF+RANKL-treated cultures between Charcot patients and healthy control subjects. Non-significant difference in the depth of bi-dented pits between Charcot patients and controls (P2>0.05).
Non-significant difference in the width, FWHM and depth of uni-dented, bi-dented and multi-dented pits in M-CSF+RANKL-treated cultures between diabetic patients and healthy control subjects (P3>0.05 for all comparisons).

To determine whether there were any differences in the pit distribution according to their shape, I compared the percentage of uni-dented, bi-dented and multi-dented pits in M-CSF+RANKL-treated cultures. The percentage of uni-dented pits was significantly reduced in Charcot patients compared with diabetic patients and healthy control subjects

(p<0.05). Although the percentage of bi-dented pits was similar between the three study groups (p>0.05), the percentage of multi-dented pits was significantly increased in Charcot patients compared with diabetic patients and healthy control subjects (p<0.05), (Table 4-6).

Table 4-6 **Percentage of uni-, bi- and multi-dented pits in M-CSF+RANKL-treated cultures in Charcot patients, diabetic patients and healthy control subjects**

Pits	Charcot	Diabetes	Controls	p-value
Uni-dented	36% [31-43]	46% [45-56]	62% [57-66]	p<0.05
Bi-dented	24% [20-28]	22% [18-25]	21% [20-22]	p>0.05
Multi-dented	40% [32-41]	32% [22-33]	17% [17-23]	p<0.05

Data expressed as median [25th-75th percentile] and analysed by the Kruskal-Wallis test; P-values indicate differences between Charcot patients, diabetic patients and healthy control subjects.
Significant increase in the percentage of multi-dented pits and significant decrease in the percentage of uni-dented pits in Charcot patients compared with diabetic patients and healthy control subjects (p<0.05 for both comparisons). Non-significant difference in the percentage of bi-dented pits between the three study groups (p>0.05).

Data on pairwise comparisons of the pit distribution according to their shape between the groups is presented below (Table 4-7).

Table 4-7 Pairwise comparisons of pit distribution (%) in M-CSF+RANKL-treated cultures

Pits	Charcot versus diabetes (P1-value)	Charcot versus control (P2-value)	Diabetes versus Controls (P3-value)
Uni-dented pits (%)	<0.05	<0.01	<0.05
Bi-dented pits (%)	>0.05	>0.05	>0.05
Multi-dented pits (%)	>0.05	<0.01	>0.05

Data is analysed with Mann-Whitney U test; Levels of significance are presented; P1-values indicate differences between Charcot patients and diabetic patients; P2-values indicate differences between Charcot patients and healthy control subjects and P3-values indicate differences between diabetic patients and healthy control subjects

Thus in M-CSF+RANKL treated cultures surface profilometry revealed that in Charcot patients newly formed osteoclasts exhibited increased resorbing activity under the surface with abnormal resorption profile, pit morphology and distribution.

4.4.8 Temporal characteristics of bone resorption in Charcot patients and healthy control subjects– the role of RANKL in osteoclastogenesis

The observed enhanced resorptive activity of monocytes derived from Charcot patients in 21 day M-CSF+RANKL-treated cultures required further investigation. I next investigated resorption on bovine bone discs at day 14. At this stage, cell proliferation and differentiation from monocytes has occurred and the resorption has commenced. It is possible that in Charcot patients, the newly-formed osteoclasts acquire their resorptive profile earlier than controls, which can explain the extensive resorption at day 21.

To explore this hypothesis, I studied 3 Charcot patients and in 3 healthy control subjects and measured bone resorption on bovine bone discs at day 14 (resorption at and under the surface, erosion profile and pit characteristics). I compared resorption at day 14 and day 21 in Charcot patients and control subjects.

4.4.8.1 Bone resorption on bovine bone discs in Charcot patients and controls subjects at day 14

At day 14, light microscopy showed the presence of pits on bovine bone discs in cultures from Charcot patients and healthy control subjects (Figure 4-23).

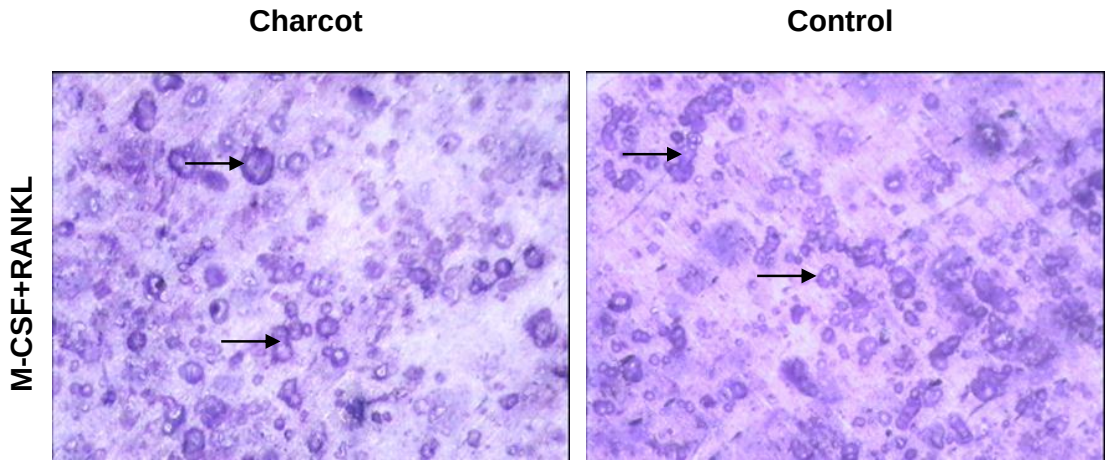

Figure 4-23 Representative images of bovine bone discs in M-CSF-RANKL-treated cultures in a Charcot patient and healthy control subject at day 14 (light microscopy).
Round resorption pits were noted in both Charcot patient and healthy control subject. In Charcot patients pits appeared larger. The arrows denote some of the pits (magnification X40).

In addition, immunofluorescent microscopy revealed bone resorbing osteoclasts formed on bovine bone discs in cultures from Charcot patients and healthy control subjects as indicated by the presence of actin ring positive multi-nucleated cells (Figure 4-24).

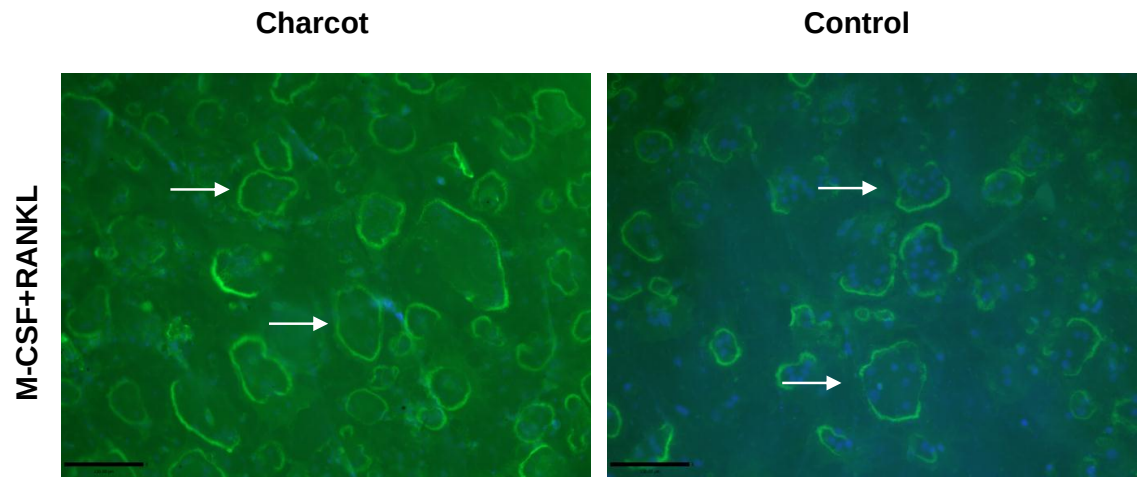

Figure 4-24 Immunofluorescent images of bovine bone discs in M-CSF+RANKL-treated cultures at day 14.
Multi-nucleated actin ring positive cells were noted on bovine bone discs in M-CSF+RANKL-treated cultures in both Charcot patient and healthy control subject. The white arrows denote some of the multi-nucleated positive cells. The blue staining denotes the nuclei; the green staining denotes the actin rings; (magnification, X100; scale bar – 130 µm)

The area of bone resorption on bone discs at day 14 in Charcot patients (15% [10.6-21.6]) was greater compared with the area of resorption in healthy control subjects (11% [9.9-11.8]) but this finding did not reach significance, ($p>0.05$).

Surface profile measurements of resorbed bovine bone discs in Charcot patients and healthy control subjects in M-CSF+RANKL-treated cultures at day 14 showed the presence of early resorption pits and representative erosion profiles are presented below (Figure 4-25).

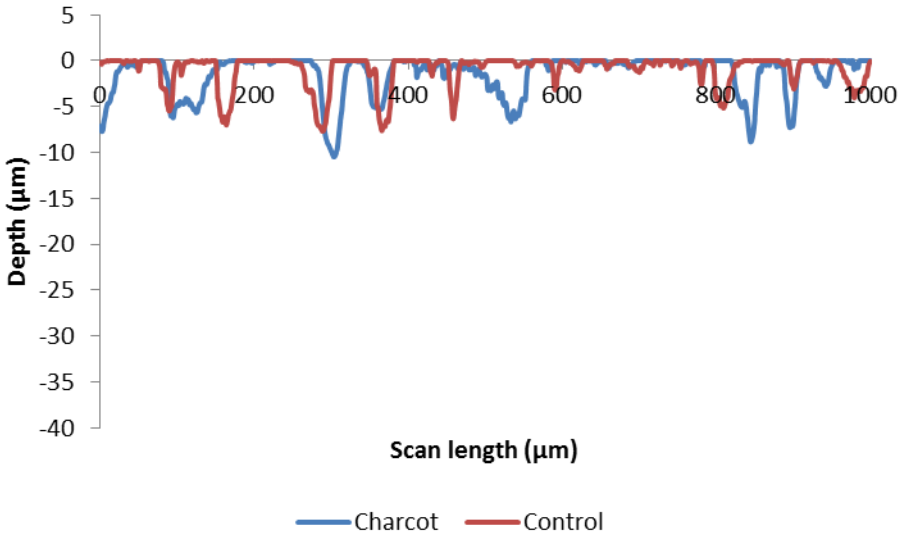

Figure 4-25 Surface profile measurements of resorbed bovine bone discs in a Charcot patient and healthy control subject in M-CSF+RANKL-treated cultures at day 14
Surface profilometry revealed multi-shaped erosions in M-CSF+RANKL-treated cultures at day 14 in a Charcot patient (blue line) and in a healthy control subject (red line).

The area of resorption under the surface at day 14 in Charcot patients ($2.5x10^3$ μm^2 [$1.8x10^3$-$2.9x10^3$]) was 3 times higher than in healthy control subjects ($0.8x10^3$ μm^2 [$0.7x10^3$-$1.0x10^3$]), but this finding did not reach significance ($p>0.05$).

4.4.8.2 Pit morphology and distribution in M-CSF+RANK-treated cultures in Charcot patients and healthy control subjects at day 14

To assess in more detail the differences in the resorption under the surface in M-CSF+RANKL-treated cultures at day 14, I next compared pit morphology. Pit parameters were different between Charcot patients and healthy control subjects. In Charcot patients, uni-dented pits were wider (both at the surface and at FWHM) compared with pits from control cultures ($p=0.05$), (Table 4-8). Moreover, multi-dented pits were significantly deeper ($p<0.05$) and wider at FWHM ($p<0.05$), (Table 4-8). In addition, bi-dented pits were also significantly wider at FWHM ($p<0.05$) in Charcot patients compared with controls (Table 4-8). Furthermore, multi-dented pits were significantly deeper in Charcot patients compared with controls.

Table 4-8 **Measurements of uni-, bi- and multi-dented pits in M-CSF+RANKL-treated cultures in Charcot patients and healthy control subjects at day 14.**

Pits	Parameter	Charcot	Control	p-value
Uni-dented	Width (µm)	56 [50-57]	40 [36-41]	0.05
	FWHM (µm)	25 [22-29]	17 [16-18]	0.05
	Depth (µm)	9 [7-9]	4 [4-6]	>0.05
Bi-dented	Width (µm)	93 [80-93]	65 [58-69]	>0.05
	FWHM (µm)	48 [44-48]	30 [25-31]	<0.05
	Depth (µm)	11 [9-11]	9 [6-9]	>0.05
Multi-dented	Width (µm)	119 [110-119]	100 [91-102]	>0.05
	FWHM (µm)	94 [89-94]	45 [34-48]	<0.05
	Depth (µm)	16 [16-19]	10 [8-12]	<0.05

Data are presented as median [25th-75th percentile] and analysed with Mann-Whitney U test; Multi-dented pits were significantly deeper and wider at FWHM in Charcot patients compared with controls (**p<0.05); bi-dented pits were significantly wider at FWHM (p<0.05). In Charcot patients, uni-dented pits were wider (both at the surface and at FWHM) compared with pits from control cultures, (p=0.05).**

There was no difference in the distribution of pits according to their shape between the two groups at day 14 and the percentage of uni-, bi- and multi-dented pits was similar between Charcot patients and controls (Table 4-9).

Table 4-9 Pairwise comparison of distribution of pits (%) in M-CSF+RANKL treated cultures in Charcot patients and controls at day 14

Percentage (%)	Charcot	Control	p-value
Uni-dented	71 [71-73]	73 [71-77]	>0.05
Bi-dented	17 [15-20]	21 [18-23]	>0.05
Multi-dented	12 [10-13]	6 [4-7]	>0.05

Data are presented as median [25th-75th percentile] and analysed with Mann-Whitney U test; Non-significant distribution of uni-dented, bi-dented and multi-dented pits between Charcot patients and healthy control subjects (p>0.05 for all comparisons).

Thus in M-CSF+RANKL-treated cultures, newly formed osteoclasts exhibited a trend of enhanced resorbing activity (at the surface and under the surface) and increased erosion profile in Charcot patients compared with healthy control subjects.

4.4.8.3 Comparison of bone resorption on bovine bone discs in Charcot patients and controls subjects in M-CSF+RANKL-treated cultures between day 14 and day 21

Observation of bovine bone discs at day 14 and at day 21 revealed an increase of bone resorption in both Charcot patients and control subjects (Figure 4-26).

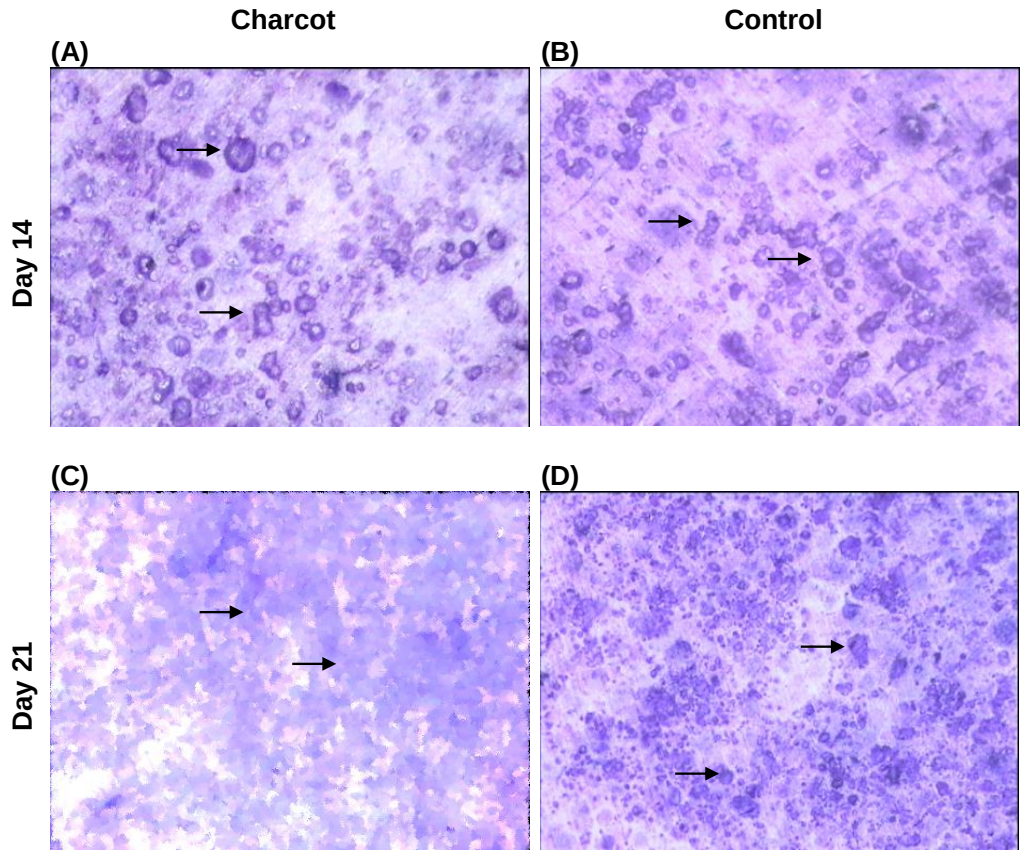

Figure 4-26 Representative images of resorbed bovine bone discs in M-CSF+RANKL-treated at day 14 and day 21 (light microscopy)
Comparison of resorption on bovine bone discs in M-CSF+RANKL-treated cultures between day 14 and day 21 in a Charcot patient (A, C) and healthy control subject (B, D). At day 14, the majority of resorption appeared as single round pits in both Charcot patient (A) and healthy control subject (B). At day 21, resorption more frequently appeared as lacunae in cultures from Charcot patient (C) compared with cultures from control subject (D). The black arrows denote some of the pits (magnification X40).

There was an increase in the area of resorption at the surface between day 14 and day 21 in M-CSF+RANKL-treated cultures in both Charcot patients (from 15% [10.6-21.6] to 46% [43.4-49.1], p=0.05) and controls (from 11% [9.9-11.8] to 15% [14.5-18.01], p=0.05) as expected. However, the response in Charcot patients was exuberant, resulting in a three-fold increase in the area of resorption at the surface in contrast to the noted 1.4 fold increase in healthy control subjects (Figure 4-27).

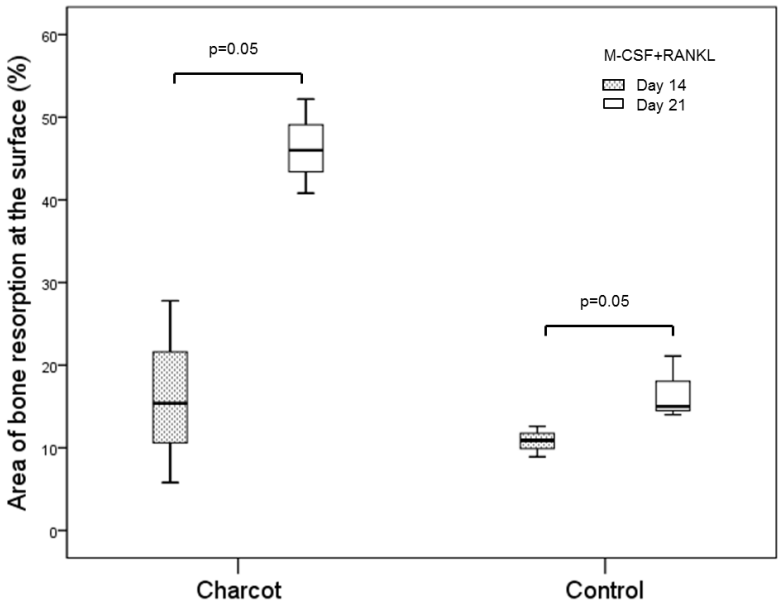

Figure 4-27 Osteoclast resorption on bovine bone discs in Charcot patients and healthy control subjects in M-CSF+RANKL-treated cultures as assessed by image analysis at day 14 and at day 21;
Significance assessed by Mann-Whitney U test, Levels of significance are demonstrated on the graph.
There was an increase in the area of resorption at the surface of bovine bone discs in both Charcot patients (p=0.05) and healthy control subjects (p=0.05) in M-CSF+RANKL-treated cultures between day 14 and day 21.

Erosion profile measurements significantly increased at day 21 compared to day 14 in both Charcot subjects and healthy controls. Resorption pits at day 21 appeared significantly deeper and wider compared with resorption pits at day 14 in both Charcot patients and controls, (Figure 4-28).

(A)

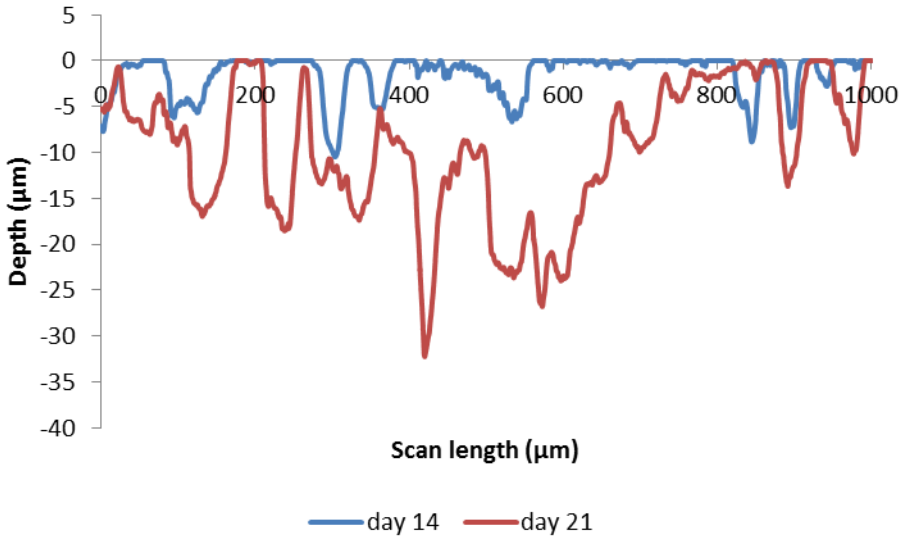

(B)

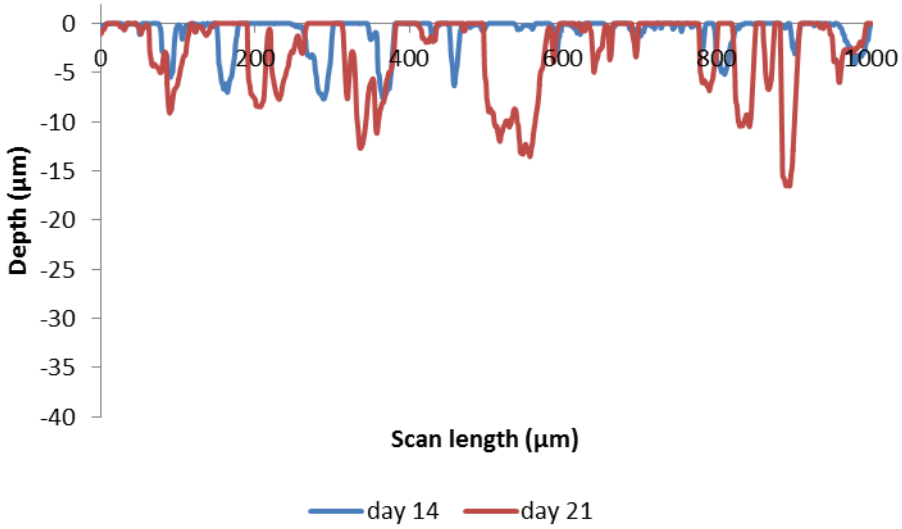

Figure 4-28 Representative surface profiles of bone discs in M-CSF+RANKL-treated cultures at day 14 and day 21.
The erosion profile increased between day 14 (blue line) and day 21 (red line) in M-CSF+RANKL-treated cultures in both Charcot patient (A) and healthy control subject (B). The increase of the erosion profile was more notable in Charcot patients compared with control subjects.

In both Charcot patients and control subjects, the area of bone resorption under the surface significantly increased between day 14 and day 21 (Charcot patients from $2.5x10^3$ µm^2 [$1.8x10^3$-$2.9x10^3$] to $8.3x10^3$ µm^2 [$6.9x10^3$-$9.5x10^3$], p=0.05 and controls from $0.8x10^3$ µm^2 [$0.7x10^3$-$1.0x10^3$] to $1.7x10^3$ µm^2 [$1.7x10^3$-$3.0x10^3$], p=0.05), resulting in a 4-fold increase in Charcot patients in contrast to a 2-fold increase noted in the healthy control subjects, (Figure 4-29)

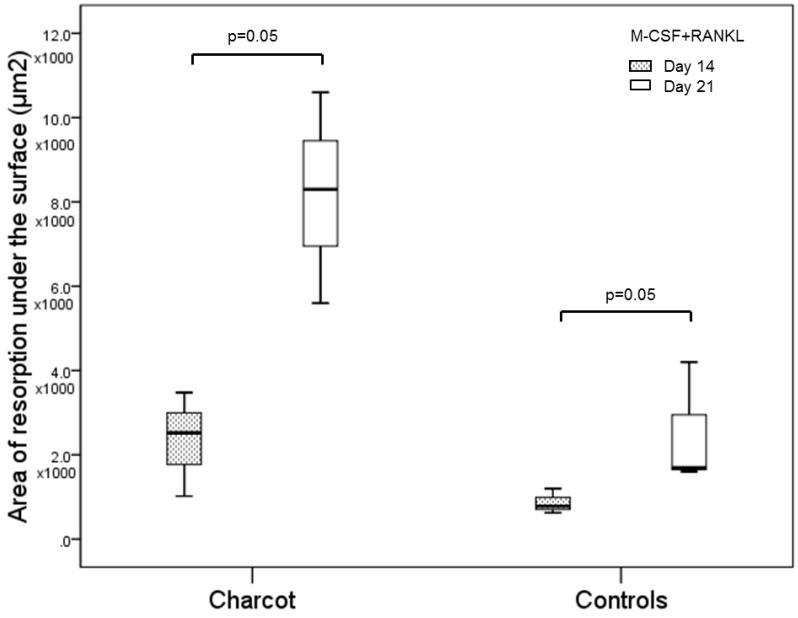

Figure 4-29 Resorption under the surface in M-CSF+RANKL-treated cultures at day 14 and day 21 in Charcot patients and healthy control subjects after;
Significance assessed by Mann-Whitney U test, Levels of significance are demonstrated on the graph.
There was an increase in the area of resorption under the surface of bovine bone discs in both Charcot patients (p=0.05) and healthy control subjects (p=0.05) in M-CSF+RANKL-treated cultures between day 14 and day 21.

The distribution of pits according to their shape between day 14 and 21 changed in both Charcot patients and healthy control subjects, (Figure 4-30).

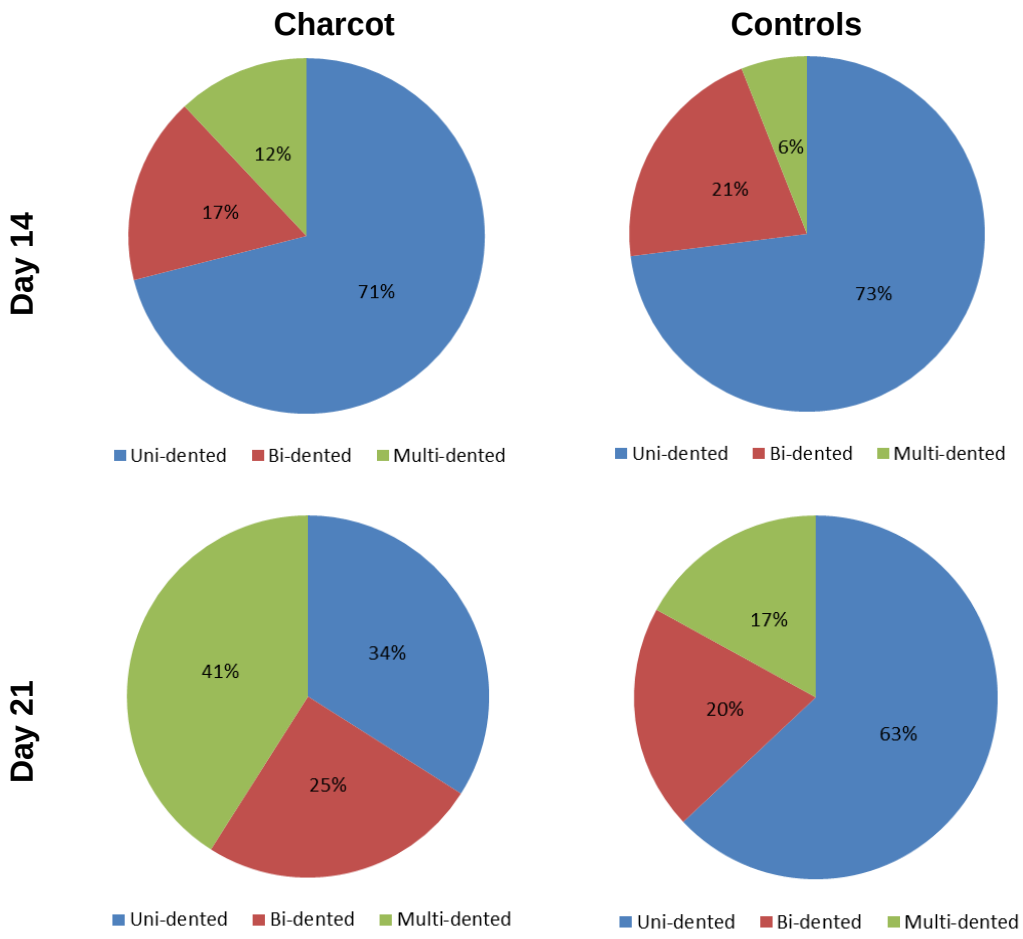

Figure 4-30 Distribution of pits according to their shape at day 14 and at day 21 in M-CSF+RANKL treated cultures in Charcot patients and healthy control subjects.
Non-significant distribution of uni-dented, bi-dented and multi-dented pits between Charcot patients and controls at day 14 ($p>0.05$). Significant increase in the percentage of multi-dented pits between day 14 and day 21 was noted in both Charcot patients ($p<0.05$) and controls ($p<0.05$). Significant decrease in the percentage of uni-dented pits was noted only in Charcot patients ($p<0.05$). At day 21, uni-dented pits were 2 times less frequent in Charcot patients compared with controls ($p<0.05$).

In Charcot patients the percentage of uni-dented pits significantly decreased from 71% [71-73] to 34% [30-36], ($p<0.05$). Although there was no significant difference in the percentage of bi-dented pits (from 17% [15-20] to 25% [21-27], $p>0.05$), there was a significant increase in the percentage of multi-dented pits between day 14 and 21 (from 12% [10-13] to 41% [37-47], $p<0.05$).

In controls, there was no significant difference in the percentage of uni-dented (73% [71-77] versus 63% [56-67], $p>0.05$) and bi-dented pits (21% [18-23] versus 20%

[20-22] p>0.05) between day 14 and 21, although a significant increase of the percentage of multi-dented pits was noted (from 6% [4-7] to 17% [13-22], p<0.05).

4.5 Discussion

Using a well-established *in vitro* assay together with the novel application of surface profilometry, I demonstrated that osteoclastic activation in acute Charcot osteoarthropathy is mediated by RANKL. Fully differentiated osteoclasts derived from Charcot patients exhibited enhanced resorbing activity both on the surface and under the surface in response to M-CSF+RANKL treatment. This resorption was blocked by the addition of excess concentrations of OPG, confirming the role of RANKL as an activator of osteoclastic activity in acute Charcot osteoarthropathy.

To assess the role of RANKL in osteoclastic activity I used three main culture conditions: 1) M-CSF-treated cultures; 2) M-CSF+RANKL- treated cultures and 3) M-CSF+RANKL+OPG-treated cultures

Data from M-CSF-treated cultures demonstrated that the infrequently noted TRAP-positive multi-nucleated cells formed on plastic were not able to carry out resorption on bovine bone discs as assessed by image analysis (toluidine blue and actin ring staining) and also by surface profilometry. Indeed, although M-CSF is an essential factor for proliferation, differentiation and survival of the monocyte-macrophage lineage, it is not an osteoclastogenic factor (Henriksen, Bollerslev et al. 2011) and therefore the lack of resorption pits and actin ring positive cells on bovine bone discs in this culture treatment was not unusual. These cultures served as negative control and the response to M-CSF was comparable between Charcot patients, diabetic patients and healthy control subjects.

The addition of RANKL to M-CSF-treatment triggered both osteoclast formation and osteoclast resorption in the three study groups, as expected and these cultures served as positive control. It is well established that osteoclastogenesis is pivotally

dependent on the presence of both cytokines as M-CSF serves as a survival factor whereas RANKL is a key factor for osteoclast differentiation and regulation, (Tanaka, Takahashi et al. 1993, Yasuda, Shima et al. 1998). In the presence of M-CSF and RANKL, monocytes, which express the receptors c-fms and RANK, proliferate and differentiate into mature multi-nucleated osteoclasts (Teitelbaum 2007, Henriksen, Bollerslev et al. 2011). My results demonstrated that newly-derived osteoclasts from monocytes isolated from Charcot patients exhibited enhanced resorbing activity to RANKL which was not associated with an increase in osteoclast formation. Although the number of TRAP-positive cells was not significantly different between Charcot patients, diabetic patients and healthy control subjects, the area of resorption on bovine bone discs in Charcot patients was significantly increased compared with controls. Thus osteoclasts generated from Charcot patients were functionally more aggressive than osteoclasts from diabetic patients and healthy control subjects in a classical resorption assay in keeping with our previous observations (Mabilleau, Petrova et al. 2008, Petrova, Petrov et al. 2014). In addition, surface profilometry demonstrated that osteoclasts from Charcot patients exhibited a considerable below-surface resorbing activity (Petrova, Petrov et al. 2014). In Charcot patients, there was an abnormal erosion profile on bovine bone discs with resorptions displaying aberrant morphological appearance and distribution. In M-CSF+RANKL-treated cultures, resorption pits appeared larger and deeper in Charcot patients compared with diabetic patients and healthy control subjects and more frequently presented as multi-dented pits. In addition, at the time of commencing of bone resorption *in vitro* (day 14), osteoclastic activity in Charcot patients was already upregulated, as indicated by the presence of larger and wider pits on bovine bone discs together with enhanced area of bone resorption. Although for some of the observed differences at day 14 between Charcot patients and controls, the p-value was equal to rather than less than 0.05, my results indicate that early osteoclasts derived from Charcot patients are primed to exhibit an enhanced resorptive profile. Furthermore, in Charcot patients but not in controls, surface profilometry revealed that in M-CSF+RANKL-treated cultures at day 14 compared to M-CSF+RANKL-treated cultures at

day 21, there was a significant increase of the percentage of multi-dented pits and a significant reduction of the percentage of uni-dented pits, indicating that Charcot-derived osteoclasts exhibit a highly- active mode of resorption.

These findings indicate a role of RANKL as an osteoclastic activator. These observations may not be unique to Charcot osteoarthropathy and indeed similar observations have been reported in other conditions associated with increased bone resorption such as rheumatoid arthritis in which the addition of RANKL resulted in a significant increase in the resorption of bone discs but did not lead to a significant increase in the number of TRAP- positive multi-nucleated cells (Hirayama, Danks et al. 2002). Overall, the observed extensive resorption activity in M-CSF+RANKL-treated cultures in Charcot patients, as compared to diabetic patients or healthy control subjects, may suggest that in patients with Charcot osteoarthropathy circulating osteoclast precursors are in a more highly activated state and as such are more primed to become osteoclasts (mediated through RANKL) with enhanced resorbing activity, than in the control groups (with and without diabetes).

The addition of OPG inhibited osteoclast formation and resorption in all study groups. This cytokine blocks the RANKL-RANK interaction on mononuclear osteoclast precursors, thus abolishing the process of osteoclast differentiation and activation. The inhibition of bone resorption after the addition of OPG to M-CSF+RANKL-treatment indicated that the up-regulated osteoclastic activity in Charcot patients is mediated by RANKL.

A limitation to my *in vitro* study is the presence of residual resorption pits in M-CSF- and M-CSF+RANKL+OPG- treated cultures. A previous *in vitro* study in Charcot patients has also reported bone resorption on dentine discs in M-CSF-treated cultures (<0.3%) and M-CSF+RANKL+OPG-treated cultures (<6%), (Mabilleau, Petrova et al. 2008). It is possible that RANKL-independent factors might have primed monocytes to differentiate into bone resorbing osteoclasts. Osteoclastogenic mediators other than RANKL that have been reported to stimulate osteoclast differentiation independently of

the RANKL pathway include TNF-α (Kobayashi, Takahashi et al. 2000), IL-6 (Kudo, Sabokbar et al. 2003), and LIGHT (homologous to lymphotoxins exhibiting inducible expression and competing with herpes simplex virus glycoprotein D for herpes virus entry mediator, a receptor expressed by T lymphocytes), (Edwards, Sun et al. 2006). The role of these which stimulate osteoclastogenesis independently of RANK/RANKL mechanisms in osteoclastic activity in Charcot osteoarthropathy is unknown. Alternatively, the relatively scattered distribution of these pits, noted sporadically in all study groups in M-CSF- and M-CSF+RANKL+OPG-treated cultures in our present study, could be due to trace (permissive) levels of RANKL.

Nevertheless, this study underscores the role of RANKL in the pathogenesis of pathological bone destruction in Charcot osteoarthropathy. This cytokine has already been identified as a mediator of vascular calcification in this condition. Peripheral artery specimens from Charcot patients, undergoing surgery identified positive RANKL staining in both medial and intimal calcified areas, which were not present in noncalcified areas or in specimens from control subjects (Ndip, Williams et al. 2011). Moreover, vascular smooth muscle cells from Charcot patients treated with RANKL showed a greater capacity to mineralise and this increased osteoblastic differentiation was inhibited by OPG, confirming the role of RANKL in the process of calcification (Ndip, Williams et al. 2011). I have shown that newly formed osteoclasts, derived from patients with Charcot osteoarthropathy, exhibit extensive resorbing activity in the presence of M-CSF+RANKL, a response which is attenuated by OPG. In the vessel wall, progenitor cells differentiate into osteoblast-like cells, depositing mineralised matrix, whereas in bone, the enhanced osteoclastic activation results in osteolysis and severe bone damage (Petrova and Shanahan 2014).

In addition to the traditional osteoclast culture assay, I have employed a novel technique to measure surface profilometry. This technique has been used for the first time as a tool to quantitate bone resorption. It revealed that in M-CSF+RANKL-treated cultures, in Charcot patients, resorption pits exhibited aberrant erosion profile and pit

morphology. It is possible that other factors or a combination of factors might have primed osteoclastic precursors to differentiate into highly aggressive osteoclastic phenotype, which requires further studies.

4.6 Conclusion

My present experiments confirmed the usefulness of the osteoclast culture assay as an important model to study the cellular mechanisms involved in the process of pathological bone resorption of the acute Charcot foot.

Using traditional cell culture assay together with surface profilometry, I have confirmed that RANKL upregulation drives the enhanced osteoclastic activity in osteoclasts derived from patients with acute Charcot osteoarthropathy.

Chapter 5 The role of the proinflammatory cytokine TNF-α on osteoclastic activity *in vitro* in patients with acute Charcot osteoarthropathy

5.1 Introduction

Using a traditional osteoclast assay, initially in a pilot study and subsequently in a more extensive study, I have demonstrated the role of RANKL as an osteoclastic activator in acute Charcot osteoarthropathy (Mabilleau, Petrova et al. 2008). Moreover, surface profilometry unmasked the aberrant erosion profile of bovine bone discs resorbed by osteoclasts derived from patients with Charcot osteoarthropathy in the presence of M-CSF+RANKL (Petrova, Petrov et al. 2014).

However, the extensive bone destruction that occurs in the affected Charcot foot can only partially be attributed to the enhanced activation of RANKL. Normally, up-regulation of RANKL would lead to systemic bone loss, but in Charcot osteoarthropathy, bone loss is limited to the inflamed affected foot, (Petrova, Foster et al. 2005), (Jirkovska, Kasalicky et al. 2001). Furthermore, there is a greater reduction of bone mineral density of the Charcot foot compared with the non-Charcot foot (Petrova, Foster et al. 2005) and peripheral osteopenia is not always associated with a reduction of bone mineral density of the axial skeleton (Jirkovska, Kasalicky et al. 2001). This suggests that factors limited to the inflamed Charcot foot may be fundamental and it is possible that proinflammatory cytokines can act as modulators of local pathological osteolysis (Jeffcoate, Game et al. 2005).

In my studies, I have explored the possible role of TNF-α and lL-6 on osteoclastogenesis as I have found that their concentrations are raised in the sera of patients with acute Charcot osteoarthropathy (Petrova, Dew et al. 2015). Furthermore, these cytokines are known to modulate osteoclastic activity in inflammatory bone loss (Zupan, Jeras et al. 2013); however, their role in Charcot osteoarthropathy is unknown.

In this chapter, I describe my experiments aiming to assess the role of TNF-α on osteoclastogenesis.

5.2 Study objective

Data from clinical observation studies of cohorts of Charcot patients reported raised serum concentrations of TNF-α in the acute active stage of the disease followed by a significant fall at the time of clinical resolution (Petrova, Dew et al. 2015), (Uccioli, Sinistro et al. 2010). Serum concentrations of TNF-α not only correlate with the bone resorption marker C-terminal telopeptide (CTX), but also with the number of osteoclastic precursors and these observations indicate a potential link between inflammation and resorption (Petrova, Dew et al. 2015), (Mabilleau, Petrova et al. 2011).

As an osteoclastogenic mediator, TNF-α induces expression of RANKL in osteoblastic cells, but it can also act directly on osteoclastic precursors (monocytes) to potentiate RANKL-induced osteoclastogenesis and thereby activity (Lam, Abu-Amer et al. 2002). This cytokine is known to enhance osteoclastogenesis in rheumatoid arthritis (Walsh and Gravallese 2004, Romas 2005) and psoriatic arthritis (Ritchlin, Haas-Smith et al. 2003), and also in other forms of inflammatory osteolysis (Redlich and Smolen 2012). However, its role in osteoclastic activity in acute Charcot osteoarthropathy is unknown.

To determine the role of this cytokine in osteoclastogenesis, I compared osteoclast formation and resorption in M-CSF+RANKL-treated cultures with and without the addition of excessive concentrations of neutralising antibody to TNF-α (anti-TNF-α).

5.3 Research design and methods

Samples from peripheral blood were obtained from 10 consecutive patients with recent onset of acute Charcot osteoarthropathy, 8 diabetic patients with no history of Charcot osteoarthropathy and 9 healthy control subjects.

The PBMCs were isolated from whole blood as described in Chapter 2 and cultured on plastic to assess osteoclast formation and on bovine bone discs to assess osteoclast resorption. Osteoclast formation was assessed by counting the number of TRAP-positive cells multi-nucleated cells on plastic. Resorption was quantitated by two methods: (1) area of resorption on the surface (%) assessed by image analysis after light microscopy and (2) area of resorption under the surface (μm^2) assessed by surface profilometry, as described in Chapters 2 and 3. In addition, I compared the concentration of CTX, as a marker of resorption, in culture supernatant before and after the addition of anti-TNF-α to M-CSF+RANKL in Charcot patients (n=5) and in healthy control subjects (n=7).

5.3.1 Rationale for the study

To ascertain whether TNF-α modulates RANKL-mediated osteoclastic activity the following cultures were set up.

Culture 1: M-CSF+RANKL- treated cultures

This culture served as a positive control (25 ng/ml M-CSF added at day 0 and 100 ng/ml human soluble RANKL added at day 7).

Culture 2: M-CSF+RANKL+anti-TNF-α- treated cultures

Excess concentration of neutralising antibody to TNF-α was added to M-CSF+RANKL-treated cultures at day 0 (25 ng/ml M-CSF + 100 ng/ml sRANKL + 10 µg/ml anti-TNF-α (R&D Systems Europe). This culture was used to assess the role of TNF-α on osteoclastogenesis. The rationale for this study was to inhibit TNF-α modulation on peripheral blood monocytes by using excess concentration of anti-TNF-α, added from the beginning until the end of the cell culture treatment.

Culture 3: M-CSF+RANKL+anti-TNF-α+OPG- treated cultures

Excess concentrations of anti-TNF-α and OPG were added to M-CSF+RANKL treated cultures at day 0 and day 7 respectively (25 ng/ml M-CSF + 100 ng/ml RANKL + 10 μg/ml anti-TNF-α + 250 ng/ml human OPG (R&D Systems Europe), (Mabilleau, Petrova et al. 2008), (Cope, Londei et al. 1994). This culture served as test culture aiming to inhibit RANKL and TNF-α.

A schematic summary of the experiment is presented below (Figure 5-1).

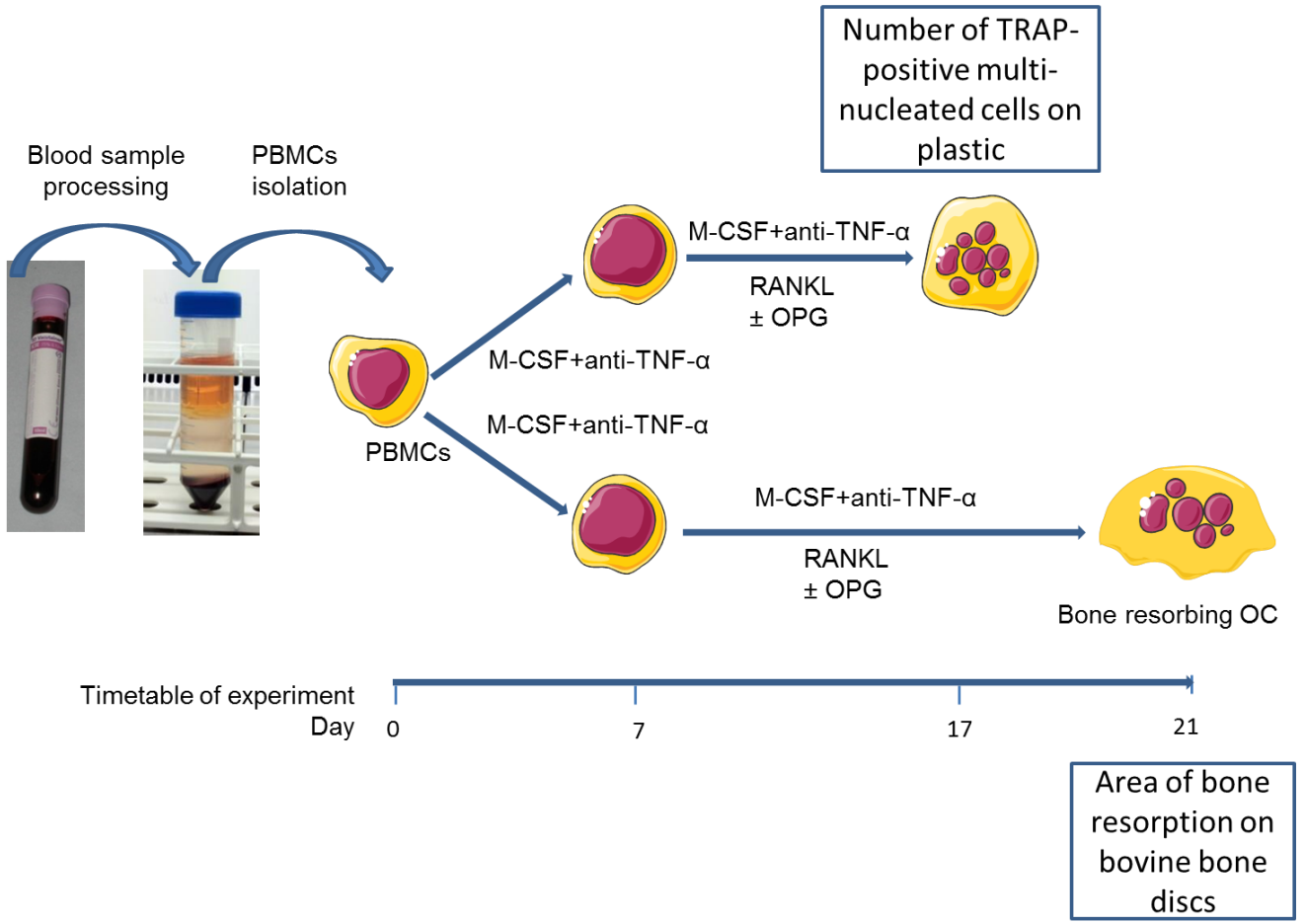

Figure 5-1 Summary of experiment.
Blood samples were processed and PBMCs were isolated and cultured in the presence of M-CSF+RANKL, M-CSF+RANKL+anti-TNF-α and M-CSF+RANKL+anti-TNF-α+OPG on plastic cell culture plates and on bovine bone discs for the assessment of osteoclast formation (number of TRAP-positive multi-nucleated cells at day 17) and resorption (area of bone resorption at day 21) respectively.

5.4 Statistical analysis

Data were analysed with Predictive Analytics Software 18 statistical package and expressed as median [25th-75th percentile]. Differences between study groups and culture treatments were analysed using the non-parametric Mann–Whitney U test (two groups) or Kruskal-Wallis test (three groups), as appropriate. Chi-square test was used for categorical variables. Differences were considered significant at $p<0.05$.

5.5 Results

5.5.1 Demographic features

Patients with acute Charcot osteoarthropathy were matched for age, gender, type and duration of diabetes with the diabetic patients and for age and gender with the healthy control subjects as described in Chapter 4.

5.5.2 Comparison of osteoclast formation on plastic between M-CSF+RANKL- and M-CSF+ RANKL +anti-TNF-α- treated cultures

Observation of the cell culture plates with light microscopy showed no difference in osteoclast formation in M-CSF+RANKL- and M-CSF+RANKL+anti-TNF-α-treated cultures in Charcot patients, diabetic patients and healthy control subjects, (Figure 5-2).

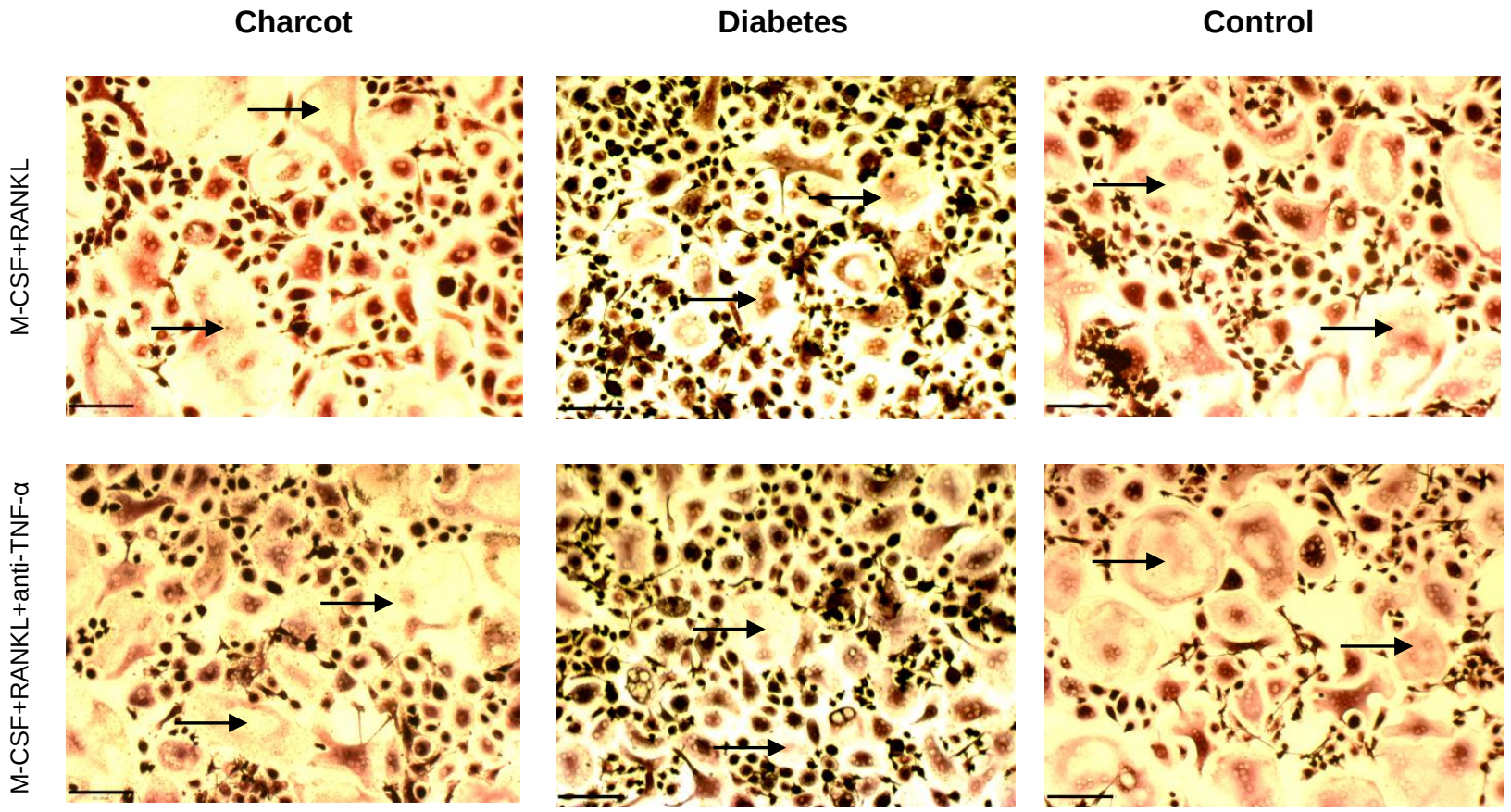

Figure 5-2 Osteoclast formation in M-CSF+RANKL-treated cultures and in M-CSF+RANKL+anti-TNF-α-treated cultures (light microscopy). Representative images of TRAP-positive multi-nucleated cells formed on plastic in a Charcot patient, diabetic patient and healthy control subject The arrows denote some of the TRAP-positive multi-nucleated cells (magnification x100, scale bar = 200μm).

The addition of anti-TNF-α to M-CSF+RANKL treatment did not lead to a significant difference in the median number of TRAP-positive multi-nucleated cells in Charcot patients, diabetic patients and healthy control subjects, (Figure 5-3).

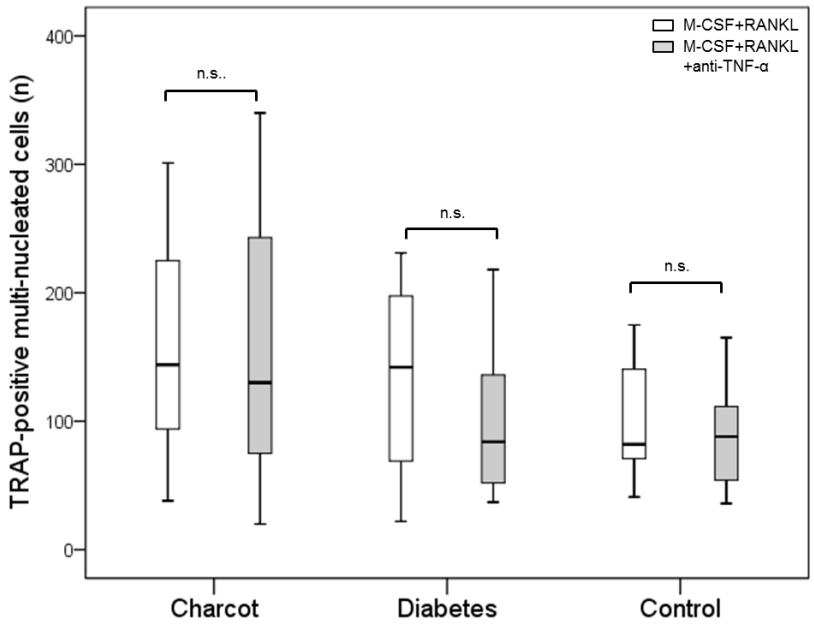

Figure 5-3 Comparison of the number of TRAP-positive multi-nucleated cells between M-CSF+RANKL-treated cultures and M-CSF+RANKL+anti-TNF-α-treated cultures
Significance assessed by Mann-Whitney U test, Levels of significance are demonstrated on the graphs; n.s. non-significant (p>0.05).
Non-significant difference in the number of TRAP-positive multi-nucleated cells between M-CSF+RANKL-treated cultures (white bars) and M-CSF+RANKL+anti-TNF-α-treated cultures (grey bars) in Charcot patients (p>0.05), diabetic patients (p>0.05) and healthy control subjects (p>0.05).

5.5.3 Comparison of osteoclast resorption on bovine bone discs between M-CSF+RANKL- and M-CSF+ RANKL +anti-TNF-α- treated cultures

Visualisation under the light microscope after toluidine blue staining showed that the extensive resorption pits noted in M-CSF+RANKL-treated cultures in Charcot patients were substituted by pits which appeared smaller and less dense. In diabetic patients and also in healthy control subjects resorption pits on bovine bone discs appeared similar between the two culture treatments in contrast to Charcot patients (Figure 5-4).

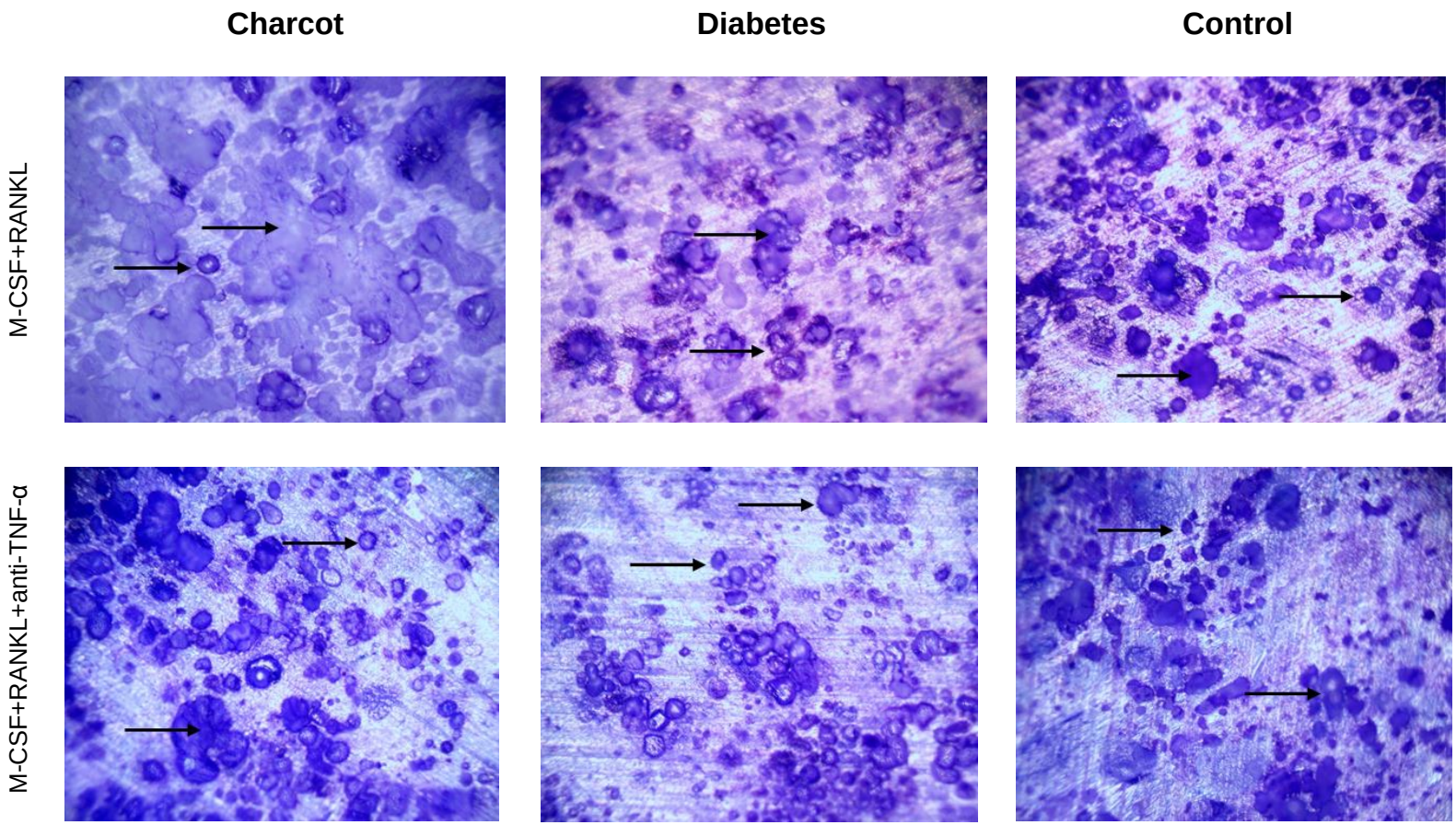

Figure 5-4 Representative images of resorbed bovine bone discs in M-CSF+RANKL-treated cultures and in M-CSF+RANKL+anti-TNF-α-treated cultures (light microscopy).
The arrows denote some of the resorption pits (magnification x200).The multiple resorption lacunae noted in M-CSF+RANKL-treated cultures in Charcot patients were less frequently noted after the addition of anti-TNF-α. The appearance of resorption pits remained unchanged between the two culture treatments in diabetic patients and also in healthy control subjects.

The addition of anti-TNF-α to M-CSF+RANKL treatment led to a significant decrease of the area of resorption at the surface only in Charcot patients but not in diabetic patients or healthy control subjects (Figure 5-5).

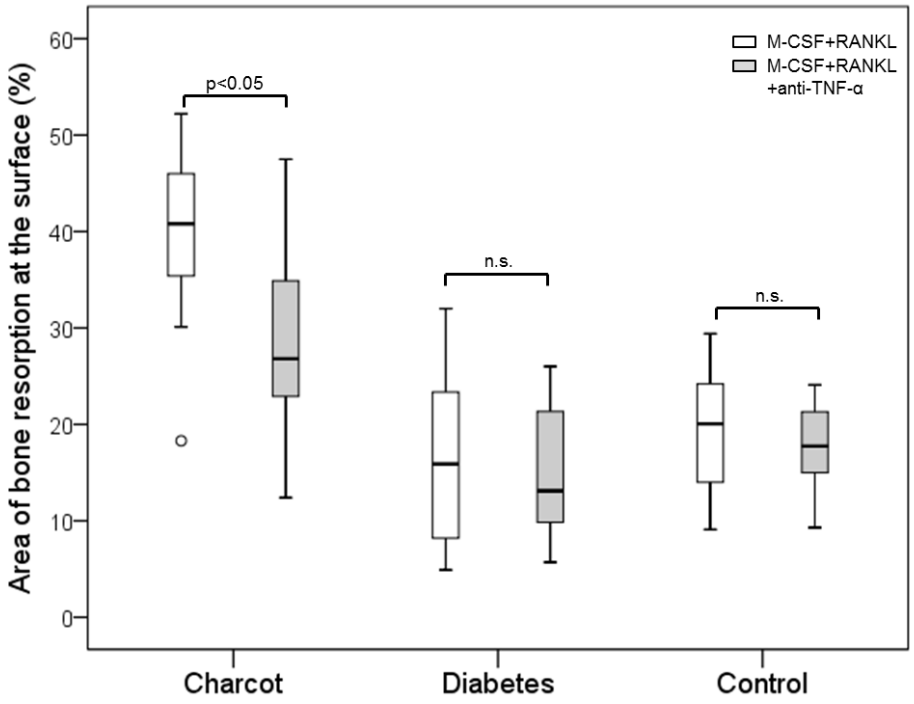

Figure 5-5 Comparison of the area of resorption at the surface of resorbed bone discs between M-CSF+RANKL-treated cultures and M-CSF+RANKL+anti-TNF-α-treated cultures
Significance assessed by Mann-Whitney U test, Levels of significance are demonstrated on the graph. (n.s.- non-significant; p>0.05)
Significant reduction in the area of resorption at the surface in response to anti-TNF-α treatment was noted only in Charcot patients (p<0.05), but not in diabetic patients (p>0.05) and healthy control subjects (p>0.05).

5.5.4 Comparison of surface profile measurements in M-CSF+RANKL- and M-CSF+RANKL +anti-TNF-α-treated cultures

After the addition of anti-TNF-α to M-CSF+RANKL treatment, the surface profile measurements of randomly selected areas revealed multi-shaped erosions of resorbed bovine bone discs in all study groups (Figure 5-6).

In contrast to M-CSF+RANKL-treated cultures where the erosions appeared greater and deeper in Charcot patients than erosions in diabetic patients and healthy controls (Chapter 4), in M-CSF+RANKL+anti-TNF-α-treated the erosion profiles of randomly selected areas of bone discs were not significantly different between the three groups (Figure 5-6).

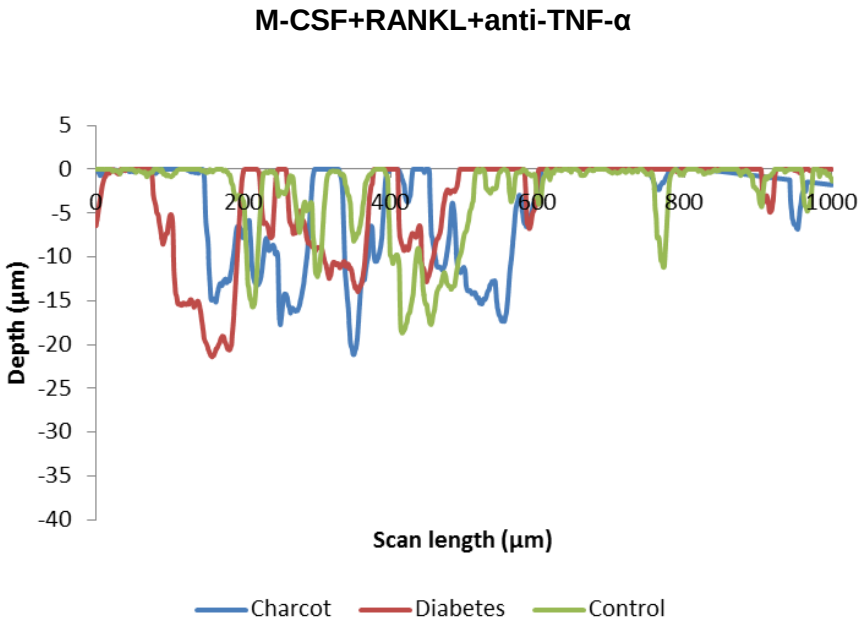

Figure 5-6 Representative erosion profiles of resorbed bone discs in a Charcot patient, diabetic patient and healthy control subject after surface profilometry in M-CSF+RANKL+anti-TNF-α-treated cultures.
The marked difference of the erosion profile in a Charcot patient compared with diabetic patient and healthy control in MCSF+RANKL-treated cultures (Chapter 4) was reversed after the addition of anti-TNF-α.

In Charcot patients, there was a “normalisation” of the erosion profile in M-CSF+RANKL+anti-TNF-α-treated cultures compared to M-CSF+RANKL-treated cultures, (Figure 5-7A), whereas anti-TNF-a had no effect on the erosion profiles of diabetic patients (Figure 5-7B) or healthy control subjects (Figure 5-7C).

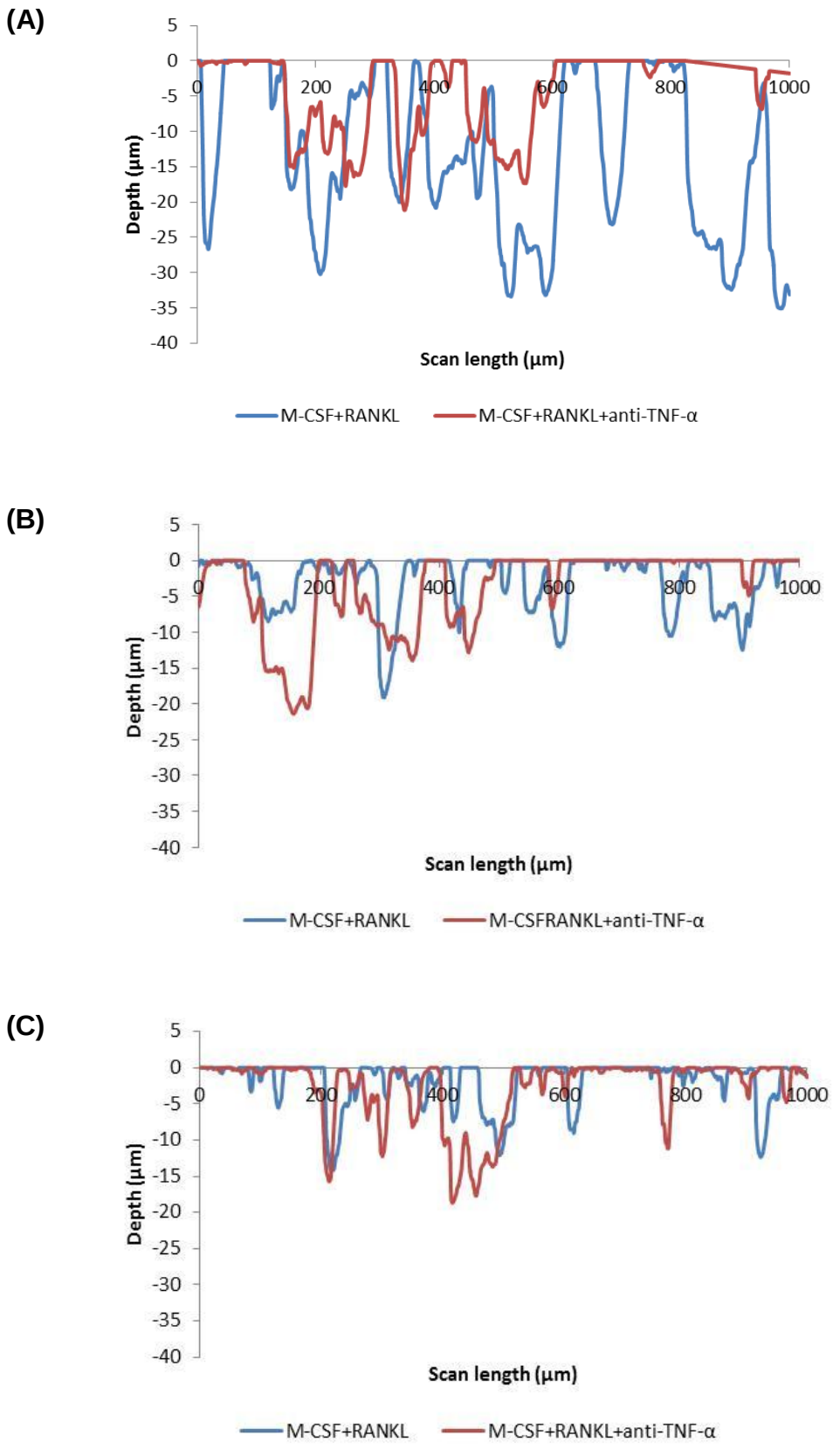

Figure 5-7 Representative erosion profiles of resorbed bone discs in M-CSF+RANKL-treated cultures and in M-CSF+RANKL+anti-TNF-α-treated cultures
Pits appeared significantly smaller in M-CSF+RANKL+anti-TNF-α-treated cultures compared with MCSF+RANKL-treated cultures in Charcot patients (A) but remained unchanged in diabetic patients (B) and in healthy controls (C).

5.5.5 Comparison of area of resorption under the surface in M-CSF+RANKL- and M-CSF+RANKL +anti-TNF-α-treated cultures after surface profilometry

After the addition of anti-TNF-α to M-CSF+RANKL treatment, the extensive erosions were reversed and the surface profile measurements were similar between Charcot patients, diabetic patients and healthy control subjects (Figure 5-6). Furthermore, in Charcot patients but not in diabetic patients and healthy control subjects, there was a significant reduction in the area of resorption under the surface in M-CSF+RANKL+anti-TNF-α-treated compared with M-CSF+RANKL-treated cultures (Figure 5-8).

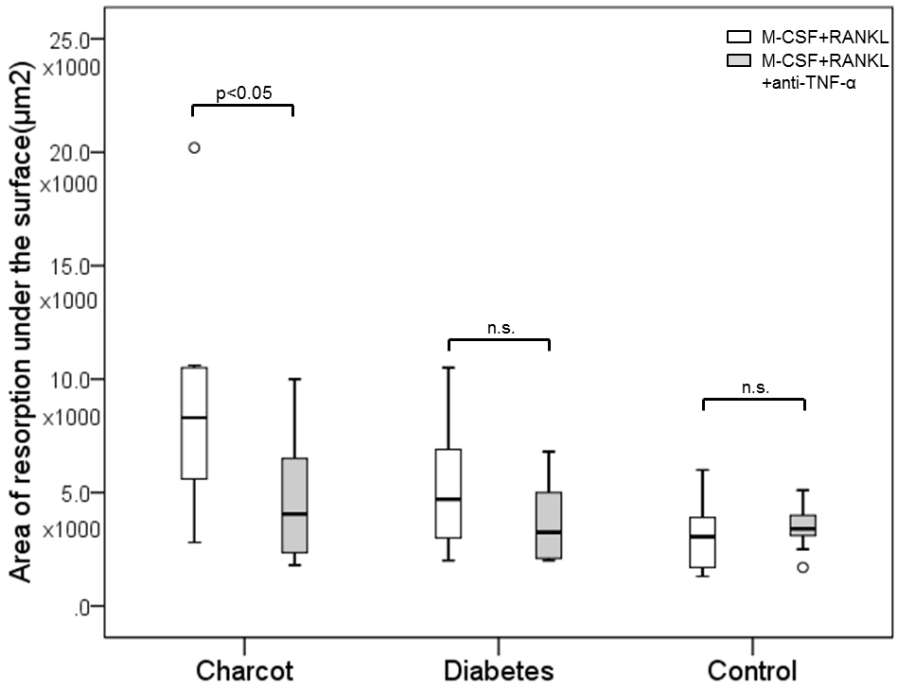

Figure 5-8 Comparison of the area of resorption under the surface of resorbed bone discs between M-CSF+RANKL-treated cultures and M-CSF+RANKL+anti-TNF-α-treated cultures. Significance assessed by Mann-Whitney U test, Levels of significance are demonstrated on the graph. (n.s.- non-significant; p>0.05).
Significant reduction in the area of resorption under the surface in response to anti-TNF-α treatment was noted only in Charcot patients (p<0.05), but not in diabetic patients (p>0.05) and healthy control subjects (p>0.05).

5.5.6 Pit morphology

To assess in more detail the differences in below surface resorption, pit morphology was evaluated and pit parameters before and after the addition of anti-TNF-α were compared. The noted differences of the pit parameters in M-CSF+RANKL-treated cultures between the groups described in Chapter 4 were lost after the inhibition of TNF-α. The pit parameters in M-CSF+RANKL+anti-TNF-α-treated cultures were not significantly different between the three study groups (Table 5-1)

Table 5-1 Measurements of uni-dented, bi-dented and multi-dented pits in M-CSF+RANKL+anti-TNF-α-treated cultures in Charcot patients, diabetic patients and healthy control subjects

Pits	Parameter	Charcot	Diabetes	Control	p-value
Uni-dented	Width (µm)	43 [37-52]	44 [37.5-57.5]	43 [40-47]	>0.05
	FWHM (µm)	22 [19-25]	19 [16.3-24]	19 [17-19]	>0.05
	Depth (µm)	6 [5-9]	5 [5-9]	6 [5-8]	>0.05
Bi-dented	Width (µm)	81 [73-98]	91 [70-101]	76 [70-87]	>0.05
	FWHM (µm)	43 [38-51]	54 [40.7-61.8]	51 [38-55]	>0.05
	Depth (µm)	12 [9-16]	15 [10-19]	12 [11-15]	>0.05
Multi-dented	Width (µm)	165 [133-188]	151 [127-178]	127 [116-141]	>0.05
	FWHM (µm)	91 [75-124]	113 [80-122]	81 [62-91]	>0.05
	Depth (µm)	18 [15.9-22.7]	22 [21-27]	16 [14-20]	>0.05

Data expressed as median [25th-75th percentile] and analysed by the Kruskal-Wallis test; P-values indicate differences between Charcot patients, diabetic patients and healthy control subjects
Non-significance difference in pit parameters (width, FWHM and depth) of the uni-dented, bi-dented and multi-dented pits between Charcot patients, diabetic patients and healthy control subjects (p>0.05 for all comparisons) in response to anti-TNF-α treatment.

The addition of anti-TNF-α to M-CSF+RANKL treatment led to a significant reduction in the width, FWHM and depth of the uni-dented pits in Charcot patients (Figure 5-9 A). Although the reduction of the bi-dented pits (Figure 5-9 B) and multi-dented pit parameters (Figure 5-9 C) was not significant, there was a general trend of

“normalisation” of pits after anti-TNF-α treatment. In contrast to Charcot patients, the addition of anti-TNF-a had no effect on pit parameters in diabetic patients or in healthy control subjects (Figure 5-9).

(A) Uni-dented pits

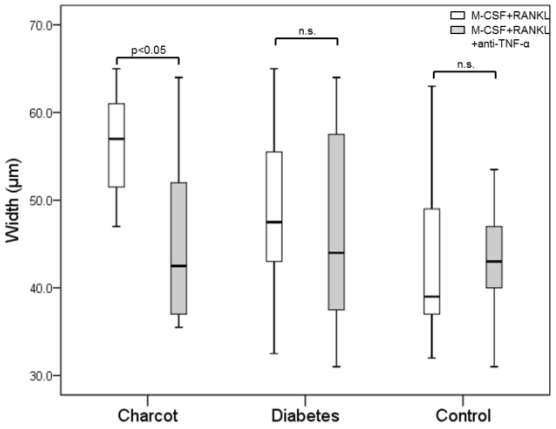

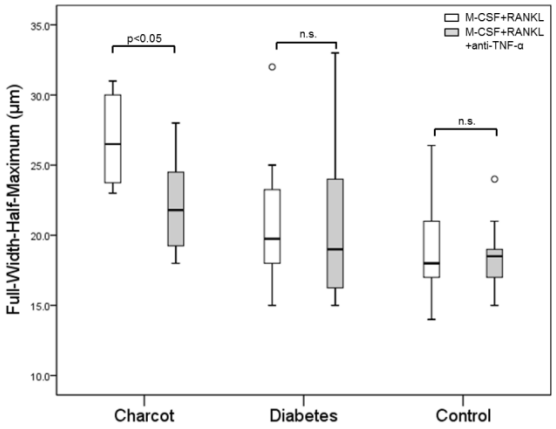

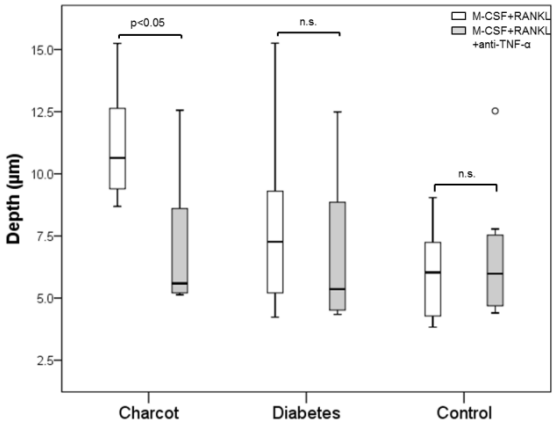

(B) Bi-dented pits

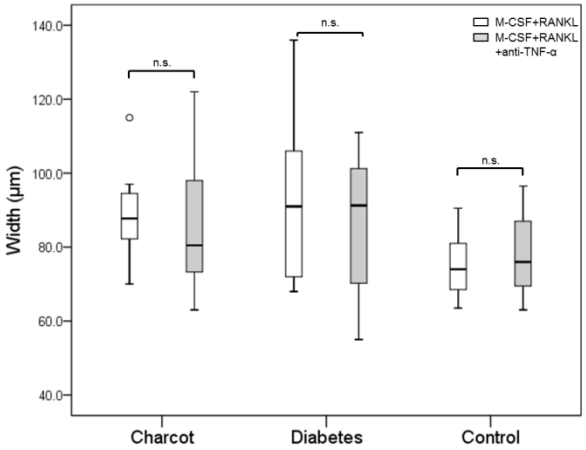

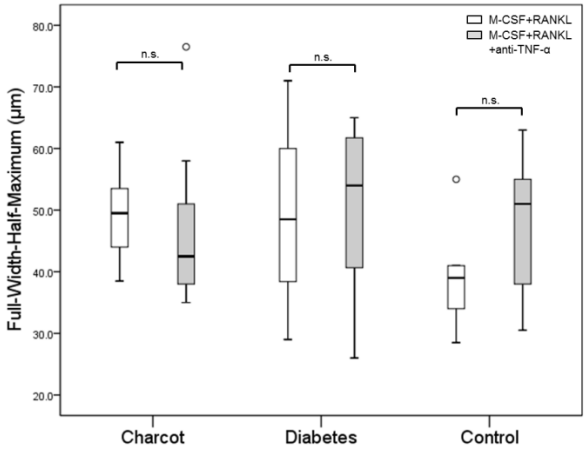

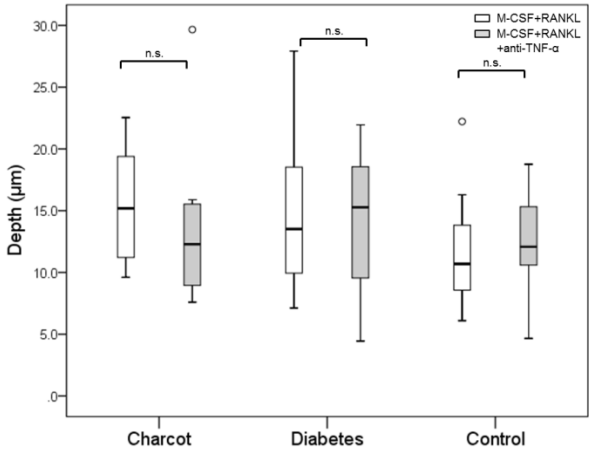

(C) Multi-dented pits

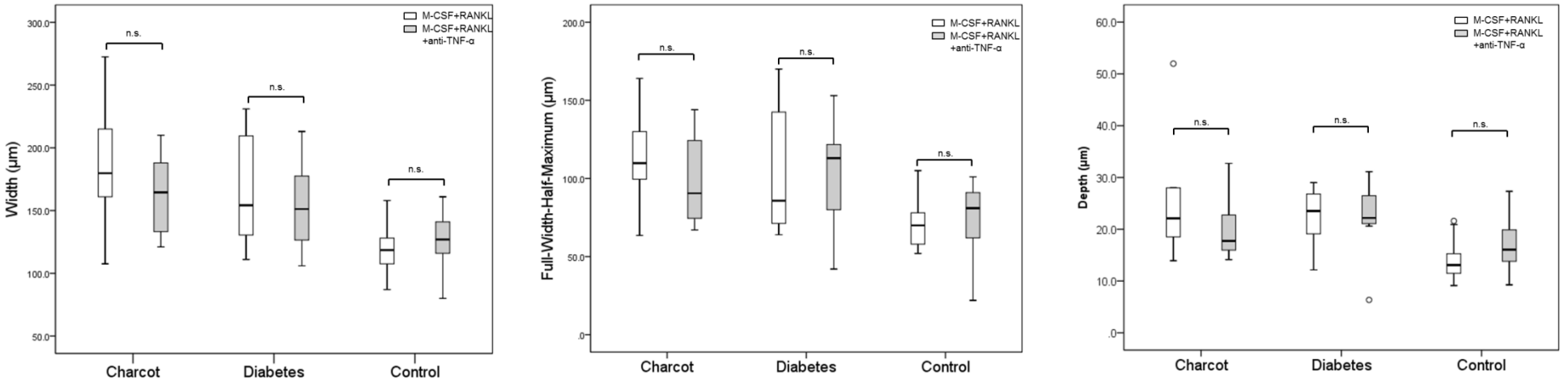

Figure 5-9 Comparison of pit measurements (width, depth and FWHM) between M-CSF+RANKL-treated cultures and M-CSF+RANKL+anti-TNF-α-treated cultures

(A) Uni-dented pits; (B) bi-dented pits; (C) multi-dented pits. Significance assessed by Mann-Whitney U test, Levels of significance are demonstrated on the graphs; ns = non-significant (p>0.05).

Significant reduction in the width, FWHM and depth of the uni-dented pits only in Charcot patients (p<0.05 for all comparisons) but not in diabetic patients (p>0.05) and healthy control subjects (p>0.05) in response to anti-TNF-α to treatment. Non-significant difference in the pit parameters of the bi-dented pits and multi-dented pit parameters was noted in all study groups (p>0.05 for all comparisons).

5.5.7 Pit distribution

To determine whether there were any differences in the distribution of the shape of the pits, the percentage of uni-dented, bi-dented and multi-dented pits was compared between the two culture treatments. In Charcot patients, the addition of anti-TNF-α to M-CSF+RANKL resulted in a significant increase in the percentage of uni-dented pits (from 36% [31-43] to 53% [43-63], $p<0.05$) and a significant decrease in the percentage of multi-dented pits (from 40% [32-42] to 25% [13-33], $p<0.05$), whereas the percentage of bi-dented pits remained unchanged (from 24% [20-28] to 22% [21-24] $p>0.05$ (Figure 5-10 A, B). There was no significant difference in the distribution of pits (uni-dented, bi-dented and multi-dented) between the two culture treatments in the diabetic patients, (Figure 5-10 C, D) and in the healthy control subjects (Figure 5-10 E, F).

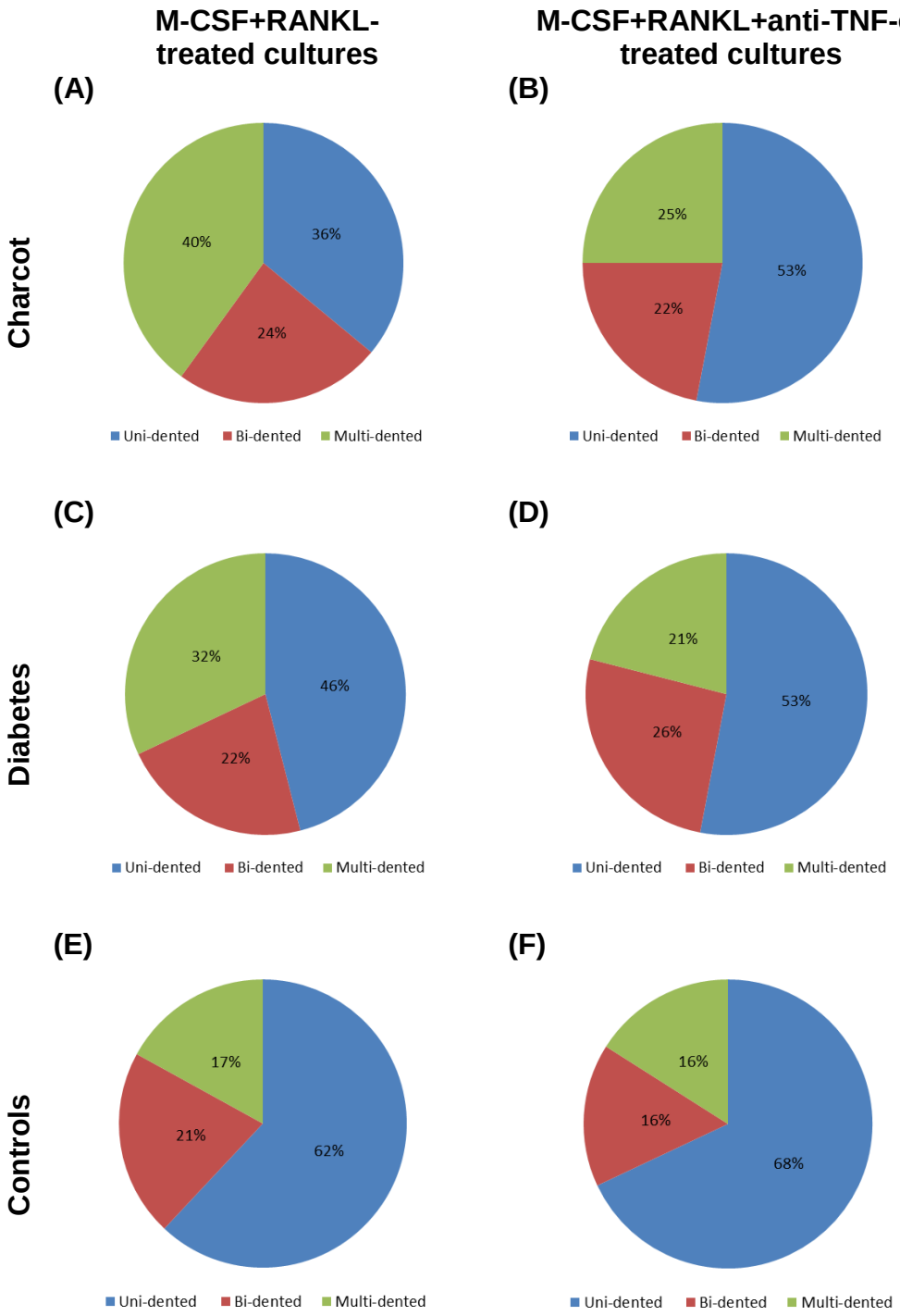

Figure 5-10 Distribution of pits according to their shape in M-CSF+RANKL and M-CSF+RANKL+anti-TNF-α-treated cultures in Charcot patients, diabetic patients and healthy control subjects respectively.

The addition of anti-TNF-α treatment led to a significant difference in the pit distribution only in Charcot patients (A, B) characterised by a significant increase in the percentage of uni-dented pits ($p<0.05$) and significant decrease ($p<0.05$) in the percentage of multi-dented pits, whereas the percentage of the bi-dented pits remained unchanged ($p>0.05$). No differences in the pit distribution were noted in diabetic patients (C, D) and in healthy control subjects (E, F); ($p>0.05$ for all comparisons).

5.5.8 Fold change of osteoclast formation and resorption (at the surface and under the surface) after anti-TNF-α treatment

The overall change in the response to anti-TNF-α treatment was determined by calculating the fold change in the number of TRAP-positive multi-nucleated cells and bone resorption on bovine bone discs both at the surface and under the surface in M-CSF+RANKL+anti-TNF-α-treated cultures compared with M-CSF+RANKL -treated cultures. The fold change of osteoclast formation (5-A) and resorption at the surface (5-B) and under the surface (5-C) was expressed as mean± SEM and was calculated as the ratio of the final value (M-CSF+RANKL+anti-TNF-α-treated cultures) and the initial value (M-CSF+RANKL-treated cultures). The fold change was compared to data for M-CSF+RANKL-treated cultures (positive control) which was expressed as 1 for the purpose of the analysis.

5-A

$$\text{Fold change (TRAP} - \text{positive multi} - \text{nucleated cells)} = \frac{\text{Number [TRAP} - \text{positive multi} - \text{nucleted cells (M} - \text{CSF} + \text{RANKL} + \text{anti} - \text{TNF} - \alpha - \text{treated cultures)]}}{\text{Number [TRAP} - \text{positive multi} - \text{nucleated cells (M} - \text{CSF} + \text{RANKL} - \text{treated cultures)]}}$$

5-B

$$\text{Fold change (Area of bone resorption at the surface)} = \frac{\text{Percentage [Area of resorption at the surface (M} - \text{CSF} + \text{RANKL} + \text{anti} - \text{TNF} - \alpha - \text{treated cultures)]}}{\text{Percentage [Area of resorption at the surface (M} - \text{CSF} + \text{RANKL} - \text{treated cultures)]}}$$

5-C

$$\text{Fold change (Area of bone resorption under the surface)} = \frac{\text{Area of resorption under the surface (M} - \text{CSF} + \text{RANKL} + \text{anti} - \text{TNF} - \alpha - \text{treated cultures)} sq.\mu m}{\text{Area of resorption under the surface (M} - \text{CSF} + \text{RANKL} - \text{treated cultures)sq.}\mu\text{m}}$$

Although the fold change in the number of TRAP-positive multi-nucleated cells was not significantly different between the two culture treatments in Charcot patients, (Figure 5-11A), the addition of anti-TNF-α to M-CSF+RANKL-treated cultures led to a significant fold change of the area of resorption at the surface (Figure 5-11B) and under the surface, (Figure 5-11C). This was in contrast to diabetic patients and healthy control subjects in whom the addition of anti-TNF-α did not result in a significant fold change in osteoclast formation and resorption (both at and under the surface), (Figure 5-11).

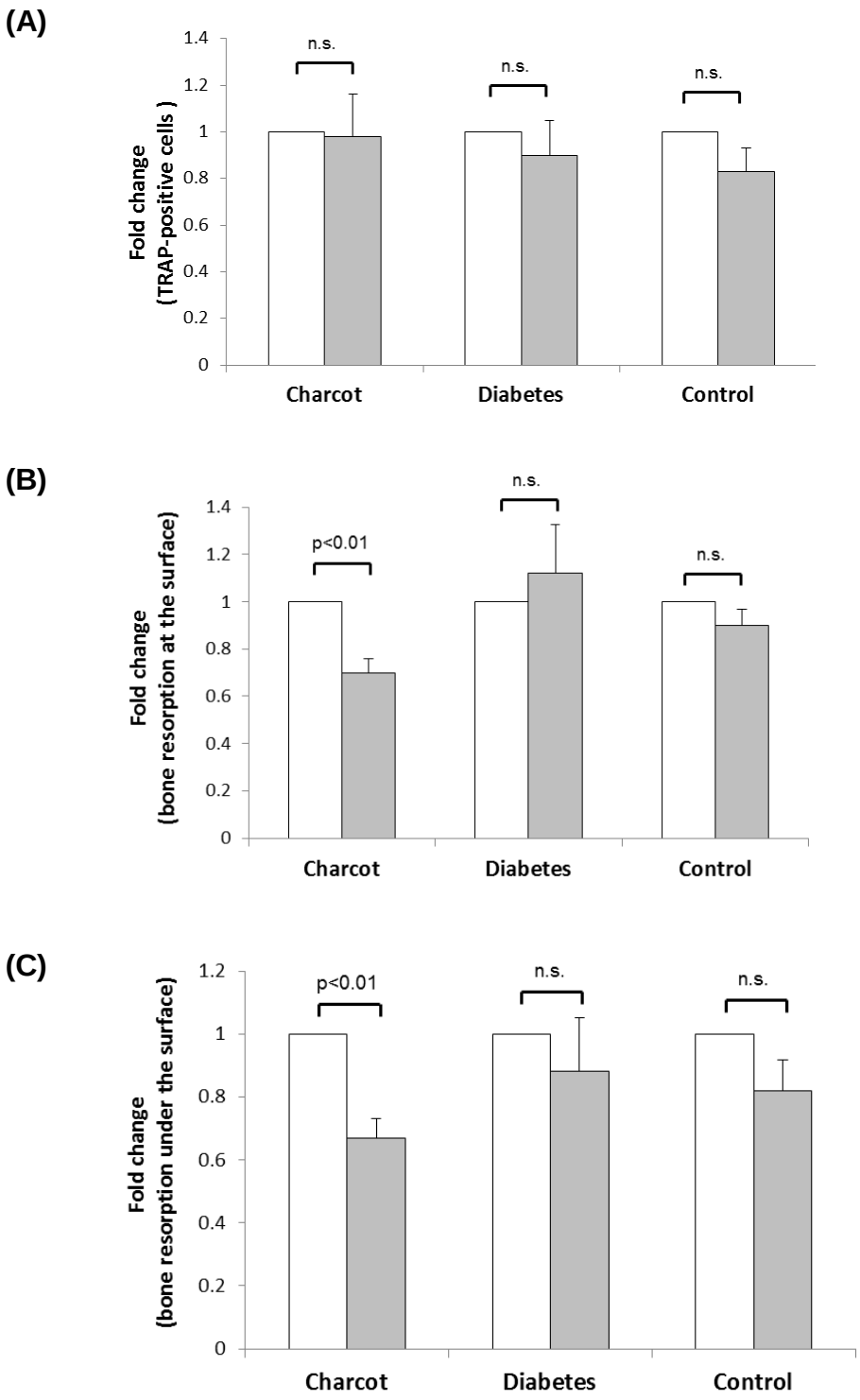

Figure 5-11 Fold change of osteoclast formation and resorption (at the surface and under the surface) in M-CSF+RANKL+anti-TNF-α treated cultures (grey bars) compared with M-CSF+RANKL-treated cultures (white bars).

(A) Number of TRAP-positive cells; (B) area of resorption at the surface; (C) area of resorption under the surface on bovine bone discs. Significance assessed by Mann-Whitney U test, Levels of significance are demonstrated on the graphs; ns = non-significant (p>0.05). Non-significant fold change in the number of TRAP-positive multi-nucleated cells in Charcot patients, diabetic patients and healthy control subjects (p>0.05 for all comparisons) in response to anti-TNF-α treatment. Significant fold-change in the area of bone resorption at the surface (p<0.01) and under the surface (p<0.01) in response to anti-TNF-α treatment only in Charcot patients but not in diabetic patients (p>0.05 for both comparisons) and healthy control subjects (p>0.05 for both comparisons).

5.5.9 The effect of anti-TNF-α treatment on CTX release in culture supernatant

The concentration of CTX released in culture supernatant is indicative of osteoclast resorption and this ELISA assay has been validated as an additional tool to assess resorption *in vitro*. I compared the concentration of CTX released over 72 hours in culture medium before and after the addition of anti-TNF-α in Charcot patients (n=5) and in healthy control subjects (n=7).

The fold change of CTX concentration in M-CSF+RANKL+anti-TNF-α-treated cultures compared with M-CSF+RANKL -treated cultures was expressed as mean± SEM and was calculated as shown below (5-D).

5-D

$$\text{Fold change (CTX in culture medium)} = \frac{\text{CTX (M-CSF+RANKL+anti-TNF-}\alpha\text{-treated cultures)}nM}{\text{CTX (M-CSF+RANKL -treated cultures)nM}}$$

The addition of anti-TNF-α in M-CSF+RANKL-treated cultures led to a significant fold change of the concentration of CTX in culture supernatant only in Charcot patients but not in healthy control subjects (Figure 5-12).

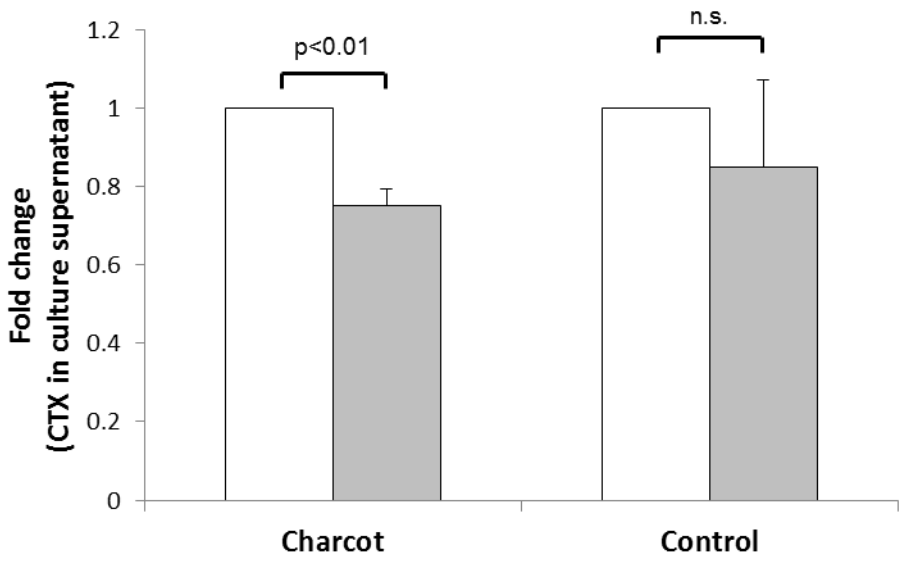

Figure 5-12 Fold change in the CTX concentration in M-CSF+RANKL+anti-TNF-α treated cultures (grey bars) compared with M-CSF+RANKL-treated cultures (white bars)
Significance assessed by Mann-Whitney U test, Levels of significance are demonstrated on the graphs; ns = non-significant (p>0.05).Significant fold-change in the concentration of CTX in culture supernatant in response to anti-TNF-α treatment only in Charcot patients (p<0.01) but not in healthy control subjects (p>0.05).

5.5.10 Bone resorption on bovine bone discs in M-CSF+RANKL+ anti-TNF-α +OPG-treated cultures

Resorption was evaluated after the addition of anti-TNF-α and OPG to M-CSF+RANKL-treated cultures. The rationale of this study was to block simultaneously TNF-α and RANKL. The addition of anti-TNF-α and OPG inhibited resorption on bovine discs in all study groups, (Figure 5-13).

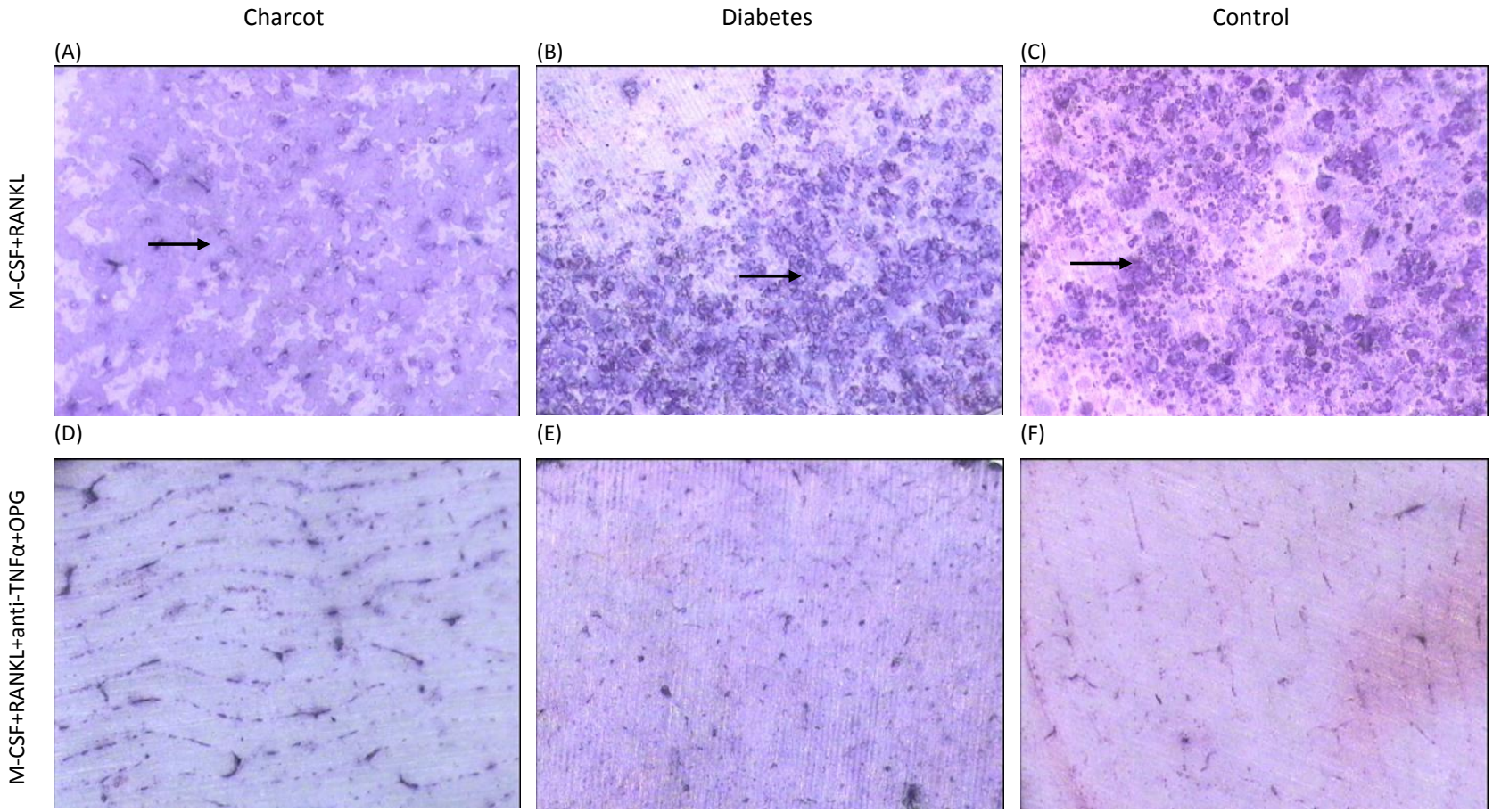

Figure 5-13 Toluidine blue staining of resorbed bovine bone discs in M-CSF+RANKL-treated cultures and in M-CSF+RANKL+anti-TNF-α+OPG-treated cultures (light microscopy)

The addition of anti-TNF-α and OPG to M-CSF+RANKL inhibited resorption in all study groups (D, E, F). The black arrows denote some of the pits in M-CSF+RANKL-treated cultures in a Charcot patient (A), diabetic patient (B) and healthy control subject (C); (magnification X40)

Non-significant isolated minute pits were noted after observation of bovine bone discs at higher magnification in 8 subjects (4 Charcot patients, 1 diabetic patient and 3 healthy control subject), (Figure 5-14) but the distribution within the groups was not significantly different, ($p>0.05$), (Table 5-2).

Table 5-2 Comparison of distribution according to presence of minute resorption pits in M-CSF+RANKL+ anti-TNFα +OPG-treated cultures in Charcot patients, diabetic patients and healthy control subjects.

Minute pits in M-CSF+ RANKL+ anti-TNF-α +OPG treated cultures	Charcot	Diabetes	Control	P-value
Absent: present	6:4	7:1	6:3	>0.05

Chi-squared test. P-value indicates the difference between Charcot patients, diabetic patient and healthy control subjects.
Non-significant difference according to presence: absence of minute isolated resorption pits in M-CSF+RANKL+ anti-TNFα+OPG-treated cultures between Charcot patients, diabetic patients and healthy control subjects ($p>0.05$)

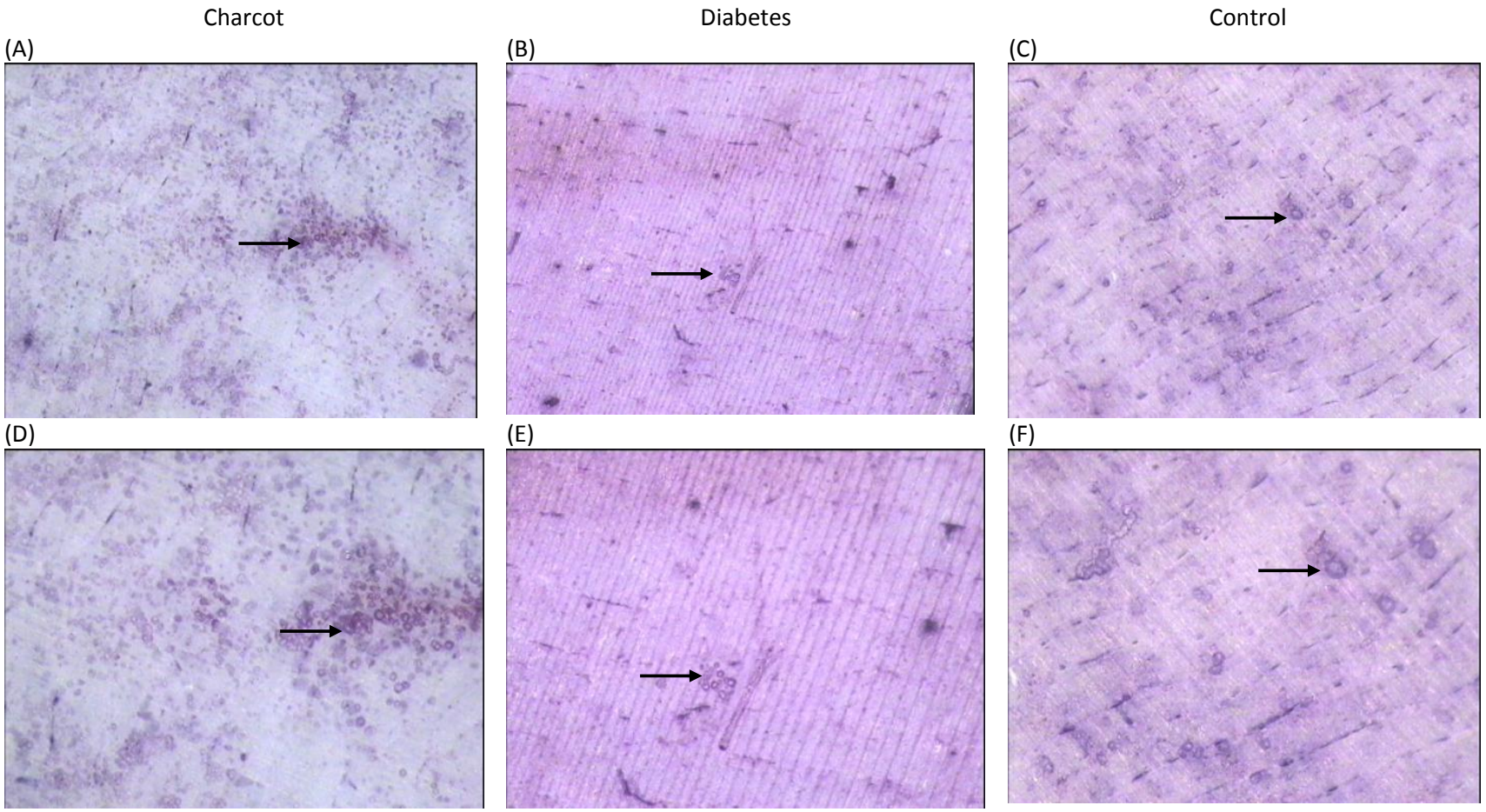

Figure 5-14 Toluidine blue staining of bovine bone discs in M-CSF+RANKL+anti-TNF-α+OPG-treated cultures in a Charcot patient, diabetic patient and healthy control subject (light microscopy)

The arrows denote presence of isolated minute pits at X40 and at X70 magnification in a Charcot patient (A, D), diabetic control patient (B, E) and healthy control subject (C, F) respectively.

5.6 Discussion

This *in vitro* study has shown that there was a significant reduction in the resorbing activity of M-CSF+RANKL-treated osteoclasts derived from Charcot patients in response to anti-TNF-α-treatment. The addition of anti-TNF-α resulted in significant reduction in the area of resorption on bovine bone discs both on the surface, as assessed by image analysis and also under the surface, as assessed by surface profilometry. The aberrant erosion profile, pit morphology and pit distribution in M-CSF+RANKL-treated cultures in Charcot patients were reversed after the addition of anti-TNF-α. These findings confirm the hypothesis that the proinflammatory cytokine TNF-α modulates increased osteoclastic activity in osteoclasts derived from patients with acute Charcot osteoarthropathy.

In this study, I sought to determine the role of TNF-α as a promoter of the observed enhanced osteoclast function in M-CSF+RANKL-treated cultures in acute Charcot osteoarthropathy. Using the traditional resorption pit assay together with surface profilometry, I have demonstrated that although osteoclast formation remained unchanged, the addition of anti-TNF-α to M-CSF+RANKL-treated cultures significantly decreased osteoclast function. This is in agreement with previous data showing that TNF-α is more potent for osteoclast activation than for osteoclast formation (Fuller, Murphy et al. 2002). The inhibition of TNF-α led to a significant reduction in the area of resorption on the surface and under the surface and a significant decrease in the concentration of CTX released in culture supernatant in cultures from Charcot patients.

These studies indicate a role of TNF-α in osteoclastic activity in Charcot osteoarthropathy. It has been previously shown that this cytokine activates osteoclasts through a direct action on osteoclastic precursors in strong synergy with RANKL (Fuller, Murphy et al. 2002). For its osteoclastogenic activity, this cytokine requires permissive levels of RANKL (Lam, Takeshita et al. 2000). Indeed, the inhibition of RANKL by OPG, as described in Chapter 3, abolished osteoclastic resorbing activity not only in diabetic patients and healthy control subjects but also in patients with Charcot osteoarthropathy.

Similarly, no resorption was noted after the combined inhibition of TNF-α and RANKL by anti-TNF-α and OPG respectively in all study groups. This suggests that TNF-α enhances RANKL mediated osteoclastic activity in Charcot osteoarthropathy.

A similar synergistic effect of RANKL and TNF-α on osteoclastogenesis has been noted in other conditions characterised by chronic inflammatory bone loss, including rheumatoid arthritis, periodontitis and inflammatory bowel disease (Zupan, Jeras et al. 2013). In Charcot osteoarthropathy, immunohistochemical analysis of surgical Charcot specimens has indicated that osteoclastic bone resorption takes place in the presence of TNF-α (Baumhauer, O'Keefe et al. 2006). In the acute stage of the osteoarthropathy, serum concentrations of TNF-α are raised (Petrova, Dew et al. 2015). Moreover, in the acute Charcot foot, inflammatory modulation of peripheral monocytes with increased spontaneous and induced production of TNF-α has been noted (Uccioli, Sinistro et al. 2010).

As well as increased resorption, in my study, there was a pathological erosion profile and aberrant morphological appearance of resorption pits on bone slices in M-CSF+RANKL-treated cultures in Charcot patients compared with healthy control subjects (Petrova, Petrov et al. 2014) and also in Charcot patients compared with diabetic patients. I demonstrated that the addition of anti-TNF-α reversed the observed differences in pit parameters and erosion profile between the study groups and in Charcot patients there was a notable “normalisation” of the erosion profile and pit morphology. This suggests that osteoclasts generated in M-CSF+RANKL-treated cultures, prior to inhibition of TNF-α, exhibit a highly aggressive resorptive profile. This exuberant resorptive activity was reduced after the addition of anti-TNF-α, which is a further evidence to support the role of this cytokine in the osteoclastogenesis in acute Charcot osteoarthropathy.

As well as changes in the morphological appearance of pits, there was a difference in the distribution of the shape of the pits in Charcot patients between the two culture treatments. The resorption pits in M-CSF+RANKL-treated cultures of the Charcot

patients were predominantly multi-dented and bi-dented whilst the uni-dented pits were less frequently seen although in diabetic patients and in healthy control subjects the pit distribution remained unchanged between the two culture treatments. The increased percentage of large multi-dented pits in M-CSF+RANKL-treated cultures suggests that osteoclasts maintain a continuous resorptive mode which is not interrupted by osteoclast migration (Soe and Delaisse 2010). The addition of anti-TNF-α to M-CSF+RANKL-treated cultures resulted in a significant reduction in the percentage of the multi-dented pits as well as a significant increase the percentage of the uni-dented pits. Thus, the inhibition of TNF-α normalised the resorptive behaviour of Charcot osteoclasts in which resorption alternated with migration as indicated by a significant increase in the percentage of uni-dented pits. It is possible that observed aberrant pit morphology and distribution were due to a TNF-α modulation of the resorption cycle. During the process of bone resorption, osteoclasts solubilise bone mineral followed by degradation of demineralised organic matrix and in control conditions, the relative rate of collagenolysis is slower than the rate of demineralisation (Soe, Merrild et al. 2013). Experimental *in vitro* studies have shown that agents which can upregulate cathepsin K expression prolong the resorption cycle and resorption events more frequently present as trenches (continuous resorption), (Soe, Merrild et al. 2013). In contrast, inhibition of cathepsin K accelerates the resorption cycle, leading to faster accumulation of collagen. This results in resorption events more frequently presenting as shallower and smaller pits (intermittent resorption). Both RANKL and TNF-α stimulate the osteoclasts to produce cathepsin K, which is the major protease responsible for the degradation of collagen (Troen 2006). In Charcot osteoarthropathy it is possible that TNF-α via enhanced cathepsin K expression may lead to imbalance between the relative rate of collagenolysis and demineralisation. This mechanism may explain the continuous resorptions which I observed as multi-dented pits in the M-CSF+RANKL treated cultures in contrast to the more frequently noted intermittent resorptions (uni-dented pits) after the addition of anti-TNF-α (Soe, Merrild et al. 2013), (Figure 5-15). Furthermore, an increased proportion of multi-dented pits similar to the trench-like lacunae which are associated

with reduction of bone stiffness (Vanderoost, Soe et al. 2013) may account for the reduction of bone mineral density that has been noted in the inflammatory stage of Charcot osteoarthropathy (Petrova and Edmonds 2010).

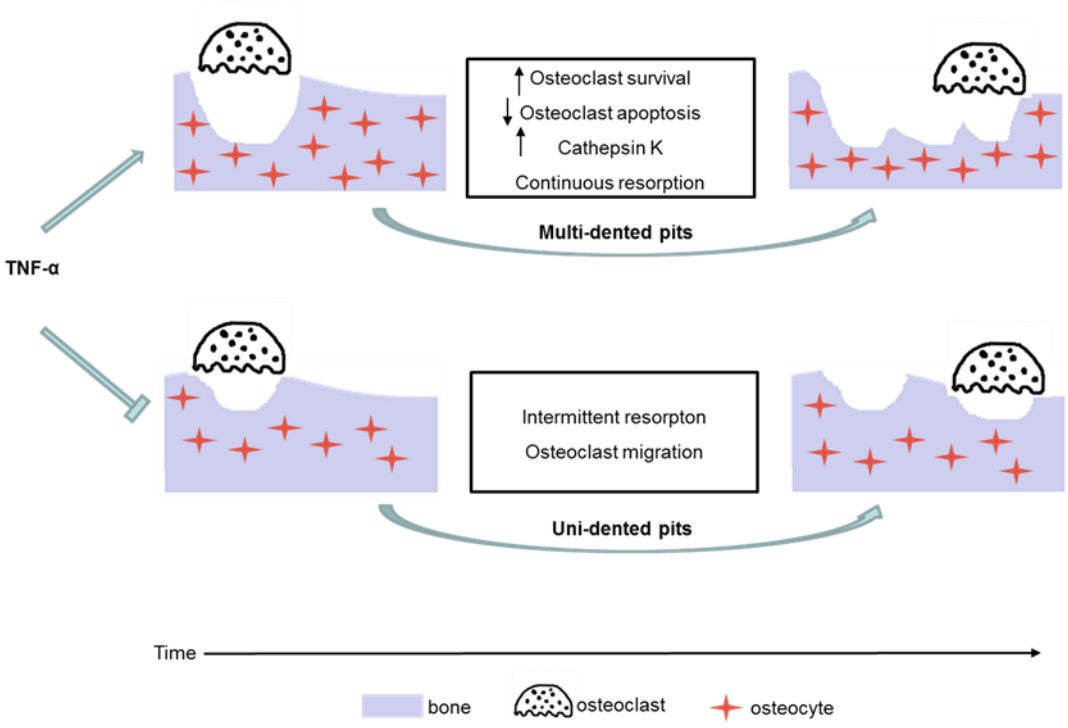

Figure 5-15 Model for osteoclast resorptive activity in Charcot osteoarthropathy in M-CSF+RANKL treated cultures before and after the addition of anti-TNF-α.
In the presence of TNF-α, continuous multi-dented pits (defined as lacunae or trenches) with increased area of resorption both on the surface and under the surface are seen more frequently compared with less frequently noted uni-dented pits (single resorption event). Resorption is prolonged and is not interrupted by migration episodes.
After the inhibition of TNF-α, the percentage of multi-dented pits is reduced with a corresponding increase in the percentage of uni-dented pits suggesting that the resorptive cycle is restored. Resorption alternates with migration and intermittent resorption events occur away from each other (uni-dented pits). The observed differences in the resorption before and after the addition of anti-TNF-α, suggest that TNF-α (via cathepsin K upregulation) modulates the resorptive behaviour of osteoclasts generated from Charcot patients and these highly-active osteoclasts are capable of extensive lacunar resorption with aberrant pit morphology and geometry due to reduced migration, increased survival and reduced apoptosis.

My data underscore the potent role of TNF-α in the RANKL-mediated osteoclastogenesis (Figure 5-16).

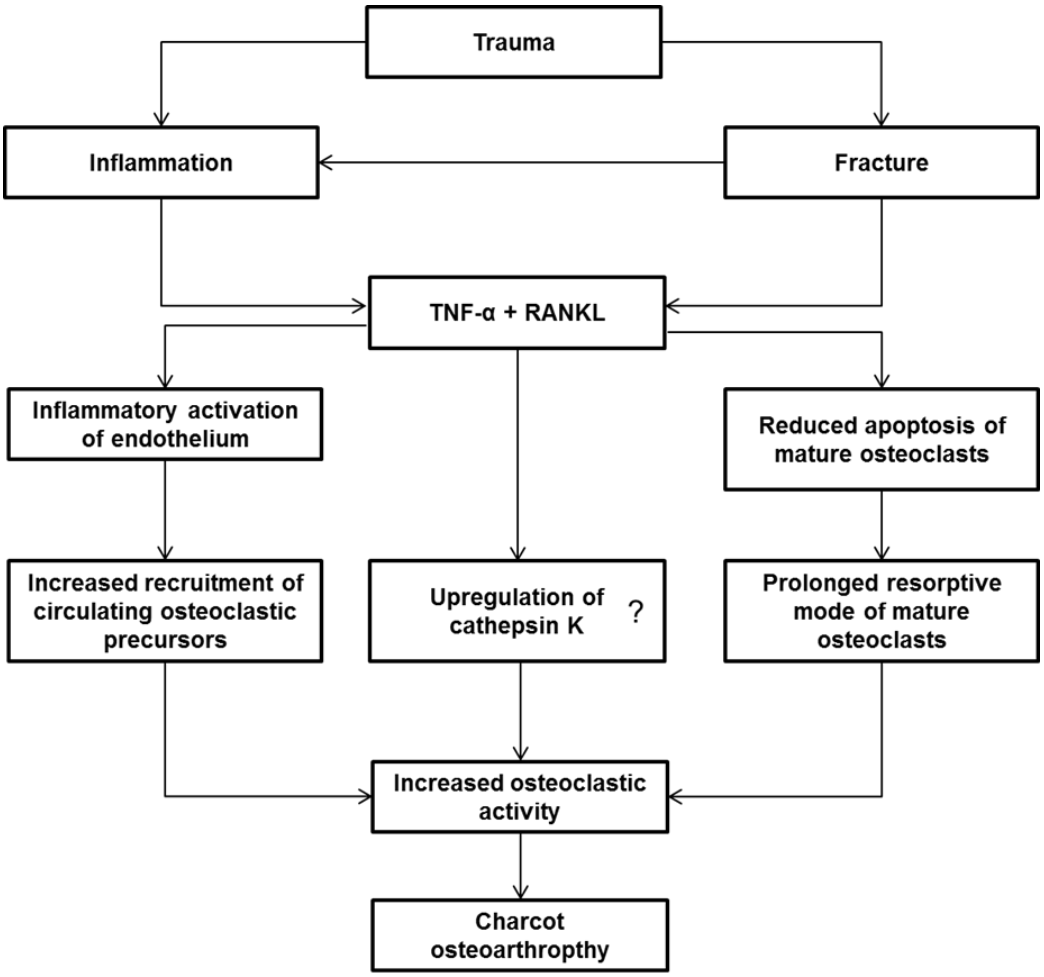

Figure 5-16 The proposed role of TNF-α in the pathogenesis of pathological bone destruction in the acute Charcot foot

Trauma to the neuropathic diabetic foot leads to bone damage and uncontrolled inflammation (Jeffcoate, Game et al. 2005). Bone fracture is the harbinger of Charcot osteoarthropathy (Johnson 1967) and it leads to changes in the bone matrix, which becomes a site of targeted remodelling with increased numbers of apoptotic osteocytes (bone matrix cells) and rapid degradation by activated osteoclasts (Heino, Kurata et al. 2009, Henriksen, Bollerslev et al. 2011). Furthermore, bone fracture triggers a coordinated healing cytokine response with the induction of pro-inflammatory cytokines, including TNF-α (Kon T 2001). In the affected Charcot foot, the inflammatory response to trauma with increased cytokine release leads to an up-regulation of receptors and adhesion molecules in the endothelium which then forms a firm attachment to osteoclast precursors resulting in enhanced recruitment of osteoclasts to sites of bone resorption

(McGowan, Walker et al. 2001). Furthermore, the activation of RANK by RANKL attracts osteoclastic precursors (Mosheimer, Kaneider et al. 2004) and its upregulation contributes to an enhanced RANKL-induced monocyte migration to the affected foot. Thus TNF-α-primed osteoclastic precursors in the presence of increased local expression of RANKL differentiate into highly aggressive osteoclasts with extensive resorbing activity characterised by increased survival, reduced apoptosis and migration. This increased osteoclastic activity may be due to cathepsin K upregulation, which requires further studies. Overall, these aberrantly activated osteoclasts play a key role in the pathological bone destruction of the acute Charcot foot.

5.7 Conclusion

Using a traditional osteoclast resorption assay together with surface profilometry, I have demonstrated for the first that the proinflammatory cytokine TNF-α modulates RANKL-mediated osteoclastic resorption *in vitro* in patients with acute Charcot osteoarthropathy and these observations shed light into the pathogenesis of this devastating condition.

Chapter 6 The role of the proinflammatory cytokine IL-6 on osteoclastic activity *in vitro* in patients with acute Charcot osteoarthropathy

6.1 Introduction

Using a traditional osteoclast assay together with surface profilometry, I have shown in Chapter 5 that in Charcot osteoarthropathy, RANKL-mediated osteoclastic activity is enhanced by the proinflammatory cytokine TNF-α. Although these studies indicate a link between inflammation and pathological bone resorption, it is possible that other proinflammatory cytokines with osteoclastogenic properties could play a role (Jeffcoate, Game et al. 2005). There is evidence to suggest that IL-6 can amplify the process of osteoclast proliferation and activation (Redlich and Smolen 2012). However, the role of this cytokine on osteoclast activation in acute Charcot osteoarthropathy is unknown.

In this chapter, I describe my experiments aiming to assess the role of IL-6 on osteoclastogenesis.

6.2 Study objective

Data from clinical observational studies of cohorts of Charcot patients have highlighted IL-6 as a potential cytokine involved in the pathogenesis of this condition as its serum concentration is raised in the acute active stage of the disease followed by a significant fall at the time of clinical resolution (Petrova, Dew et al. 2015), (Uccioli, Sinistro et al. 2010). Furthermore, the serum concentration of IL-6 correlates with the bone resorption marker C-terminal telopeptide (CTX), (Petrova, Dew et al. 2015). As an osteoclastogenic mediator, IL-6 up-regulates expression of RANKL in osteoblastic cells, but it can also induce the differentiation and activation of osteoclasts from osteoclastic

precursors and it cellular effects are mediated through the IL-6 receptor (IL-6R), (Redlich and Smolen 2012), (Kudo, Sabokbar et al. 2003). There is evidence to suggest that this cytokine is involved in the pathogenesis of systemic osteoporosis (Redlich and Smolen 2012), pathological bone loss in rheumatoid arthritis, multiple myeloma and Paget's disease (Duplomb, Baud'huin et al. 2008).

To determine the role of IL-6 in osteoclastogenesis in acute Charcot osteoarthropathy, I compared osteoclast formation and resorption in M-CSF+RANKL-treated cultures with and without the addition of excessive concentration of neutralising antibody to IL-6 (anti-IL-6).

6.3 Research design and methods

Samples from peripheral blood were obtained from 6 consecutive patients with recent onset of acute Charcot osteoarthropathy, 5 diabetic patients with no history of Charcot osteoarthropathy and 5 healthy control subjects.

The PBMCs were isolated from whole blood as described in Chapter 2 and cultured on plastic to assess osteoclast formation and on bovine bone discs to assess osteoclast resorption. Osteoclast formation was assessed by counting the number of TRAP-positive cells multi-nucleated cells on plastic. Resorption was quantitated by two methods: (1) area of resorption on the surface (%) assessed by image analysis after light microscopy and (2) area of resorption under the surface (μm^2) assessed by surface profilometry, as described in Chapters 2 and 3. In addition, I compared the concentration of CTX, as a marker of resorption, in culture supernatant before and after the addition of anti-IL-6 to M-CSF+RANKL in Charcot patients (n=4) and in healthy control subjects (n=4).

6.3.1 Rationale for the study

To ascertain whether IL-6 modulates RANKL-mediated osteoclastic activity the following culture treatments were set up.

Culture 1: M-CSF+RANKL- treated cultures

This culture served as a positive control (25 ng/ml M-CSF added at day 0 and 100 ng/ml human soluble RANKL added at day 7).

Culture 2: M-CSF+RANKL+anti-IL-6- treated cultures

Excess concentration of neutralising antibody to IL-6 was added to M-CSF+RANKL-treated culture at day 0 (25 ng/ml M-CSF + 100 ng/ml sRANKL + 10 µg/ml anti-IL-6 (R&D Systems Europe). This culture was used to assess the role of IL-6 on osteoclastogenesis. The rationale for this study was to inhibit IL-6 modulation on peripheral blood monocytes by using excess concentration of anti-IL-6, added from the beginning until the end of the cell culture treatment.

Culture 3: M-CSF+RANKL+anti-L-6 +OPG- treated cultures

Excess concentrations of anti-IL-6 and OPG were added to M-CSF+RANKL treated cultures at day 0 and day 7 respectively (25 ng/ml M-CSF + 100 ng/ml RANKL + 10 µg/ml anti-IL-6 + 250 ng/ml human OPG (R&D Systems Europe), (Mabilleau, Petrova et al. 2008), (Axmann, Bohm et al. 2009). This culture served as test culture aiming to inhibit RANKL and IL-6.

A summary of the experiment is illustrated below (Figure 6-1).

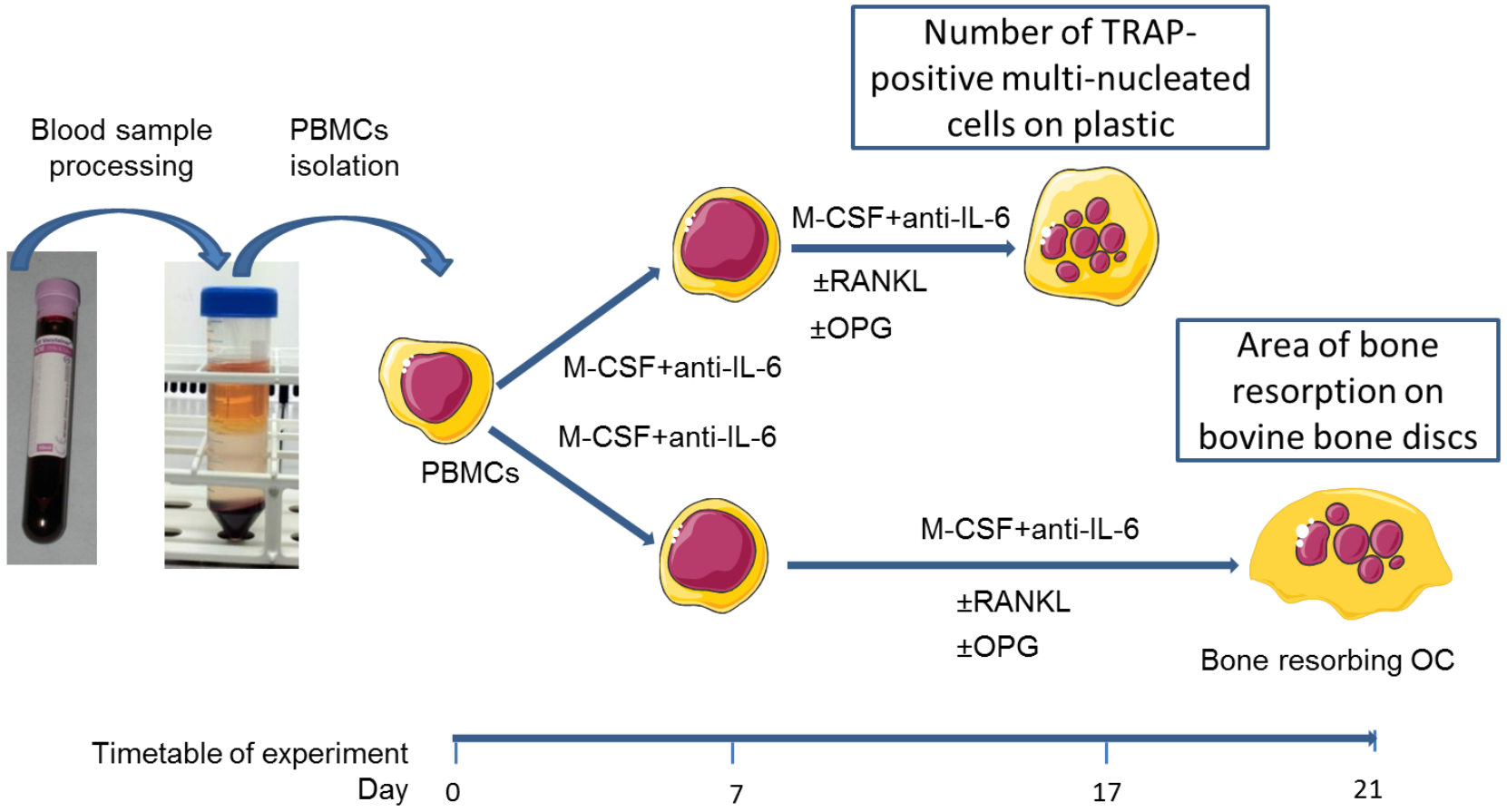

Figure 6-1 Summary of experiment.
Blood samples were processed and PBMCs were isolated and cultured in the presence of M-CSF+RANKL, M-CSF+RANKL+anti-IL-6 and M-CSF+RANKL+anti-IL-6+OPG on plastic cell culture plates and on bovine bone discs for the assessment of osteoclast formation (number of TRAP-positive multi-nucleated cells at day 17) and resorption (area of bone resorption at day 21) respectively.

6.4 Statistical analysis

Data were analysed with Predictive Analytics Software 18 statistical package and expressed as median [25th-75th percentile]. Differences between study groups and culture treatments were analysed using the non-parametric Mann–Whitney U test (two groups) or Kruskal-Wallis test (three groups), as appropriate. Chi-square test was used for categorical variables. Differences were considered significant at $p<0.05$.

6.5 Results

6.5.1 Demographic features

Patients with acute Charcot osteoarthropathy were matched for age, gender, type and duration of diabetes with the diabetic patients and for age and gender with the healthy control subjects. The age, gender distribution, type and duration of diabetes were not significantly different between the Charcot patients and diabetic patients nor were the age and gender distribution between the Charcot patients and healthy control subjects (Table 6-1).

Table 6-1 Demographic features of the study patients

	Charcot	Diabetes	Control
Age (years)	57 [47-57]	61 [55-67]	45 [42-49]
Gender (male: female)	3:3	3:2	4:1
Type 1: Type 2 diabetes	3:3	1:4	-
Duration of diabetes (years)	24 [8-29]	10 [8-24]	-

Data expressed as median [25^{th}-75^{th} percentile]; Data assessed with Mann-Whitney U test. Non-significant difference in age, gender distribution, type and duration of diabetes (Charcot patients versus diabetic patients) and age and gender (Charcot patients versus healthy control subjects), ($p>0.05$ for all pairwise comparisons).

6.5.2 Comparison of osteoclast formation on plastic between M-CSF+RANKL- and M-CSF+ RANKL +anti-IL-6- treated cultures

Observation of the cell culture plates with light microscopy showed no difference in osteoclast formation in M-CSF+RANKL and M-CSF+RANKL+anti-IL-6-treated cultures in Charcot patients, diabetic patients and healthy control subjects (Figure 6-2).

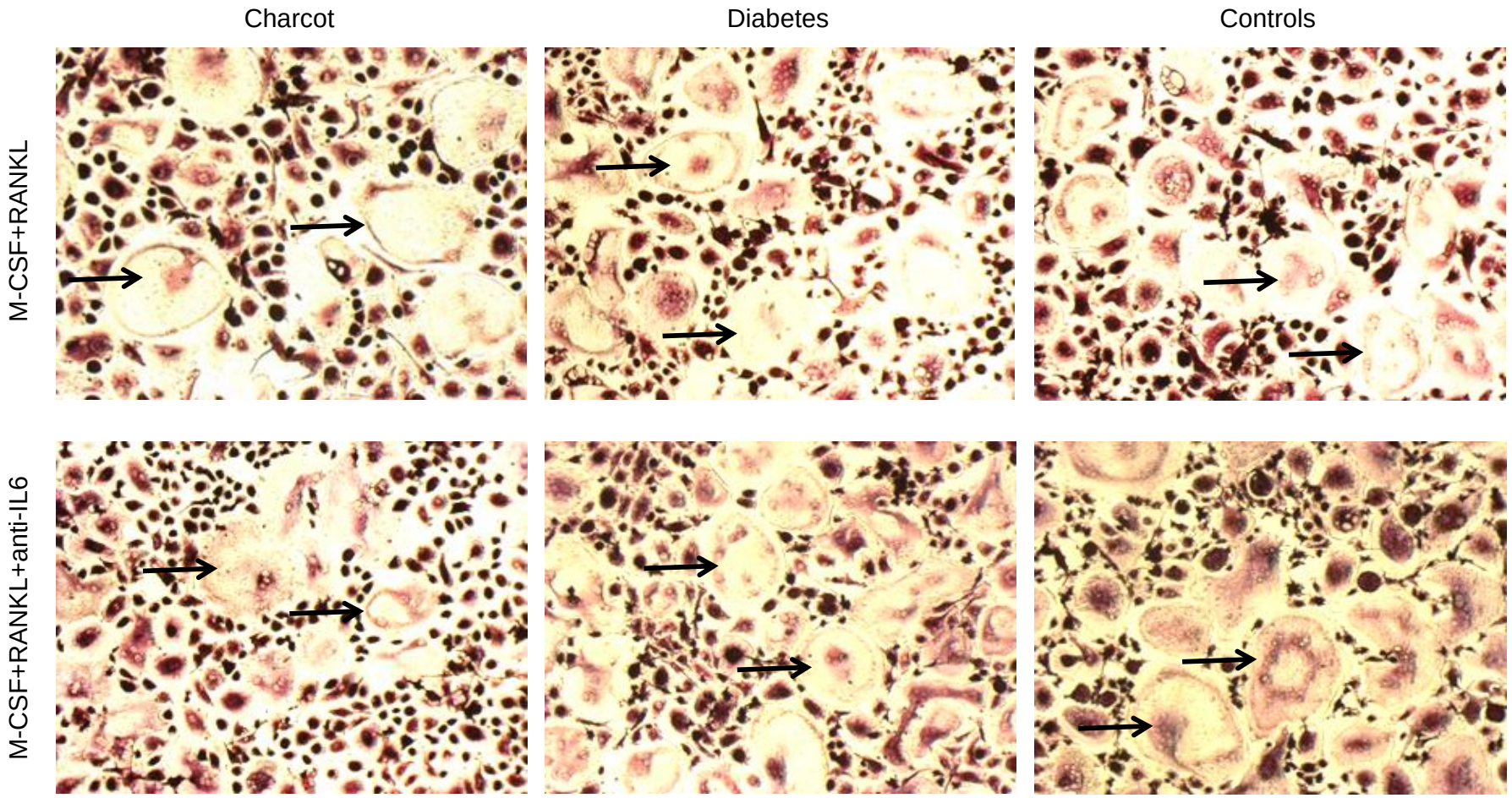

Figure 6-2 Osteoclast formation in M-CSF+RANKL-treated cultures and in M-CSF+RANKL+anti-IL-6-treated cultures (light microscopy). Representative images of TRAP-positive multi-nucleated cells formed on plastic in a Charcot patient, diabetic patient and healthy control subject. The arrows denote some of the TRAP-positive multi-nucleated cells (magnification x100)

The addition of anti-IL-6 to M-CSF+RANKL treatment did not lead to a significant difference in the median number of TRAP-positive multi-nucleated cells in Charcot patients, diabetic patients and healthy control subjects, (Figure 6-3).

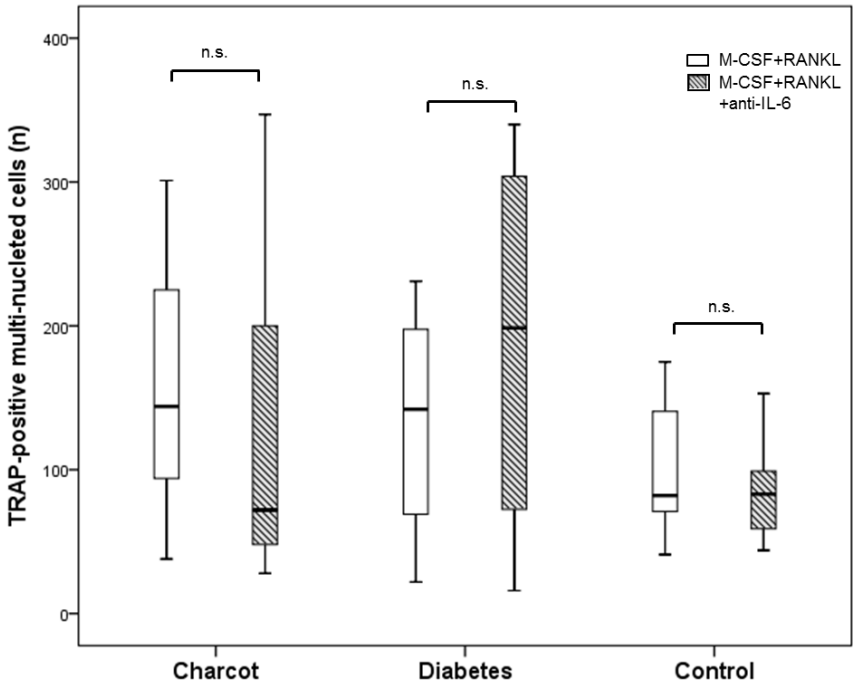

Figure 6-3 Comparison of the number of TRAP-positive multi-nucleated cells between M-CSF+RANKL-treated cultures and M-CSF+RANKL+anti-IL-6-treated cultures
Significance assessed by Mann-Whitney U test, Levels of significance are demonstrated on the graphs; n.s. non-significant (p>0.05).
Non-significant difference in the number of TRAP-positive multi-nucleated cells between M-CSF+RANKL-treated cultures (white bars) and M-CSF+RANKL+anti-IL-6-treated cultures (grey striped bars) in Charcot patients (p>0.05), diabetic patients (p>0.05) and healthy control subjects (p>0.05).

6.5.3 Comparison of osteoclast resorption on bovine bone discs between M-CSF+RANKL- and M-CSF+ RANKL +anti-IL-6- treated cultures

Visualisation under the light microscope after toluidine blue staining showed that in Charcot patients the extensive resorption pits noted in M-CSF+RANKL-treated cultures were substituted by pits which appeared smaller in size but with similar density. In contrast to Charcot patients, the resorption pits on bovine bone discs appeared similar

between the two culture treatments in diabetic patients and also in healthy control subjects (Figure 6-4).

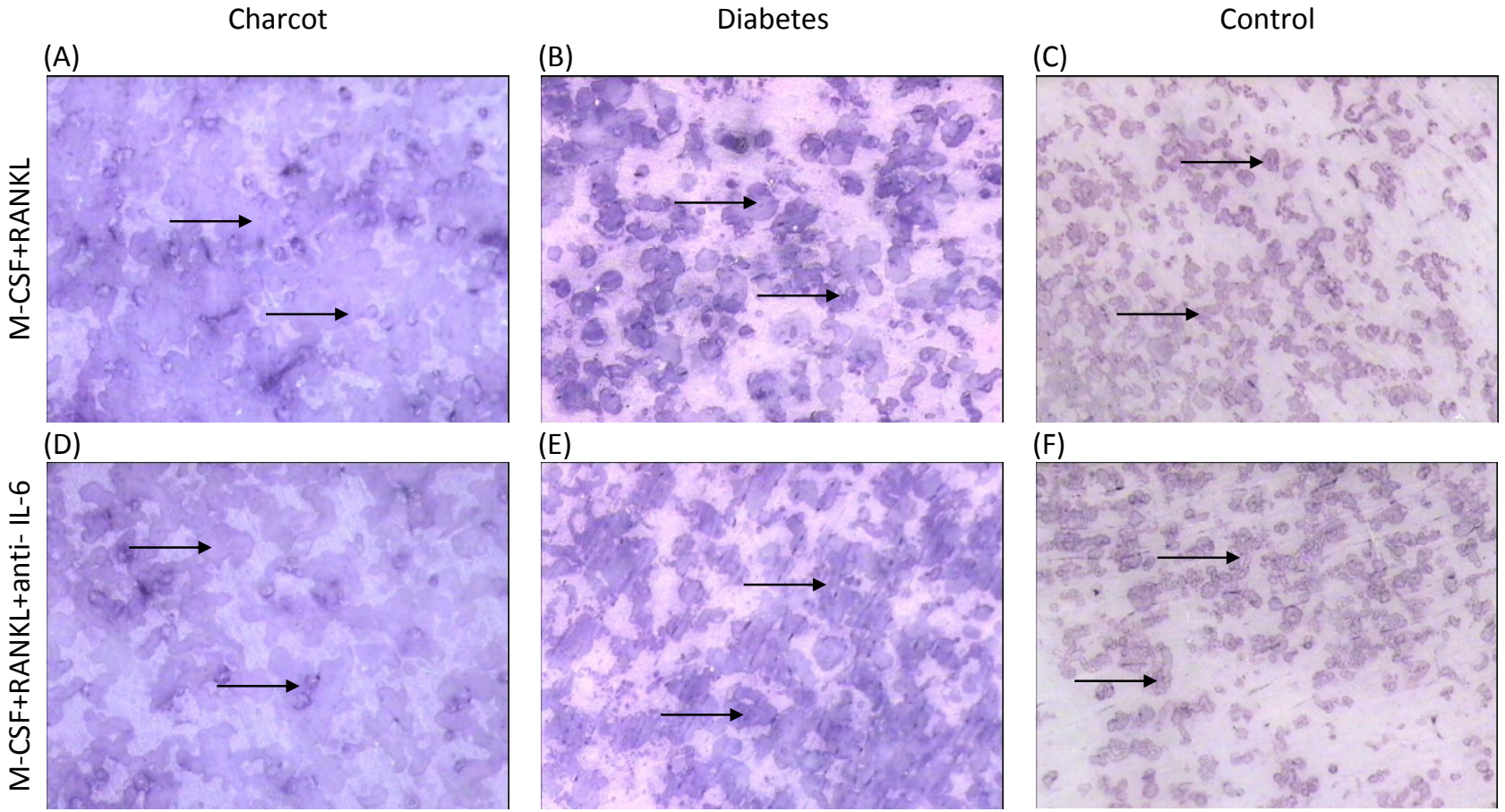

Figure 6-4 Representative images of resorbed bovine bone discs in M-CSF+RANKL-treated cultures and in M-CSF+RANKL+anti-IL-6 -treated cultures (light microscopy).

The arrows denote some of the resorption pits (magnification x40). The multiple resorption lacunae noted in M-CSF+RANKL-treated cultures in Charcot patients were still noted after the addition of anti-IL-6 treatment. The appearance of resorption pits remained unchanged between the two culture treatments in diabetic patients and also in healthy control subjects.

The addition of anti-IL-6 to M-CSF+RANKL treatment led to a significant decrease in the area of resorption at the surface only in Charcot patients but not in diabetic patients or healthy control subjects (Figure 6-5).

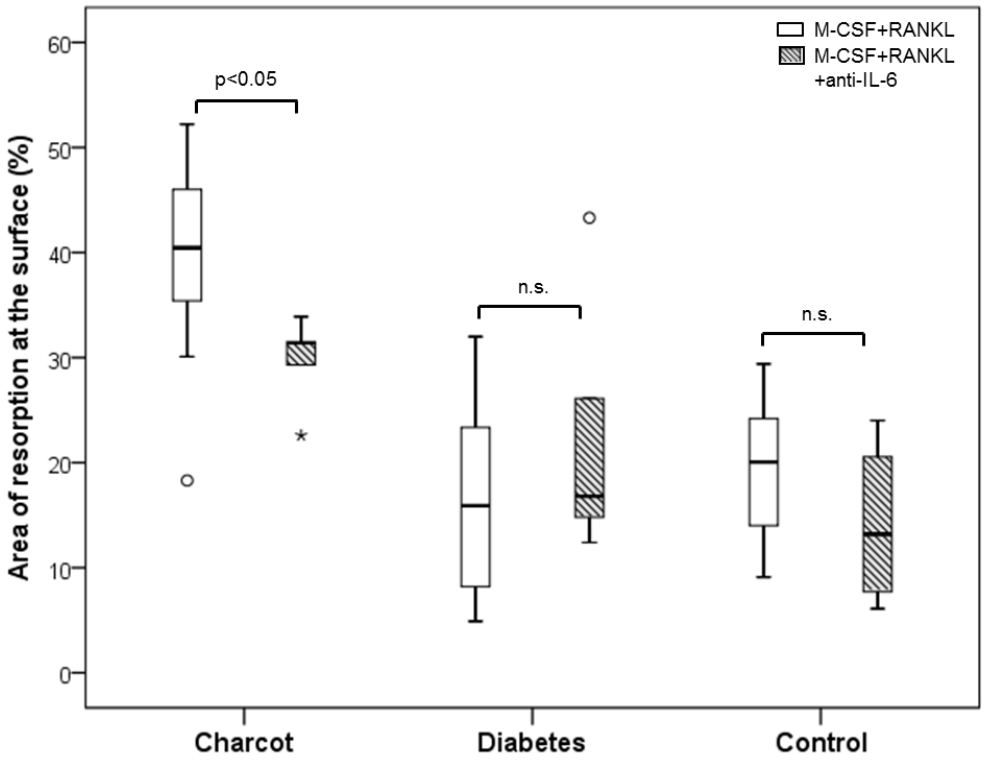

Figure 6-5 Comparison of the area of resorption at the surface of resorbed bone discs between M-CSF+RANKL-treated cultures and M-CSF+RANKL+anti-IL-6-treated cultures.
Significance assessed by Mann-Whitney U test, Levels of significance are demonstrated on the graph. (n.s.- non-significant; p>0.05)
Significant reduction in the area of resorption at the surface in response to anti-IL-6 treatment was noted only in Charcot patients (p<0.05), but not in diabetic patients (p>0.05) and healthy control subjects (p>0.05).

In Charcot patients, the observed reduction of the area of resorption at the surface as assessed by image analysis (Figure 6-5) was not associated with a significant reduction of the area of resorption under the surface, as assessed by surface profilometry (Figure 6-6). There was no significant difference in the area of resorption under the surface between M-CSF+RANKL+anti-IL-6-treated cultures compared with M-

CSF+RANKL-treated cultures in Charcot patients as well as in diabetic patients and healthy control subjects (Figure 6-6).

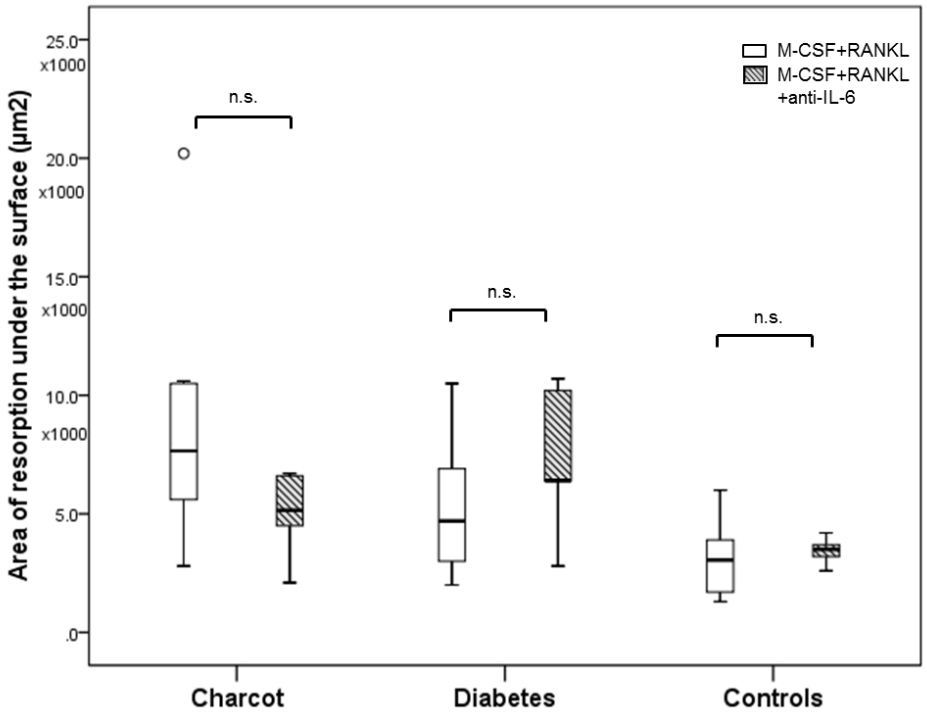

Figure 6-6 Comparison of the area of resorption under the surface of resorbed bone discs measured by surface profilometry between M-CSF+RANKL-treated cultures and M-CSF+RANKL+anti-IL-6-treated cultures.
Significance assessed by Mann-Whitney U test, Levels of significance are demonstrated on the graph. (n.s.- non-significant; p>0.05)
The area of resorption under the surface remained unchanged in response to anti-IL-6 treatment in Charcot patients (p>0.05), diabetic patients (p>0.05) and healthy control subjects (p>0.05).

6.5.4 Comparison of surface profile measurements in M-CSF+RANKL- and M-CSF+RANKL +anti-IL-6-treated cultures

After the addition of anti-IL-6 to M-CSF+RANKL treatment, the surface profile measurements of randomly selected areas revealed multi-shaped erosions of resorbed bovine bone discs in all study groups (Figure 6-7).

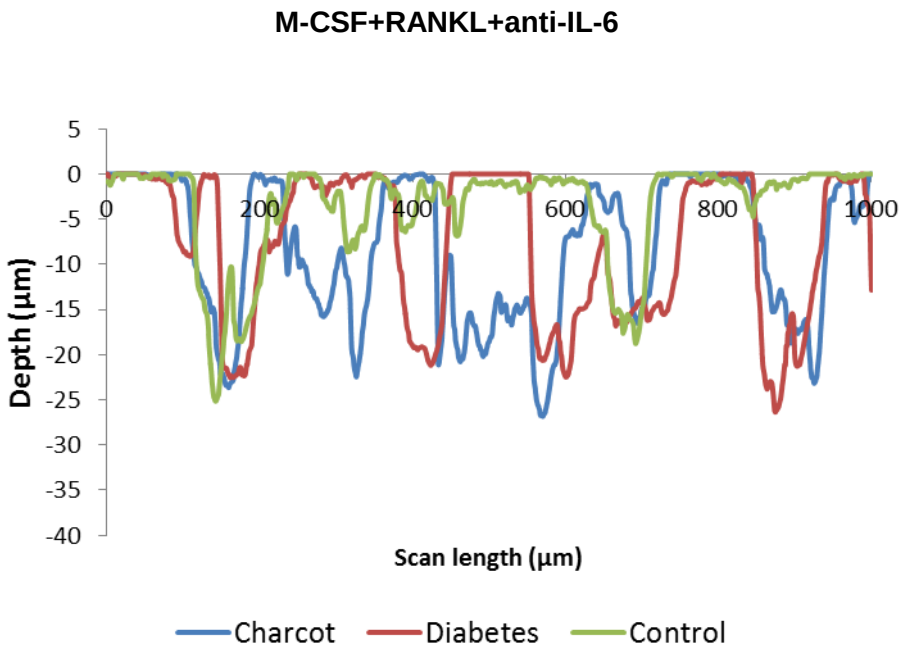

Figure 6-7 Representative erosion profiles of resorbed bone discs in a Charcot patient, diabetic patient and healthy control subject after surface profilometry in M-CSF+RANKL+anti-IL-6-treated cultures.
Pits appear larger in Charcot patients compared with pits in healthy control subjects and similarly, pits appeared larger in diabetic patients compared with healthy control subjects.

The addition of anti-IL-6 had an ambiguous effect on surface profile measurements in all study groups (Figure 6-8). In Charcot patients, pits appeared smaller in size and area in M-CSF+RANKL+anti-IL-6-treated cultures compared with M-CSF+RANKL-treated cultures (Figure 6-8A). In diabetic patients, pits appeared larger in size and area, (Figure 6-8B) whereas in healthy control subjects, the morphological appearance of pits remained unchanged (Figure 6-8) in M-CSF+RANKL+anti-IL-6-treated cultures compared with M-CSF+RANKL-treated cultures.

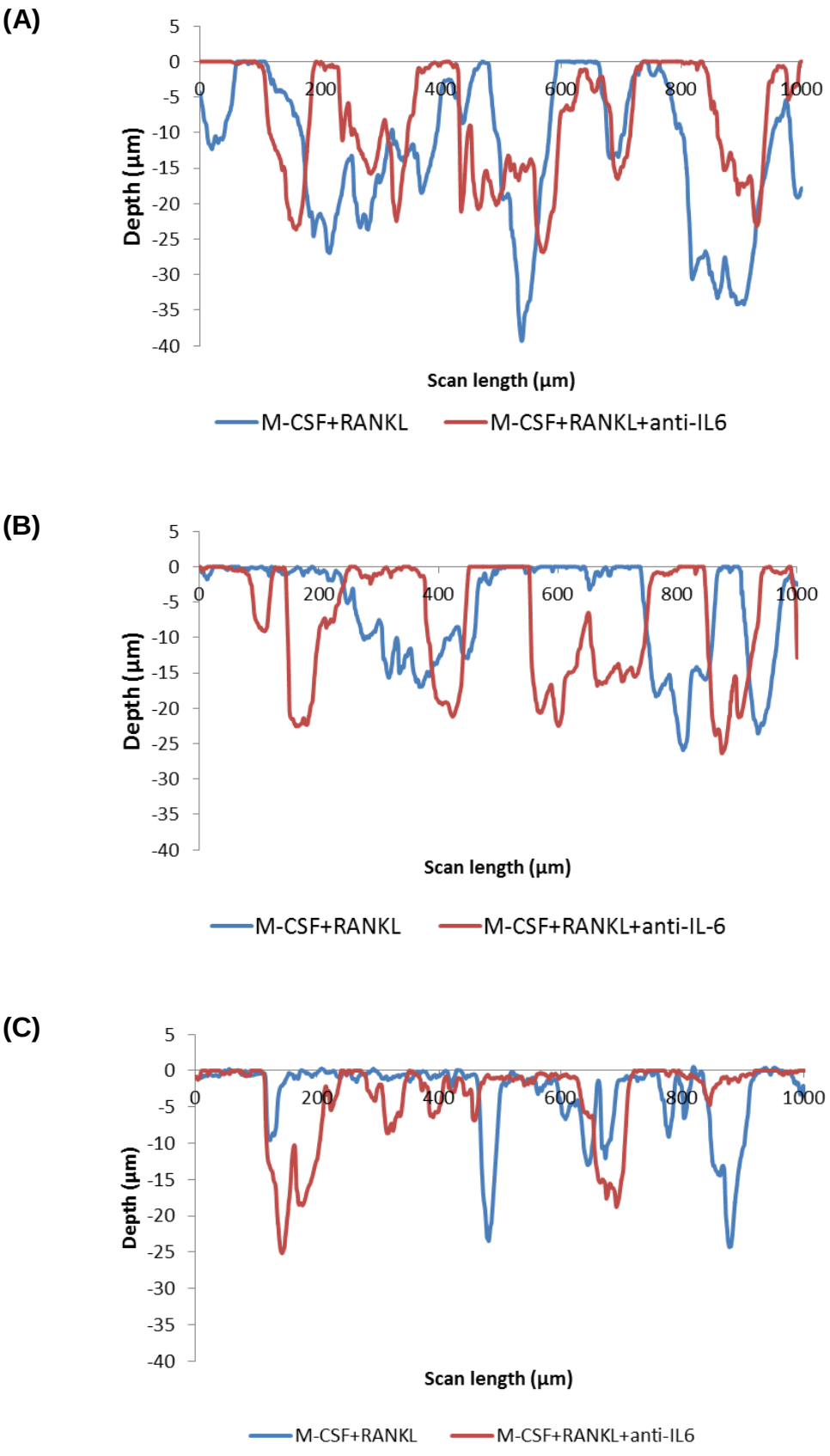

Figure 6-8 Representative erosion profiles of resorbed bone discs in M-CSF+RANKL-treated cultures and in M-CSF+RANKL+anti-IL-6-treated cultures
Non-remarkable changes of the erosion profile were noted in response to anti-IL-6 treatment in Charcot patients (A), diabetic patients (B) and healthy control subject (C).

6.5.5 Pit morphology

To quantitate the differences in below surface resorption, I evaluated pit morphology and compared pit parameters before and after the addition of anti-IL-6. The pit parameters in M-CSF+RANKL+anti-IL-6-treated cultures were not significantly different between the three study groups (Table 6-2).

Table 6-2 Measurements of uni-dented, bi-dented and multi-dented pits in M-CSF+RANKL+anti-IL-6-treated cultures in Charcot patients, diabetic patients and healthy control subjects

Pits	Parameter	Charcot	Diabetes	Control	p-value
Uni-dented	Width (µm)	45 [45-52]	50 [46-53]	43 [43-45]	>0.05
	FWHM (µm)	23 [22-24]	25 [23-26]	22 [21-23]	>0.05
	Depth (µm)	8 [7-8]	9 [8-9]	6 [6-8]	>0.05
Bi-dented	Width (µm)	86 [81-88]	81 [78-84]	90 [82-96]	>0.05
	FWHM (µm)	51 [45-56]	53 [45-60]	48 [48-54]	>0.05
	Depth (µm)	14 [9-1]	17 [15-17]	13 [12-14]	>0.05
Multi-dented	Width (µm)	148 [136-200]	191 [176-238]	133 [126-135]	>0.05
	FWHM (µm)	96 [91-121]	142 [129-162]	99 [87-101]	>0.05
	Depth (µm)	22 [20-23]	26 [25-27]	19 [15-23]	>0.05

Data expressed as median [25th-75th percentile] and analysed by the Kruskal-Wallis test; P-values indicate differences between Charcot patients, diabetic patients and healthy control subjects.
Non-significance difference in pit parameters (width, FWHM and depth) of the uni-dented, bi-dented and multi-dented pits between Charcot patients, diabetic patients and healthy control subjects (p>0.05 for all comparisons) in response to anti-IL-6 treatment.

No differences were noted between any of the pit parameters in all pairwise comparisons (Charcot patients versus diabetic patients, Charcot patients versus healthy control subjects and diabetic patients versus healthy control subjects, (p>0.05 for all comparisons).

The comparison of the pit parameters before and after the addition of anti-IL-6 revealed that in Charcot patents, there was a trend of a non-significant reduction of the width, FWHM and depth of uni-dented, bi-dented and multi-dented pits, (Figure 6-9). In contrast to Charcot patients, there was a trend of non-significant increase of the pit parameters in cultures from diabetic patients. In particular, multi-dented pits appeared enlarged both at the surface and under the surface (Figure 6-9). In controls, there was not a notable difference in the pit parameters between the two culture conditions (Figure 6-9).

(A) Uni-dented pits μ

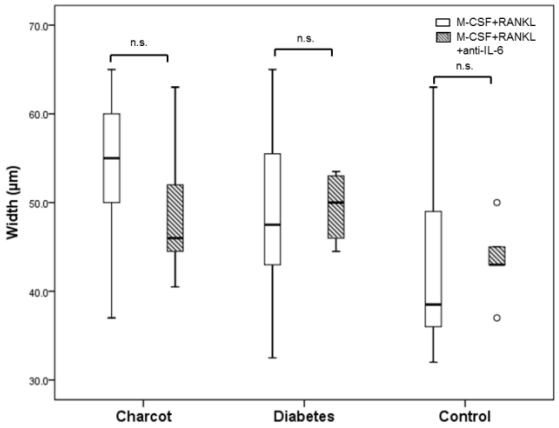

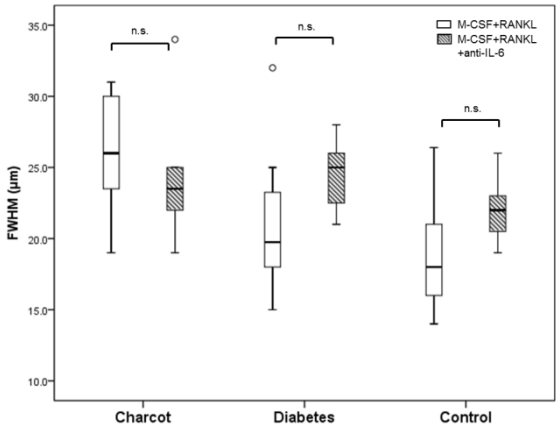

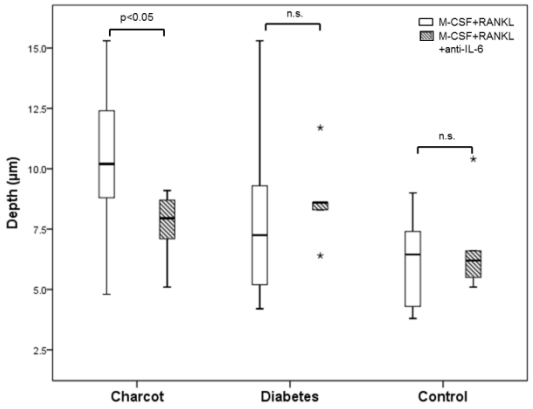

(B) Bi-dented pits

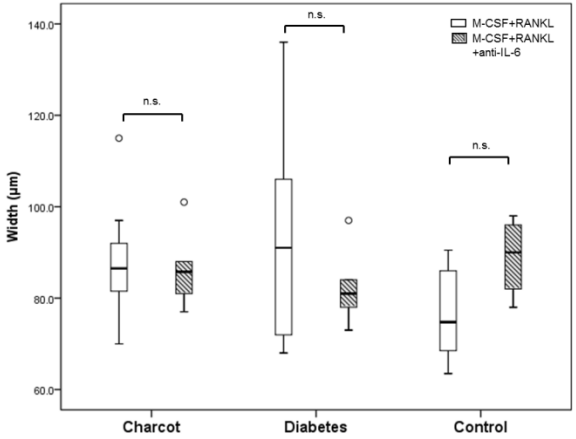

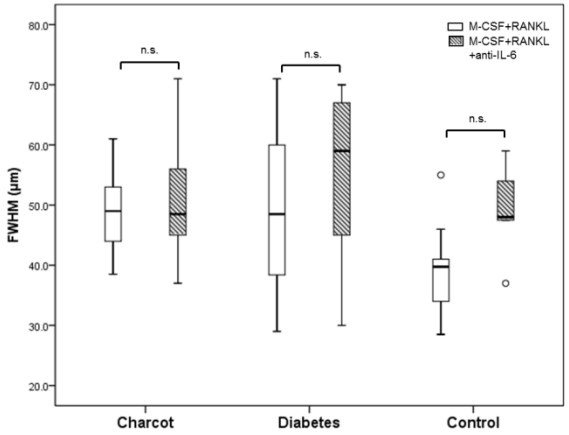

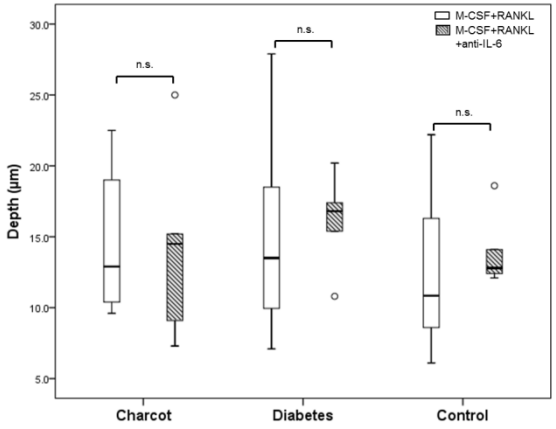

(C) Multi-dented pits

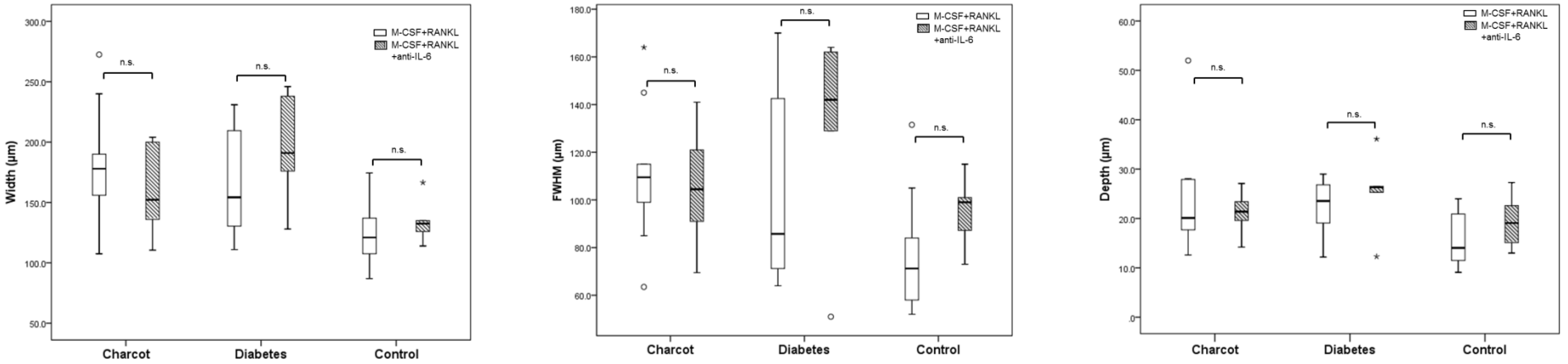

Figure 6-9 Comparison of pit measurements (width, depth and FWHM) between M-CSF+RANKL-treated cultures and M-CSF+RANKL+anti-IL-6-treated cultures

(A) Uni-dented pits; (B) bi-dented pits; (C) multi-dented pits. Significance assessed by Mann-Whitney U test, Levels of significance are demonstrated on the graphs; ns = non-significant (p>0.05).

Non-significant difference in the pit parameters of uni-dented, bi-dented pits and multi-dented pit parameters was noted in all study groups (p>0.05 for all comparisons) in response to anti-IL-6 treatment.

6.5.6 Pit distribution in M-CSF+RANKL- and M-CSF+RANKL +anti-IL-6-treated cultures

To determine whether there were any differences in the distribution of the shape of the pits, the percentage of uni-dented, bi-dented and multi-dented pits was compared between the two culture treatments. In Charcot patients, the addition of anti-IL-6 to M-CSF+RANKL resulted in a non-significant increase in the percentage of uni-dented pits (from 36% [31-43] to 43% [40-55], and a non-significant decrease in the percentage of multi-dented pits (from 40% [32-42] to 33% [27-38], whereas the percentage of bi-dented pits remained unchanged (from 24% [20-28] to 24% [17-28], (Figure 6-10A, B). There was a non-significant difference in the distribution of pits (uni-dented, bi-dented and multi-dented) between the two culture treatments in the diabetic patients (Figure 6-10 C, D) and in the healthy controls (Figure 6-10 E, F).

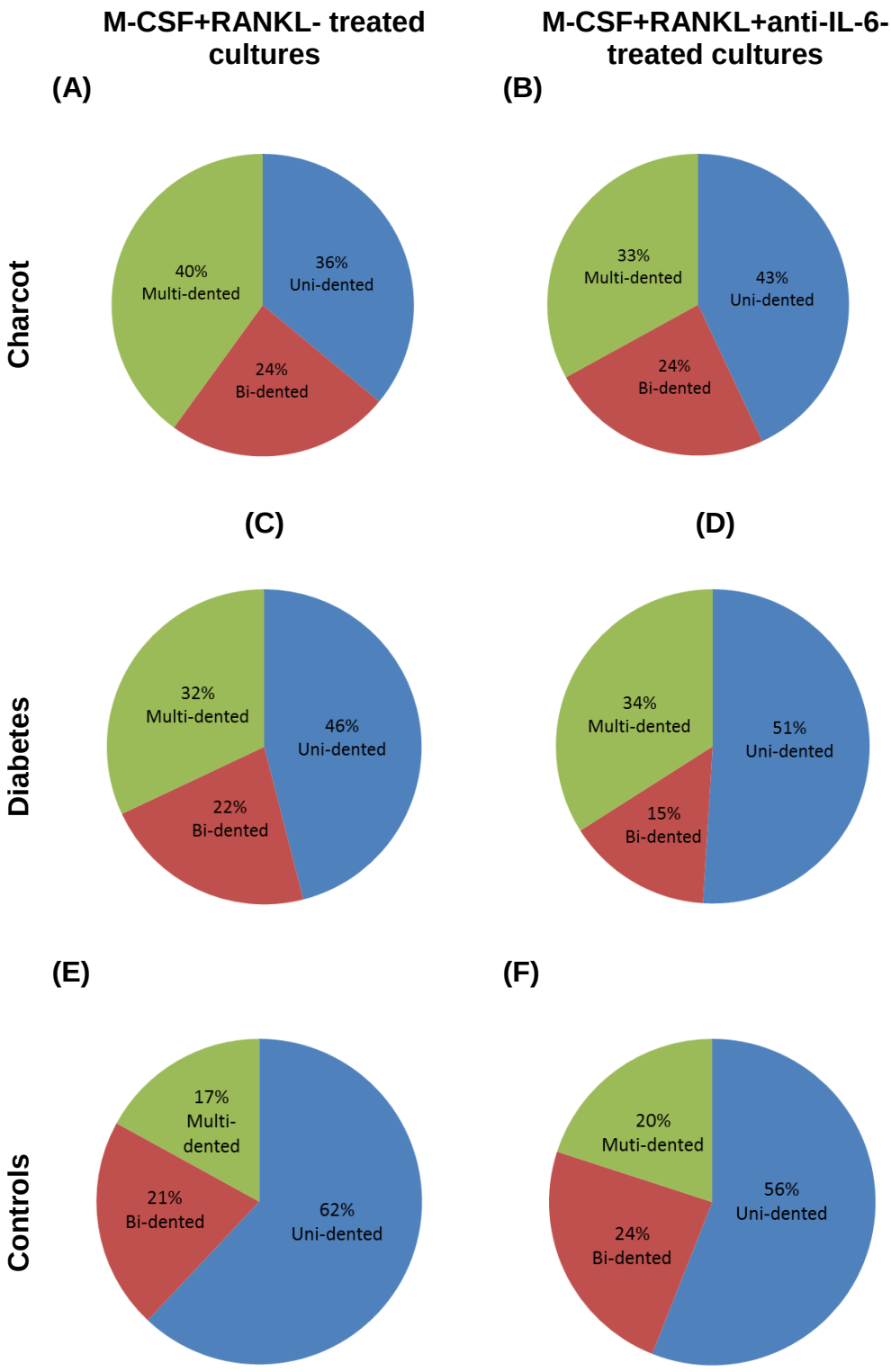

Figure 6-10 Distribution of pits according to their shape in M-CSF+RANKL and M-CSF+RANKL+anti-IL-6-treated cultures in Charcot patients, diabetic patients and healthy control subjects respectively

In Charcot patients the addition of anti-IL-6 treatment led to a non-significant increase in the percentage of uni-dented pits ($p>0.05$) and non-significant decrease ($p>0.05$) in the percentage of multi-dented pits, whereas the percentage of the bi-dented spits remained unchanged (A, B). No differences in the pit distribution were noted in diabetic patients (C, D) and in healthy control subjects (E, F); ($p>0.05$ for all comparisons).

6.5.7 Fold change of osteoclast formation and resorption (at the surface and under the surface) in culture medium after anti-IL-6 treatment

The overall change in the response to anti-IL-6 treatment was determined by calculating the fold change in the number of TRAP-positive multi-nucleated cells, bone resorption at the surface and under the surface in M-CSF+RANKL+anti-IL-6-treated cultures compared with M-CSF+RANKL -treated cultures. The fold change of osteoclast formation (6-A) and resorption both at the surface (6-B) and under the surface (6-C) was expressed as mean± SEM and was calculated as the ratio of the final value (M-CSF+RANKL+anti-IL-6-treated cultures) and the initial value (M-CSF+RANKL-treated cultures). The fold change was compared to data for M-CSF+RANKL-treated cultures (positive control) which was expressed as 1 for the purpose of the analysis.

6-A

$$\text{Fold change (TRAP} - \text{positive multi} - \text{nucleated cells)} = \frac{\text{Number [TRAP} - \text{positive multi} - \text{nucleted cells (M} - \text{CSF} + \text{RANKL} + \text{anti} - \text{IL} - 6 - \text{treated cultures)]}}{\text{Number [TRAP} - \text{positive multi} - \text{nucleated cells (M} - \text{CSF} + \text{RANKL} - \text{treated cultures)]}}$$

6-B

$$\text{Fold change (Area of bone resorption at the surface)} = \frac{\text{Percentage [Area of resorption at the surface (M} - \text{CSF} + \text{RANKL} + \text{anti} - \text{IL} - 6 - \text{treated cultures)]}}{\text{Percentage [Area of resorption at the surface (M} - \text{CSF} + \text{RANKL} - \text{treated cultures)]}}$$

6-C

$$\text{Fold change (Area of bone resorption under the surface)} = \frac{\text{Area of resorption under the surface (M} - \text{CSF} + \text{RANKL} + \text{anti} - \text{IL} - 6 - \text{treated cultures)} sq.\mu m}{\text{Area of resorption under the surface (M} - \text{CSF} + \text{RANKL} - \text{treated cultures) sq.}\mu\text{m}}$$

The addition of anti-IL-6 to M-CSF+RANKL-treated cultures led to a non-significant fold change in the number of TRAP-positive multi-nucleated cells in Charcot patients, diabetic patients and healthy control subjects (Figure 6-11A). However, in Charcot patients but not in diabetic patients and healthy control subjects, there was a significant fold change of the area of resorption at the surface (Figure 6-11B) but not under the surface, (Figure 6-11C).

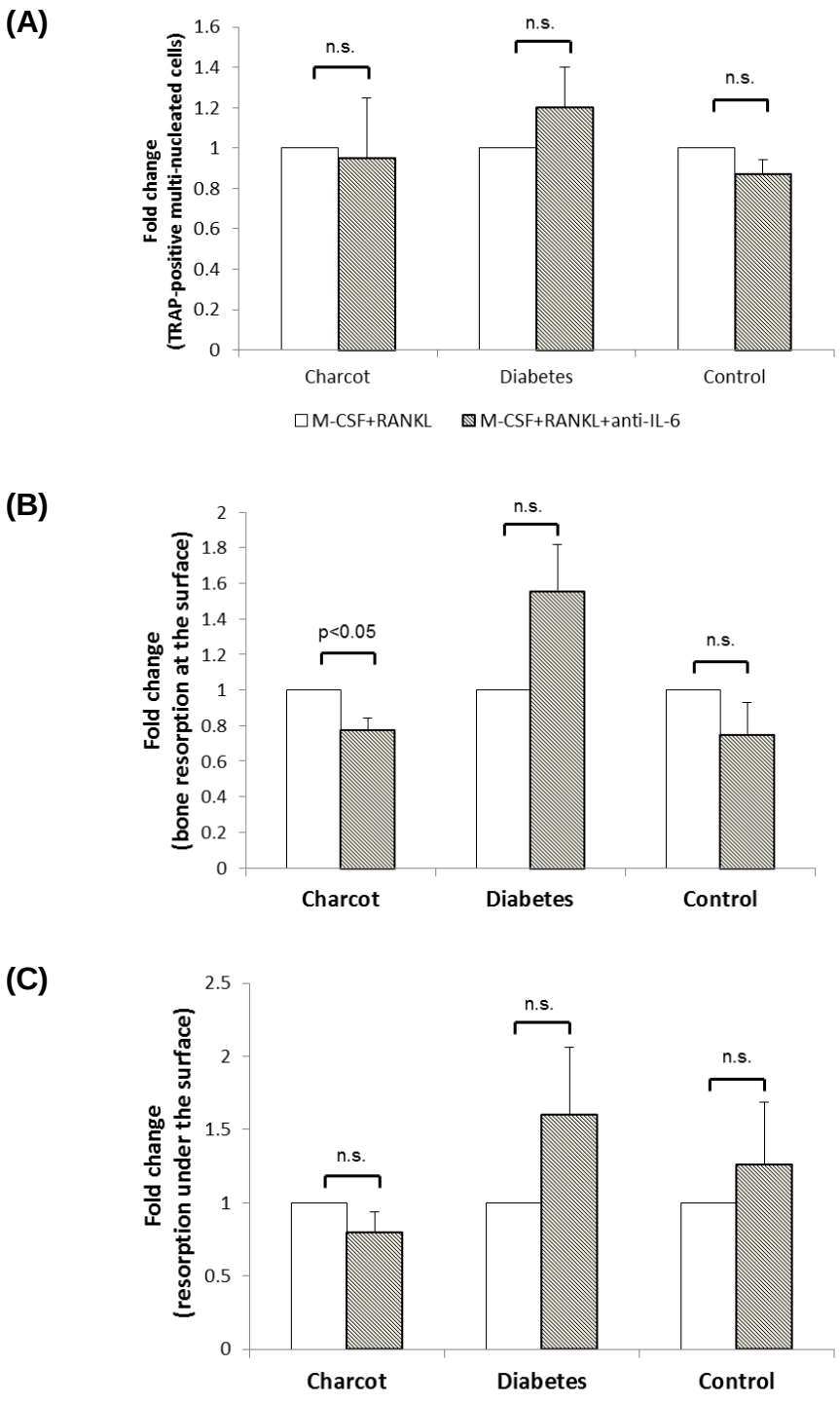

Figure 6-11 Fold change of osteoclast formation and resorption (at the surface and under the surface) in M-CSF+RANKL+anti-IL-6 treated cultures (grey striped bars) compared with M-CSF+RANKL-treated cultures (white bars).

(A) Number of TRAP-positive cells; (B) area of resorption at the surface; (C) area of resorption under the surface on bovine bone discs. Significance assessed by Mann-Whitney U test, Levels of significance are demonstrated on the graphs; ns = non-significant ($p>0.05$). Non-significant fold change in the number of TRAP-positive multi-nucleated cells in response to anti-IL-6 treatment in Charcot patients, diabetic patients and healthy control subjects ($p>0.05$ for all comparisons). Significant fold-change in the area of bone resorption at the surface ($p<0.05$) in response to anti-IL-6 treatment in Charcot patients but not in diabetic patients ($p>0.05$) and healthy control subjects ($p>0.05$); non-significant difference in the fold change of resorption under the surface in all study groups in response to anti-IL-6 ($p>0.05$ for both comparisons).

6.5.8 The effect of anti-IL-6 treatment on CTX release in culture supernatant

To assess the extent of bone resorption, I compared the concentration of CTX released over 72 hours in culture medium before and after the addition of anti-IL-6 in Charcot patients (n=4) and in healthy control subjects (n=4).

The fold change of CTX concentration in M-CSF+RANKL+anti-IL-6-treated cultures compared with M-CSF+RANKL-treated cultures was expressed as mean± SEM and was calculated as shown below (6-D).

6-D

$$\text{Fold change (CTX in culture medium)} = \frac{CTX\ (M-CSF+RANKL+anti-IL-6-treated\ cultures)nM}{CTX\ (M-CSF+RANKL-treated\ cultures)nM}$$

The addition of anti-IL-6 in M-CSF+RANKL-treated cultures led to a significant fold change of the concentration of CTX in culture supernatant only in Charcot patients but not in healthy control subjects (Figure 6-12).

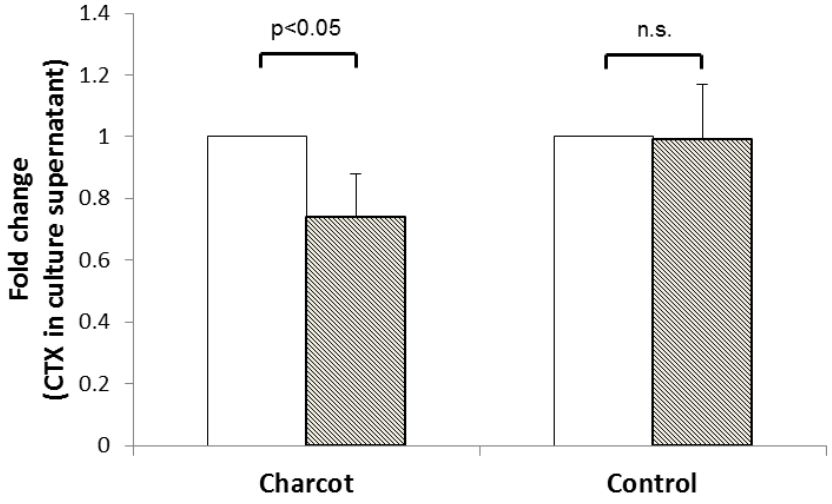

Figure 6-12 Fold change in the CTX concentration in M-CSF+RANKL+anti-IL-6-treated cultures (grey striped bars) compared with M-CSF+RANKL-treated cultures (white bars) Significance assessed by Mann-Whitney U test, Levels of significance are demonstrated on the graphs; ns = non-significant (p>0.05).Significant fold-change in the concentration of CTX in culture supernatant in response to anti-IL-6 treatment only in Charcot patients (p<0.05) but not in healthy control subjects (p>0.05).

6.5.9 Bone resorption on bovine bone discs in M-CSF+RANKL+anti-IL-6+OPG-treated cultures

Resorption was evaluated after the addition of anti-IL-6 and OPG to M-CSF+RANKL-treated cultures. The rationale of this study was to block simultaneously IL-6 and RANKL. The addition of anti-IL-6 and OPG inhibited resorption on bovine discs in all study groups, (Figure 6-13).

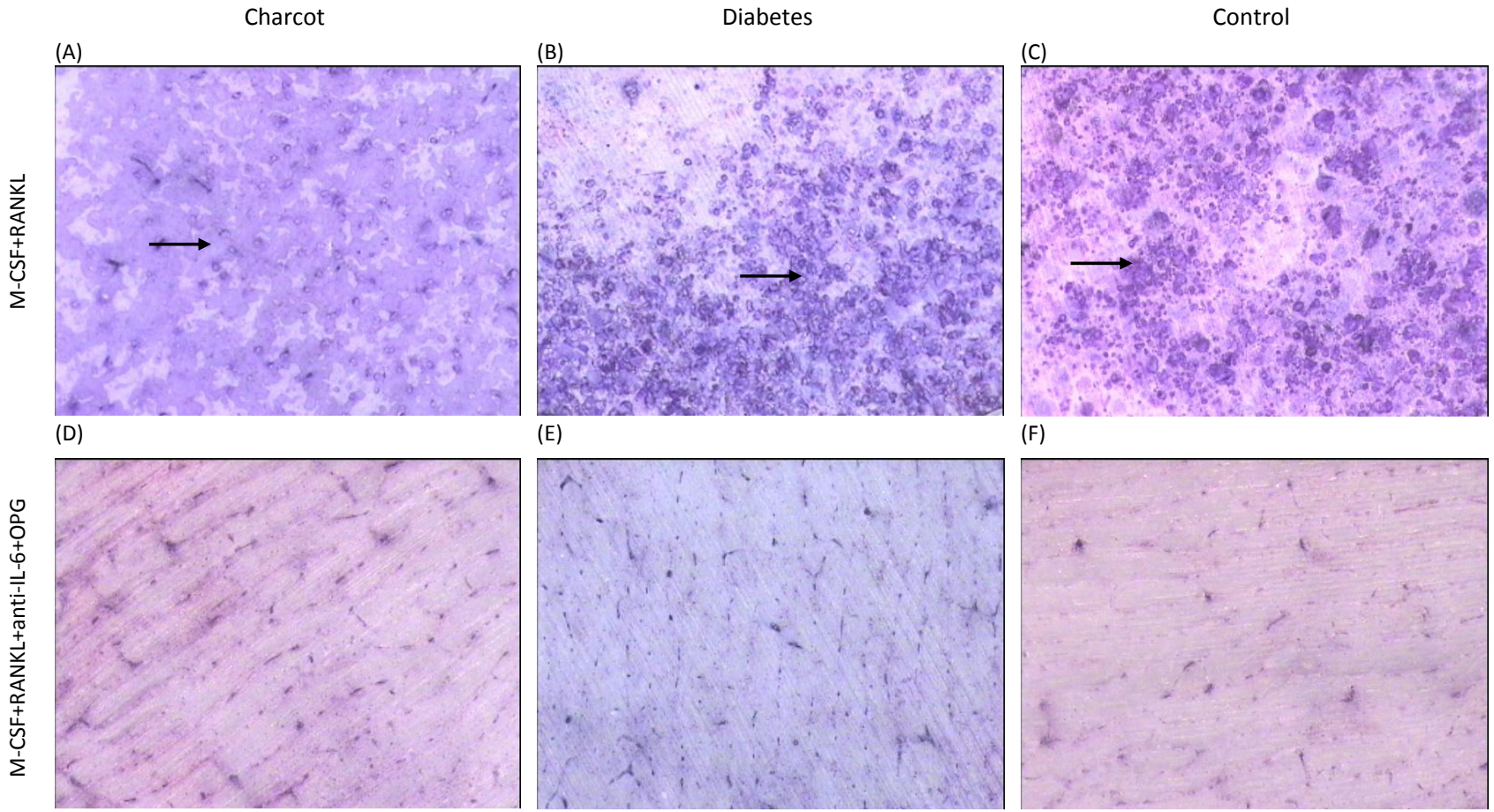

Figure 6-13 Toluidine blue staining of resorbed bovine bone discs in M-CSF+RANKL-treated cultures and in M-CSF+RANKL+anti-IL-6-treated cultures (light microscopy)

The addition of anti-IL-6 and OPG to M-CSF+RANKL inhibited resorption in all study groups (D, E, F). The black arrows denote some of the pits in M-CSF+RANKL-treated cultures in a Charcot patient (A), diabetic patient (B) and healthy control subject (C); (magnification X40)

Non-significant isolated minute pits were noted after observation of bovine bone discs at higher magnification in 5 subjects (3 Charcot patients, 1 diabetic patient and 1 healthy control subject), (Figure 6-14), but the distribution within the groups was not significant (p>0.05), (Table 6-3).

Table 6-3 Comparison of distribution according to presence of minute resorption pits in M-CSF+RANKL+anti-IL-6+OPG-treated cultures in Charcot patients, diabetic patients and healthy control subjects.

Minute pits in M-CSF+ RANKL+ anti-IL-6 +OPG treated cultures	Charcot	Diabetes	Control	P-value
Absent: present	3:3	4:1	5:1	>0.05

Chi-squared test; P-value indicates the difference between Charcot patients, diabetic patients ad healthy control subjects.
Non-significant difference according to presence: absence of minute isolated resorption pits in M-CSF+RANKL+anti-IL-6+OPG-treated cultures between Charcot patients, diabetic patients and healthy control subjects (p>0.05)

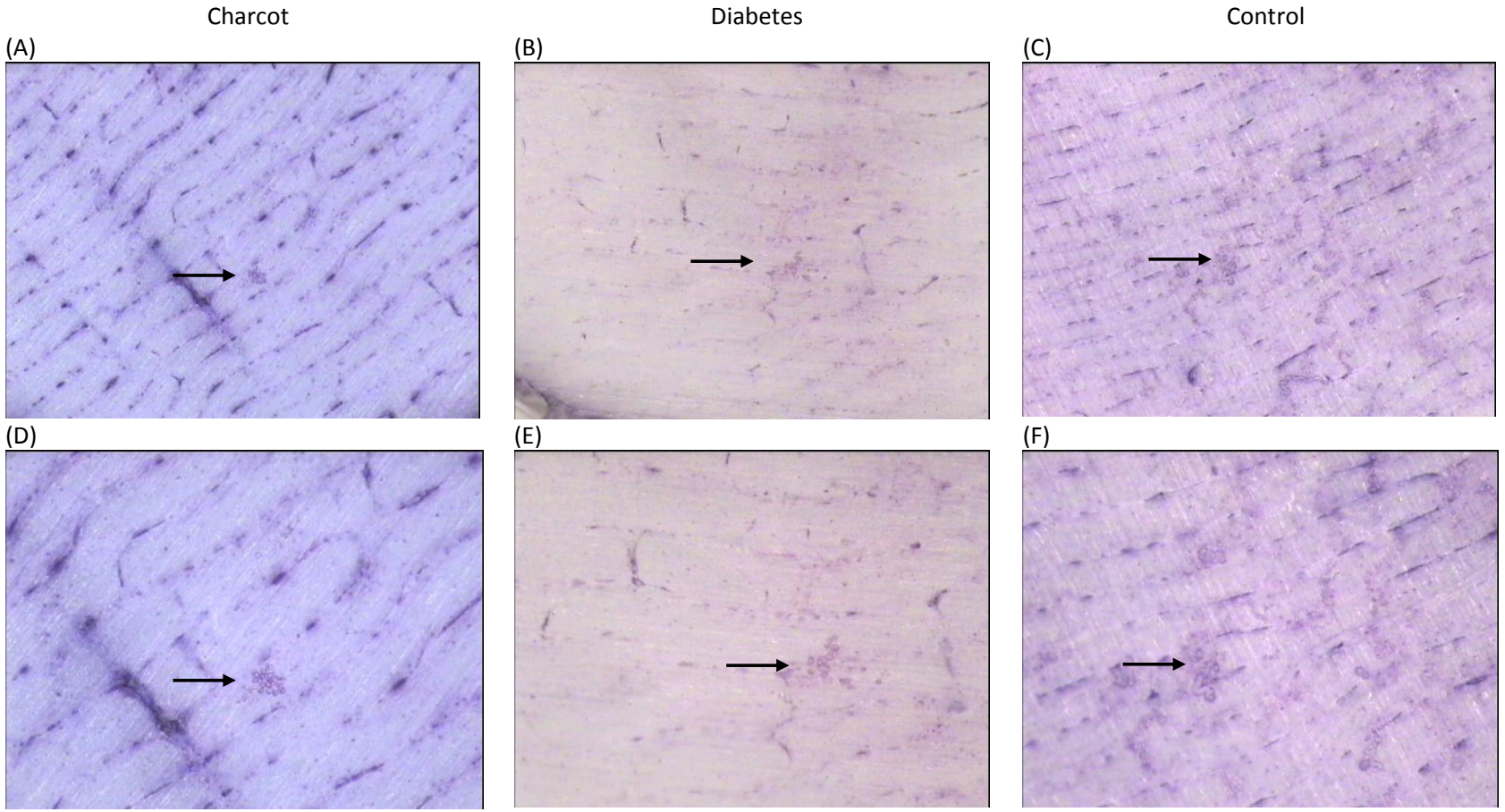

Figure 6-14 Toluidine blue staining of bovine bone discs in M-CSF+RANKL+anti-IL-6+OPG-treated cultures in a Charcot patient, diabetic patient and healthy control subject (light microscopy)

The arrows denote presence of isolated minute pits at X40 and at X70 magnification in a Charcot patient (A, D), diabetic control patient (B, E) and healthy control subject (C, F) respectively.

6.6 Discussion

This *in vitro* study has shown that there was a significant reduction in the resorbing activity of M-CSF+RANKL-treated osteoclasts derived from Charcot patients in response to anti-IL-6 treatment. The addition of anti-IL-6 resulted in significant reduction in the area of resorption on bovine bone discs on the surface, as assessed by image analysis but not in the area of resorption under the surface as assessed by surface profilometry. The aberrant erosion profile, pit morphology and pit distribution in M-CSF+RANKL-treated cultures remained unchanged after the addition of anti-IL-6. This suggests that the proinflammatory cytokine IL-6 reduced osteoclastic activity on the surface but had no effect on the resorption under the surface, erosion profile, pit morphology and pit distribution.

In this study, I sought to determine the role of IL-6 as a modulator of enhanced osteoclast function in M-CSF+RANKL-treated cultures in acute Charcot osteoarthropathy. Using the traditional resorption pit assay together with surface profilometry, I have demonstrated that although osteoclast formation in M-CSF+RANKL+anti-IL-6-treated cultures was similar between Charcot patients, diabetic patients and healthy control subjects, there was a significant reduction in the area of bone resorption on bovine bone discs only in Charcot patients. The reduction of the resorbing activity of Charcot-derived osteoclasts was confirmed by a significant reduction of the concentration of the CTX released in culture supernatant. However, in contrast to TNF-α, the inhibition of IL-6 did not reverse the aberrant pathological profile of resorbed bone discs from Charcot patients in M-CSF+RANKL-treated cultures.

There is evidence to suggest that IL-6 positively regulates osteoclast differentiation not only by inducing RANKL on the surface of osteoblasts, but also has a direct stimulatory effect on osteoclastic precursors (Duplomb, Baud'huin et al. 2008). IL-6 is the most abundant cytokine in the circulation and this *in vitro* experiment suggests a possible priming of osteoclastic precursors by IL-6. Inhibition of IL-6 led to a significant reduction of the area of resorption on bovine bone discs at the surface only in Charcot patients,

indicating a possible role of this cytokine in modulating osteoclast activity. The lack of significant changes in the erosion profile and pit morphology suggests that this cytokine does not alter the mode of resorption of newly-formed osteoclasts. This cytokine has been linked with inflammatory bone loss (12) and bone specimens from Charcot patients stained positive for IL-6 (Baumhauer, O'Keefe et al. 2006). Moreover, the serum concentration of IL-6 is raised in the acute active stage of Charcot osteoarthropathy and correlates with CTX, a marker of bone resorption (Petrova, Dew et al. 2015).

There is controversy regarding the role of IL-6 in driving osteoclastogenesis and bone resorption (Axmann, Bohm et al. 2009). Some studies have shown that in physiological conditions, IL-6 acts directly on osteoclast precursors to inhibit their differentiation and thus IL-6 acts to suppress bone resorption (Yoshitake, Itoh et al. 2008). However, under inflammatory conditions, IL-6 provides discordant signals to osteoclasts and osteoblasts – it directly inhibits osteoclast differentiation of osteoclastic precursors but at the same time up-regulates RANKL expression of osteoblasts and thereby indirectly induces osteoclast differentiation (Yoshitake, Itoh et al. 2008). The cellular effects of IL-6 are mediated through the IL-6R. Recent studies have shown that neutralising antibody to IL-6R directly blocks RANKL-mediated osteoclast formation by binding to monocytic precursor cells and thus inhibiting their differentiation into osteoclasts. (Axmann, Bohm et al. 2009). In addition, it was also shown that the blockade of IL-6R through neutralising antibodies specifically inhibits inflammatory osteoclastogenesis *in vitro* and also in vivo in a transgenic mouse model (Axmann, Bohm et al. 2009). Thus recent evidence supports that IL-6 modulates RANKL-mediated activity on osteoclasts and moreover, there is evidence to suggest that this cytokine is directly capable of inducing osteoclast formation by a RANKL-independent mechanism (Kudo, Sabokbar et al. 2003).

The exact role of IL-6 in the pathogenesis of Charcot osteoarthropathy is yet to be established. However, my *in vitro* experiment has shown that IL-6 modulates osteoclastic activity in the presence of RANKL. Indeed, the inhibition of RANKL by OPG abolished

osteoclastic resorbing activity not only in diabetic patients and healthy control subjects but also in patients with Charcot osteoarthropathy. Similarly, no resorption was noted after the combined inhibition of IL-6 and RANKL by anti-IL-6 and OPG respectively in all study groups. This suggests that IL-6 enhances RANKL-mediated osteoclastic activity in Charcot osteoarthropathy

Interestingly, the response to anti-IL-6 treatment was not as potent as the response to anti-TNF-α treatment and a possible interaction between these two cytokines in the osteoclastogenesis in acute Charcot osteoarthropathy is proposed (Figure 6-15). It has been postulated that there is an “add-on” effect of IL-6 on TNF-α-mediated inflammatory bone loss, as IL-6 mediates the effect of TNF-α on osteoclastogenesis but not vice versa (Redlich and Smolen 2012), (Axmann, Bohm et al. 2009). It is possible that in Charcot osteoarthropathy, IL-6 and TNF-α up-regulated RANKL-mediated osteoclastic resorption on the surface, whereas the enhanced resorption under the surface was modulated solely by TNF-α. Overall, this interaction resulted in enhanced RANKL-mediated activity leading to bone destruction and ultimately Charcot osteoarthropathy.

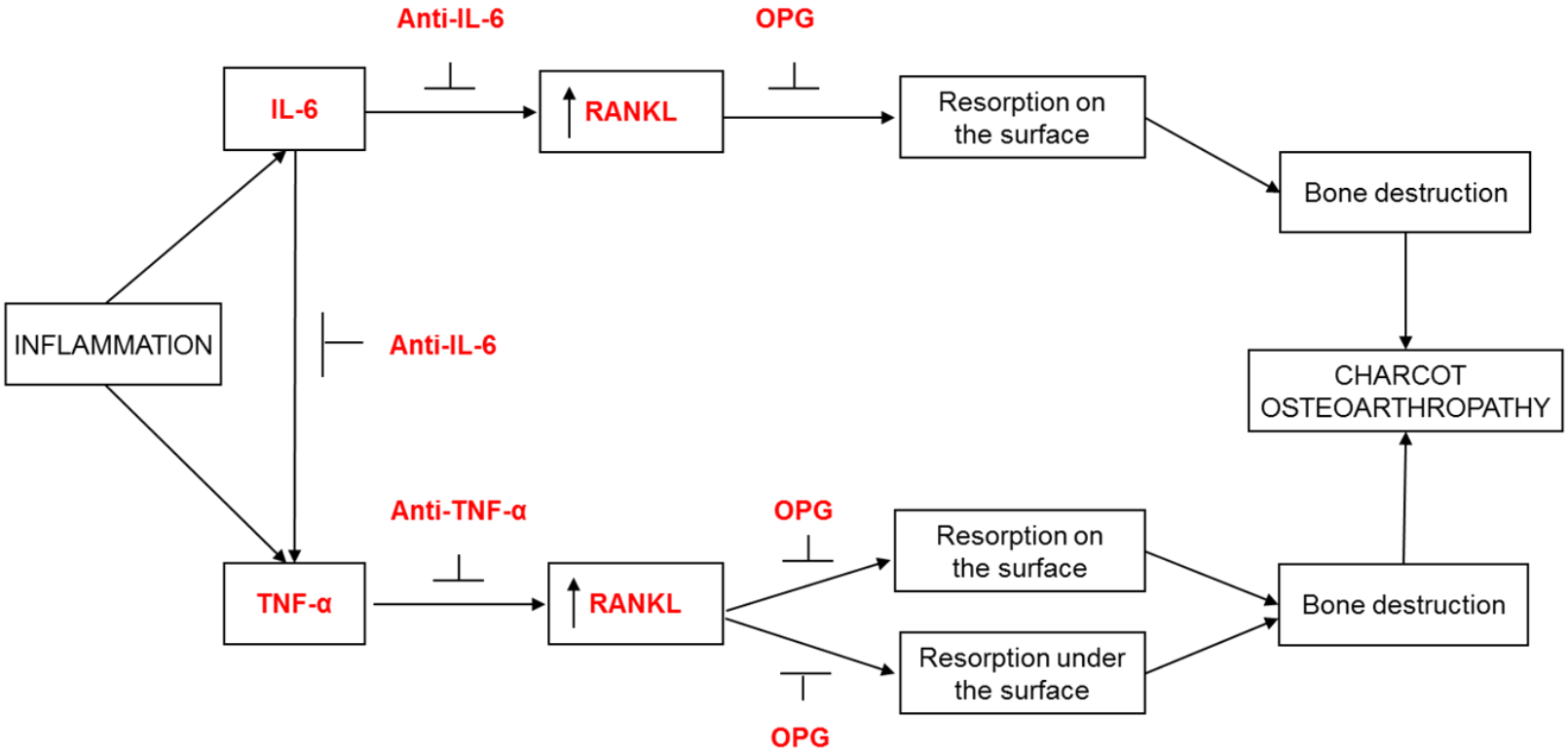

Figure 6-15 The hypothetical interaction between the proinflammatory cytokines IL-6 and TNF-α on RANKL-mediated osteoclastic activity in acute Charcot osteoarthropathy

In Charcot osteoarthropathy, the proinflammatory cytokines, IL-6 and TNF-α, modulated osteoclastic activity in the presence of RANKL. The addition of anti-IL-6 and anti-TNF-α to M-CSF+RANKL-treated cultures significantly reduced the area of resorption on the surface of resorbed bone discs. In addition, anti-TNF-α but not anti-IL-6 significantly reduced the area of resorption under the surface. The response to anti-IL-6 treatment was not as potent as the response to anti-TNF-α treatment. It is possible that there is an "add-on" effect of IL-6 on TNF-α-mediated bone resorption. Although the interaction between these cytokines is unknown, I demonstrated that IL-6 and TNF-α modulate RANKL-mediated osteoclastic activity leading to increased bone destruction and ultimately Charcot osteoarthropathy.

6.7 Conclusion

Although the exact role of action of IL-6 on the osteoclastogenesis in inflammatory bone loss is still disputed, I have demonstrated that IL-6 modulated osteoclast resorption in Charcot patients by using a classical resorption pit assay. The addition of anti-IL-6 significantly reduced bone resorption on the surface as assessed by image analysis, but had no impact on the erosion profile, pit morphology and distribution, as assessed by surface profiliometry.

Chapter 7 Conclusions and future directions

7.1 Introduction

This thesis contributes to our understanding of the pathogenesis of Charcot osteoarthropathy and sheds light on the mechanisms of increased osteoclastic activity in the acute Charcot foot.

KEY FINDINGS OF THIS THESIS:

7.2 Osteoclastic culture assay and surface profilometry, novel techniques to investigate the pathological bone resorption in acute Charcot osteoarthropathy

The main purpose of this research was to explore the hypothesis that aberrantly activated osteoclasts play a key role in the pathological bone destruction of the acute Charcot foot. To explore this hypothesis, I introduced for the first time in the field of Charcot osteoarthropathy the osteoclast culture assay. This is based on the observation that RANKL and OPG are the key extracellular regulators of osteoclast development and this has led to extensive research in studying the mechanisms of osteoclast differentiation and function in both physiological and pathological conditions. The osteoclastic culture assay has been validated as a suitable test to determine the capacity of osteoclast precursors to generate bone resorbing osteoclasts in a variety of diseases and also as an assay to monitor the bone resorbing activity of novel drugs (Susa, Luong-Nguyen et al. 2004).

The increased bone resorption of the acute Charcot foot has long been noted, although its exact cellular mechanisms have not been previously investigated. Using this

well-established *in vitro* technique, I assessed osteoclast formation and function in cultures treated with M-CSF+RANKL with and without inhibitors (OPG; neutralising antibody to TNF-α and neutralising antibody to IL-6) and demonstrated the usefulness of this technique to study osteoclast formation and function at the cellular level in patients with Charcot osteoarthropathy (Mabilleau, Petrova et al. 2008).

In addition, I developed a novel method to quantitate resorption on bone discs using surface profilometry (Petrova, Petrov et al. 2014). This technique provided a new perspective for measuring osteoclastic activity and was used to evaluate erosion patterns and pit parameters of resorbed bone discs under different culture treatments. It unmasked differences of the resorption pit profiles between osteoclasts generated from Charcot patients and controls (with and without diabetes) which were not previously noted using only the traditional pit assay (Petrova, Petrov et al. 2014).

Overall, these new techniques provided a contemporary approach to study the cellular mechanisms of osteoclast activation in this devastating condition. The proposed methodology could become fundamental in exploring osteoclast activity not only in the acute, active stage of the disease but also in the stage of resolution of the Charcot foot to monitor disease activity. There is a great clinical need to implement suitable techniques in the management of this condition to enable clinicians to diagnose the transition of the Charcot foot from the acute active stage into the chronic stable stage (Rogers, Frykberg et al. 2011). Furthermore, this novel approach could become fundamental in the monitoring of novel pharmacological therapies aiming to arrest the pathological bone destruction of the acute Charcot foot.

7.3 RANKL is the main activator of increased activity of newly formed osteoclasts in patients with acute Charcot osteoarthropathy

My main objective was to assess the role of RANKL in osteoclastic activation in acute Charcot osteoarthropathy. I generated functional human osteoclasts *in vitro* from PBMCs, isolated from Charcot patients, diabetic patients and healthy control subjects.

The research in this thesis has proved that in comparison to osteoclasts derived from diabetic patients and healthy control subjects, newly-formed osteoclasts from patients with acute Charcot osteoarthropathy exhibited enhanced response to RANKL as indicated by increased resorbing activity, which was not associated with an increase in osteoclast formation.

At the time of commencing of bone resorption *in vitro* (day 14), osteoclastic activity in Charcot patients was already upregulated, as indicated by the presence of larger and wider pits on bovine bone discs together with enhanced area of bone resorption.

The differences in the morphological appearance of the resorption pits between Charcot patients and controls were more clearly detected after 21 days in culture. Image analysis of resorbed bone discs revealed that in cultures from Charcot patients in comparison to cultures from diabetic patients and healthy control subjects, resorption pits were not only spread over an extensive area, but also appeared significantly larger and more frequently presented as lacunae or trenches. It is likely that the predominant single resorption events (identified as uni-dented pits by surface profilometry) were the results of the proteolytic activity of individual osteoclasts, as previously described, whereas pits which appeared as lacunae or trenches were the result of resorption carried out by osteoclasts which have migrated over the bone surface, leaving behind continuous trails of resorption (Hefti, Frischherz et al. 2010), (Jeon, Jeong et al. 2012).

The exuberant resorbing activity in M-CSF+RANKL-treated cultures from Charcot patients was morphologically characterised by surface profilometry. Resorbed bone

discs from cultures from Charcot patients exhibited aberrant erosion profiles with increased area of resorption under the surface, abnormal pit morphology and pit distribution. Uni-dented pits were predominantly seen in M-CSF+RANKL-treated cultures in both Charcot patients and controls at day 14. In contrast to control cultures in which the uni-dented pits remained the predominant type of resorption at day 21, in cultures from Charcot patients there was a shift in the distribution of pits from a high proportion of uni-dented pits at day 14 to a high proportion of multi-dented pits at day 21. This suggested that osteoclasts generated from Charcot patients displayed enhanced motility allowing them to carry out continuous resorption. Furthermore, the increased osteoclast function in cultures from Charcot patients in M-CSF+RANKL-treated cultures could be due to increased osteoclast survival, allowing the cells to maintain an active resorptive cycle rather than undergo apoptosis.

The response to RANKL was attenuated by OPG, a decoy inhibitor for RANKL, confirming the role of RANKL as an essential cytokine in osteoclast activation in acute Charcot osteoarthropathy. Overall, these studies revealed that in the presence of M-CSF+RANKL, osteoclastic precursors derived from patients with acute Charcot osteoarthropathy were primed to differentiate into highly-aggressive osteoclasts with increased resorbing activity.

7.4 The proinflammatory cytokine TNF-α modulates RANKL-mediated osteoclastic activity in acute Charcot osteoarthropathy

The addition of anti-TNF-α to M-CSF+RANKL-treated cultures significantly reduced bone resorption on bovine bone discs in Charcot patients but not in diabetic patients and healthy control subjects. The addition of anti-TNF-α in cultures from Charcot patients modulated osteoclast function only and not osteoclast formation.

Image analysis demonstrated that the addition of anti-TNF-α decreased by 30% the area of resorption on bovine bone discs. Surface profilometry revealed that the below

surface area of resorption was also decreased by 30% after the addition of anti-TNF-α. Moreover, there was a 30% reduction of the concentration of CTX released in culture supernatant before and after the addition of anti-TNF-α to M-CSF+RANKL-treated cultures.

In addition to reduction of osteoclast resorption on bovine bone discs from cultures from Charcot patients, TNF-α inhibition reversed the pathological erosion profile of resorbed bone discs in M-CSF+RANKL-treated cultures and normalised the pit distribution and pit morphology. The relative increase of multi-dented pits together with the relative decrease of the uni-dented pits in M-CSF+RANKL-treated cultures was reversed after the addition of anti-TNF-α, indicating that TNF-α modified the resorptive behaviour of newly-formed osteoclasts derived from Charcot patients. This may result from a TNF-α induced imbalance between the relative rate of collagenolysis and demineralisation (Soe, Merrild et al. 2013), which requires further studies.

Overall these studies demonstrated that in addition to RANKL, TNF-α primed osteoclastic precursors differentiated into highly-active osteoclasts with enhanced resorbing activity.

7.5 The proinflammatory cytokine IL-6 decreased bone resorption only at the surface of resorbed bone disc in cultures from Charcot patients

The addition of anti-IL-6 to M-CSF+RANKL-treated cultures significantly reduced bone resorption on bovine bone discs in Charcot patients but not in diabetic patients and healthy control subjects. Anti-IL-6-treatment significantly reduced osteoclast function but did not alter osteoclast formation. Image analysis demonstrated that the addition of anti-IL-6 decreased by 22% the area of resorption on bovine bone discs. There was also a 20% reduction of the concentration of CTX released in culture supernatant before and after the addition of anti-IL-6 to M-CSF+RANKL-treated cultures. Although the inhibition

of IL-6 resulted in a significant reduction in the area of resorption at the surface of bone discs, as assessed by image analysis, surface profilometry revealed that the area of resorption under the surface was similar before and after the addition of anti-IL-6. This is in contrast to anti-TNF-α treatment which resulted in a significant reduction of the area of resorption both at and below surface. Furthermore, the aberrant erosion profile, pit morphology and pit distribution in M-CSF+RANKL-treated cultures remained unchanged after the addition of anti-IL-6.

The overall reduction of the area of resorption on the surface after the addition of anti-IL-6 could be due to a shift of the distribution of the type of the resorption pits in M-CSF+RANKL-treated cultures compared with M-SF+RANKL+anti-IL-6-treated cultures. The addition of anti-IL-6 led to a non-significant reduction of the percentage of multi-dented pits and a non-significant increase of the percentage of uni-dented pits. The overall response to anti-IL-6 treatment was not as potent as the response to anti-TNF-α. It is possible that IL-6 potentiated the TNF-α mediated modulation of RANKL activity, as a result of a possible “add-on” effect (Redlich and Smolen 2012). Alternatively, the cross-talk of these two cytokines on osteoclastic precursors is unknown (Zupan, Jeras et al. 2013).

7.6 TNF-α and IL-6 modulate osteoclastic activity in the presence of RANKL

Bone resorption on bovine bone discs was abolished in M-CSF+RANKL+OPG-treated cultures before and after the addition of anti-TNF-α or anti-IL-6 respectively not only in diabetic patients and healthy controls but also in cultures from Charcot patients. Thus in the absence of RANKL, the enhanced resorbing activity of Charcot osteoclasts was blocked.

This confirms that RANKL is the main activator of increased osteoclastic activity whereas TNF-α and IL-6 have an additive effect.

7.7 Study limitations

Although this study reported that the pattern of resorption on bovine bone discs was different between Charcot patients and controls (with and without diabetes) and also between culture treatments, it did not explore the possible driving mechanisms.

The enhanced resorbing activity in M-CSF+RANKL-treated cultures in Charcot patients could be due to cathepsin K upregulation. It has been previously shown that the extent of resorption over bone surfaces results from the balance between factors upregulating or downregulating cathepsin K (Soe and Delaisse 2010). Enlarged resorption pits similar to the lacunae and trenches, predominantly noted in M-CSF+RANKL-treated cultures in Charcot patients, have been reported in cultures treated with cathepsin K inducers (Soe and Delaisse 2010). In contrast, osteoclasts treated with cathepsin K inhibitors form small round shallow pits (Leung, Pickarski et al. 2011) similar to the pits which I reported in control cultures. The possible RANKL and TNF-α-induced upregulaton of cathepsin K in cultures from Charcot patents could explain the observed differences in the type of resorption noted in M-CSF+RANKL-treated cultures before and after the addition of anti-TNF-α. In contrast to TNF-α, it is likely that IL-6 did not modulate cathepsin K activity as the addition of anti-IL-6 did not alter the pit morphology and the shape of the pits as well as the area of resorption under the surface. Upregulation of cathepsin K in acute Charcot osteoarthropathy requires further studies as this mechanism may potentially indicate a novel treatment target to reduce the enhanced bone resorption in patients with this condition by using cathepsin K inhibitors.

As well as cathepsin K upregulation, a further explanation of the extensive bone resorption observed on bone discs from Charcot patients could be a TNF-α driven increased migration, increased survival and reduced apoptosis of Charcot derived osteoclasts. It has been shown that TNF-α activated Charcot monocytes display a significant resistance to apoptosis (Uccioli, Sinistro et al. 2010). Further studies are needed to demonstrate how TNF-α may modulate the resorptive behaviour of activated osteoclasts in Charcot osteoarthropathy. It may be possible to activate osteoclastic

precursors, isolated from healthy control subjects and diabetic patients with neuropathy who are at risk of Charcot osteoarthropathy, with varying concentrations of TNF-α to assess osteoclastic activity after the addition of RANKL.

In addition, the interaction between IL-6 and TNF-α in the pathological bone resorption of the acute Charcot foot is unknown (Uccioli, Sinistro et al. 2010). It has been shown that IL-6 can potentiate the response to TNF-α (Redlich and Smolen 2012). In my studies, I assessed the role of TNF-α and IL-6 in separate experiments rather than in combination. The rate of osteoclastogenesis in vivo is a result of the sum of activating and inhibitory signals (Kwan Tat, Padrines et al. 2004) and in the complex Charcot patient, the interplay of various stimulating and inhibitory stimuli determines the severity of bone destruction.

A further limitation to my study was that I assessed bone resorption in two levels, one at the surface and the other under the surface. There are a number of methods that can be used to measure the volume and the depth of eroded areas, including scanning electron microscopy, confocal laser microscopy, and contact profilometry [13]. However, 3D reconstruction images do not always provide a true representation of the resorption lacuna [13]. To overcome this limitation it may be possible to carry out a 3D analysis of resorption of the entire bovine bone disc by using novel X-ray micro-CT technique (Xradia Versa, Carl Zeiss Microscopy GmbH). I have already contacted the company, which have suggested a measurement protocol. Furthermore, I have discussed this project with Professors Kimmel and Akhter from Creighton University, USA, who have already expressed an interest in collaborating to develop this novel technique.

7.8 Future prospective

My observations not only shed light on the pathogenesis of Charcot osteoarthropathy but may also have important implications for future management of this condition.

This study has pointed out several possible cellular targets that may be important for planning future therapies in this devastating condition- RANKL blockade or anti-TNF-α therapy aiming to inhibit the TNF-α modulation of osteoclastic precursors. Alternatively, cathepsin K inhibitors could be important to arrest the extensive bone resorption, which characterises the acute stage of this condition.

The results of this thesis demonstrated that in acute Charcot osteoarthropathy there is aberrant osteoclast activation with enhanced response to RANKL, which is further modulated by the proinflammatory cytokines TNF-α and IL-6. These observations provide a scientific basis for future intervention by raising the possibility of using RANKL inhibition in the management of Charcot foot. This cytokine is important for the pathogenesis of vascular calcification in this condition and with my observations I have also confirmed its role as the main osteoclast activator.

Although the relative importance of TNF-α and IL-6 in the osteoclastogenesis has not to be underestimated, it will be difficult for anti-TNF-α agents or anti-IL-6 to be useful in the management of Charcot osteoarthropathy as the window of opportunity to administer these therapies in the inflamed neuropathic Charcot foot is limited. Once osteoclastic precursors are primed to differentiate into highly resorbing osteoclasts by TNF-α and IL-6 the response to their blockade is uncertain, as they target not only osteoclastic precursors to differentiate into osteoclasts, but also enhance RANKL-expression of osteoblasts (Redlich and Smolen 2012). In addition, these proinflammatory cytokines could upregulate RANKL expression by activated T-lymphocytes due to uncontrolled inflammation (Zupan, Jeras et al. 2013). The benefit/ risk of these anti-

inflammatory therapies in diabetes is uncertain, due to an increased risk of infection and side effects. Moreover, in agreement with previous studies, I have confirmed that for their osteogenic action, TNF-α and IL-6 require RANKL (Lam, Takeshita et al. 2000). Thus Denusomab, a monoclonal antibody against RANKL, could be a treatment of choice which may directly inhibit osteoclast activation and indirectly arrest the inflammatory modulation on osteoclastic precursors. Indeed, Denusomab has been used in the treatment of osteoporosis and rheumatoid arthritis. There is firm evidence to suggest the usefulness of this therapy to prevent bone reduction in postmenopausal women (Papapoulos, Chapurlat et al. 2012). With regard to patients with rheumatoid arthritis, the addition of Denusomab to ongoing treatment with methotrexate led to inhibition of structural changes and improved bone mineral density (Cohen, Dore et al. 2008).

In addition to Denusomab, cathepsin K inhibitors could provide a further possible target to arrest the pathological bone resorption of the acute active stage of the disease. My studies have suggested that in the acute Charcot foot, RANKL and TNF-α could upregulate cathepsin K activity. Furthermore, the latter can be upregulated by small fibre neuropathy via lack of CGRP control on bone as evidence from experimental work has demonstrated that CGRP inhibits bone resorption by down-regulating osteoclastic genes including cathepsin K. At present, a phase 3 clinical study is underway to explore the usefulness of the cathepsin K inhibitor Odanacatib in the management of generalised bone loss (http://clinicaltrials.gov/ct2/show/NCT01803607). Future studies are needed to explore this mechanism as a potential target in the management of Charcot osteoarthropathy.

Although at present there is speculation about the possible benefit of treatment with biologic agents, I am not aware of any cases of Charcot osteoarthropathy where such therapies have been used. Nevertheless, my studies provide the basis for scientific intervention for future trials in patients with acute Charcot osteoarthropathy.

Reference list

Alexander, M. Y. (2009). "RANKL links arterial calcification with osteolysis." Circ Res **104**(9): 1032-1034.

Armstrong, D. G. and L. A. Lavery (1997). "Monitoring healing of acute Charcot's arthropathy with infrared dermal thermometry." Journal of Rehabilitation Research & Development **34**(3): 317-321.

Armstrong, D. G. and L. A. Lavery (1998). "Elevated peak plantar pressures in patients who have Charcot arthropathy." Journal of Bone & Joint Surgery - American Volume **80**(3): 365-369.

Armstrong, D. G., W. F. Todd, L. A. Lavery, L. B. Harkless and T. R. Bushman (1997). "The natural history of acute Charcot's arthropathy in a diabetic foot specialty clinic." Diabetic Medicine **14**(5): 357-363.

Axmann, R., C. Bohm, G. Kronke, J. Zwerina, J. Smolen and G. Schett (2009). "Inhibition of interleukin-6 receptor directly blocks osteoclast formation in vitro and in vivo." Arthritis & Rheumatism **60**(9): 2747-2756.

Baumhauer, J. F., R. J. O'Keefe, L. C. Schon and M. S. Pinzur (2006). "Cytokine-induced osteoclastic bone resorption in charcot arthropathy: an immunohistochemical study." Foot & Ankle International **27**(10): 797-800.

Bem, R., A. Jirkovska, M. Dubsky, V. Fejfarova, M. Buncova, J. Skibova and E. B. Jude (2010). "Role of quantitative bone scanning in the assessment of bone turnover in patients with Charcot foot." Diabetes Care **33**(2): 348-349.

Bernard, G. W. and C. Shih (1990). "The osteogenic stimulating effect of neuroactive calcitonin gene-related peptide." Peptides **11**(4): 625-632.

Bjurholm, A., A. Kreicbergs, M. Schultzberg and U. H. Lerner (1992). "Neuroendocrine regulation of cyclic AMP formation in osteoblastic cell lines (UMR-106-01, ROS 17/2.8, MC3T3-E1, and Saos-2) and primary bone cells." Journal of Bone & Mineral Research **7**(9): 1011-1019.

Boulton, A. J., A. I. Vinik, J. C. Arezzo, V. Bril, E. L. Feldman, R. Freeman, R. A. Malik, R. E. Maser, J. M. Sosenko, D. Ziegler and A. American Diabetes (2005). "Diabetic neuropathies: a statement by the American Diabetes Association." Diabetes Care **28**(4): 956-962.

Boyce, B. F. and L. Xing (2008). "Functions of RANKL/RANK/OPG in bone modeling and remodeling." Archives of Biochemistry & Biophysics **473**(2): 139-146.

Boyle, W. J., W. S. Simonet and D. L. Lacey (2003). "Osteoclast differentiation and activation." Nature **423**(6937): 337-342.

Bucay, N., I. Sarosi, C. R. Dunstan, S. Morony, J. Tarpley, C. Capparelli, S. Scully, H. L. Tan, W. Xu, D. L. Lacey, W. J. Boyle and W. S. Simonet (1998). "osteoprotegerin-deficient mice develop early onset osteoporosis and arterial calcification." Genes & Development **12**(9): 1260-1268.

Cavanagh, P. R., M. J. Young, J. E. Adams, K. L. Vickers and A. J. Boulton (1994). "Radiographic abnormalities in the feet of patients with diabetic neuropathy." Diabetes Care **17**(3): 201-209.

Chantelau, E. (2005). "The perils of procrastination: effects of early vs. delayed detection and treatment of incipient Charcot fracture." Diabet Med **22**(12): 1707-1712.

Chantelau, E. and G. Grutzner (2014). "Is the Eichenholtz classification still valid for the diabetc Charcot foot?" Swiss Medical Weekly(144): w13948.

Chantelau, E. and L. W. Poll (2006). "Evaluation of the diabetic charcot foot by MR imaging or plain radiography--an observational study." Experimental & Clinical Endocrinology & Diabetes **114**(8): 428-431.

Chantelau, E., T. Wienemann and A. Richter (2012). "Pressure pain thresholds at the diabetic Charcot-foot: an exploratory study.[Erratum appears in J Musculoskelet Neuronal Interact. 2013 Jun;13(2):263]." Journal of Musculoskeletal Neuronal Interactions **12**(2): 95-101.

Cherruau, M., P. Facchinetti, B. Baroukh and J. L. Saffar (1999). "Chemical sympathectomy impairs bone resorption in rats: a role for the sympathetic system on bone metabolism." Bone **25**(5): 545-551.

Childs, M., D. G. Armstrong and G. W. Edelson (1998). "Is Charcot arthropathy a late sequela of osteoporosis in patients with diabetes mellitus?" Journal of Foot & Ankle Surgery **37**(5): 437-439; discussion 449.

Christensen, T. M., J. Bulow, L. Simonsen, P. E. Holstein and O. L. Svendsen (2010). "Bone mineral density in diabetes mellitus patients with and without a Charcot foot." Clinical Physiology & Functional Imaging **30**(2): 130-134.

Christensen, T. M., L. Simonsen, P. E. Holstein, O. L. Svendsen and J. Bulow (2011). "Sympathetic neuropathy in diabetes mellitus patients does not elicit Charcot osteoarthropathy." Journal of Diabetes & its Complications **25**(5): 320-324.

Clasen, S. (2000). "Is diabetic Charcot foot related to lower limb osteopaenia?" Foot and ankle surgery **6**: 255-259.

Cohen, S. B., R. K. Dore, N. E. Lane, P. A. Ory, C. G. Peterfy, J. T. Sharp, D. van der Heijde, L. Zhou, W. Tsuji, R. Newmark and G. Denosumab Rheumatoid Arthritis Study (2008). "Denosumab treatment effects on structural damage, bone mineral density, and bone turnover in rheumatoid arthritis: a twelve-month, multicenter, randomized, double-blind, placebo-controlled, phase II clinical trial." Arthritis & Rheumatism **58**(5): 1299-1309.

Cope, A. P., M. Londei, N. R. Chu, S. B. Cohen, M. J. Elliott, F. M. Brennan, R. N. Maini and M. Feldmann (1994). "Chronic exposure to tumor necrosis factor (TNF) in vitro impairs the activation of T cells through the T cell receptor/CD3 complex; reversal in vivo by anti-TNF antibodies in patients with rheumatoid arthritis." Journal of Clinical Investigation **94**(2): 749-760.

Cundy, T. F., M. E. Edmonds and P. J. Watkins (1985). "Osteopenia and metatarsal fractures in diabetic neuropathy." Diabetic Medicine **2**(6): 461-464.

Dhawan, V., K. F. Spratt, M. S. Pinzur, J. Baumhauer, S. Rudicel and C. L. Saltzman (2005). "Reliability of AOFAS diabetic foot questionnaire in Charcot arthropathy: stability, internal consistency, and measurable difference." Foot & Ankle International **26**(9): 717-731.

Dhore, C. R., J. P. Cleutjens, E. Lutgens, K. B. Cleutjens, P. P. Geusens, P. J. Kitslaar, J. H. Tordoir, H. M. Spronk, C. Vermeer and M. J. Daemen (2001). "Differential

expression of bone matrix regulatory proteins in human atherosclerotic plaques." Arteriosclerosis, Thrombosis & Vascular Biology **21**(12): 1998-2003.

Duplomb, L., M. Baud'huin, C. Charrier, M. Berreur, V. Trichet, F. Blanchard and D. Heymann (2008). "Interleukin-6 inhibits receptor activator of nuclear factor kappaB ligand-induced osteoclastogenesis by diverting cells into the macrophage lineage: key role of Serine727 phosphorylation of signal transducer and activator of transcription 3." Endocrinology **149**(7): 3688-3697.

Edmonds, M. E., A. Korzon-Burakowska, R. Saldana Chaparro, T. Dew, S. Stock, C. Moniz and N. L. Petrova (2009). "Serum levels of osteoprotegerin are raised in diabetic peripheral neuropathy and are significantly correlated with peripheral arterial calcification." Diabetologia **52**: S97.

Edmonds, M. E., N. Morrison, J. W. Laws and P. J. Watkins (1982). "Medial arterial calcification and diabetic neuropathy." British Medical Journal Clinical Research Ed. **284**(6320): 928-930.

Edoff, K., J. Hellman, J. Persliden and C. Hildebrand (1997). "The developmental skeletal growth in the rat foot is reduced after denervation." Anatomy & Embryology **195**(6): 531-538.

Edwards, J. R., S. G. Sun, R. Locklin, C. M. Shipman, I. E. Adamopoulos, N. A. Athanasou and A. Sabokbar (2006). "LIGHT (TNFSF14), a novel mediator of bone resorption, is elevated in rheumatoid arthritis." Arthritis & Rheumatism **54**(5): 1451-1462.
El-Khoury, G. Y. and M. H. Kathol (1980). "Neuropathic fractures in patients with diabetes mellitus." Radiology **134**(2): 313-316.

Fabrin, J., K. Larsen and P. E. Holstein (2000). "Long-term follow-up in diabetic Charcot feet with spontaneous onset." Diabetes Care **23**(6): 796-800.

Fujikawa, Y., J. M. Quinn, A. Sabokbar, J. O. McGee and N. A. Athanasou (1996). "The human osteoclast precursor circulates in the monocyte fraction." Endocrinology **137**(9): 4058-4060.

Fuller, K., C. Murphy, B. Kirstein, S. W. Fox and T. J. Chambers (2002). "TNFalpha potently activates osteoclasts, through a direct action independent of and strongly synergistic with RANKL." Endocrinology **143**(3): 1108-1118.

Game, F. L., R. Catlow, G. R. Jones, M. E. Edmonds, E. B. Jude, G. Rayman and W. J. Jeffcoate (2012). "Audit of acute Charcot's disease in the UK: the CDUK study.[Erratum appears in Diabetologia. 2012 Mar;55(3):862]." Diabetologia **55**(1): 32-35.

Gazis, A., N. Pound, R. Macfarlane, K. Treece, F. Game and W. Jeffcoate (2004). "Mortality in patients with diabetic neuropathic osteoarthropathy (Charcot foot)." Diabetic Medicine **21**(11): 1243-1246.
Goto, T., T. Yamaza, M. A. Kido and T. Tanaka (1998). "Light- and electron-microscopic study of the distribution of axons containing substance P and the localization of neurokinin-1 receptor in bone." Cell & Tissue Research **293**(1): 87-93.

Gough, A., H. Abraha, F. Li, T. S. Purewal, A. V. Foster, P. J. Watkins, C. Moniz and M. E. Edmonds (1997). "Measurement of markers of osteoclast and osteoblast activity in patients with acute and chronic diabetic Charcot neuroarthropathy." Diabetic Medicine **14**(7): 527-531.

Hara-Irie, F., N. Amizuka and H. Ozawa (1996). "Immunohistochemical and ultrastructural localization of CGRP-positive nerve fibers at the epiphyseal trabecules facing the growth plate of rat femurs." Bone **18**(1): 29-39.

Hefti, T., M. Frischherz, N. D. Spencer, H. Hall and F. Schlottig (2010). "A comparison of osteoclast resorption pits on bone with titanium and zirconia surfaces." Biomaterials **31**(28): 7321-7331.

Heino, T. J., K. Kurata, H. Higaki and H. K. Vaananen (2009). "Evidence for the role of osteocytes in the initiation of targeted remodeling." Technology & Health Care **17**(1): 49-56.

Henriksen, K., J. Bollerslev, V. Everts and M. A. Karsdal (2011). "Osteoclast activity and subtypes as a function of physiology and pathology--implications for future treatments of osteoporosis." Endocrine Reviews **32**(1): 31-63.

Herbst, S. A., K. B. Jones and C. L. Saltzman (2004). "Pattern of diabetic neuropathic arthropathy associated with the peripheral bone mineral density." Journal of Bone & Joint Surgery - British Volume **86**(3): 378-383.

Hill, E. L. and R. Elde (1991). "Distribution of CGRP-, VIP-, D beta H-, SP-, and NPY-immunoreactive nerves in the periosteum of the rat." Cell & Tissue Research **264**(3): 469-480.

Hill, E. L., R. Turner and R. Elde (1991). "Effects of neonatal sympathectomy and capsaicin treatment on bone remodeling in rats." Neuroscience **44**(3): 747-755.

Hirayama, T., L. Danks, A. Sabokbar and N. A. Athanasou (2002). "Osteoclast formation and activity in the pathogenesis of osteoporosis in rheumatoid arthritis." Rheumatology **41**(11): 1232-1239.

Hofbauer, L. C., C. C. Brueck, S. K. Singh and H. Dobnig (2007). "Osteoporosis in patients with diabetes mellitus." Journal of Bone & Mineral Research **22**(9): 1317-1328.

Hohmann, E. L., R. P. Elde, J. A. Rysavy, S. Einzig and R. L. Gebhard (1986). "Innervation of periosteum and bone by sympathetic vasoactive intestinal peptide-containing nerve fibers." Science **232**(4752): 868-871.

Hukkanen, M., Y. T. Konttinen, S. Santavirta, L. Nordsletten, J. E. Madsen, R. Almaas, A. B. Oestreicher, T. Rootwelt and J. M. Polak (1995). "Effect of sciatic nerve section on neural ingrowth into the rat tibial fracture callus." Clinical Orthopaedics & Related Research(311): 247-257.

Husheem, M., J. K. Nyman, J. Vaaraniemi, H. K. Vaananen and T. A. Hentunen (2005). "Characterization of circulating human osteoclast progenitors: development of in vitro resorption assay." Calcified Tissue International **76**(3): 222-230.

Jeffcoate, W. (2004). "Vascular calcification and osteolysis in diabetic neuropathy-is RANK-L the missing link?" Diabetologia **47**(9): 1488-1492.

Jeffcoate, W. J. (2005). "Theories concerning the pathogenesis of the acute charcot foot suggest future therapy." Current Diabetes Reports **5**(6): 430-435.

Jeffcoate, W. J., F. Game and P. R. Cavanagh (2005). "The role of proinflammatory cytokines in the cause of neuropathic osteoarthropathy (acute Charcot foot) in diabetes." Lancet **366**(9502): 2058-2061.

Jeon, O. K., S. H. Jeong, Y. M. Yoo, K. H. Kim, D. S. Yoon and C. H. Kim (2012). "Quantification of temporal changes in 3D osteoclastic resorption pit using confocal laser scanning microscopy." J Tissue Eng Regen Med **9**(1): 29-35.

Jirkovska, A., P. Kasalicky, P. Boucek, J. Hosova and J. Skibova (2001). "Calcaneal ultrasonometry in patients with Charcot osteoarthropathy and its relationship with densitometry in the lumbar spine and femoral neck and with markers of bone turnover." Diabetic Medicine **18**(6): 495-500.

Johnson, J. T. (1967). "Neuropathic fractures and joint injuries. Pathogenesis and rationale of prevention and treatment." Journal of Bone & Joint Surgery - American Volume **49**(1): 1-30.

Kathol, M. H., G. Y. el-Khoury, T. E. Moore and J. L. Marsh (1991). "Calcaneal insufficiency avulsion fractures in patients with diabetes mellitus." Radiology **180**(3): 725-729.

Katoulis, E. C., M. Ebdon-Parry, H. Lanshammar, L. Vileikyte, J. Kulkarni and A. J. Boulton (1997). "Gait abnormalities in diabetic neuropathy." Diabetes Care **20**(12): 1904-1907.

Kobayashi, K., N. Takahashi, E. Jimi, N. Udagawa, M. Takami, S. Kotake, N. Nakagawa, M. Kinosaki, K. Yamaguchi, N. Shima, H. Yasuda, T. Morinaga, K. Higashio, T. J. Martin and T. Suda (2000). "Tumor necrosis factor alpha stimulates osteoclast differentiation by a mechanism independent of the ODF/RANKL-RANK interaction." Journal of Experimental Medicine **191**(2): 275-286.

Kon, T., T. J. Cho, T. Aizawa, M. Yamazaki, N. Nooh, D. Graves, L. C. Gerstenfeld and T. A. Einhorn (2001). "Expression of osteoprotegerin, receptor activator of NF-kappaB ligand (osteoprotegerin ligand) and related proinflammatory cytokines during fracture healing." Journal of Bone & Mineral Research **16**(6): 1004-1014.

Kon T, C. T., Aizawa T, Yamazaki M, Nooh N, Graves D, Gerstenfeld LC, Einhorn TA (2001). "Expression of osteoprotegerin, receptor activator of NF-kappaB ligand (osteoprotegerin ligand) and related proinflammatory cytokines during fracture healing." J Bone Miner Res **16**(6): 1004-1014.

Konttinen, Y., S. Imai and A. Suda (1996). "Neuropeptides and the puzzle of bone remodeling. State of the art." Acta Orthopaedica Scandinavica **67**(6): 632-639.

Kostenuik, P. J. (2005). "Osteoprotegerin and RANKL regulate bone resorption, density, geometry and strength." Current Opinion in Pharmacology **5**(6): 618-625.

Kudo, O., A. Sabokbar, A. Pocock, I. Itonaga, Y. Fujikawa and N. A. Athanasou (2003). "Interleukin-6 and interleukin-11 support human osteoclast formation by a RANKL-independent mechanism." Bone **32**(1): 1-7.

Kwan Tat, S., M. Padrines, S. Theoleyre, D. Heymann and Y. Fortun (2004). "IL-6, RANKL, TNF-alpha/IL-1: interrelations in bone resorption pathophysiology." Cytokine & Growth Factor Reviews **15**(1): 49-60.

Lam, J., Y. Abu-Amer, C. A. Nelson, D. H. Fremont, F. P. Ross and S. L. Teitelbaum (2002). "Tumour necrosis factor superfamily cytokines and the pathogenesis of inflammatory osteolysis." Annals of the Rheumatic Diseases **61 Suppl 2**: ii82-83.

Lam, J., S. Takeshita, J. E. Barker, O. Kanagawa, F. P. Ross and S. L. Teitelbaum (2000). "TNF-alpha induces osteoclastogenesis by direct stimulation of macrophages

exposed to permissive levels of RANK ligand." Journal of Clinical Investigation **106**(12): 1481-1488.

Lee, L., P. A. Blume and B. Sumpio (2003). "Charcot joint disease in diabetes mellitus." Annals of Vascular Surgery **17**(5): 571-580.

Leung, P., M. Pickarski, Y. Zhuo, P. J. Masarachia and L. T. Duong (2011). "The effects of the cathepsin K inhibitor odanacatib on osteoclastic bone resorption and vesicular trafficking." Bone **49**(4): 623-635.

Li, J., T. Ahmad, M. Spetea, M. Ahmed and A. Kreicbergs (2001). "Bone reinnervation after fracture: a study in the rat." Journal of Bone & Mineral Research **16**(8): 1505-1510.

Mabilleau, G. and M. E. Edmonds (2010). "Role of neuropathy on fracture healing in Charcot neuro-osteoarthropathy." J Musculoskelet Neuronal Interact **10**(1): 84-91.

Mabilleau, G., N. Petrova, M. E. Edmonds and A. Sabokbar (2011). "Number of circulating CD14-positive cells and the serum levels of TNF-alpha are raised in acute charcot foot." Diabetes Care **34**(3): e33.

Mabilleau, G., N. L. Petrova, M. E. Edmonds and A. Sabokbar (2008). "Increased osteoclastic activity in acute Charcot's osteoarthropathy: the role of receptor activator of nuclear factor-kappaB ligand." Diabetologia **51**(6): 1035-1040.

Marino, S., J. G. Logan, D. Mellis and M. Capulli (2014). "Generation and culture of osteoclasts." BoneKEy Reports **3**: 570.

McCrory, J. L., E. Morag, A. J. Norkitis, M. S. Barr, R. P. Moser, G. M. Caputo, P. R. Cavanagh and J. S. Ulbrecht (1998). "Healing of Charcot fractures: skin temperature and radiographic correlates." The Foot **8**: 158-165.

McGill, M., L. Molyneaux, T. Bolton, K. Ioannou, R. Uren and D. K. Yue (2000). "Response of Charcot's arthropathy to contact casting: assessment by quantitative techniques." Diabetologia **43**(4): 481-484.

McGowan, N. W., E. J. Walker, H. Macpherson, S. H. Ralston and M. H. Helfrich (2001). "Cytokine-activated endothelium recruits osteoclast precursors." Endocrinology **142**(4): 1678-1681.

Meyer, S. (1992). "The pathogenesis of diabetic Chrcot joints." Iowa Orthop J(12): 63-70.

Miller, D. (2001). " Spinal cord disorders: Syringomyelia. In Donaghy M ed. Brain's diseases of the nervous system, 11ed., ." Oxford: Oxford University Press(20): 618-622.

Min, H., S. Morony, I. Sarosi, C. R. Dunstan, C. Capparelli, S. Scully, G. Van, S. Kaufman, P. J. Kostenuik, D. L. Lacey, W. J. Boyle and W. S. Simonet (2000). "Osteoprotegerin reverses osteoporosis by inhibiting endosteal osteoclasts and prevents vascular calcification by blocking a process resembling osteoclastogenesis." Journal of Experimental Medicine **192**(4): 463-474.

Mosheimer, B. A., N. C. Kaneider, C. Feistritzer, D. H. Sturn and C. J. Wiedermann (2004). "Expression and function of RANK in human monocyte chemotaxis." Arthritis & Rheumatism **50**(7): 2309-2316.

Mueller, M. J., D. Zou, K. L. Bohnert, L. J. Tuttle and D. R. Sinacore (2008). "Plantar stresses on the neuropathic foot during barefoot walking." Physical Therapy **88**(11): 1375-1384.

Munson, M. E., J. S. Wrobel, C. M. Holmes and D. A. Hanauer (2014). "Data Mining for Identifying Novel Associations and Temporal Relationships with Charcot Foot." Journal of Diabetes Research **2014:214353. doi: 10.1155/2014/214353**.

Ndip, A., A. Williams, E. B. Jude, F. Serracino-Inglott, S. Richardson, J. V. Smyth, A. J. Boulton and M. Y. Alexander (2011). "The RANKL/RANK/OPG signaling pathway mediates medial arterial calcification in diabetic Charcot neuroarthropathy." Diabetes **60**(8): 2187-2196.

Papapoulos, S., R. Chapurlat, C. Libanati, M. L. Brandi, J. P. Brown, E. Czerwinski, M. A. Krieg, Z. Man, D. Mellstrom, S. C. Radominski, J. Y. Reginster, H. Resch, J. A. Roman Ivorra, C. Roux, E. Vittinghoff, M. Austin, N. Daizadeh, M. N. Bradley, A. Grauer, S. R. Cummings and H. G. Bone (2012). "Five years of denosumab exposure in women with postmenopausal osteoporosis: results from the first two years of the FREEDOM extension." Journal of Bone & Mineral Research **27**(3): 694-701.

Pascaretti-Grizon, F., G. Mabilleau, M. F. Basle and D. Chappard (2011). "Measurement by vertical scanning profilometry of resorption volume and lacunae depth caused by osteoclasts on dentine slices." Journal of Microscopy **241**(2): 147-152.

Pedersen, L. M., O. R. Madsen and H. Bliddal (1993). "Charcot arthropathy as an unusual initial manifestation of diabetes mellitus." British Journal of Rheumatology **32**(9): 854-855.

Petrova, N. L., T. K. Dew, R. L. Musto, R. A. Sherwood, M. Bates, C. F. Moniz and M. E. Edmonds (2015). "Inflammatory and bone turnover markers in a cross-sectional and prospective study of acute Charcot osteoarthropathy." Diabetic Medicine **32**(2): 267-273.

Petrova, N. L. and M. E. Edmonds (2008). "Charcot neuro-osteoarthropathy-current standards." Diabetes/Metabolism Research Reviews **24 Suppl 1**: S58-61.

Petrova, N. L. and M. E. Edmonds (2010). "A prospective study of calcaneal bone mineral density in acute Charcot osteoarthropathy." Diabetes Care **33**(10): 2254-2256.

Petrova, N. L. and M. E. Edmonds (2013). "Medical management of Charcot arthropathy." Diabetes, Obesity & Metabolism **15**(3): 193-197.

Petrova, N. L., A. V. Foster and M. E. Edmonds (2004). "Difference in presentation of charcot osteoarthropathy in type 1 compared with type 2 diabetes." Diabetes Care **27**(5): 1235-1236.

Petrova, N. L., A. V. Foster and M. E. Edmonds (2005). "Calcaneal bone mineral density in patients with Charcot neuropathic osteoarthropathy: differences between Type 1 and Type 2 diabetes." Diabetic Medicine **22**(6): 756-761.

Petrova, N. L., C. Moniz, D. A. Elias, M. Buxton-Thomas, M. Bates and M. E. Edmonds (2007). "Is there a systemic inflammatory response in the acute charcot foot?" Diabetes Care **30**(4): 997-998.

Petrova, N. L., P. K. Petrov, M. E. Edmonds and C. M. Shanahan (2014). "Novel Use of a Dektak 150 Surface Profiler Unmasks Differences in Resorption Pit Profiles Between Control and Charcot Patient Osteoclasts." Calcif Tissue Int **94**: 403-411.

Petrova, N. L. and C. M. Shanahan (2014). "Neuropathy and the vascular-bone axis in diabetes: lessons from Charcot osteoarthropathy." Osteoporos Int. 2014 Apr;25(4):. **25**(4): 1197-1207.

Piaggesi, A., L. Rizzo, F. Golia, D. Costi, F. Baccetti, S. Ciaccio, S. De Gregorio, E. Vignali, D. Trippi, V. Zampa, C. Marcocci and S. Del Prato (2002). "Biochemical and ultrasound tests for early diagnosis of active neuro-osteoarthropathy (NOA) of the diabetic foot." Diabetes Res Clin Pract **58**: 1-9.

Pickwell, K. M., M. J. van Kroonenburgh, R. E. Weijers, P. V. van Hirtum, M. S. Huijberts and N. C. Schaper (2011). "F-18 FDG PET/CT scanning in Charcot disease: a brief report." Clinical Nuclear Medicine **36**(1): 8-10.

Pittenger, G. and A. Vinik (2003). "Nerve growth factor and diabetic neuropathy." Experimental Diabesity Research **4**(4): 271-285.

Ramnemark, A., L. Nyberg, R. Lorentzon, U. Englund and Y. Gustafson (1999). "Progressive hemiosteoporosis on the paretic side and increased bone mineral density in the nonparetic arm the first year after severe stroke." Osteoporosis International **9**(3): 269-275.

Redlich, K. and J. S. Smolen (2012). "Inflammatory bone loss: pathogenesis and therapeutic intervention." Nature Reviews. Drug Discovery **11**(3): 234-250.

Richard, J. L., M. Almasri and S. Schuldiner (2012). "Treatment of acute Charcot foot with bisphosphonates: a systematic review of the literature." Diabetologia **55**(5): 1258-1264.

Ritchlin, C. T., S. A. Haas-Smith, P. Li, D. G. Hicks and E. M. Schwarz (2003). "Mechanisms of TNF-alpha- and RANKL-mediated osteoclastogenesis and bone resorption in psoriatic arthritis." Journal of Clinical Investigation **111**(6): 821-831.

Rix, M., H. Andreassen and P. Eskildsen (1999). "Impact of peripheral neuropathy on bone density in patients with type 1 diabetes." Diabetes Care **22**(5): 827-831.

Rogers, L. C., R. G. Frykberg, D. G. Armstrong, A. J. Boulton, M. Edmonds, G. H. Van, A. Hartemann, F. Game, W. Jeffcoate, A. Jirkovska, E. Jude, S. Morbach, W. B. Morrison, M. Pinzur, D. Pitocco, L. Sanders, D. K. Wukich and L. Uccioli (2011). "The Charcot foot in diabetes." Diabetes Care **34**(9): 2123-2129.

Romas, E. (2005). "Bone loss in inflammatory arthritis: mechanisms and therapeutic approaches with bisphosphonates." Best Practice & Research in Clinical Rheumatology **19**(6): 1065-1079.

Ross, A. J., R. W. Mendicino and A. R. Catanzariti (2013). "Role of body mass index in acute charcot neuroarthropathy." Journal of Foot & Ankle Surgery **52**(1): 6-8.

Ruotolo, V., B. Di Pietro, L. Giurato, S. Masala, M. Meloni, O. Schillaci, A. Bergamini and L. Uccioli (2013). "A new natural history of Charcot foot: clinical evolution and final outcome of stage 0 Charcot neuroarthropathy in a tertiary referral diabetic foot clinic." Clinical Nuclear Medicine **38**(7): 506-509.

Sabokbar, A. and N. S. Athanasou (2003). "Generating human osteoclasts from peripheral blood." Methods in Molecular Medicine **80**: 101-111.

Sanders, L. J. and R. G. Frykberg (2001). "Charcot neuroarthropathy of the foot." In: Bowker JH, Phiefer MA (eds) Levin & O'Neal's the diabetic foot **6th edn. Mosby, St Louis**: 439-466.

Santavirta, S., Y. T. Konttinen, D. Nordstrom, A. Makela, T. Sorsa, M. Hukkanen and P. Rokkanen (1992). "Immunologic studies of nonunited fractures." Acta Orthopaedica Scandinavica **63**(6): 579-586.

Schaper, N. C., M. Huijberts and K. Pickwell (2008). "Neurovascular control and neurogenic inflammation in diabetes." Diabetes/Metabolism Research Reviews **24 Suppl 1**: S40-44.

Schwartz, A. V., T. A. Hillier, D. E. Sellmeyer, H. E. Resnick, E. Gregg, K. E. Ensrud, P. J. Schreiner, K. L. Margolis, J. A. Cauley, M. C. Nevitt, D. M. Black and S. R. Cummings (2002). "Older women with diabetes have a higher risk of falls: a prospective study." Diabetes Care **25**(10): 1749-1754.

Serre, C. M., D. Farlay, P. D. Delmas and C. Chenu (1999). "Evidence for a dense and intimate innervation of the bone tissue, including glutamate-containing fibers." Bone **25**(6): 623-629.

Shanahan, C. M., N. R. Cary, J. R. Salisbury, D. Proudfoot, P. L. Weissberg and M. E. Edmonds (1999). "Medial localization of mineralization-regulating proteins in association with Mönckeberg's sclerosis: evidence for smooth muscle cell-mediated vascular calcification." Circulation **100**(21): 2168-2176.

Sharma, A., B. E. Scammell, K. J. Fairbairn, M. J. Seagrave, F. L. Game and W. J. Jeffcoate (2010). "Prevalence of calcification in the pedal arteries in diabetes complicated by foot disease." Diabetes Care **33**(5): e66.

Shibuya, N., J. La Fontaine and S. J. Frania (2008). "Alcohol-induced neuroarthropathy in the foot: a case series and review of literature." Journal of Foot & Ankle Surgery **47**(2): 118-124.

Simonet, W. S., D. L. Lacey, C. R. Dunstan, M. Kelley, M. S. Chang, R. Luthy, H. Q. Nguyen, S. Wooden, L. Bennett, T. Boone, G. Shimamoto, M. DeRose, R. Elliott, A. Colombero, H. L. Tan, G. Trail, J. Sullivan, E. Davy, N. Bucay, L. Renshaw-Gegg, T. M. Hughes, D. Hill, W. Pattison, P. Campbell, S. Sander, G. Van, J. Tarpley, P. Derby, R. Lee and W. J. Boyle (1997). "Osteoprotegerin: a novel secreted protein involved in the regulation of bone density." Cell **89**(2): 309-319.

Sinacore, D. R. and N. C. Withrington (1999). "Recognition and management of acute neuropathic (Charcot) arthropathies of the foot and ankle." J Orthop Sports Phys Ther **29**(12): 736-746.

Sinha, S., C. S. Munichoodappa and G. P. Kozak (1972). "Neuro-arthropathy (Charcot joints) in diabetes mellitus (clinical study of 101 cases)." Medicine **51**(3): 191-210.

Soe, K. and J. M. Delaisse (2010). "Glucocorticoids maintain human osteoclasts in the active mode of their resorption cycle." Journal of Bone & Mineral Research **25**(10): 2184-2192.

Soe, K., D. M. Merrild and J. M. Delaisse (2013). "Steering the osteoclast through the demineralization-collagenolysis balance." Bone **56**(1): 191-198.

Stevens, M. J., M. E. Edmonds, A. V. Foster and P. J. Watkins (1992). "Selective neuropathy and preserved vascular responses in the diabetic Charcot foot." Diabetologia **35**(2): 148-154.

Susa, M., N. H. Luong-Nguyen, D. Cappellen, N. Zamurovic and R. Gamse (2004). "Human primary osteoclasts: in vitro generation and applications as pharmacological and clinical assay." Journal of Translational Medicine **2**(4).

Tanaka, S., N. Takahashi, N. Udagawa, T. Tamura, T. Akatsu, E. R. Stanley, T. Kurokawa and T. Suda (1993). "Macrophage colony-stimulating factor is indispensable for both proliferation and differentiation of osteoclast progenitors." Journal of Clinical Investigation **91**(1): 257-263.

Teitelbaum, S. L. (2000). "Bone resorption by osteoclasts." Science **289**(5484): 1504-1508.

Teitelbaum, S. L. (2007). "Osteoclasts: what do they do and how do they do it?" American Journal of Pathology **170**(2): 427-435.

Tracey, K. J. (2007). "Physiology and immunology of the cholinergic anti-inflammatory pathway." J Clin Investigations **117**(2): 289-296.

Troen, B. R. (2006). "The regulation of cathepsin K gene expression." Annals of the New York Academy of Sciences **1068**: 165-172.

Uccioli, L., A. Sinistro, C. Almerighi, C. Ciaprini, A. Cavazza, L. Giurato, V. Ruotolo, F. Spasaro, E. Vainieri, G. Rocchi and A. Bergamini (2010). "Proinflammatory modulation of the surface and cytokine phenotype of monocytes in patients with acute Charcot foot." Diabetes Care **33**(2): 350-355.

Valabhji, J., R. C. Marshall, S. Lyons, L. Bloomfield, D. Hogg, P. Rosenfeld and C. M. Gabriel (2012). "Asymmetrical attenuation of vibration sensation in unilateral diabetic Charcot foot neuroarthropathy." Diabetic Medicine **29**(9): 1191-1194.

van Baal, J., R. Hubbard, F. Game and W. Jeffcoate (2010). "Mortality associated with acute Charcot foot and neuropathic foot ulceration." Diabetes Care **33**(5): 1086-1089.

Vanderoost, J., K. Soe, D. M. Merrild, J. M. Delaisse and G. H. van Lenthe (2013). "Glucocorticoid-induced changes in the geometry of osteoclast resorption cavities affect trabecular bone stiffness." Calcified Tissue International **92**(3): 240-250.

Walsh, N. C. and E. M. Gravallese (2004). "Bone loss in inflammatory arthritis: mechanisms and treatment strategies." Current Opinion in Rheumatology **16**(4): 419-427.

Wang, H., M. Yu, M. Ochani, C. A. Amella, M. Tanovic, S. Susarla, J. H. Li, H. Wang, H. Yang, L. Ulloa, Y. Al-Abed, C. J. Czura and K. J. Tracey (2003). "Nicotinic acetylcholine receptor alpha7 subunit is an essential regulator of inflammation." Nature **421**(6921): 384-388.

Wang, L., X. Shi, R. Zhao, B. P. Halloran, D. J. Clark, C. R. Jacobs and W. S. Kingery (2010). "Calcitonin-gene-related peptide stimulates stromal cell osteogenic differentiation and inhibits RANKL induced NF-kappaB activation, osteoclastogenesis and bone resorption." Bone **46**(5): 1369-1379.

Wrobel, J. S. and B. Najafi (2010). "Diabetic foot biomechanics and gait dysfunction." Journal of Diabetes Science & Technology **4**(4): 833-845.

Yasuda, H., N. Shima, N. Nakagawa, K. Yamaguchi, M. Kinosaki, S. Mochizuki, A. Tomoyasu, K. Yano, M. Goto, A. Murakami, E. Tsuda, T. Morinaga, K. Higashio, N. Udagawa, N. Takahashi and T. Suda (1998). "Osteoclast differentiation factor is a ligand

for osteoprotegerin/osteoclastogenesis-inhibitory factor and is identical to TRANCE/RANKL." Proceedings of the National Academy of Sciences of the United States of America **95**(7): 3597-3602.

Yoshitake, F., S. Itoh, H. Narita, K. Ishihara and S. Ebisu (2008). "Interleukin-6 directly inhibits osteoclast differentiation by suppressing receptor activator of NF-kappaB signaling pathways." Journal of Biological Chemistry **283**(17): 11535-11540.

Young, M. J., A. Marshall, J. E. Adams, P. L. Selby and A. J. Boulton (1995). "Osteopenia, neurological dysfunction, and the development of Charcot neuroarthropathy." Diabetes Care **18**(1): 34-38.

Young, N., K. Neiderer, B. Martin, D. Jolley and J. F. Dancho (2012). "HIV neuropathy induced Charcot neuroarthropathy: a case discussion." Foot **22**(3): 112-116.

Yu, G. V. and J. R. Hudson (2002). "Evaluation and treatment of stage 0 Charcot's neuroarthropathy of the foot and ankle." J Am Podiatr Med Assoc **92**(4): 210-220.

Zampa, V., I. Bargellini, L. Rizzo, F. Turini, S. Ortori, A. Piaggesi and C. Bartolozzi (2011). "Role of dynamic MRI in the follow-up of acute Charcot foot in patients with diabetes mellitus." Skeletal Radiology **40**(8): 991-999.

Zupan, J., M. Jeras and J. Marc (2013). "Osteoimmunology and the influence of pro-inflammatory cytokines on osteoclasts." Biochemia Medica **23**(1): 43-63.

Appendix 1 List of publications

Original research articles

1. Petrova NL, Petrov PK, Edmonds ME, Shanahan CM. Inhibition of TNF-α reverses the pathological resorption pit profile of osteoclasts from patients with acute Charcot osteoarthropathy. J Diabetes Res. 2015; 2015: 917945. doi: 10.1155/2015/917945

2. Petrova NL, Petrov PK, Edmonds ME, Shanahan CM. Novel use of a Dektak 150 surface profiler unmasks differences in resorption pit profiles between control and charcot patient osteoclasts. Calcif Tissue Int. 2014 Apr;94(4):403-11.

3. Petrova NL, Dew TK, Musto RL, Sherwood RA, Bates M, Moniz CF, Edmonds ME. Inflammatory and bone turnover markers in a cross-sectional and prospective study of acute Charcot osteoarthropathy. Diabet Med. 2015; 32 (2): 267-273.

4. Petrova NL, Edmonds ME. A prospective study of calcaneal bone mineral density in acute Charcot osteoarthropathy. Diabetes Care. 2010 Oct;33(10):2254-6.

5. Mabilleau G, Petrova NL, Edmonds ME, Sabokbar A. Increased osteoclastic activity in acute Charcot's osteoarthropathy: the role of receptor activator of nuclear factor-kappaB ligand. Diabetologia. 2008 Jun;51(6):1035-40.

6. Petrova NL, Moniz C, Elias DA, Buxton-Thomas M, Bates M, Edmonds ME. Is there a systemic inflammatory response in the acute Charcot foot? Diabetes Care. 2007 Apr;30(4):997-8.

Refereed review articles

7. Petrova NL, Shanahan CM. Neuropathy and the vascular-bone axis in diabetes: lessons from Charcot osteoarthropathy. Osteoporos Int. 2014 Apr;25(4):1197-207.

8. Petrova NL, Edmonds ME. Medical management of Charcot arthropathy. Diabetes Obes Metab. 2013 Mar;15(3):193-7.

9. Petrova NL, Edmonds ME. Charcot neuro-osteoarthropathy-current standards. Diabetes Metab Res Rev. 2008 May Jun;24 Suppl 1:S58-61.

Hindawi Publishing Corporation
Journal of Diabetes Research
Volume 2015, Article ID 917945, 10 pages
http://dx.doi.org/10.1155/2015/917945

Research Article

Inhibition of TNF-α Reverses the Pathological Resorption Pit Profile of Osteoclasts from Patients with Acute Charcot Osteoarthropathy

Nina L. Petrova,[1] Peter K. Petrov,[2] Michael E. Edmonds,[1] and Catherine M. Shanahan[3]

[1]*Diabetic Foot Clinic, King's College Hospital, London SE5 9RS, UK*
[2]*Department of Materials, Imperial College London, London SW7 2AZ, UK*
[3]*Cardiovascular Division, King's College London, London SE5 9NU, UK*

Correspondence should be addressed to Nina L. Petrova; petrovanl@yahoo.com

Received 12 February 2015; Revised 23 April 2015; Accepted 23 April 2015

Academic Editor: Andrea Scaramuzza

We hypothesised that tumour necrosis factor-α (TNF-α) may enhance receptor activator of nuclear factor-$\kappa\beta$ ligand- (RANKL-) mediated osteoclastogenesis in acute Charcot osteoarthropathy. Peripheral blood monocytes were isolated from 10 acute Charcot patients, 8 diabetic patients, and 9 healthy control subjects and cultured *in vitro* on plastic and bone discs. Osteoclast formation and resorption were assessed after treatment with (1) macrophage-colony stimulating factor (M-CSF) and RANKL and (2) M-CSF, RANKL, and neutralising antibody to TNF-α (anti-TNF-α). Resorption was measured on the surface of bone discs by image analysis and under the surface using surface profilometry. Although osteoclast formation was similar in M-CSF + RANKL-treated cultures between the groups ($p > 0.05$), there was a significant increase in the area of resorption on the surface ($p < 0.01$) and under the surface ($p < 0.01$) in Charcot patients compared with diabetic patients and control subjects. The addition of anti-TNF-α resulted in a significant reduction in the area of resorption on the surface ($p < 0.05$) and under the surface ($p < 0.05$) only in Charcot patients as well as a normalisation of the aberrant erosion profile. We conclude that TNF-α modulates RANKL-mediated osteoclastic resorption *in vitro* in patients with acute Charcot osteoarthropathy.

1. Introduction

Charcot osteoarthropathy is a severe complication of diabetes, which is associated with significant morbidity and mortality [1–5]. Inflammation and increased osteoclastic activity are well-recognised drivers of the rapid bone destruction that occurs in the Charcot foot, although the link between them is not fully understood [6].

We have recently demonstrated that, in acute Charcot osteoarthropathy, there is increased osteoclastic activity in response to the osteoclastogenic cytokine receptor activator of nuclear factor-$\kappa\beta$ ligand (RANKL) [7]. Osteoclasts, generated from peripheral blood monocytes of Charcot patients in the presence of the stimulating factor macrophage-colony stimulating factor (M-CSF) and RANKL, excessively resorb bone slices. Using the novel technique of surface profilometry, in addition to traditional light microscopy, we have shown that osteoclasts derived from Charcot patients eroded bone surfaces with an aberrant pit profile and geometry [8]. Resorption pits from cultures of Charcot patients appeared more frequently as multidented pits and were significantly deeper and wider compared with resorption pits in healthy controls [8].

The reason for this increased resorbing activity is unknown, but it is possible that it is driven by uncontrolled inflammation due to upregulation of proinflammatory cytokines and in particular tumour necrosis factor-α (TNF-α) [6]. As an osteoclastogenic mediator, TNF-α induces expression of RANKL in osteoblastic cells, but it can also act directly on osteoclastic precursors (monocytes) to potentiate RANKL-induced osteoclastogenesis and thereby activity [9]. This cytokine is known to enhance osteoclastogenesis in rheumatoid arthritis [10, 11] and psoriatic arthritis [12] and also in other forms of inflammatory osteolysis [13] and we

hypothesised that TNF-α may also modulate osteoclastic activity in acute Charcot osteoarthropathy. Thus the aim of this study was to determine the role of this cytokine by comparing the extent of osteoclast formation and resorption in M-CSF + RANKL-treated cultures with and without the addition of neutralising antibody to TNF-α (anti-TNF-α).

2. Materials and Methods

2.1. Patients. Samples from peripheral blood were obtained from 10 consecutive patients with recent onset of acute Charcot osteoarthropathy, 8 diabetic patients with no history of Charcot osteoarthropathy, and 9 healthy control subjects. All patients with Charcot osteoarthropathy presented with a unilateral red hot swollen foot and radiological evidence of acute Charcot fractures, demonstrated on plain foot and ankle radiographs [1, 5]. All participants had intact feet and had no features of foot infection or sepsis. The study was approved by the Outer West London Research Ethics Committee and was carried out in accordance with institutional guidelines and the Declaration of Helsinki with all patients and control subjects signing written informed consent.

2.2. Isolation and Culture of Peripheral Blood Mononuclear Cells (PBMCs). Peripheral blood mononuclear cells (PBMCs) were isolated from whole blood as previously described [8]. The PBMCs were separated after gradient centrifugation and resuspended in culture medium and 2×10^6 cells were cultured on 24-well plates and 5×10^5 cells were cultured on bovine bone discs (Immunodiagnostic Systems Ltd., Boldon, UK) in duplicate to assess osteoclast formation and resorption, respectively. Cultures were maintained in α-minimal essential medium (α-MEM, Lonza, Wokingham, UK) supplemented with penicillin (50 U/mL)/streptomycin (50 μg/mL) (Sigma-Aldrich Ltd., Poole, UK), L-glutamine (2 mM) (Sigma-Aldrich Ltd., Poole, UK), and 10% heat-inactivated FBS (Lonza Ltd., Wokingham, UK) under the following conditions:

(i) Cultures with M-CSF 25 ng/mL (added at day 0) (R&D Systems Europe, Ltd., Abingdon, UK) and soluble RANKL 100 ng/mL (added at day 7) (PeproTech EC Ltd., London, UK): M-CSF + RANKL-treated cultures served as a positive control.

(ii) Cultures with M-CSF (added at day 0), anti-TNF-α 10 μg/mL (added at day 0), (R&D Systems Europe, Ltd., Abingdon, UK), and soluble RANKL 100 ng/mL (added at day 7): M-CSF + RANKL + anti-TNF-α-treated cultures were used to assess the role of TNF-α on osteoclastogenesis. The rationale for this study was to inhibit TNF-α modulation on peripheral blood monocytes by using excess concentration of anti-TNF-α, added from the beginning until the end of the cell culture treatment [14].

Culture medium was refreshed every 3-4 days supplemented with the appropriate agents as described above. After 17 days in culture, 24-well plates were stained for tartrate-resistant acid phosphatase (TRAP). Plates were viewed by light microscopy and TRAP-positive cells with three or more nuclei were counted as osteoclasts. The ability of these cells to resorb bone was demonstrated by culturing PBMCs on bovine bone discs for 21 days. The bone discs were stained with toluidine blue and mounted on glass slides. Resorption was quantitated by two methods: (1) area of resorption on the surface (%) assessed by image analysis after light microscopy and (2) area of resorption under the surface (μm^2) assessed by surface profilometry, as previously described [8]. The erosion profile of resorbed bone discs was measured by the Dektak 150 Surface Profiler (Veeco, New York, USA) fitted with a stylus (radius 2.5 μm), as previously described [8]. The stylus was dragged across the surface of the sample in hills and valleys mode with ten scans per subject carried out at random sites on each of the two discs. Each measurement had the following scan parameters: stylus force: 3.00 mg, scan length: 1000 μm, scan duration: 60 seconds, vertical measurement range: 65.5 μm, scan resolution: 0.056 μm/scan. On average, 75 pits per condition/per subject were analysed and the median area of disc erosion was calculated in μm^2 using Origin Pro 8.6 software.

According to their shape, pits were defined as unidented (erosion with one dent starting from and finishing at the level of the unresorbed surface), bidented (erosion with two clearly defined dents starting from and finishing at the level of the unresorbed surface), and multidented (erosion with three or more dents starting from and finishing at the level of the unresorbed surface). Each pit was characterised by the following parameters: width at the surface (μm), maximum depth (μm), and full-width-half-maximum (FWHM) (μm), where the width was measured at the half of the maximum depth. The median width, depth, and FWHM for the unidented, bidented, and multidented pits were calculated for each subject [8].

2.3. Statistical Analyses. Data were analysed with Predictive Analytics Software 18 statistical package and expressed as median (25th–75th percentile). Differences between study groups and culture treatments were analysed using the non-parametric Mann-Whitney U test (two groups) or Kruskal-Wallis test (three groups), as appropriate. Chi-square test was used for categorical variables. Differences were considered significant at $p < 0.05$.

3. Results

3.1. Demographical Features. Patients with acute Charcot osteoarthropathy were matched for age, gender, and type and duration of diabetes with the diabetic patients and for age and gender with the healthy control subjects. The age, gender distribution, and type and duration of diabetes were not significantly different between the Charcot patients and diabetic patients nor were the age and gender distribution between the Charcot patients and healthy control subjects (Table 1).

3.2. Osteoclast Formation. Observation of the cell culture plates with light microscopy showed no difference in osteoclast formation in M-CSF + RANKL-treated cultures between

Table 1: Demographic features of the study patients.

	Charcot	Diabetes	Healthy control subjects
Age (years)	57 [53–64]	60 [55–66]	45 [42–48]
Gender (male : female)	6 : 4	3 : 4	5 : 3
Type 1 : type 2 diabetes	4 : 6	1 : 6	—
Duration of diabetes (years)	17 [8–29]	10 [9–26]	—

Data expressed as median [25th–75th percentile].
Nonsignificant difference in age, gender distribution, type and duration of diabetes (Charcot patients versus diabetic patients), and age and gender (Charcot patients versus healthy control subjects); ($p > 0.05$ for all pairwise comparisons).

the three groups (Figure 1(a)). The median number of TRAP-positive multinucleated cells in M-CSF + RANKL-treated cultures in Charcot patients was not significantly different from the median number of TRAP-positive multinucleated cells in diabetic patients and healthy control subjects (Figure 1(b)).

The addition of anti-TNF-α to M-CSF + RANKL treatment did not lead to a significant difference in the median number of TRAP-positive multinucleated cells in Charcot patients, diabetic patients, and healthy control subjects (Figures 1(a) and 1(b)).

3.3. Osteoclast Resorption. Traditional light microscopy (Figure 1(c)) together with surface profilometry revealed that the newly formed osteoclasts isolated from patients with acute Charcot osteoarthropathy exhibited increased resorbing activity in M-CSF + RANKL-treated cultures compared with osteoclasts generated from diabetic patients and healthy controls, as indicated by a significantly increased area of resorption on the surface (Figure 1(d)) and under the surface (Figure 1(e)).

The addition of anti-TNF-α to M-CSF + RANKL treatment led to a significant reduction in the area of resorption on the surface (Figures 1(c) and 1(d)) and under the surface (Figure 1(e)) only in Charcot patients but not in diabetic patients or healthy control subjects. In Charcot patients, the area of resorption on the surface assessed by image analysis was 30% smaller in M-CSF + RANKL + anti-TNF-α-treated cultures compared with M-CSF + RANKL-treated cultures (Figure 1(d)) as was the area of resorption under the surface after surface profilometry (Figure 1(e)).

3.4. Erosion Profile of Resorbed Bovine Bone Discs after Surface Profilometry. The surface profile measurements of randomly selected areas revealed multishaped erosions of resorbed bovine bone discs in all study groups in both culture treatments (Figures 2(a) and 2(b)).

However, in M-CSF + RANKL-treated cultures, the erosion profiles were markedly different between the three groups (Figure 2(a)). The erosions appeared greater and deeper in Charcot patients compared to erosions in diabetic patients and healthy controls (Figure 2(a)).

After the addition of anti-TNF-α to M-CSF + RANKL treatment, the observed differences in the erosion profile between the three groups were lost (Figure 2(b)). In Charcot patients, there was a "normalisation" of the erosion profile in M-CSF + RANKL + anti-TNF-α-treated cultures compared to M-CSF + RANKL-treated cultures (Figure 2(c)), whereas anti-TNF-α had no effect on the erosion profiles of diabetic patients (Figure 2(d)) or healthy control subjects (Figure 2(e)).

3.5. Pit Morphology. To assess in more detail the differences in resorption under the surface, pit morphology was evaluated. In M-CSF + RANKL-treated cultures, the pit parameters (median width, FWHM and depth) were greater in Charcot patients compared with diabetic patients and healthy control subjects (Figures 2(f), 2(g), and 2(h)). The addition of anti-TNF-α to M-CSF + RANKL treatment led to a significant reduction in the width, FWHM, and depth of the unidented pits in Charcot patients (Figure 2(f)). Although the reduction of the bidented pit parameters (Figure 2(g)) and multidented pit parameters (Figure 2(h)) was not significant, there was a general trend of "normalisation" of pits after anti-TNF-α. In contrast to Charcot patients, the addition of anti-TNF-α had no effect on pit parameters in diabetic patients or in healthy control subjects (Figures 2(f), 2(g), and 2(h)).

3.6. Pit Distribution. To determine whether there were any differences in the distribution of the shape of the pits, the percentage of unidented, bidented, and multidented pits between the two culture treatments was compared. In Charcot patients, the addition of anti-TNF-α to M-CSF + RANKL resulted in a significant increase in the percentage of unidented pits (from 36% [31–43] to 53% [43–63], $p < 0.05$) and a significant decrease in the percentage of multidented pits (from 40% [32–42] to 25% [13–33], $p < 0.05$), whereas the percentage of bidented pits remained unchanged (from 24% [20–28] to 22% [21–24], $p > 0.05$) (Figure 2(i)). There was no significant difference in the distribution of pits (unidented, bidented, and multidented) between the two culture treatments in the diabetic patients and in the healthy controls (Figure 2(i)).

4. Discussion

This *in vitro* study has shown that there was a significant reduction in the resorbing activity of M-CSF + RANKL-treated osteoclasts derived from Charcot patients in response to anti-TNF-α treatment. The addition of anti-TNF-α resulted in significant reduction in the area of resorption on bovine bone discs both on the surface, as assessed by image analysis,

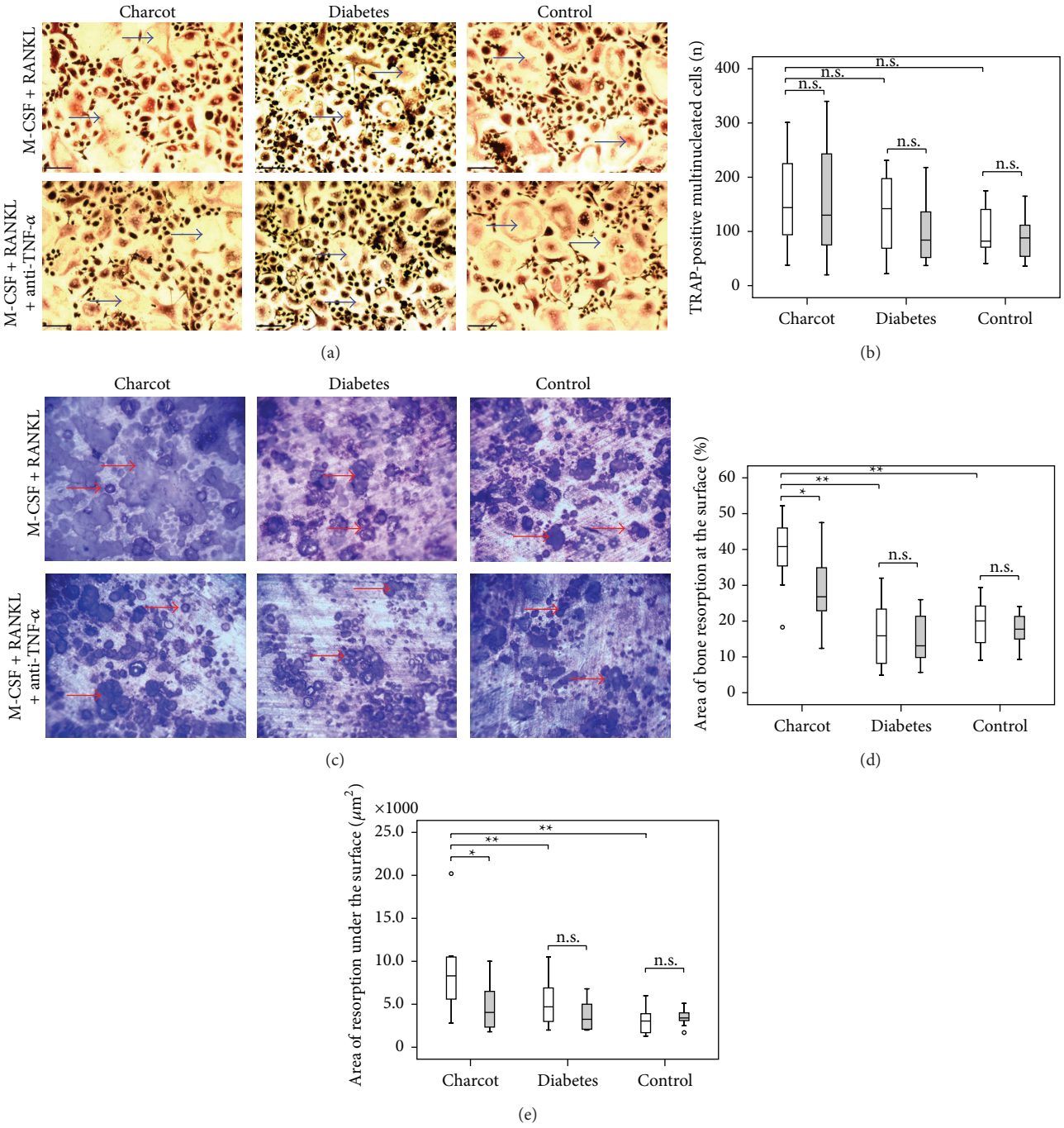

FIGURE 1: Osteoclast formation and resorption in Charcot patients, diabetic patients, and healthy control subjects in M-CSF + RANKL-treated cultures and in M-CSF + RANKL + anti-TNF-α-treated cultures. Representative images of TRAP-positive multinucleated cells formed on plastic (Olympus; original magnification ×100, scale bar = 200 μm) (a) and resorbed bovine bone discs (Olympus BX60; original magnification ×200) (c). The arrows denote some of the TRAP-positive multinucleated cells (a) and some of the resorption pits (c). Comparison of the number of TRAP-positive multinucleated cells (b), the area of resorption at the surface (d), and the area of resorption under the surface (e) of resorbed bone discs between M-CSF + RANKL-treated cultures (white bars) and M-CSF + RANKL + anti-TNF-α-treated cultures (grey bars). Significance assessed by Mann-Whitney U test, levels of significance are demonstrated on the graphs; $^{*}p < 0.05$; $^{**}p < 0.01$; ns = nonsignificant ($p > 0.05$).

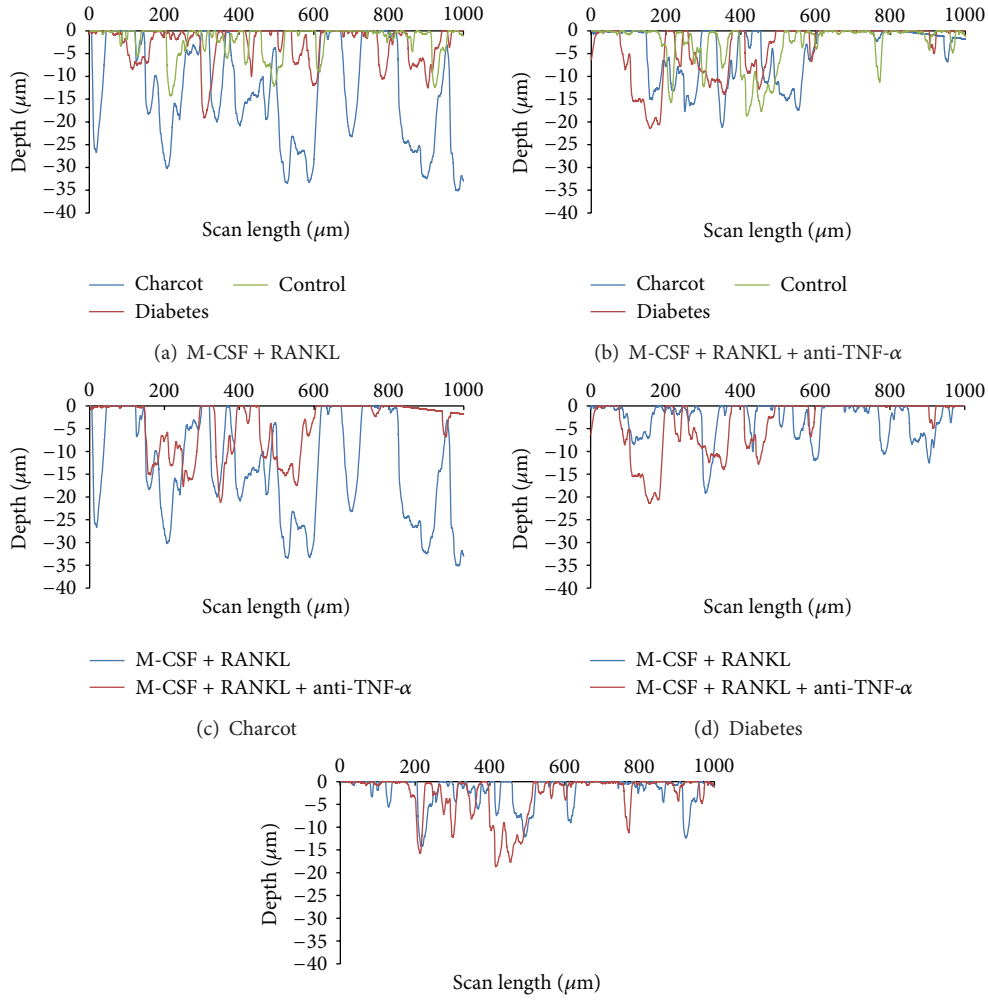

(a) M-CSF + RANKL

(b) M-CSF + RANKL + anti-TNF-α

(c) Charcot

(d) Diabetes

(e) Control

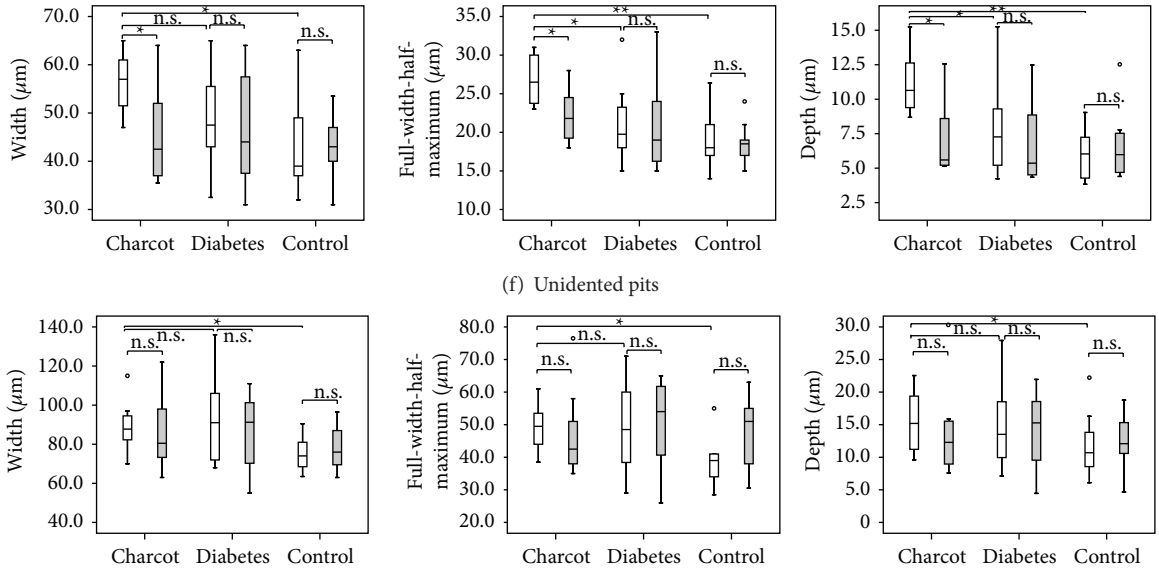

(f) Unidented pits

(g) Bidented pits

Figure 2: Continued.

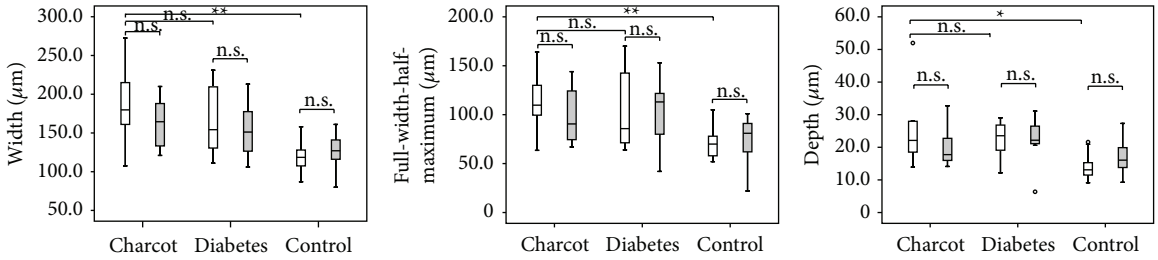

(h) Multidented pits

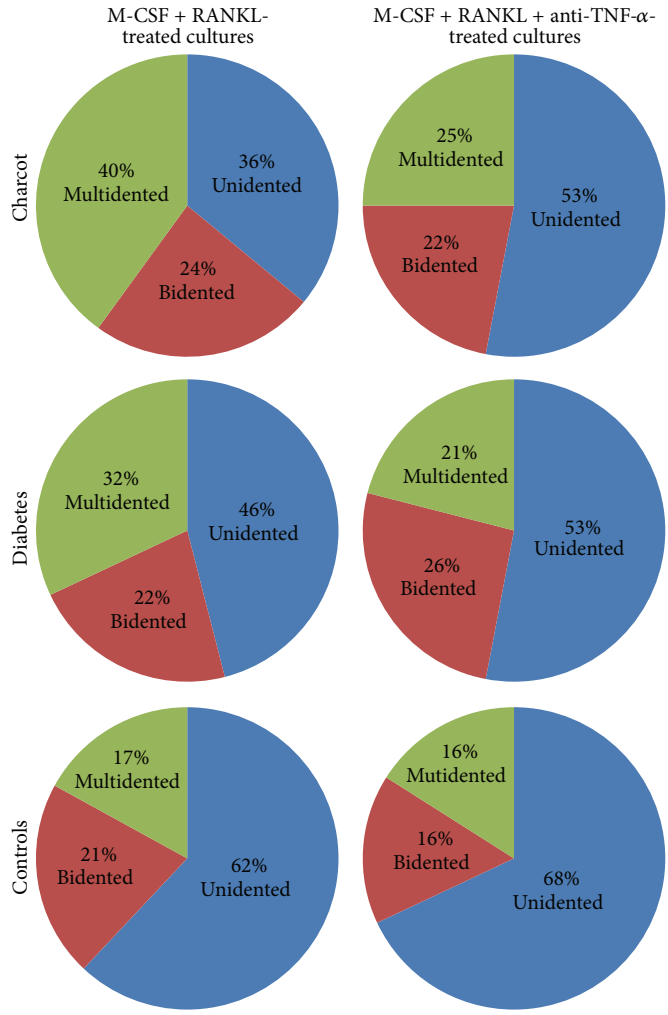

(i)

Figure 2: Surface profilometry in Charcot patients, diabetic patients, and healthy control subjects in M-CSF + RANKL-treated cultures and in M-CSF + RANKL + anti-TNF-α-treated cultures. Representative erosion profiles of resorbed bone discs in Charcot patient (blue line), diabetic patient (red line), and healthy control subject (green line) after surface profilometry in M-CSF + RANKL-treated cultures (a) and in M-CSF + RANKL + anti-TNF-α-treated cultures (b). Representative erosion profiles of resorbed bone discs in M-CSF + RANKL-treated cultures (blue line) and M-CSF + RANKL + anti-TNF-α-treated cultures (red line) in Charcot patient (c), diabetic patient (d), and healthy control subject (e). The marked difference of the erosion profile in a Charcot patient compared with diabetic patient and healthy control in MCSF + RANKL-treated cultures (a) was reversed after the addition of anti-TNF-α (b). Pits appeared significantly smaller in M-CSF + RANKL + anti-TNF-α-treated cultures compared with MCSF + RANKL-treated cultures in Charcot patients (c) but remained unchanged in diabetic patients (d) and in healthy controls (e). Comparison of pit measurements (width, FWHM, and depth) between M-CSF + RANKL-treated cultures (white bars) and M-CSF + RANKL + anti-TNF-α-treated cultures (grey bars); unidented pits (f), bidented pits (g), and multidented pits (h). Significance assessed by Mann-Whitney U test, levels of significance are demonstrated on the graphs; $^{*}p < 0.05$; $^{**}p < 0.01$; ns = nonsignificant ($p > 0.05$). Distribution of pits (%) according to their shape in M-CSF + RANKL and M-CSF + RANKL + anti-TNF-α-treated cultures in Charcot patients, diabetic patients, and healthy control subjects (i). In M-CSF + RANKL-treated cultures, there was a significant reduction in the percentage of unidented ($p < 0.05$) and a significant increase in the percentage of multidented pits ($p < 0.05$) in Charcot patients compared with diabetic patients and healthy controls. The addition of anti-TNF-α treatment led to a significant difference in the pit distribution only in Charcot patients characterised by a significant increase in the percentage of unidented pits ($p < 0.05$) and significant decrease in the percentage of multidented pits ($p < 0.05$). No differences in the pit distribution were noted in diabetic patients and in healthy control subjects.

and also under the surface, as assessed by surface profilometry. The aberrant erosion profile, pit morphology, and pit distribution in M-CSF + RANKL-treated cultures in Charcot patients were reversed after the addition of anti-TNF-α. These findings confirm the hypothesis that the proinflammatory cytokine TNF-α modulates increased osteoclastic activity in acute Charcot osteoarthropathy.

In the present study, we have shown that newly derived osteoclasts from monocytes isolated from Charcot patients exhibit an enhanced response to RANKL. Osteoclastogenesis is pivotally dependant on M-CSF (a survival factor) and RANKL (key factor for osteoclast differentiation and regulation) [15, 16]. In the presence of these two cytokines, monocytes, which express the receptors c-fms and RANK, proliferate and differentiate into mature multinucleated osteoclasts [17, 18]. The osteoclasts generated from Charcot patients were functionally more aggressive compared to osteoclasts from diabetic patients and healthy control subjects in a classical resorption assay [7, 8]. In addition, surface profilometry demonstrated that osteoclasts from Charcot patients exhibited a considerable below-surface resorbing activity, which was not associated with an increase in osteoclast formation [8]. However, the mechanisms of this enhanced response are unknown.

In Charcot osteoarthropathy bone loss is limited to the inflamed affected foot [19, 20] and it is possible that local inflammatory factors released after initial trauma to the Charcot foot may act as osteoclastogenic mediators [6]. In this study, we sought to determine the role of TNF-α as a promoter of the observed enhanced osteoclast function. This cytokine has been linked with inflammatory bone loss [12] and immunohistochemical analysis of surgical Charcot specimens has indicated that osteoclastic bone resorption takes place in the presence of TNF-α [21]. In the acute stage of the osteoarthropathy, serum concentrations of TNF-α are raised [22]. Moreover, in the acute Charcot foot, inflammatory modulation of peripheral monocytes with increased spontaneous and induced production of TNF-α has been noted [23]. In this study, using the traditional resorption pit assay together with surface profilometry, we have demonstrated that although osteoclast formation remained unchanged, the addition of anti-TNF-α to M-CSF + RANKL-treated cultures significantly decreased osteoclast function. This is in agreement with previous data showing that TNF-α is more potent for osteoclast activation than for osteoclast formation [24]. The inhibition of TNF-α led to a significant reduction in the area of resorption on the surface and under the surface in cultures from Charcot patients.

As well as increased resorption, in our study, there were a pathological erosion profile and aberrant morphological appearance of resorption pits on bone slices in M-CSF + RANKL-treated cultures in Charcot patients compared with healthy control subjects [8] and also in Charcot patients compared with diabetic patients. We demonstrated that the addition of anti-TNF-α reversed the observed differences in pit parameters and erosion profile between the study groups and in Charcot patients there was a notable "normalisation" of the erosion profile and pit morphology. This suggests that osteoclasts generated in M-CSF + RANKL-treated cultures, prior to inhibition of TNF-α, exhibit a highly aggressive resorptive profile. This exuberant resorptive activity was reduced after the addition of anti-TNF-α, providing further evidence to support the role of this cytokine in the osteoclastogenesis of acute Charcot osteoarthropathy.

As well as changes in the morphological appearance of pits, there was a difference in the distribution of the shape of the pits in Charcot patients between the two culture treatments. The resorption pits in M-CSF + RANKL-treated cultures of the Charcot patients were predominantly multidented and bidented whilst the unidented pits were less frequently seen although in diabetic patients and in healthy control subjects the pit distribution remained unchanged between the two culture treatments.

The addition of anti-TNF-α to M-CSF + RANKL-treated cultures resulted in a significant reduction in the percentage of the multidented pits as well as a significant increase the percentage of the unidented pits. Thus, the inhibition of TNF-α normalised the resorptive behaviour of Charcot osteoclasts in which resorption alternated with migration as indicated by a significant increase in the percentage of unidented pits. It is possible that observed aberrant pit morphology and distribution were due to a TNF-α modulation of the resorption cycle (Figure 3(a)). During the process of bone resorption, osteoclasts solubilise bone mineral followed by degradation of demineralised organic matrix and in control conditions, the relative rate of collagenolysis is slower than the rate of demineralisation [25]. Experimental *in vitro* studies have shown that agents which can upregulate cathepsin K expression prolong the resorption cycle and resorption events more frequently present as trenches (continuous resorption) [25]. In contrast, inhibition of cathepsin K accelerates the resorption cycle, leading to faster accumulation of collagen. This results in resorption events more frequently presenting as shallower and smaller pits (intermittent resorption). Both RANKL and TNF-α stimulate the osteoclasts to produce cathepsin K, which is the major protease responsible for the degradation of collagen [26]. In Charcot osteoarthropathy it is possible that TNF-α via enhanced cathepsin K expression may lead to imbalance between the relative rate of collagenolysis and demineralisation. This mechanism may explain the continuous resorptions which we observed as multidented pits in the M-CSF + RANKL-treated cultures in contrast to the more frequently noted intermittent resorptions (unidented pits) after the addition of anti-TNF-α [25] (Figure 3(a)).

These findings have important implications for understanding the pathogenesis of this condition. Our data underscores the potent role of TNF-α in the RANKL-mediated osteoclastogenesis (Figure 3(b)). Trauma to the neuropathic diabetic foot leads to bone damage and uncontrolled inflammation [6]. Bone fracture is the harbinger of Charcot osteoarthropathy [27] and it leads to changes in the bone matrix, which becomes a site of targeted remodelling with increased numbers of apoptotic osteocytes (bone matrix cells) and rapid degradation by activated osteoclasts [18, 28]. Furthermore, bone fracture triggers a coordinated healing cytokine response with the induction of proinflammatory cytokines, including TNF-α [29]. In the affected Charcot foot,

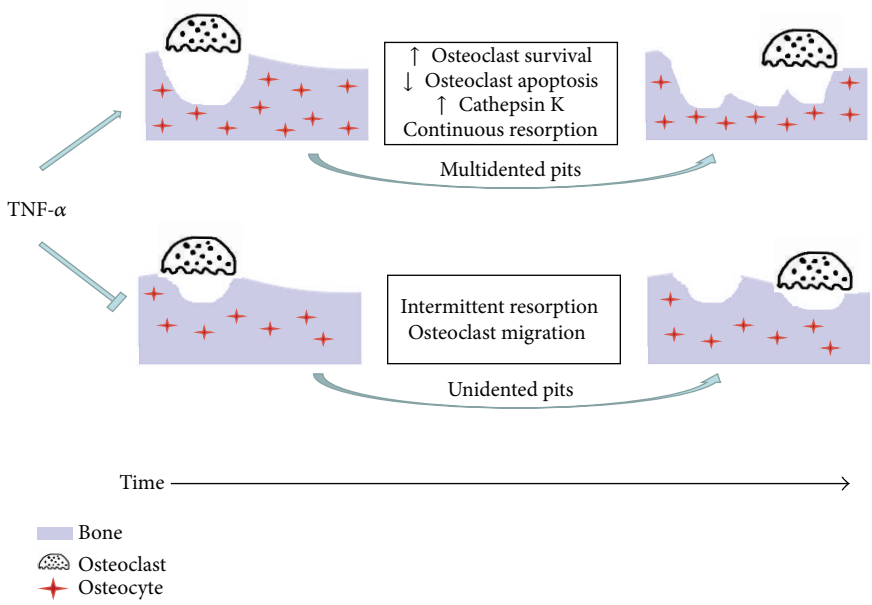

(a)

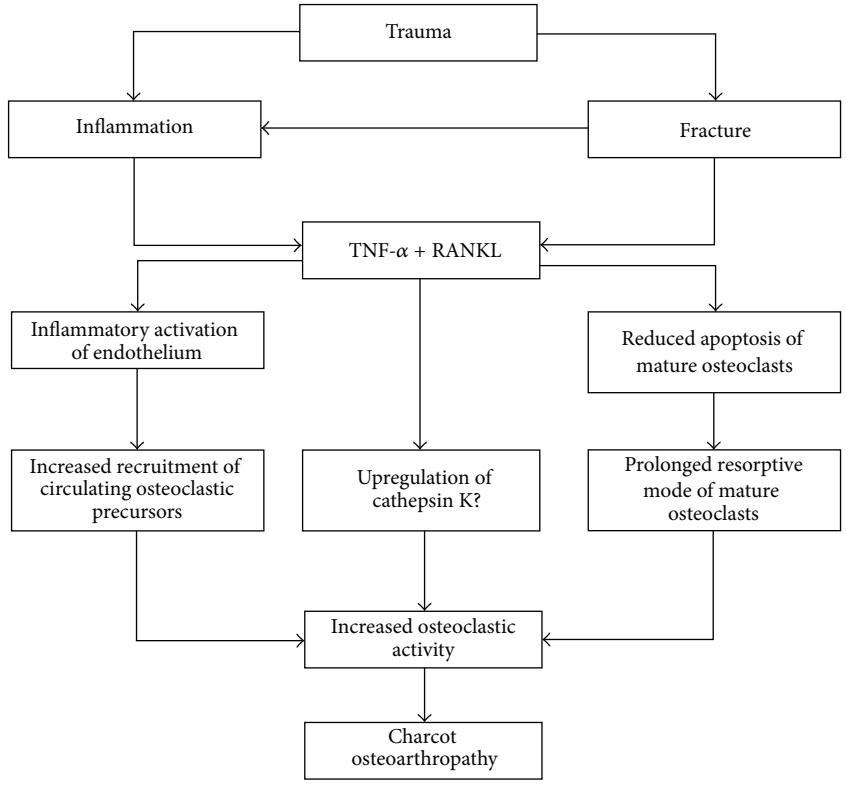

(b)

Figure 3: Model for osteoclast resorptive activity in Charcot osteoarthropathy in M-CSF + RANKL-treated cultures before and after the addition of anti-TNF-α (a). In the presence of TNF-α, continuous multidented pits (defined as lacunae or trenches) with increased area of resorption both on the surface and under the surface are seen more frequently compared with less frequently noted unidented pits (single resorption event). Resorption is prolonged and is not interrupted by migration episodes. After the inhibition of TNF-α, the percentage of multidented pits is reduced with a corresponding increase in the percentage of unidented pits suggesting that the resorptive cycle is restored. Resorption alternates with migration and intermittent resorption events occur away from each other (unidented pits). The observed differences in the resorption before and after the addition of anti-TNF-α suggest that TNF-α (via cathepsin K upregulation) modulates the resorptive behaviour of osteoclasts generated from Charcot patients and these highly active osteoclasts are capable of extensive lacunar resorption with aberrant pit morphology and geometry due to reduced migration, increased survival, and reduced apoptosis. The proposed role of TNF-α in the pathogenesis of pathological bone destruction in the acute Charcot foot (b).

the inflammatory response to trauma with increased cytokine release leads to an upregulation of receptors and adhesion molecules in the endothelium which then forms a firm attachment to osteoclast precursors resulting in enhanced recruitment of osteoclasts to sites of bone resorption [30]. Furthermore, the activation of RANK by RANKL attracts osteoclastic precursors [31] and its upregulation contributes to an enhanced RANKL-induced monocyte migration to the affected foot. Thus TNF-α-primed osteoclastic precursors in the presence of increased local expression of RANKL differentiate into highly aggressive osteoclasts with extensive resorbing activity characterised by increased survival and reduced apoptosis and migration. This increased osteoclastic activity may be due to cathepsin K upregulation, which requires further studies, as this may provide scientific basis for novel intervention with cathepsin K inhibitors. Overall, these aberrantly activated osteoclasts play a key role in the pathological bone destruction of the acute Charcot foot.

In conclusion, using a traditional osteoclast resorption assay together with surface profilometry, this study has demonstrated for the first time that the proinflammatory cytokine TNF-α modulated RANKL-mediated osteoclastic resorption *in vitro* in patients with acute Charcot osteoarthropathy and these observations shed light into the pathogenesis of this devastating condition.

Disclosure

Michael E. Edmonds and Catherine M. Shanahan are joint senior authors.

Conflict of Interests

The authors declare that there is no conflict of interests regarding the publication of this paper.

Acknowledgments

This paper is supported by Diabetes Research and Wellness Foundation. Nina L. Petrova is a holder of Diabetes Research and Wellness Foundation Clinical Fellowship.

References

[1] N. L. Petrova and M. E. Edmonds, "Charcot neuro-osteoarthropathy—current standards," *Diabetes/Metabolism Research and Reviews*, vol. 24, supplement 1, pp. S58–S61, 2008.

[2] A. Gazis, N. Pound, R. Macfarlane, K. Treece, F. Game, and W. Jeffcoate, "Mortality in patients with diabetic neuropathic osteoarthropathy (Charcot foot)," *Diabetic Medicine*, vol. 21, no. 11, pp. 1243–1246, 2004.

[3] J. van Baal, R. Hubbard, F. Game, and W. Jeffcoate, "Mortality associated with acute charcot foot and neuropathic foot ulceration," *Diabetes Care*, vol. 33, no. 5, pp. 1086–1089, 2010.

[4] M.-W. Sohn, T. A. Lee, R. M. Stuck, R. G. Frykberg, and E. Budiman-Mak, "Mortality risk of charcot arthropathy compared with that of diabetic foot ulcer and diabetes alone," *Diabetes Care*, vol. 32, no. 5, pp. 816–821, 2009.

[5] L. C. Rogers, R. G. Frykberg, D. G. Armstrong et al., "The Charcot foot in diabetes," *Diabetes Care*, vol. 34, no. 9, pp. 2123–2129, 2011.

[6] W. J. Jeffcoate, F. Game, and P. R. Cavanagh, "The role of proinflammatory cytokines in the cause of neuropathic osteoarthropathy (acute Charcot foot) in diabetes," *The Lancet*, vol. 366, no. 9502, pp. 2058–2061, 2005.

[7] G. Mabilleau, N. L. Petrova, M. E. Edmonds, and A. Sabokbar, "Increased osteoclastic activity in acute Charcot's osteoarthopathy: the role of receptor activator of nuclear factor-kappaB ligand," *Diabetologia*, vol. 51, no. 6, pp. 1035–1040, 2008.

[8] N. L. Petrova, P. K. Petrov, M. E. Edmonds, and C. M. Shanahan, "Novel use of a Dektak 150 surface profiler unmasks differences in resorption pit profiles between control and Charcot patient osteoclasts," *Calcified Tissue International*, vol. 94, no. 4, pp. 403–411, 2014.

[9] J. Lam, Y. Abu-Amer, C. A. Nelson, D. H. Fremont, F. P. Ross, and S. L. Teitelbaum, "Tumour necrosis factor superfamily cytokines and the pathogenesis of inflammatory osteolysis," *Annals of the Rheumatic Diseases*, vol. 61, no. 2, pp. ii82–ii83, 2002.

[10] E. Romas, "Bone loss in inflammatory arthritis: mechanisms and therapeutic approaches with bisphosphonates," *Best Practice and Research: Clinical Rheumatology*, vol. 19, no. 6, pp. 1065–1079, 2005.

[11] N. C. Walsh and E. M. Gravallese, "Bone loss in inflammatory arthritis: mechanisms and treatment strategies," *Current Opinion in Rheumatology*, vol. 16, no. 4, pp. 419–427, 2004.

[12] C. T. Ritchlin, S. A. Haas-Smith, P. Li, D. G. Hicks, and E. M. Schwarz, "Mechanisms of TNF-α- and RANKL-mediated osteoclastogenesis and bone resorption in psoriatic arthritis," *Journal of Clinical Investigation*, vol. 111, no. 6, pp. 821–831, 2003.

[13] K. Redlich and J. S. Smolen, "Inflammatory bone loss: pathogenesis and therapeutic intervention," *Nature Reviews Drug Discovery*, vol. 11, no. 3, pp. 234–250, 2012.

[14] A. P. Cope, M. Londei, N. R. Chu et al., "Chronic exposure to tumor necrosis factor (TNF) in vitro impairs the activation of T cells through the T cell receptor/CD3 complex; reversal in vivo by anti-TNF antibodies in patients with rheumatoid arthritis," *The Journal of Clinical Investigation*, vol. 94, no. 2, pp. 749–760, 1994.

[15] S. Tanaka, N. Takahashi, N. Udagawa et al., "Macrophage colony-stimulating factor is indispensable for both proliferation and differentiation of osteoclast progenitors," *The Journal of Clinical Investigation*, vol. 91, no. 1, pp. 257–263, 1993.

[16] H. Yasuda, N. Shima, N. Nakagawa et al., "Osteoclast differentiation factor is a ligand for osteoprotegerin/osteoclastogenesis-inhibitory factor and is identical to TRANCE/RANKL," *Proceedings of the National Academy of Sciences of the United States of America*, vol. 95, no. 7, pp. 3597–3602, 1998.

[17] S. L. Teitelbaum, "Osteoclasts: what do they do and how do they do it?" *American Journal of Pathology*, vol. 170, no. 2, pp. 427–435, 2007.

[18] K. Henriksen, J. Bollerslev, V. Everts, and M. A. Karsdal, "Osteoclast activity and subtypes as a function of physiology and pathology—implications for future treatments of osteoporosis," *Endocrine Reviews*, vol. 32, no. 1, pp. 31–63, 2011.

[19] A. Jirkovská, P. Kasalický, P. Bouček, J. Hosová, and J. Skibová, "Calcaneal ultrasonometry in patients with Charcot osteoarthropathy and its relationship with densitometry in the lumbar spine and femoral neck and with markers of bone turnover," *Diabetic Medicine*, vol. 18, no. 6, pp. 495–500, 2001.

[20] N. L. Petrova, A. V. M. Foster, and M. E. Edmonds, "Calcaneal bone mineral density in patients with Charcot neuropathic osteoarthropathy: differences between Type 1 and Type 2 diabetes," *Diabetic Medicine*, vol. 22, no. 6, pp. 756–761, 2005.

[21] J. F. Baumhauer, R. J. O'Keefe, L. C. Schon, and M. S. Pinzur, "Cytokine-induced osteoclastic bone resorption in charcot arthropathy: an immunohistochemical study," *Foot & Ankle International*, vol. 27, no. 10, pp. 797–800, 2006.

[22] N. L. Petrova, T. K. Dew, R. L. Musto et al., "Inflammatory and bone turnover markers in a cross-sectional and prospective study of acute Charcot osteoarthropathy," *Diabetic Medicine*, vol. 32, no. 2, pp. 267–273, 2015.

[23] L. Uccioli, A. Sinistro, C. Almerighi et al., "Proinflammatory modulation of the surface and cytokine phenotype of monocytes in patients with acute Charcot foot," *Diabetes Care*, vol. 33, no. 2, pp. 350–355, 2010.

[24] K. Fuller, C. Murphy, B. Kirstein, S. W. Fox, and T. J. Chambers, "TNFα potently activates osteoclasts, through a direct action independent of and strongly synergistic with RANKL," *Endocrinology*, vol. 143, no. 3, pp. 1108–1118, 2002.

[25] K. Søe, D. M. H. Merrild, and J.-M. Delaissé, "Steering the osteoclast through the demineralization-collagenolysis balance," *Bone*, vol. 56, no. 1, pp. 191–198, 2013.

[26] B. R. Troen, "The regulation of cathepsin K gene expression," *Annals of the New York Academy of Sciences*, vol. 1068, no. 1, pp. 165–172, 2006.

[27] J. T. Johnson, "Neuropathic fractures and joint injuries. Pathogenesis and rationale of prevention and treatment," *The Journal of Bone & Joint Surgery—American Volume*, vol. 49, no. 1, pp. 1–30, 1967.

[28] T. J. Heino, K. Kurata, H. Higaki, and H. K. Väänänen, "Evidence for the role of osteocytes in the initiation of targeted remodeling," *Technology and Health Care*, vol. 17, no. 1, pp. 49–56, 2009.

[29] T. Kon, T.-J. Cho, T. Aizawa et al., "Expression of osteoprotegerin, receptor activator of NF-κB ligand (osteoprotegerin ligand) and related proinflammatory cytokines during fracture healing," *Journal of Bone and Mineral Research*, vol. 16, no. 6, pp. 1004–1014, 2001.

[30] N. W. A. McGowan, E. J. Walker, H. Macpherson, S. H. Ralston, and M. H. Helfrich, "Cytokine-activated endothelium recruits osteoclast precursors," *Endocrinology*, vol. 142, no. 4, pp. 1678–1681, 2001.

[31] B. A. Mosheimer, N. C. Kaneider, C. Feistritzer, D. H. Sturn, and C. J. Wiedermann, "Expression and function of RANK in human monocyte chemotaxis," *Arthritis & Rheumatism*, vol. 50, no. 7, pp. 2309–2316, 2004.

Calcif Tissue Int (2014) 94:403–411
DOI 10.1007/s00223-013-9820-9

ORIGINAL RESEARCH

Novel Use of a Dektak 150 Surface Profiler Unmasks Differences in Resorption Pit Profiles Between Control and Charcot Patient Osteoclasts

Nina L. Petrova · Peter K. Petrov · Michael E. Edmonds · Catherine M. Shanahan

Received: 21 August 2013 / Accepted: 22 November 2013 / Published online: 10 December 2013

Abstract We hypothesized that newly formed osteoclasts from patients with acute Charcot osteoarthropathy can resorb surfaces of bone more extensively compared with controls. Peripheral blood monocytes, isolated from eight Charcot patients and nine controls, were cultured in vitro on 24-well plates and bovine bone discs in duplicate with macrophage colony-stimulating factor (M-CSF) and receptor activator of nuclear factor κβ ligand (RANKL). Osteoclast formation was assessed by tartrate-resistant acid phosphatase staining (TRAcP) at day 17. Resorption was measured at day 21 after toluidine blue staining by two methods: (1) area of resorption at the surface by image analysis (%) and (2) area of resorption under the surface (μm^2) measured by a Dektak 150 Surface Profiler. Ten 1,000 μm-long scans were performed per disc. Pits were classified as unidented, bidented, and multidented according to their shape. Although the number of newly formed TRAcP positive multinucleated cells (>3 nuclei) was similar in M-CSF + RANKL-treated cultures between controls and Charcot patients, the latter exhibited increased resorbing activity. The area of resorption on the surface by image analysis was significantly greater in Charcot patients compared with controls (21.1 % [14.5–26.2] vs. 40.8 % [35.4–46.0], median [25–75th percentile], $p < 0.01$), as was the area of resorption under the surface (2.7 μm^2 [1.6–3.9] vs. 8.3 μm^2 [5.6–10.6], $p < 0.01$) after profilometry. In Charcot patients pits were deeper and wider and more frequently presented as multidented pits. This application of the Dektak 150 Surface Profiler revealed novel differences in resorption pit profile from osteoclasts derived from Charcot patients compared with controls. Resorption in Charcot patients was mediated by highly aggressive newly formed osteoclasts from monocytes eroding large and deep areas of bone.

Keywords Charcot osteoarthropathy · Osteoclasts · Resorption pits · Surface profilometry

The authors report that they have no conflict of interest.

N. L. Petrova (✉) · M. E. Edmonds
Diabetic Foot Clinic, King's College Hospital, Denmark Hill, London SE5 9RS, UK
e-mail: petrovanl@yahoo.com

M. E. Edmonds
e-mail: michael.edmonds@nhs.net

P. K. Petrov
Department of Materials, Imperial College, Prince Consort Road, London SW7 2AZ, UK
e-mail: p.petrov@imperial.ac.uk

C. M. Shanahan
Cardiovascular Division, James Black Centre, King's College London, 125 Coldharbour Lane, London SE5 9NU, UK
e-mail: cathy.shanahan@kcl.ac.uk

Introduction

Charcot osteoarthropathy (or Charcot foot) is one of the most challenging foot complications of diabetes in the twenty first century [1]. Trauma of the insensate diabetic neuropathic foot triggers inflammation and aggressive osteolysis which result in multiple fractures, bone fragmentations, and joint dislocations [2]. The mechanisms of severe bone destruction seen in the acute Charcot foot are not fully understood, but we have recently hypothesized that aberrantly activated osteoclasts play a key role in this pathological process.

Osteoclasts are the principal cell type responsible for bone resorption [3] and are derived from mononuclear cell precursors of the monocyte/macrophage lineage that

circulate in the blood in the monocytic fraction [4]. Osteoclastogenesis is regulated by receptor activator of nuclear factor κβ ligand (RANKL), a cytokine from the TNF-ligand superfamily, which acts via its receptor RANK, expressed on osteoclastic precursors and osteoclasts [5]. Another cytokine required for proliferation and survival of mononuclear cells is macrophage-colony stimulating factor (M-CSF), which acts via its receptor, c-fms [6]. Osteoclastic precursors in the presence of RANKL and M-CSF undergo differentiation and fusion resulting in large multinucleated cells, which express a series of osteoclast markers, including tartrate-resistant acid phosphatase (TRAcP) and calcitonin receptors [7]. To degrade mineralized matrix, these cells have a unique cytoskeleton. In contact with bone, they form ruffled membrane and actin rings, characteristic of actively resorbing osteoclasts [8].

The discovery of M-CSF and RANKL has led to the development of an in vitro resorption assay to generate functional human osteoclasts from peripheral blood mononuclear cells (PBMCs) in the presence of these cytokines [9]. Recently, using this technique, we have shown that newly formed osteoclasts generated from Charcot patients exhibit an increased response to RANKL, as demonstrated by large areas of resorption on dentine slices after toluidine blue staining [10]. Although the technique to generate functional human osteoclasts is widely used to assess osteoclastic activity, measurement of the percentage area resorbed by image analysis has its limitations because it does not provide information on the depth and shape of erosions. Thus, measurement of the erosion profile could be a useful method to describe the resorptive capacity of newly formed osteoclasts in vitro as it may provide more information on how osteoclasts exert their resorbing activity. We hypothesized that osteoclasts from Charcot patients have increased osteoclastic potential and can carry out extensive resorption not only at the surface but also under the surface of bovine discs.

In order to investigate this hypothesis, we used a Dektak 150 Surface Profiler to measure the surface profile of eroded bovine discs from osteoclasts generated in the presence of M-CSF and RANKL from PBMCs isolated from Charcot patients and controls.

Materials and Methods

Patients

Samples from peripheral blood were obtained from 8 diabetic patients with acute Charcot osteoarthropathy (4 men and 4 women, 4 type 1 diabetes and 4 type 2 diabetes) and 9 healthy control subjects (5 men and 4 women).

Patients with acute Charcot osteoarthropathy were matched for age and gender with the healthy subjects. The median age was similar between Charcot patients and control subjects (57 years [43–60.5], median [25–75th percentile] vs. 45 years [41–51.5], $p > 0.05$), and there was no difference in the gender distribution between the two groups ($p > 0.05$). All patients with acute Charcot osteoarthropathy presented with a unilateral red, hot, swollen foot and radiological evidence of acute Charcot fractures, demonstrated on plain foot and ankle radiographs [1]. The study was approved by the Outer West London Research Ethics Committee, and all patients and control subjects gave written informed consent.

Isolation and Culture of PBMCs

PBMCs were isolated from patients and control subjects as previously described [10]. Briefly, blood was diluted with α-minimal essential medium (α-MEM; Lonza Ltd., Wokingham, UK) in 1:1, layered over Histopaque (Sigma-Aldrich Ltd., Poole, UK), and centrifuged for 25 min at 4 °C at 2,300 rpm. The interface layer was washed in α-MEM and centrifuged at 1,500 rpm at 4 °C for 15 min. Cells were resuspended in α-MEM, and after a second round of centrifugation (1,500 rpm at 4 °C for 15 min), the pellet was resuspended in culture medium and 2×10^6 cells were cultured on 24-well plates and 5×10^5 cells were cultured on bovine bone discs in duplicate to assess osteoclast formation and resorption, respectively. The bone discs (IDS Ltd., Boldon, UK) were made from the cortical part of the femur of bovine bones (6 mm in diameter and approximately 200 μm thick).

After 2 h of incubation at 37 °C, plates and bovine bone discs were washed to remove nonadherent cells and then maintained in culture medium, supplemented with penicillin (50 U/ml)/streptomycin (50 μg/ml) (Sigma-Aldrich Ltd., Poole, UK), L-glutamine (2 mM) (Sigma-Aldrich Ltd., Poole, UK), and 10 % heat-inactivated FBS (Lonza Ltd., Wokingham, UK) under the following conditions: cultures with M-CSF 25 ng/ml (added at day 0)—negative control (M-CSF, R&D Systems Europe, Ltd., Abingdon, UK); cultures with M-CSF and soluble RANKL 100 ng/ml (added at day 7)—positive control (RANKL-PeproTech EC Ltd., London, UK). Culture medium was refreshed every 3 or 4 days and was supplemented with the appropriate agents as described above.

Osteoclast formation was assessed at day 17 after tartrate-resistant acid phosphatase (TRAcP) staining, as previously described [10]. TRAcP-positive ($TRAcP^+$) cells with more than three nuclei were identified as osteoclasts. The number of newly generated osteoclasts on plastic (24-well plates) was assessed by light microscopy.

Functional evidence of osteoclast resorption was assessed on bovine bone discs after 21 days of culture. The discs

were initially placed in NH_4OH (1 mol/l) overnight and sonicated to remove any adherent cells, then stained with 1 % toluidine blue for 5 min. Excess staining was removed by washing with distilled water. After air drying, the bovine bone discs were mounted onto a glass slide. Resorption pits were identified by light microscopy. The extent of eroded surface on each bovine bone disc was determined using image analysis and expressed as the percentage of surface area resorbed. Additional bovine bone discs were stained with FitC-phalloidin (Sigma-Aldrich Ltd., Poole, UK) and mounted with Vectashield mounting medium with DAPI (Vector Laboratories, Peterborough, UK) for the assessment of actin ring formation, a marker of actively resorbing osteoclasts [11].

Surface Profilometry

The erosion profile of each bovine bone disc was measured by the Dektak 150 Surface Profiler (Veeco, New York, NY, USA), fitted with a stylus which had a radius of 2.5 μm. The glass slide with the mounted bovine bone disc was placed on the stage and positioned under the stylus. Initially, the surface of each disc was examined for the presence of erosions using the camera integrated with the profiler. The resorbed areas appeared as dark areas surrounded by grey areas. In order to set up the unresorbed bone at the zero level, the starting point of each measurement was preset away from a randomly selected eroded area. Then the stylus was dragged across the surface of the sample in hills and valleys mode with vertical measurement range of 65.5 μm. Each measurement was carried out with the following scan parameters: stylus force 3.00 mg, scan length 1,000 μm, and scan duration 60 s, which resulted in a resolution of 0.056 μm/scan. The Veeco software graphically reproduced the measured erosion profile. In order to compensate for the tilt of the mounted discs, the profiler software was used to level the measurement and to set the unresorbed bovine surface as the zero level. The measurement data was exported and saved as an Excel-formatted document for further analysis. Ten scans for each subject were carried out at random sites on each of the two bovine discs. The median area of disc erosion under the surface (μm^2) was calculated for each subject by Origin Pro 8.6 software. A total of 1,233 pits (median of 48 and 73 pits per Charcot patient and control subject, respectively) were evaluated. According to their shape, pits were defined as unidented (erosion with one dent starting from and finishing at the level of the unresorbed surface), bidented (erosion with two clearly defined dents starting from and finishing at the level of the unresorbed surface), and multidented (erosion with three or more dents starting from and finishing at the level of the unresorbed surface). Each pit was characterized by the following parameters: width at the surface (μm), maximum depth (μm), and full-width–half-maximum (FWHM), where the width was measured at the half of the maximum depth. The median width, depth, and FWHM for the unidented, bidented, and multidented pits were calculated for each subject.

Statistical Analyses

Data were expressed as median [25–75th percentile] and analysed by the Mann–Whitney nonparametric test. Resorption on bovine bone discs was quantitated by two methods: (1) resorption at the surface by image analysis (%), and (2) area of resorption under the surface (μm^2) by profilometry. The area of resorption (at the surface and under the surface), together with the pit parameters (width, FWHM, and maximum depth) for the unidented, bidented, and multidented pits were compared between the controls and the Charcot patients. Differences were considered significant at $p < 0.05$.

Results

Microscopy

Observation of the 24-well plates with light microscopy showed no difference in osteoclast formation in M-CSF-treated cultures and also in M-CSF + RANKL-treated cultures between the two groups. The median number of $TRAP^+$ multinucleated cells in controls was not significantly different from the median number of $TRAP^+$ multinucleated cells in Charcot patients in MCSF-treated cultures (controls 18 [1–52]) vs. Charcot 39 [12–65]), $p > 0.05$) and also in M-CSF + RANKL-treated cultures (controls 82 [71–141] vs. Charcot 140 [87–208], $p > 0.05$).

Observation of bovine bone discs by light microscopy showed no evidence of pit formation in M-CSF-treated cultures in both control subjects and Charcot patients (Fig. 1a, b). In contrast, numerous pits were noted in M-CSF + RANKL-treated cultures on bovine bone discs in both controls and Charcot patients (Fig. 1c, d). Furthermore, actin ring formation assessed with immunofluorescent microscopy was noted only in M-CSF + RANKL-treated cultures (Fig. 1g, h) but not in cultures treated with M-CSF alone (Fig. 1e, f). Thus, M-CSF on its own did not trigger osteoclastic resorptive activity; these cultures served as a negative control, whereas M-CSF + RANKL-treated cultures served as a positive control.

Visualization under the light microscope after toluidine blue staining revealed that there was a remarkable difference in the morphology of the pits between the two groups. In control subjects, the resorption events more commonly

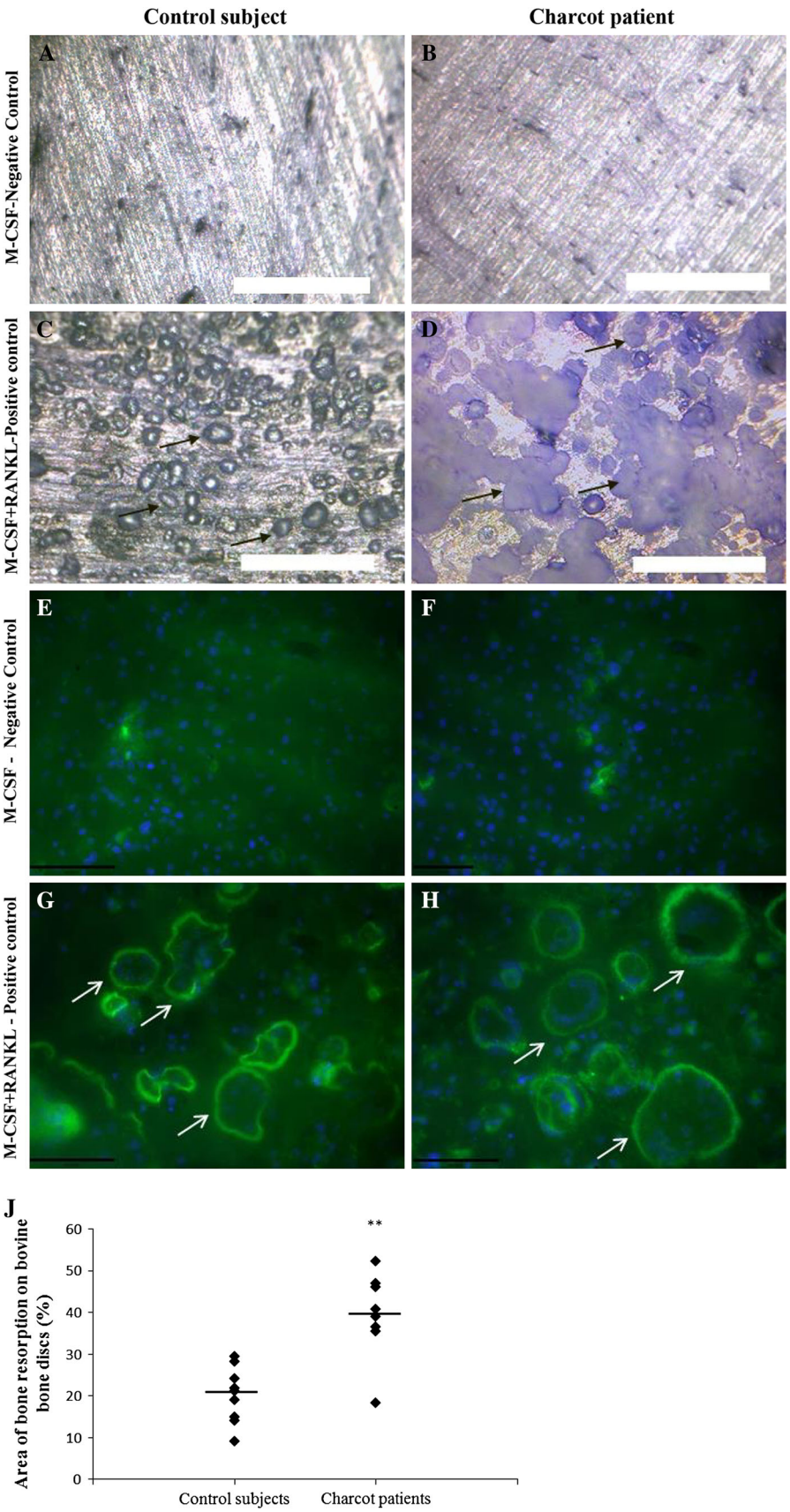

Fig. 1 Typical appearance of bovine bone discs after toluidine blue staining in M-CSF-treated cultures and M-CSF + RANKL-treated cultures in a control subject (**a**, **c**) and in a Charcot patient (**b**, **d**), respectively (Olympus BX60; original magnification, ×200; *scale bar* =200 μm). No resorption pits were identified in M-CSF-treated cultures in both groups (**a**, **b**). RANKL-induced osteoclastic resorption in a control subject (**c**) and a Charcot patient (**d**). The *arrows* denote some of the resorption pits (**c**, **d**). Immunofluorescent images of bovine bone discs (Olympus IX81; original magnification, ×200; *scale bar* =100 μm) stained with FitC-phalloidin and mounted with Vectashield with DAPI mounting medium for visualization of actin rings and nuclei in M-CSF-treated cultures and M-CSF + RANKL-treated cultures in a control subject (**e**, **g**) and a Charcot patient (**f**, **h**) respectively. No actin ring formation was observed in both groups in M-CSF-treated cultures (**e**, **f**). Multinucleated actin ring positive cells were noted in M-CSF + RANKL-treated cultures in both control subject and Charcot patient (**g**, **h**; *white arrows* denote some of the multinucleated actin ring positive cells). *Scatter plot* graph represents the total area of bone resorption on bovine bone discs (%) in control subjects and Charcot patients in M-CSF + RANKL-treated cultures (**j**). *Lines* represent medians; ** $p < 0.01$

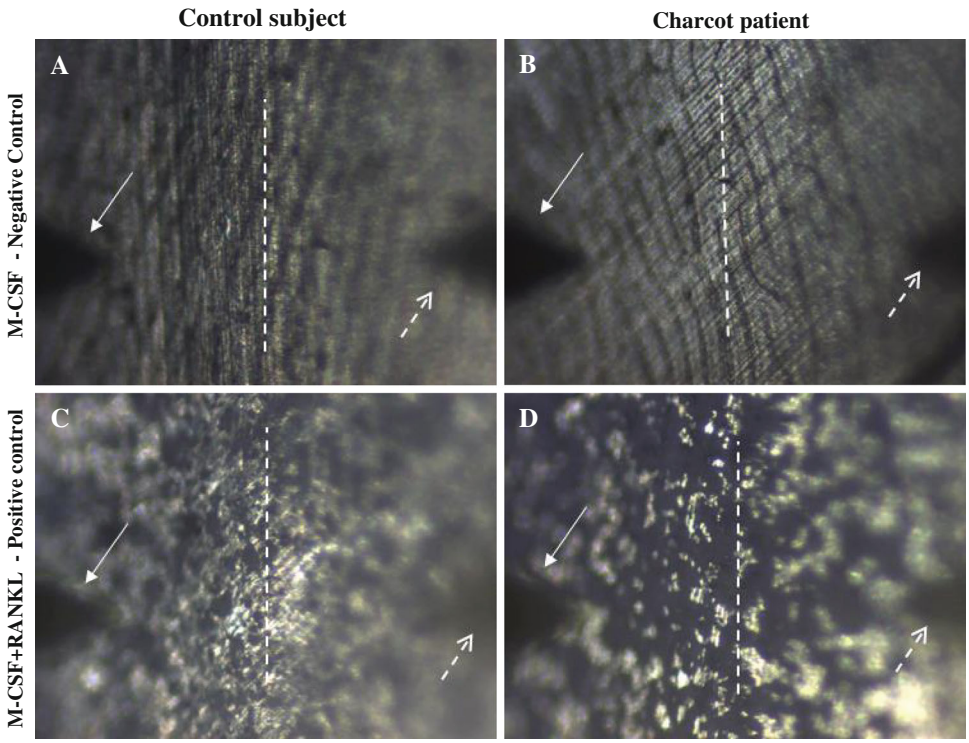

Fig. 2 Appearance of the bovine bone disc surface as viewed during machine operation. Images were taken with the integrated camera of the Profiler prior surface measurement. The stylus is lifted above the surface of the sample. *White arrow* stylus, *white dashed arrow* stylus shadow, *white dashed line* scan line). The edges of the images appear out of focus as a result of the acquisition setup of the camera supplied with a mirror positioned at a 45° angle in respect to the sample plane. Typical appearance of bovine bone discs observed with the integrated camera in M-CSF-treated cultures and in M-CSF + RANKL-treated cultures in a control subject (**a**, **c**) and in a Charcot patient (**b**, **d**), respectively. No erosions were noted in M-CSF-treated cultures in control subjects (**a**) and Charcot patients (**b**) in contrast to numerous erosions in M-CSF + RANKL-treated cultures, as seen in both control subjects (**c**) and Charcot patients (**d**). Erosions appeared as dark areas surrounded by grey areas of unresorbed bone (**c**, **d**)

appeared as discrete round pits, sometimes separated from each other and sometimes in clusters (Fig. 1c), whereas those in Charcot patients tended to be elongated, appearing as continuous grooves described as lacunae or trenches (Fig. 1d). Furthermore, the total area of the resorbed surface measured by light microscopy was significantly different between control subjects (21.1 % [14.5–26.2]) and Charcot patients (40.8 % [35.4–46.0]), resulting in a two-fold increase in Charcot patients compared with controls ($p < 0.01$) (Fig. 1j).

Surface Profilometry

Observation of the surface of each bone disc with the camera integrated with the profiler revealed no evidence of pits (erosions) in M-CSF-treated cultures in control subjects (Fig. 2a) and Charcot patients (Fig. 2b). However, in M-CSF + RANKL-treated cultures, there were numerous erosions in both control subjects (Fig. 2c) and Charcot patients (Fig. 2d). The eroded surface appeared as dark areas surrounded by grey areas of unresorbed bone. These observations with the profiler camera were in agreement with the data from light and immunofluorescent microscopy, which showed no resorption and no evidence of actin ring positive cells in M-CSF-treated cultures (negative control) (Fig. 1a, b, e, f, respectively) but numerous resorptive events and actin ring–positive cells in M-CSF + RANKL-treated cultures (positive control), as seen in both control subjects and Charcot patients (Fig. 1c, d, g, h, respectively).

The surface profile of bovine bone discs from M-CSF-treated cultures measured with the Dektak 150 Surface Profiler appeared as an almost straight line with a fluctuation of ±1 μm after levelling for the tilt of the mounted discs, and this was observed in both control subjects (Fig. 3a, solid line) and Charcot patients (Fig. 3c, solid line). In M-CSF + RANKL-treated cultures, the surface profile measurements of randomly selected areas revealed multishaped erosions of resorbed bovine bone discs in control subjects and Charcot patients. Examples of typical profiles are shown in Fig. 3a, c, respectively (dashed lines).

The shapes of pits were categorized into three main types according to the number of clearly defined dents below the unresorbed bone surface as unidented, bidented,

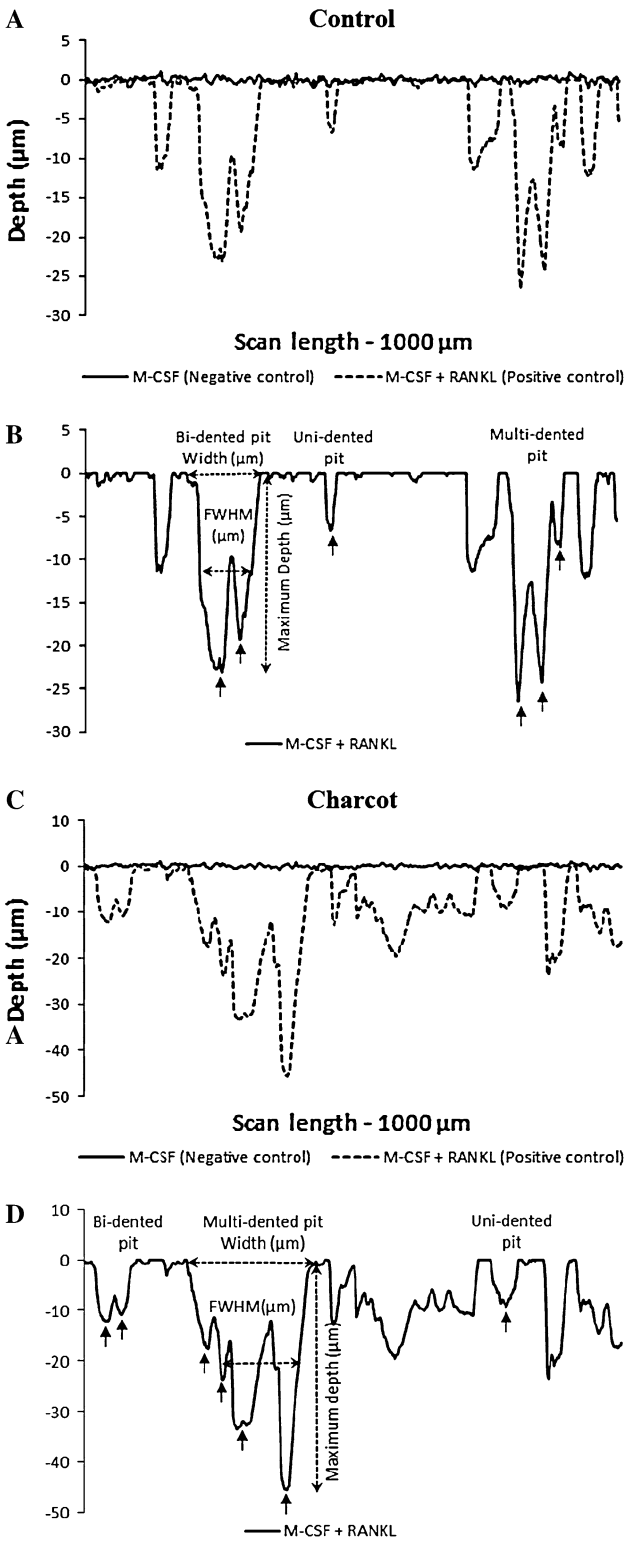

◀ **Fig. 3** Erosion profile of bovine bone discs in M-CSF-treated cultures (*solid line*) and M-CSF + RANKL-treated cultures (*dashed line*) in a control subject (**a**) and a Charcot patient (**c**) after profilometry. Erosion profile in M-CSF-treated cultures (*solid line*) appeared as almost a straight line, in contrast to the multishaped erosion profiles in M-CSF + RANKL-treated cultures (*dashed line*) in a control subject (**a**) and a Charcot patient (**c**). Examples of unidented, bidented, and multidented pits together with an illustration of the dents (*arrow*) and pit parameters (width at the surface; FWHM and maximum depth: *dashed arrow*) are shown for a control subject (**b**) and a Charcot patient (**d**)

and multidented. Examples of each type of pit, together with the dents and the measured parameters (width at the surface, FWHM depth, and maximum depth) in a control subject and a Charcot patient, are shown in Fig. 3b, d, respectively.

Comparison of controls and Charcot patients using surface profilometry showed a marked difference in the erosion profile in M-CSF + RANKL-treated cultures between the two groups. The erosions on bovine discs in Charcot patients appeared greater and deeper compared to erosions in control subjects (Fig. 4a). The total area of the resorbed bone under the surface was significantly different between control subjects (2.7 μm^2 [1.6–3.9]) and Charcot patients (8.3 μm^2 [5.6–10.6]), and there was a threefold increase in the area of resorption under the surface in M-CSF + RANKL-treated cultures between Charcot patients and controls ($p < 0.01$) (Fig. 4b).

Furthermore, there was a significant difference in the pit parameters in the two groups. The median pit width, median FWHM, and median depth were significantly greater in Charcot patients compared with controls for the unidented ($p < 0.05$, $p < 0.01$, $p < 0.01$) and multidented pits ($p < 0.01$, $p < 0.01$, $p < 0.05$), respectively (Table 1). The median pit width and median FWHM for the bidented pits were also significantly greater in Charcot patients compared with controls ($p < 0.05$, $p < 0.05$, respectively), although there was no difference in the median pit depth between the two groups ($p > 0.05$) (Table 1).

Discussion

We have shown for the first time the utility of the Dektak 150 Surface Profiler in measuring the surface profile of eroded bovine discs and pit characteristics. Using traditional light microscopy techniques, we have demonstrated that although osteoclast formation was similar between controls and Charcot patients, the percentage of the area resorbed at the surface by Charcot osteoclasts was significantly increased compared with controls. In addition, using surface profilometry, we have shown that there is a notable difference in the way osteoclasts generated from monocytes from controls and Charcot patients exert their resorbing activity. This technique revealed that pits on bovine discs were significantly wider and deeper in Charcot patients compared with controls and more frequently appeared as multidented pits. Thus, we have overcome the limitations of the resorption pit

assay by introducing a novel method of measurement of erosion profile and pit parameters. These new observations of highly aggressive (active) osteoclasts in acute Charcot osteoartropathy may explain the extremely destructive nature of the pathological bone resorption observed in this devastating condition.

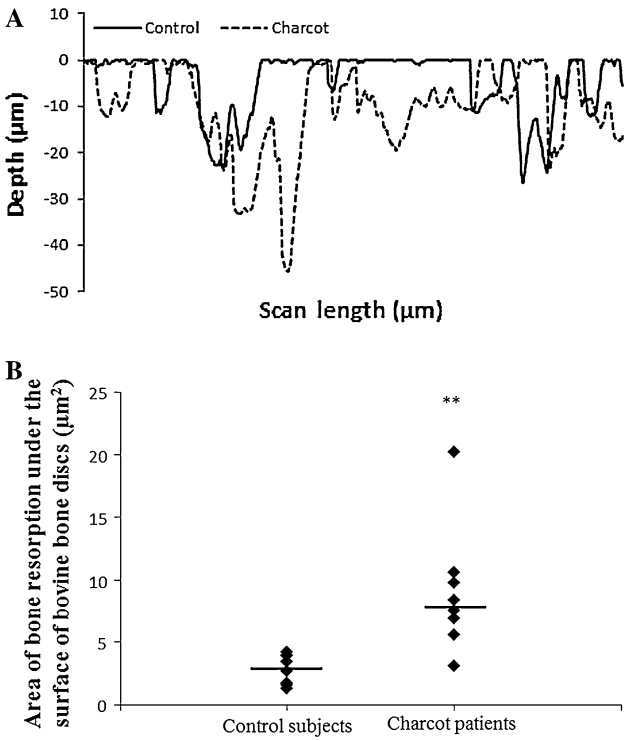

Fig. 4 Erosion profiles in a control subject (*solid line*) and a Charcot patient (*dashed line*) in M-CSF + RANKL-treated cultures after profilometry (**a**). Scatter plot graph represents the area of resorption under the surface on bovine bone discs (μm^2) in control subjects and Charcot patients in M-CSF + RANKL-treated cultures (**b**). *Lines* represent medians; $^{**}p < 0.01$

By using a well-established osteoclastic culture assay, we have demonstrated that there was a similar number of $TRAcP^+$ multinucleated cells between controls and Charcot patients in M-CSF-treated cultures and also after the addition of RANKL. Although TRAP staining did not differentiate between osteoclasts and TRAP-positive macrophage polykaryons, osteoclast differentiation was unlikely to be different between controls and Charcot patients on the basis of $TRAcP^+$ multinucleated cell data. Furthermore, these newly derived cells from monocytes were able to resorb bone only in M-CSF + RANKL-treated cultures, but not in cultures treated with M-CSF alone. This was demonstrated by both resorption assay and actin ring formation on bovine bone discs. However, these newly formed osteoclasts from Charcot patients had increased osteoclastic activity, as indicated by a twofold increase in the percentage area resorbed on bovine bone discs. Measurement of pit area by image analysis on the surface of bone discs is not always fully representative of osteoclastic resorbing activity [12, 13]. Pit depth can be different in the presence of the same pit area [14] and can be modulated by various factors. For example, eroded depth and volume were significantly increased in osteoclasts generated in M-CSF + RANKL-treated cultures compared to cultures treated with M-CSF plus lipopolysaccharides [13]. Estrogen treatment added to osteoclast cultures significantly decreased the depth of resorption pits with no effects on the total area resorbed [15]. Furthermore, glucocorticoids can act directly on osteoclasts and can alter the morphology of resorption lacunae, resulting in elongated continuous groves of resorption with a significant increase in depth [16].

Similarly, by using surface profilometry, we have shown a difference in the erosion profile of bovine bone discs as well as a difference in the morphological appearance of pits in Charcot patients compared with control subjects. In the

Table 1 Measurements of uni-, bi-, and multidented pits in M-CSF + RANKL-treated cultures in control subjects and Charcot patients

Pits	Parameter	Control subjects, median [25–75th percentile]	Charcot patients, median [25–75th percentile]	*p* value
Unidented	Width (μm)	39 [36–52]	59 [50–62]	<0.05
	FWHM (μm)	18 [17–21]	27 [24–30]	<0.01
	Depth (μm)	6 [4–7]	10 [9–12]	<0.01
Bidented	Width (μm)	74 [67–84]	89 [82–97]	<0.05
	FWHM (μm)	39 [32–41]	50 [39–54]	<0.05
	Depth (μm)	11 [8–15]	13 [10–19]	>0.05
Multidented	Width (μm)	118 [98–133]	182 [166–240]	<0.01
	FWHM (μm)	70 [56–81]	110 [99–145]	<0.01
	Depth (μm)	13 [11–18]	20 [18–28]	<0.05

Median number of pits analysed in control subjects: 43 unidented pits, 17 bidented pits, 13 multidented pits. Median number of pits analysed in Charcot patients: 17 unidented pits, 13 bidented pits, 18 multidented pits

M-CSF macrophage colony-stimulating factor, *RANKL* receptor activator of nuclear factor κβ ligand, *FWHM* full-width–half-maximum

latter, the unidented pits were most frequently found, whereas in Charcot patients the majority of pits were bi-dented and multidented. These observations may suggest that newly formed osteoclasts from controls and Charcot patients exert their resorbing activity in a different way. It is possible that under control conditions, resorption alternates with migration, which results in punching out bone at different points away from each other, whereas in Charcot-derived osteoclasts resorption tends to proceed without being interrupted by migration and osteoclasts carry out erosions of the bovine surface over an extended length. This may explain the severity of bone destruction seen in Charcot patients and the presence of multifragmented fractures and extensive osseous damage.

The mechanisms that determine resorption depth and erosion profile are currently unclear [17]. Increased survival and reduced osteoclast apoptosis could modify the eroded surface area and pit characteristics [15]. Although the mechanisms leading to these alterations in osteoclastic function remain unknown, we have shown that newly formed osteoclasts from Charcot patients have increased resorbing potential after RANKL stimulation and have confirmed the role of this cytokine in this condition. Osteoclastic bone resorption in acute Charcot osteoarthropathy takes place on the background of severe inflammation, and it is possible that this response to RANKL is modified by proinflammatory cytokines [18]. Indeed, in acute Charcot osteoarthropathy, there is an inflammatory modulation of the surface and cytokine phenotype of monocytes with increased expression of the proinflammatory cytokines tumour necrosis factor-α (TNF-α) and interleukin-1β (IL-1β), decreased secretion of the anti-inflammatory cytokines IL-4 and IL-10, and increased resistance to apoptosis [19]. Thus, it is possible that proinflammatory modulation of the surface and cytokine phenotype of monocytes in Charcot patients [19] can give rise to aberrant osteoclasts. Indeed, TNF-α and IL-1β are known to enhance osteoclastic activity [8]. In addition, inflammatory-activated endothelium recruits osteoclastic precursors to the site of bone resorption [20], and in the context of the Charcot foot, this relates to the site of foot trauma and subsequent bone destruction. Alternatively, there may be an increased expression of RANKL by activated T lymphocytes which are involved in the inflammatory response to trauma and bone destruction. Further studies are now required to determine how these pathways may affect osteoclastic activation.

A limitation to our study was that we assessed bone resorption in two planes, one at the surface and the other under the surface. There are a number of methods that could be used to measure the volume and the depth of eroded areas, including scanning electron microscopy, confocal laser microscopy, and contact profilometry [13]. However, these methods are time-consuming, and the 3D reconstruction images do not always provide a true representation of the resorption lacuna [13]. In contrast, surface profilometry is a quick and simple method which allows direct and unbiased measurement of the erosion profile of resorbed discs.

In conclusion, we have clearly demonstrated, using the Dektak 150 Surface Profiler, that bone destruction in Charcot osteoarthropathy is mediated by highly aggressive osteoclasts with increased resorbing activity in response to RANKL. We have shown that surface profile measurements of resorbed bone discs provide additional information compared to the classical resorption pit assay. Surface profilometry provides a new perspective for measuring osteoclastic activity and may be used to evaluate erosion patterns and parameters (depth, width, and FWHM) in a variety of conditions associated with increased osteoclastic activity.

Acknowledgments Supported in part by Diabetes Research and Wellness Foundation. NLP is a holder of a Diabetes Research and Wellness Foundation Clinical Fellowship.

References

1. Petrova NL, Edmonds ME (2008) Charcot neuro-osteoarthropathy—current standards. Diabetes Metab Res Rev 24(1):S58–S61
2. Jeffcoate WJ (2005) Theories concerning the pathogenesis of the acute Charcot foot suggest future therapy. Curr Diabetes Rep 5:430–435
3. Teitelbaum SL (2000) Bone resorption by osteoclasts. Science 289:1504–1508
4. Fujikawa Y, Quinn JM, Sabokbar A, McGee JO, Athanasou NA (1996) The human osteoclast precursor circulates in the monocyte fraction. Endocrinology 137:4058–4060
5. Yasuda H, Shima N, Nakagawa N, Yamaguchi K, Kinosaki M, Mochizuki S, Tomoyasu A, Yano K, Goto M, Murakami A, Tsuda E, Morinaga T, Higashio K, Udagawa N, Takahashi N, Suda T (1998) Osteoclast differentiation factor is a ligand for osteoprotegerin/osteoclastogenesis-inhibitory factor and is identical to TRANCE/RANKL. Proc Natl Acad Sci USA 95:3597–3602
6. Tanaka S, Takahashi N, Udagawa N, Tamura T, Akatsu T, Stanley ER, Kurokawa T, Suda T (1993) Macrophage colony-stimulating factor is indispensable for both proliferation and differentiation of osteoclast progenitors. J Clin Invest 91:257–263
7. Henriksen K, Bollerslev J, Everts V, Karsdal MA (2011) Osteoclast activity and subtypes as a function of physiology and pathology—implications for future treatments of osteoporosis. Endocr Rev 32:31–63
8. Teitelbaum SL (2007) Osteoclasts: what do they do and how do they do it? Am J Pathol 170:427–435
9. Husheem M, Nyman JK, Vääräniemi J, Vaananen HK, Hentunen TA (2005) Characterization of circulating human osteoclast progenitors: development of in vitro resorption assay. Calcif Tissue Int 76:222–230
10. Mabilleau G, Petrova NL, Edmonds ME, Sabokbar A (2008) Increased osteoclastic activity in acute Charcot's osteoarthropathy: the role of receptor activator of nuclear factor–kappaB ligand. Diabetologia 51:1035–1040

11. Fuller K, Murphy C, Kirstein B, Fox SW, Chambers TJ (2002) TNFα potently activates osteoclasts, through a direct action independent of and strongly synergistic with RANKL. Endocrinology 143:1108–1118
12. Soysa NS, Alles N, Aoki K, Ohya K (2009) Three-dimensional characterization of osteoclast bone-resorbing activity in the resorption lacunae. J Med Dent Sci 56:107–112
13. Pascaretti-Grizon F, Mabilleau G, Basle MF, Chappard D (2011) Measurement by vertical scanning profilometry of resorption volume and lacunae depth caused by osteoclasts on dentine slices. J Microsc 241:147–152
14. Asagiri M, Hirai T, Kunigami T, Kamano S, Gober HJ, Okamoto K, Nishikawa K, Latz E, Golenbock DT, Aoki K, Ohya K, Imai Y, Morishita Y, Miyazono K, Kato S, Saftig P, Takayanagi H (2008) Cathepsin K-dependent toll-like receptor 9 signaling revealed in experimental arthritis. Science 319:624–627
15. Parikka V, Lehenkari P, Sassi ML, Halleen J, Risteli J, Härkönen P, Väänänen HK (2001) Estrogen reduces the depth of resorption pits by disturbing the organic bone matrix degradation activity of mature osteoclasts. Endocrinology 142:5371–5378
16. Soe K, Delaisse JM (2010) Glucocorticoids maintain human osteoclasts in the active mode of their resorption cycle. J Bone Miner Res 25:2184–2192
17. Goff MG, Slyfield CR, Kummari SR, Tkachenko EV, Fischer SE, Yi YH, Jekir MG, Keaveny TM, Hernandez CJ (2012) Three-dimensional characterization of resorption cavity size and location in human vertebral trabecular bone. Bone 51:28–37
18. Jeffcoate WJ, Game F, Cavanagh PR (2005) The role of proinflammatory cytokines in the cause of neuropathic osteoarthropathy (acute Charcot foot) in diabetes. Lancet 366:2058–2061
19. Uccioli L, Sinistro A, Almerighi C, Ciaprini C, Cavazza A, Giurato L, Ruotolo V, Spasaro F, Vainieri E, Rocchi G, Bergamini A (2010) Proinflammatory modulation of the surface and cytokine phenotype of monocytes in patients with acute Charcot foot. Diabetes Care 33:350–355
20. McGowan NW, Walker EJ, Macpherson H, Ralston SH, Helfrich MH (2001) Cytokine-activated endothelium recruits osteoclast precursors. Endocrinology 142:1678–1681

Calcif Tissue Int (2014) 94:412–413
DOI 10.1007/s00223-014-9841-z

ERRATUM

Erratum to: Novel Use of a Dektak 150 Surface Profiler Unmasks Differences in Resorption Pit Profiles Between Control and Charcot Patient Osteoclasts

Nina L. Petrova · Peter K. Petrov · Michael E. Edmonds · Catherine M. Shanahan

Published online: 18 February 2014

Erratum to: Calcif Tissue Int
DOI 10.1007/s00223-013-9820-9

Unfortunately, all reported values representing the area of resorption under the surface were missing the 10^3 multiplication factor in abstract, surface profilometry section and Fig. 4 in the original publication. The correct presentation is shown in this erratum.

The eighth sentence of the abstract should read "The area of resorption on the surface by image analysis was significantly greater in Charcot patients compared with controls (21.1 % [14.5–26.2] versus 40.8 % [35.4–46.0], median [25–75th percentile], $p < 0.01$), as was the area of resorption under the surface (2.7×10^3 μm^2 [1.6×10^3–3.9×10^3] versus 8.3×10^3 μm^2 [5.6×10^3–10.6×10^3], $p < 0.01$) after profilometry".

The last sentence of the fourth paragraph in the Results (section surface profilometry) should read "The total area of the resorbed bone under the surface was significantly different between control subjects (2.7 x10^3 μm^2 [1.6×10^3–3.9×10^3]) and Charcot patients (8.3×10^3 μm^2 [5.6×10^3–10.6×10^3]), and there was a threefold increase in the area of resorption under the surface in M-CSF + RANKL-treated cultures between Charcot patients and controls ($p < 0.01$) (Fig. 4b)".

The correct version of Fig. 4 is presented below.

The online version of the original article can be found under doi:10.1007/s00223-013-9820-9.

N. L. Petrova (✉) · M. E. Edmonds
Diabetic Foot Clinic, King's College Hospital, Denmark Hill, London SE5 9RS, UK
e-mail: petrovanl@yahoo.com

M. E. Edmonds
e-mail: michael.edmonds@nhs.net

P. K. Petrov
Department of Materials, Imperial College, Prince Consort Road, London SW7 2AZ, UK
e-mail: p.petrov@imperial.ac.uk

C. M. Shanahan
Cardiovascular Division, James Black Centre, King's College London, 125 Coldharbour Lane, London SE5 9NU, UK
e-mail: cathy.shanahan@kcl.ac.uk

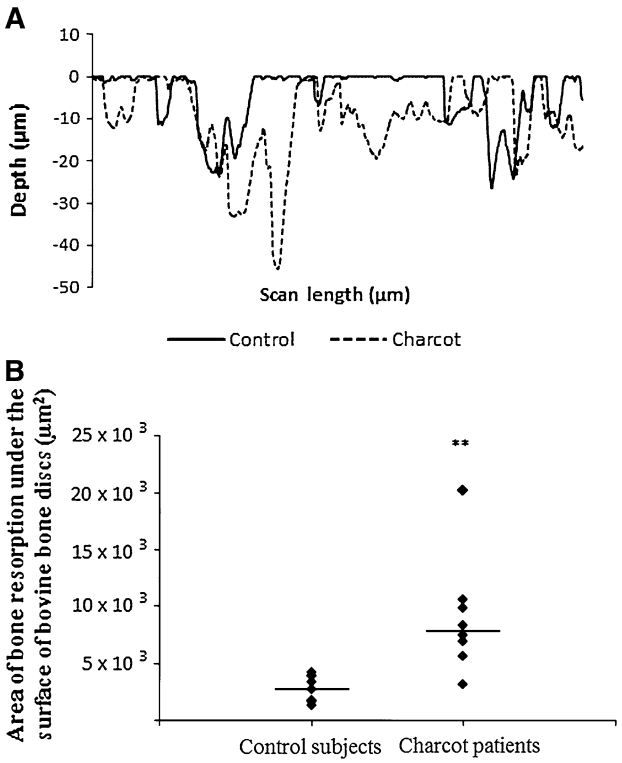

Fig. 4 Erosion profiles in a control subject (*solid line*) and a Charcot patient (*dashed line*) in M-CSF + RANKL-treated cultures after profilometry (**a**). Scatter plot graph represents the area of resorption under the surface on bovine bone discs (μm^2) in control subjects and Charcot patients in M-CSF + RANKL-treated cultures (**b**). *Lines* represent medians; $^{**}p < 0.01$

DIABETICMedicine

DOI: 10.1111/dme.12590

Research: Complications

Inflammatory and bone turnover markers in a cross-sectional and prospective study of acute Charcot osteoarthropathy

N. L. Petrova[1], T. K. Dew[2], R. L. Musto[2], R. A. Sherwood[2], M. Bates[1], C. F. Moniz[2] and M. E. Edmonds[1]

[1]Diabetic Foot Clinic and [2]Department of Clinical Biochemistry, King's College Hospital NHS Foundation Trust, London, UK

Accepted 8 September 2014

Abstract

Aims To assess markers of inflammation and bone turnover at presentation and at resolution of Charcot osteoarthropathy.

Methods We measured serum inflammatory and bone turnover markers in a cross-sectional study of 35 people with Charcot osteoarthropathy, together with 34 people with diabetes and 12 people without diabetes. In addition, a prospective study of the subjects with Charcot osteoarthropathy was conducted until clinical resolution.

Results At presentation, C-reactive protein ($P = 0.007$), tumour necrosis factor-α ($P = 0.010$) and interleukin-6 ($P = 0.002$), but not interleukin-1β, ($P = 0.254$) were significantly higher in people with Charcot osteoarthropathy than in people with and without diabetes. Serum C-terminal telopeptide ($P = 0.004$), bone alkaline phosphatase ($P = 0.006$) and osteoprotegerin ($P < 0.001$), but not tartrate-resistant acid phosphatase ($P = 0.126$) and soluble receptor activator of nuclear factor-κβ ligand ($P = 0.915$), were significantly higher in people with Charcot osteoarthropathy than in people with and without diabetes. At follow-up it was found that tumour necrosis factor-α ($P = 0.012$) and interleukin-6 ($P = 0.003$), but not C-reactive protein ($P = 0.101$), interleukin-1β ($P = 0.457$), C-terminal telopeptide ($P = 0.743$), bone alkaline phosphatase ($P = 0.193$), tartrate-resistant acid phosphatase ($P = 0.856$), osteoprotegerin ($P = 0.372$) or soluble receptor activator of nuclear factor-kβ ligand ($P = 0.889$), had significantly decreased between presentation and the 3 months of casting therapy time point, and all analytes remained unchanged from 3 months of casting therapy until resolution. In people with Charcot osteoarthropathy, there was a positive correlation between interleukin-6 and C-terminal telopeptide ($P = 0.028$) and tumour necrosis factor-α and C-terminal telopeptide ($P = 0.013$) only at presentation.

Conclusions At the onset of acute Charcot foot, serum concentrations of tumour necrosis factor-α and interleukin-6 were elevated; however, there was a significant reduction in these markers at resolution and these markers may be useful in the assessment of disease activity.

Diabet. Med. 00, 000–000(2014)

Introduction

The excessive inflammatory response to trauma and the well described rapid bone resorption are established features of acute Charcot osteoarthropathy [1]. Recent studies have reported either inflammatory markers or markers of bone turnover in small cohorts of people with Charcot osteoarthropathy, but have not measured these at the same time and therefore have not explored any possible association between inflammation and bone resorption [2–5]. In a clinical study, we reported an association between inflammation and bone mineral density as indicated by a significant reduction in bone mineral density of the Charcot foot after 3 months of casting therapy with no further reduction of bone mineral density at the time of resolution [6].

The aim of the present study was to measure serum markers of inflammation and bone turnover, firstly, in a cross-sectional study of people with acute Charcot osteoarthropathy together with people with diabetes and people without diabetes and, secondly, in a prospective study of those people with Charcot osteoarthropathy, with

Correspondence to: Nina L. Petrova. E-mail: petrovanl@yahoo.com

What's new?

- At the onset of Charcot osteoarthropathy, serum concentrations of tumour necrosis factor-α and interleukin-6 are significantly higher in people with Charcot osteoarthropathy than in people with and without diabetes.
- At presentation, in people with Charcot osteoarthropathy, tumour necrosis factor-α and interleukin-6 are positively correlated to C-terminal telopeptide, a marker of bone turnover.
- On follow-up, serum tumour necrosis factor-α and interleukin-6 decreased significantly between time of presentation and 3 months of casting therapy and remained unchanged from the 3 months of casting time point until resolution.
- Serum tumour necrosis factor-α and interleukin-6 could serve as markers of disease activity.

assessment after 3 months of casting therapy and then at clinical resolution.

Subjects and methods

We studied 35 consecutive people with diabetes and acute Charcot osteoarthropathy (group 1), matched for age and gender with 34 people with diabetes and no previous history of Charcot osteoarthropathy (group 2) and 12 people with no previous history of diabetes (group 3). Subjects from group 1 presented to the diabetic foot clinic at King's College Hospital over a 3-year period with a red, swollen, intact foot and a skin temperature > 2°C compared with the same site on the contralateral foot. Foot skin temperatures were measured using a DermaTemp 1001 thermometer (Exergen, Watertown, MA, USA). The diagnosis of acute Charcot osteoarthropathy was made in keeping with the diagnostic criteria defined in the recent task force document [7] and was confirmed in 24 cases by evidence of subluxation, dislocation or fragmentation of bone on standard foot radiographs and, in 11 cases, by the presence of an increased focal uptake on the blood flow, blood pool and bony uptake phases of the triphasic technetium-diphosphonate bone scan (Tyco Healthcare, Gosport, UK), indicative of early bone damage.

People with diabetes (group 2) were recruited consecutively from King's Diabetes Centre when attending routinely for their annual diabetes review. People without diabetes (group 3) included members of staff and relatives who agreed to take part in the study.

There was no evidence of any skin breakdown, foot ulceration or infection in any of the groups. None of the subjects was on any treatment for osteoporosis, including hormone replacement therapy or bisphosphonates. None of the people with diabetes was treated with thiazolidinediones. All participants gave informed written consent. The study was approved by King's College Hospital NHS Trust Research Ethics Committee and carried out in accordance with the Declaration of Helsinki.

People from group 1 were monitored in the diabetic foot clinic and treated by off-loading and cast immobilization. Foot skin temperatures were measured monthly. When the temperature difference between the feet was < 2°C at two consecutive visits, the Charcot foot was deemed to have resolved and the people with Charcot osteoarthropathy were then changed from casts to orthotic footwear [8]. The duration of casting treatment was recorded in weeks.

Blood samples were obtained by venepuncture from the forearm veins. Serum was immediately separated by centrifugation and stored at −80°C. A single blood sample was obtained from groups 2 and 3. Markers of inflammation and bone turnover were compared between the three groups as part of a cross-sectional study.

To assess changes in these measurements in the natural history of the osteoarthropathy, further blood samples were obtained from subjects from group 1 after 3 months of casting and at the time of resolution. Two people were withdrawn from the study at 3 months because of the development of foot ulceration. Eight further people did not complete the study because of foot ulceration (n = 4), reconstructive surgery (n = 1), non-compliance with casting therapy (n = 1), needle phobia (n = 1) and a new tibial fracture (n = 1; Fig. 1).

The following markers of inflammation were measured in the sera: C-reactive protein (CRP), measured by Cormay high-sensitivity (hs) CRP assay (Cormay, Warsaw, Poland; inter- and intra-assay coefficients of variation 4.1 and 3.4%,

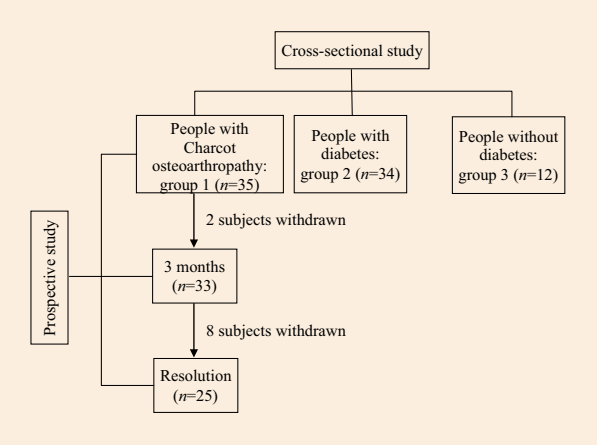

FIGURE 1 Flow chart showing the two study arms: a cross-sectional study in people with Charcot osteoarthropathy, people with diabetes and people without diabetes and a prospective study in which the people with Charcot osteoarthropathy were followed up from presentation until clinical resolution.

respectively), human hs tumour necrosis factor-α (TNF-α), measured by Quantikine enzyme-linked immunosorbent assay (ELISA) hs-TNF-α assay (R&D Systems, Abingdon, UK; inter- and intra- coefficients of variation 8.4 and 5.3%, respectively), human interleukin-6, measured by Quantikine ELISA hs interleukin-6 assay (R&D Systems; inter-assay and intra-assay coefficients of variation 7.8 and 7.4%, respectively), and human hs interleukin-1β, measured by Quantikine ELISA hs interleukin-1β assay (R&D Systems; inter- and intra-assay coefficients of variation 8.9 and 6.7%, respectively).

Markers of bone turnover were serum C-terminal telopeptide, a breakdown product of type 1 collagen, measured by serum CrossLaps ELISA kits (Nordic Bioscience Diagnostics, Herlev, Denmark; inter- and intra-assay coefficients of variation 7.7 and 2.2%, respectively), serum tartrate-resistant acid phosphatase, measured by bone tartrate-resistant acid phosphatase assay (Immunodiagnostic Systems, Bolden, UK; inter- and intra-assay coefficients of variation 10.0 and 4.1%, respectively), serum bone-specific alkaline phosphatase, measured by Ostase bone alkaline phosphatase immunoenzymetric assay (Immunodiagnostic Systems; inter- and intra-assay coefficients of variation 5.5 and 4.1%, respectively). Serum osteoprotegerin and soluble receptor activator of nuclear factor κβ ligand (RANKL) cytokines, which modulate bone turnover and osteoclastic activity, were measured by Osteoprotegerin ELISA assay (Biomedica, Vienna, Austria; inter- and intra-assay coefficients of variation 7.5 and 6%, respectively) and soluble RANKL was measured by human ELISA ampli-sRANKL assay (Biomedica, Vienna, Austria; inter- and intra-assay coefficients of variation 4.5 and 8.5%, respectively).

Small fibre function was assessed by measurement of temperature perception threshold to hot and cold using the method of limits (Thermotest; Somedic, Stockholm, Sweden), in groups 1 and 2 as previously described [9,10]. The average detected change of five stimuli towards higher (temperature perception to hot) and lower temperatures (temperature perception to cold) was recorded in degrees centigrade (°C). Temperature perception threshold to hot and temperature perception threshold to cold > 15°C was recorded as 15°C for the purpose of the analysis.

Large fibre function was assessed by measurement of vibration perception threshold in volts (range 0–50 V) at the apex of the hallux in groups 1 and 2 (Neurothesiometer; Horwell Scientific Laboratory Supplies, Nottingham, UK) and was determined as an average of three readings [11]. Vibration perception threshold > 50 V was taken as 50 V for the purpose of the analysis.

Statistical analyses

Baseline characteristics were recorded for all groups. Data were analysed with Predictive Analytics Software 18 statistical package. Comparisons between people with Charcot osteoarthropathy, people with diabetes and people without diabetes at baseline were carried out using non-parametric Kruskal–Wallis analysis for the three-group comparisons and a Mann–Whitney *U*-test for the two-group comparisons. A chi-squared test was used for categorical variables. In group 1, a paired *t*-test was used to assess the longitudinal changes of markers of inflammation and bone turnover between presentation and the 3-month follow-up, and also the change between the 3-month follow-up and clinical resolution. The association between markers of inflammation and bone turnover was determined by Spearman's correlation coefficient (r_s) at baseline and at follow-up. Results are presented as median (25^{th}–75^{th} percentile). A P value < 0.05 was considered to indicate statistical significance.

Results

Demographic and clinical details are shown in Table 1. Age and gender distribution were similar between the three groups. Duration and type of diabetes, as well as diabetes control as indicated by glycated haemoglobin (HbA_{1c}) were also similar between groups 1 and 2. People with Charcot osteoarthropathy had impaired small and large nerve fibre function as shown by a significantly higher vibration perception threshold, temperature perception threshold to cold and temperature perception threshold to hot than those of people with diabetes (Table 1).

Baseline data

With regard to markers of inflammation, there was a significant difference in serum CRP ($P = 0.007$), TNF-α ($P = 0.010$), interleukin-6 ($P = 0.002$) but not interleukin-1β (0.254) between the three groups, (Table 2). Furthermore, serum concentrations of CRP, TNF-α, interleukin-6 were significantly higher in people with Charcot osteoarthropathy than in people with diabetes ($P = 0.045$, $P = 0.009$ and $P = 0.013$, respectively) and were also significantly higher in people with Charcot osteoarthropathy than in people without diabetes ($P = 0.005$, $P = 0.021$ and $P = 0.003$, respectively).

With regard to markers of bone turnover, there was a significant difference in serum C-terminal telopeptide ($P = 0.004$), bone alkaline phosphatase ($P = 0.006$) and osteoprotegerin ($P < 0.001$), but not tartrate-resistant acid phosphatase ($P = 0.126$) and soluble RANKL ($P = 0.915$) between the three groups (Table 2). Serum C-terminal telopeptide and osteoprotegerin, but not serum bone alkaline phosphatase, were significantly higher in people with Charcot osteoarthropathy than in people with diabetes ($P = 0.001$, $P = 0.019$ and $P = 0.158$, respectively). Serum bone alkaline phosphatase and osteoprotegerin, but not serum C-terminal telopeptide were significantly higher in

Table 1 Demographic and clinical characteristics of the study subjects

	People with Charcot osteoarthropathy (group 1)	People with diabetes (group 2)	People without diabetes (group 3)	*P*
Number of subjects, *n*	35	34	12	
Gender (M: F), *n*	23:12	21:13	8:4	0.926
Age, years	53 (44–75)	56.5 (47–62)	44 (37.3–51)	0.066
Duration of diabetes, years	26 (12–31.3)	19 (7.8–28.3)	n/a	0.259*
Type 1: Type 2 diabetes, *n*	17:18	17:17	n/a	0.503
HbA_{1c} mmol/mol	63 (53–86)	72 (60–84)	n/a	0.513*
%	7.9 (7.0–10.0)	8.7 (7.6–9.8)		
Vibration perception threshold, V	48.3 (20.8–50.0)	19.3 (9.3–25.8)	Not measured	< 0.001*
Temperature perception threshold to cold, °C	15.0 (8.4–15)	7.0 (4.3–10.4)	Not measured	< 0.001*
Temperature perception threshold to hot, °C	15.0 (9.0–15.0)	4.1 (2.7–6.5)	Not measured	< 0.001*

Data are median (25^{th}–75^{th} percentile) values, unless otherwise indicated.
**P* values indicate the comparison between people with Charcot osteoarthropathy and people with diabetes (group 1 vs group 2).

Table 2 Markers of inflammation and bone turnover of the study subjects at baseline

	People with Charcot osteoarthropathy (group 1)	People with diabetes (group 2)	People without diabetes (group 3)	*P*
CRP, mg/l	5.4 (1.8–19.9)	3.7 (1.1–5.7)	0.8 (0.4–2.1)	0.007
TNF-α, ng/l	1.3 (1.0–1.85)	1.0 (0.8–1.3)	0.8 (0.5–1.4)	0.010
Interleukin-6, ng/l	3.3 (1.7–9.3)	2.0 (1.3–2.9)	1.4 (0.5–2.3)	0.002
Interleukin-1β, ng/l	0.27 (0.19–0.62)	0.20 (0.10–0.67)	0.18 (0.08–0.89)	0.254
C-terminal telopeptide, µg/l	0.24 (0.13–0.61)	0.12 (0.08–0.28)	0.15 (0.12–0.22)	0.004
Bone alkaline phosphatase, µg/l	16.4 (11.7–26.2)	13.6 (11.1–17.5)	10.1 (8.0–11.9)	0.006
Tartrate-resistant acid phosphatase, U/l	3.9 (2.9–5.3)	3.9 (3.3–4.7)	2.7 (2.0–4.3)	0.126
Osteoprotegerin, pmol/l	5.4 (4.2–6.8)	4.4 (3.1–5.6)	2.9 (2.7–3.7)	< 0.001
Soluble RANKL†, pmol/l	0.29 (0.22–0.58)	0.41 (0.20–0.56)	0.13 (0.06–0.22)	0.915

TNF-α, tumour necrosis factor-α; RANKL, receptor activator of nuclear factor-κβ ligand; CRP, C-reactive protein.
Kruskal–Wallis non-parametrical test *P* values indicate differences between the three groups.
Data are median (25th–75th percentile) values.
Serum soluble RANKL† was detected in only 22 people with Charcot osteoarthropathy, 18 people with diabetes and 12 people without diabetes.

people with Charcot osteoarthropathy than in people without diabetes ($P = 0.006$, $P < 0.001$ and $P = 0.128$, respectively).

Prospective study

The people with Charcot osteoarthropathy were followed up from presentation until clinical resolution. The median (25th–75th percentile) duration of follow-up was 29 (23–36.5) weeks. The serum concentrations of the inflammatory and bone turnover markers were compared between time of presentation and the 3 months of casting therapy time point and also between the 3 months of casting therapy time point and time of clinical resolution.

There was a significant fall in serum TNF-α ($P = 0.012$) and interleukin-6 ($P = 0.003$) but not serum CRP ($P = 0.101$), interleukin-1β ($P = 0.457$), C-terminal telopeptide ($P = 0.743$), bone alkaline phosphatase ($P = 0.193$), tartrate-resistant acid phosphatase ($P = 0.856$), osteoprotegerin ($P = 0.372$) and soluble RANKL ($P = 0.889$) from time of presentation to the 3 months of casting therapy time point (Table 3). Despite the ongoing casting treatment, there was no further reduction in the serum concentrations of TNF-α ($P = 0.388$) and interleukin-6 ($P = 0.472$) from the 3 months of casting therapy time point to the time of clinical resolution (Table 3). Similarly, serum C-reactive protein ($P = 0.489$), interleukin-1β ($P = 0.996$), C-terminal telopeptide ($P = 0.351$), bone alkaline phosphatase ($P = 0.847$), tartrate-resistant acid phosphatase ($P = 0.365$), osteoprotegerin ($P = 0.767$) and soluble RANKL ($P = 0.211$) remained unchanged from 3 months of casting therapy to clinical resolution (Table 3).

Table 3 Markers of inflammation and bone turnover of people with Charcot osteoarthropathy at presentation and during follow-up (after 3 months of casting therapy and at the time of resolution)

People with Charcot osteoarthropathy (group 1)	Presentation (n = 35)	3 months (n = 33)	Resolution (n = 25)	P*	P†
CRP, mg/l	5.4 (1.8–19.9)	2.5 (0.9–11.1)	2.5 (0.6–4.9)	0.101	0.489
TNF-α, ng/l	1.3 (1.0–1.85)	1.1 (0.8–1.8)	1.1 (0.6–2.0)	0.012	0.388
Interleukin-6, ng/l	3.3 (1.7–9.3)	2.5 (1.5–4.1)	2.2 (1.4–3.2)	0.003	0.472
Interleukin-β, ng/l	0.27 (0.19-0.62)	0.35 (0.16-0.63)	0.34 (0.18-0.56)	0.457	0.996
C-terminal telopeptide, μg/l	0.24 (0.13–0.61)	0.35 (0.16–0.63)	0.19 (0.12–0.69)	0.743	0.351
Bone alkaline phosphatase, μg/l	16.4 (11.7–26.2)	16.4 (11.7–20.6)	16.4 (12.4–21.5)	0.193	0.847
Tartrate-resistant acid phosphatase, U/l	3.9 (2.9–5.3)	4.0 (3.1–5.4)	3.6 (2.9–5.0)	0.856	0.365
Osteoprotegerin, pmol/l	5.4 (4.2–6.8)	5.2 (3.9–6.6)	5.0 (3.7–6.0)	0.372	0.767
Soluble RANKL, pmol/l	0.29 (0.22–0.58)	0.39 (0.26–0.55)	0.37 (0.18–0.50)	0.889	0.211

TNF-α, tumour necrosis factor-α; RANKL, receptor activator of nuclear factor-κβ ligand; CRP, C-reactive protein.
*Pair-wise comparison between presentation and after 3 months of casting therapy.
†Pair-wise comparison between 3 months of casting timepoint and resolution.

Correlation between inflammatory and bone turnover markers in people with Charcot osteoarthropathy

At presentation, there was a significant positive correlation between serum TNF-α and C-terminal telopeptide concentrations (r_s =0.457, P = 0.013) and between serum interleukin-6 and C-terminal telopeptide concentrations (r_s =0.401, P = 0.028). These correlations were only noted at presentation and were not present after 3 months of casting therapy or at clinical resolution. There was also a significant positive correlation between TNF-α concentrations and osteoprotegerin at presentation (r_s =0.376, P = 0.031) but not after 3 months of casting or at resolution.

Discussion

We believe this is the first study to evaluate the role of inflammatory markers and their correlation with bone turnover markers in Charcot osteoarthropathy. It has shown that presentation of the acute Charcot foot was characterized by increased concentrations of the proinflammatory cytokines TNF-α and interleukin-6, thus supporting the pro-inflammatory cytokine hypothesis of the pathogenesis of the osteoarthropathy [1]. There was a positive correlation between the proinflammatory cytokines and serum bone markers C-terminal telopeptide and osteoprotegerin. The prospective arm of the study showed that TNF-α and interleukin-6 significantly declined from the time of presentation to the 3 months of casting therapy time point and then showed no further change until the time of clinical resolution.

In our previous study of systemic serological markers of inflammation, we have shown that in the acute stage of Charcot osteoarthropathy, C-reactive protein was normal or slightly increased, white blood cell count was normal and there was a mild increase in the erythrocyte sedimentation rate [4]; however, in almost 50% of our patients, C-reactive protein was below the limit of detection of the assay (< 5 mg/l), [4]. In the present study, we measured CRP with a high-sensitivity assay to detect concentrations of this marker in all samples. Serum concentrations of CRP were elevated at presentation in people with Charcot osteoarthropathy compared with control subjects. Although CRP showed a trend to decline at resolution, this decline was not significant. This is in contrast to the situation with osteomyelitis, when CRP, together with white blood cell count and erythrocyte sedimentation rate have been shown to be reliable markers for both diagnosis and prognosis [12].

At presentation, serum concentrations of TNF-α and interleukin-6 were significantly higher in people with acute Charcot osteoarthropathy than in aged-matched people with diabetes and people without diabetes. On follow-up, there was a significant reduction in the concentration of these cytokines after 3 months of casting therapy but no further change was noted at clinical resolution. These proinflammatory cytokines may therefore be useful in assessing the activity of acute Charcot feet and, indeed, TNF-α and interleukin-6 have been shown to be helpful in assessing fracture healing in fragility fractures and high-energy fractures in people without diabetes [13].

With regard to bone turnover markers, two previous studies have shown increased concentration of the bone resorption marker carboxyterminal telopeptide of type 1 collagen, but this elevation was not coupled with a rise of the bone formation markers procollagen carboxyterminal and bone alkaline phosphatase isoenzyme [2,3]. In the present study, we have shown that serum C-terminal telopeptide, but not bone alkaline phosphatase, was significantly higher in people with Charcot osteoarthropathy at presentation than in people with diabetes. The observed lack of increased levels of bone alkaline phosphatase in response to the raised C-terminal telopeptide suggests that, in people with Charcot osteoarthropathy, there may be adynamic bone, related to the presence of diabetic neuropathy, which could impair the regulation of bone remodelling [14,15]. Alternatively, it is

possible that these systemic bone turnover markers fail to represent the extent of the localized bone destruction that takes place in the affected Charcot foot. A similar situation may occur in osteomyelitis in which bone turnover markers do not differentiate between those with osteomyelitis and control subjects [16]. Our longitudinal study indicated that the moderate elevation of serum C-terminal telopeptide at presentation in people with Charcot osteoarthropathy was followed by a further rise after 3 months of casting therapy and then decreased to its initial concentration at the time of resolution. These observations are consistent with a large population-based study of people with fractures that showed a significant rise in C-terminal telopeptide concentration at 4 months after fracture, followed by a decrease to its pre-injury concentration 5–6 months after the fracture [17]. Although the present study, together with previous studies, has shown higher levels of markers of bone turnover in acute Charcot osteoarthropathy, the lack of longitudinal changes at the time of resolution indicates that bone turnover markers may not be useful in monitoring the activity of the Charcot foot. Furthermore, the lack of reduction may be attributable to the continued presence of the inflammatory condition or to the ongoing fractures.

Serum osteoprotegerin, but not soluble RANKL, was also elevated in people with Charcot osteoarthropathy. It is possible that the increased serum osteoprotegerin reflects enhanced RANKL activation and osteoclastic activity. Early studies that have measured the serum concentration of RANKL have shown that in the majority of cases, the levels were below the sensitivity of the assay used [18]. Although in the present study we could only detect soluble RANKL in 50% of our cohort, we have clearly shown, through *in vitro* studies, that RANKL is essential for osteoclastic activation in acute Charcot osteoarthropathy [19]. Furthermore, more recent studies have reported elevated RANKL concentrations and an elevated RANKL–osteoprotegerin ratio in people with Charcot osteoarthropathy [20]. Alternatively, the elevated serum osteoprotegerin level may be associated with the presence of neuropathy in people with Charcot osteoarthropathy, who had significantly impaired small and large nerve fibre function compared with patients with diabetes [21]. Larger studies are needed to establish the role of RANKL and osteoprotegerin in the natural history of Charcot osteoarthropathy [22].

The present study has shown a significant positive correlation between the pro-inflammatory cytokines TNF-α and interleukin-6 and the bone turnover marker C-terminal telopeptide; however, such an association does not prove causation. It is difficult to be sure whether the observed increase in the inflammatory and bone turnover markers may be related to the presence of the acute active osteoarthropathy itself or to the presence of fractures *per se*. Nevertheless, recent *in vitro* studies on newly formed osteoclasts in people with Charcot osteoarthropathy have suggested that TNF-α, interleukin-6 and RANKL can be modulators of increased osteoclastic activity [23]. Also osteoclastic bone resorption has been shown to take place in the presence of TNF-α and interleukin-6 [24] accompanied by lymphocyte and eosinophil infiltration [25] in bone specimens from people with Charcot osteoarthropathy.

A limitation of the present study is that blood samples were obtained from the forearm veins rather than from the affected foot. It is possible that there is a difference in the concentrations of the pro-inflammatory cytokines, bone turnover markers, RANKL and osteoprotegerin between the local and systemic circulations [26]. A further limitation is the impact of neuropathy on people with Charcot osteoarthropathy who had a significantly greater small and large nerve fibre deficit compared with people with diabetes.

In conclusion, at the onset of the acute Charcot foot, serum concentrations of TNF-α and interleukin-6 were increased; however, there was a significant reduction in these markers at resolution and these markers may be useful in the assessment of disease activity.

Funding sources

This study was supported by a Diabetes UK project grant: RD 05/0003025. N.L.P. was funded by Diabetes UK.

Competing interests

None declared.

References

1 Jeffcoate WJ, Game F, Cavanagh PR. The role of proinflammatory cytokines in the cause of neuropathic osteoarthropathy (acute Charcot foot) in diabetes. *Lancet* 2005; **366**: 2058–2061.
2 Gough A, Abraha H, Li F, Purewal TS, Foster AV, Watkins PJ *et al*. Measurement of markers of osteoclast and osteoblast activity in patients with acute and chronic diabetic Charcot neuroarthropathy. *Diabet Med* 1997; **14**: 527–531.
3 Piaggesi A, Rizzo L, Golia F, Costi D, Baccetti F, Ciaccio S *et al*. Biochemical and ultrasound tests for early diagnosis of active neuro-osteoarthropathy (NOA) of the diabetic foot. *Diabetes Res Clin Pract* 2002; **58**: 1–9.
4 Petrova NL, Moniz C, Elias DA, Buxton-Thomas M, Bates M, Edmonds ME. Is there a systemic inflammatory response in the acute charcot foot? *Diabetes Care* 2007; **30**: 997–998.
5 Uccioli L, Sinistro A, Almerighi C, Ciaprini C, Cavazza A, Giurato L *et al*. Proinflammatory modulation of the surface and cytokine phenotype of monocytes in patients with acute Charcot foot. *Diabetes Care* 2010; **33**: 350–355.
6 Petrova NL, Edmonds ME. A prospective study of calcaneal bone mineral density in acute Charcot osteoarthropathy. *Diabetes Care* 2010; **33**: 2254–2256.
7 Rogers LC, Frykberg RG, Armstrong DG, Boulton AJ, Edmonds M, Van GH *et al*. The Charcot foot in diabetes. *Diabetes Care* 2011; **34**: 2123–2129.
8 Petrova NL, Edmonds ME. Charcot neuro-osteoarthropathy-current standards. *Diabetes Metab Res Rev* 2008; **24**(Suppl 1): S58–61.
9 Hansson P, Lindblom U, Lindstrom P. Graded assessment and classification of impaired temperature sensibility in patients with

diabetic polyneuropathy. *J Neurol Neurosurg Psychiatry* 1991; **54**: 527–530.
10 Petrova NL, Foster AVM, Edmonds ME. Calcaneal bone mineral density in patients with Charcot neuropathic osteoarthropathy: differences between Type 1 and Type 2 diabetes. *Diabet Med* 2005; **22**: 756–761.
11 Young MJ, Breddy JL, Veves A, Boulton AJ. The prediction of diabetic neuropathic foot ulceration using vibration perception thresholds A prospective study. *Diabetes Care* 1994; **17**: 557–560.
12 Michail M, Jude E, Liaskos C, Karamagiolis S, Makrilakis K, Dimitroulis D *et al*. The performance of serum inflammatory markers for the diagnosis and follow-up of patients with osteomyelitis. *Int J Low Extrem Wounds* 2013; **12**: 94–99.
13 Giganti MG, Liuni F, Celi M, Gasbarra E, Zenobi R, Tresoldi I *et al*. Changes in serum levels of TNF-alpha, IL-6, osteoprotegerin, RANKL and their correlation with radiographic and clinical assessment in fragility fractures and high energy fractures. *J Biol Regul Homeost Agents*; **26**: 671–680.
14 Rasul S, Ilhan A, Wagner L, Luger A, Kautzky-Willer A. Diabetic polyneuropathy relates to bone metabolism and markers of bone turnover in elderly patients with type 2 diabetes: greater effects in male patients. *Gend Med* 2012; **9**: 187–196.
15 Elefteriou F. Regulation of bone remodeling by the central and peripheral nervous system. *Arch Biochem Biophys* 2008; **473**: 231–236.
16 Nyazee HA, Finney KM, Sarikonda M, Towler DA, Johnson JE, Babcock HM. Diabetic foot osteomyelitis: bone markers and treatment outcomes. *Diabetes Res Clin Pract* 2012; **97**: 411–417.
17 Ivaska KK, Gerdhem P, Akesson K, Garnero P, Obrant KJ. Effect of fracture on bone turnover markers: a longitudinal study comparing marker levels before and after injury in 113 elderly women. *J Bone Miner Res*; **22**: 1155–1164.
18 Pearson R G S, Divyateja H, Seagrave M, Game FL, Jeffcoate WJ *et al*. Charcot neuropathic osteoarthropathy, proinflammatoty cytokines and bone turnover markers. Abstract. *J Bone Joint Surg Br* 2012; 95–B.
19 Mabilleau G, Petrova NL, Edmonds ME, Sabokbar A. Increased osteoclastic activity in acute Charcot's osteoarthropathy: the role of receptor activator of nuclear factor-kappaB ligand. *Diabetologia* 2008; **51**: 1035–1040.
20 Ndip A, Williams A, Jude EB, Serracino-Inglott F, Richardson S, Smyth JV *et al*. The RANKL/RANK/osteoprotegerin signaling pathway mediates medial arterial calcification in diabetic Charcot neuroarthropathy. *Diabetes* 2011; **60**: 2187–2196.
21 Nybo M, Poulsen MK, Grauslund J, Henriksen JE, Rasmussen LM. Plasma osteoprotegerin concentrations in peripheral sensory neuropathy in Type 1 and Type 2 diabetic patients. *Diabet Med* 2010; **27**: 289–294.
22 Petrova NL, Shanahan CM. Neuropathy and the vascular-bone axis in diabetes: lessons from Charcot osteoarthropathy. *Osteoporos Int* 2014; **25**: 1197–1207.
23 Petrova NL, Shanahan C, Edmonds M. The proinflammatory cytokines TNF-a and IL-6 modulate RANKL-mediated osteoclastic resorption in vitro in patients with acute Charcot osteoarthropathy. Abstract. *Diabetologia* 2011; **54**(Suppl 1):S11.
24 Baumhauer JF, O'Keefe RJ, Schon LC, Pinzur MS. Cytokine-induced osteoclastic bone resorption in charcot arthropathy: an immunohistochemical study. *Foot Ankle Int* 2006; **27**: 797–800.
25 Aragón-Sánchez J, Lázaro-Martínez JL, Cabrera-Galván JJ. Additional information on the role of histopathology in diagnosing diabetic foot osteomyelitis. *Diabet Med* 2013; **31**: 113–116.
26 Divyateja H, Shu KSS, Pearson RG, Scammell BE, Game FL, Jeffcoate WJ. Local and systemic concentrations of pro-inflammatory cytokines, osteoprotegerin, sRANKL and bone turnover markers in acute Charcot foot and in controls. Abstract. *Diabetologia* 2011; **54**(Suppl 1): S11–S12.

A Prospective Study of Calcaneal Bone Mineral Density in Acute Charcot Osteoarthropathy

NINA L. PETROVA, MD
MICHAEL E. EDMONDS, FRCP

OBJECTIVE — To measure prospectively bone mineral density (BMD) of the Charcot and non-Charcot foot in 36 diabetic patients presenting with acute Charcot osteoarthropathy.

RESEARCH DESIGN AND METHODS — Calcaneal BMD was measured with quantitative ultrasound at presentation, at 3 months of casting, and at the time of the clinical resolution.

RESULTS — BMD of the Charcot foot was significantly reduced compared with BMD of the non-Charcot foot at presentation ($P = 0.001$), at 3 months of casting ($P < 0.001$), and at the time of clinical resolution ($P < 0.001$). Overall, from the time of presentation to the time of resolution there was a significant fall of BMD of the Charcot foot ($P < 0.001$) but not of the non-Charcot foot ($P = 0.439$).

CONCLUSIONS — Although the Charcot foot was treated with casting until clinical resolution, there was a significant fall of BMD only from presentation up until 3 months of casting.

Diabetes Care 33:2254–2256, 2010

Studies on bone mineral density (BMD) have shown a reduction of BMD of the Charcot foot compared with the contralateral non-Charcot foot (1–4). However, it is not known what happens to BMD in the natural history of the osteoarthropathy. The aim of this study was to measure prospectively the longitudinal changes of BMD of the Charcot and non-Charcot foot in patients presenting with acute Charcot osteoarthropathy.

RESEARCH DESIGN AND METHODS

— We studied 36 consecutive patients (19 type 1 diabetic patients; 20 male subjects; mean age 54 years [95% CI 49.4–57.9]; mean duration of diabetes 22 years [16.9–26.3]) who presented to the Diabetic Foot Clinic between February 2002 and October 2008 with a red, hot, swollen foot and a skin temperature >2°C compared with that of the contralateral foot and who had no previous offloading treatment. Foot skin temperatures were measured by Dermatemp 1001 (Exergen, Watertown, MA). All patients were treated with offloading and cast immobilization until the temperature difference between the feet was <2°C at two consecutive monthly visits (5,6).

BMD of the calcaneum was measured by quantitative ultrasound (Sahara Clinical Bone Sonometer; Hologic, Waltham, MA) as described previously (1). BMD of the Charcot foot was compared with BMD of the non-Charcot foot at presentation, at 3 months, and at the time of the clinical resolution at the end of the casting treatment using a paired Student *t* test. One-way repeated-measures ANOVA was used to assess the longitudinal change of BMD and foot skin temperature difference between feet. Pairwise comparisons between the means for BMD at presentation, at 3 months, and at clinical resolution were carried out to assess the effect of time. Results are presented as means (95% CI). Differences were considered significant at $P < 0.05$. All subjects gave informed written consent to participate. The study was approved by King's College Hospital NHS Trust Research Ethics Committee and carried out in accordance with the Declaration of Helsinki.

RESULTS

— BMD of the Charcot foot was significantly reduced compared with BMD of the non-Charcot foot at presentation (0.456 g/cm^2 [95% CI 0.411–0.502] vs. 0.494 g/cm^2 [0.456–0.533]; $P = 0.001$), at 3 months of casting (0.433 g/cm^2 [0.389–0.476] vs. 0.482 g/cm^2 [0.393–0.564]; $P < 0.001$), and at the time of clinical resolution (0.432 g/cm^2 [0.388–0.477] vs. 0.479 g/cm^2 [0.393–0.579]; $P < 0.001$).

Time to clinical resolution was 8.2 months (95% CI 6.9–9.5). The multivariate analysis demonstrated a significant fall of BMD of the Charcot foot from the time of presentation to the time of clinical resolution (Wilks $\Lambda = 0.525$, $P < 0.001$). This was noted in both type 1 (Wilks $\Lambda = 0.528$, $P = 0.006$) (Fig. 1*A*) and type 2 diabetes (Wilks $\Lambda = 0.497$, $P = 0.015$) (Fig. 1*B*).

The pairwise comparisons between the different time points demonstrated a significant fall of BMD of the Charcot foot from presentation to clinical resolution ($P = 0.015$). The fall of BMD from presentation (0.456 g/cm^2 [95% CI 0.411–0.502]) to 3 months of casting (0.433 g/cm^2 [0.389–0.476]) was highly significant ($P < 0.001$), both in type 1 ($P = 0.002$) and type 2 diabetes ($P = 0.004$), but the subsequent fall of BMD from 3 months of casting to clinical resolution was not significant (0.433 g/cm^2 [0.389–0.476] to 0.432 g/cm^2 [0.388–0.477]; $P = 0.949$). This applied to both type 1 ($P = 0.748$) and type 2 diabetes ($P = 0.832$).

In contrast to the Charcot foot, the multivariate analysis in the non-Charcot foot indicated that there was a nonsignificant fall of BMD from the time of presentation (0.494 g/cm^2 [95% CI 0.456–0.533]) to the time of resolution (0.479 g/cm^2 [0.393–0.579], Wilks $\Lambda = 0.947$; $P = 0.439$), and this was present in both type 1 (Wilks $\Lambda = 0.935$, $P = 0.583$)

From the Diabetic Foot Clinic, King's College Hospital, London, U.K.
Corresponding author: Nina L. Petrova, petrovanl@yahoo.com.
Received 13 April 2010 and accepted 4 July 2010. Published ahead of print at http://care.diabetesjournals.org on 13 July 2010. DOI: 10.2337/dc10-0636.

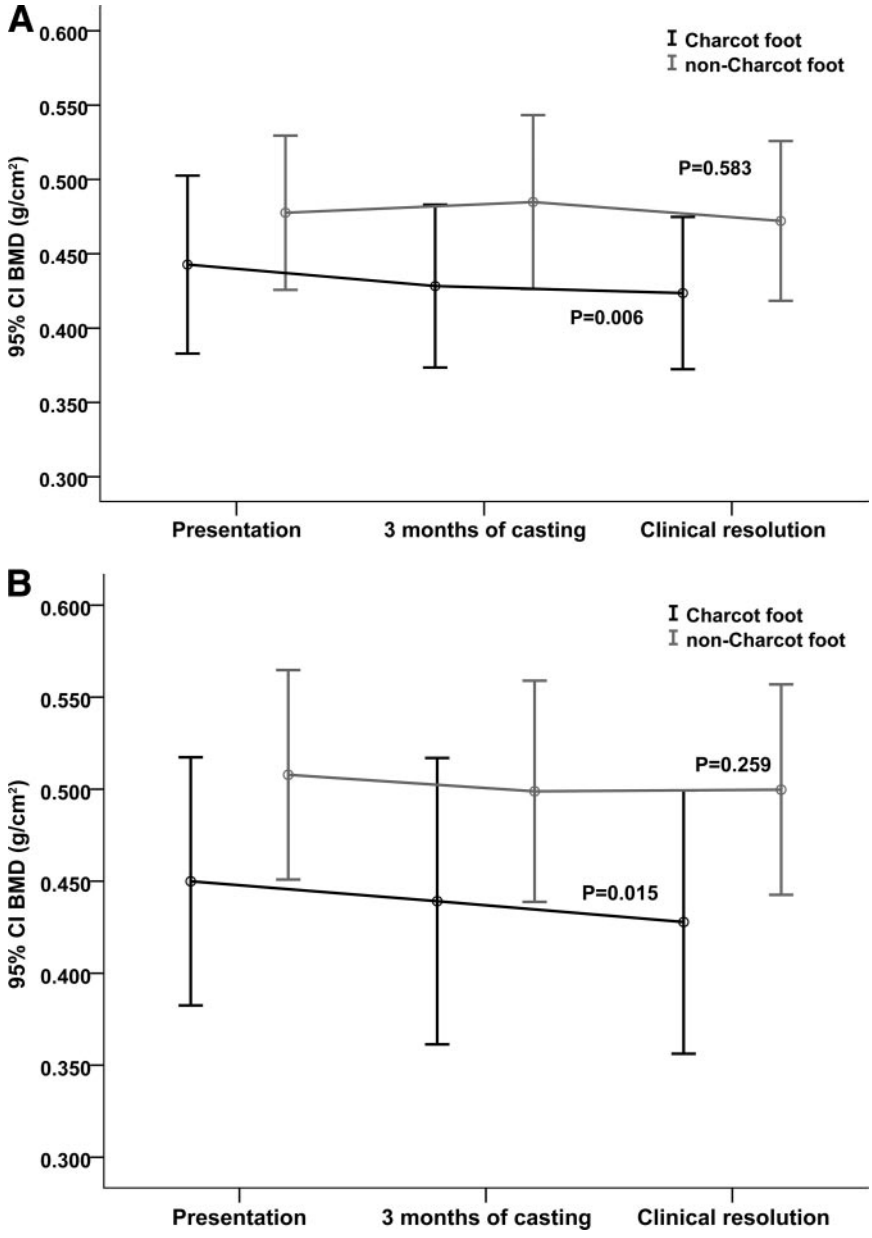

Figure 1—*Longitudinal changes of BMD of the Charcot and non-Charcot foot in patients with type 1 diabetes* (A) *and in patients with type 2 diabetes* (B). *Data are means (95% CI).* P *values indicate significance of the changes of BMD of the Charcot and non-Charcot foot from the time of presentation until the time of clinical resolution.*

(Fig. 1*A*) and type 2 diabetes (Wilks $\Lambda = 0.799$, $P = 0.259$) (Fig. 1*B*).

There was a significant fall of the foot skin temperature difference between the Charcot and non-Charcot foot from the time of presentation to the time of resolution (Wilks $\Lambda = 0.423$, $P < 0.001$). The foot skin temperature difference also fell significantly from 3.5°C (95% CI 3.1–4.1) at presentation to 2.2°C (1.8–2.2) at 3 months of casting ($P < 0.001$), and the latter further significantly reduced to 1.4°C (1.1–1.8) at clinical resolution ($P = 0.001$).

CONCLUSIONS — This study demonstrated that from the time of presentation to clinical resolution there was a significant fall of BMD of the Charcot foot but not of the non-Charcot foot. Although there was a significant fall of BMD of the Charcot foot at 3 months of casting compared with BMD at presentation, there was no further significant reduction of BMD from 3 months of casting up until clinical resolution, despite the ongoing casting of the Charcot foot.

Our study showed a fall of BMD at 3 months of casting in the Charcot foot both in type 1 and type 2 diabetes. The foot skin temperature of the Charcot foot was still 2°C greater compared with that of the non-Charcot foot, and this may have been related to inflammatory osteolysis that would have resulted in a fall of BMD (4). Increased levels of proinflammatory cytokines have been reported in patients with acute Charcot osteoarthropathy, and this may explain this observed reduction of BMD (7–9).

However, this fall of BMD may have been aggravated by the cast immobilization of the Charcot foot, and a recent case report has documented a fall of BMD in a total contact cast, highlighting the effect of immobilization (10). In our study, although there was a significant fall of BMD of the Charcot foot from presentation to 3 months of casting, this was not followed by a further significant fall of BMD up until clinical resolution despite the ongoing casting. Thus, it is more likely that the overall fall of BMD was related to inflammatory osteolysis rather than casting immobilization.

A limitation of this study is that we measured BMD of the calcaneum not BMD at the site of Charcot osteoarthropathy. Nevertheless, the calcaneum is a disease-responsive bone with a high metabolic turnover rate (11) and should have reflected overall changes of BMD in the foot.

In conclusion, although the Charcot foot was treated with casting until clinical resolution, there was a significant fall of BMD only from presentation until 3 months of casting. This may be related to the inflammatory osteolysis of Charcot osteoarthropathy.

Acknowledgments— N.L.P. was supported by Diabetes U.K. Grants BDA: RD 01/002284 and BDA: 05/0003025.

No potential conflicts of interest relevant to this article were reported.

N.L.P. and M.E.E. researched data, contributed to the discussion, wrote the manuscript, and reviewed/edited the manuscript.

References

1. Petrova NL, Foster AV, Edmonds ME. Calcaneal bone mineral density in patients with Charcot neuropathic osteoarthropathy: differences between Type 1 and Type 2 diabetes. Diabet Med 2005; 22:756–761
2. Young MJ, Marshall A, Adams JE, Selby PL, Boulton AJ. Osteopenia, neurological dysfunction, and the development of Charcot neuroarthropathy. Diabetes Care 1995;18:34–38

3. Jirkovská A, Kasalický P, Boucek P, Hosová J, Skibová J, Kasalicky P, Boucek P, Hosova J, Skibova J. Calcaneal ultrasonometry in patients with Charcot osteoarthropathy and its relationship with densitometry in the lumbar spine and femoral neck and with markers of bone turnover. Diabet Med 2001;18:495–500
4. Sinacore DR, Hastings MK, Bohnert KL, Fielder FA, Villareal DT, Blair VP 3rd, Johnson JE. Inflammatory osteolysis in diabetic neuropathic (charcot) arthropathies of the foot. Phys Ther 2008; 88:1399–1407
5. Armstrong DG, Lavery LA, Liswood PJ, Todd WF, Tredwell JA. Infrared dermal thermometry for the high-risk diabetic foot. Phys Ther 1997;77:169–175
6. Petrova NL, Edmonds ME. Charcot neuro-osteoarthropathy: current standards. Diabete Metab Res Rev 2008; 24(Suppl. 1):S58–S61
7. Jeffcoate WJ, Game F, Cavanagh PR. The role of proinflammatory cytokines in the cause of neuropathic osteoarthropathy (acute Charcot foot) in diabetes. Lancet 2005;366:2058–2061
8. Jeffcoate WJ. Abnormalities of vasomotor regulation in the pathogenesis of the acute charcot foot of diabetes mellitus. Int J Low Extrem Wounds 2005;4:133–137
9. Petrova NL, Dew T, Musto R, Langworthy R, Sherwood R, Moniz C, Edmonds ME. The proinflammatory cytokines, TNF-alpha and IL-6, are linked with pathological bone turnover in the acute Charcot foot (Abstract). Diabet Med 2008;25:A22
10. Hastings MK, Sinacore DR, Fielder FA, Johnson JE. Bone mineral density during total contact cast immobilization for a patient with neuropathic (Charcot) arthropathy. Phys Ther 2005;85:249–256
11. Langton CM, Palmer SB, Porter RW. The measurement of broadband ultrasonic attenuation in cancellous bone. Eng Med 1984;13:89–91

Diabetologia
DOI 10.1007/s00125-008-0992-1

ARTICLE

Increased osteoclastic activity in acute Charcot's osteoarthopathy: the role of receptor activator of nuclear factor-kappaB ligand

G. Mabilleau · N. L. Petrova · M. E. Edmonds · A. Sabokbar

Received: 19 December 2007 / Accepted: 22 February 2008

Abstract
Aims/hypothesis Our aims were to compare osteoclastic activity between patients with acute Charcot's osteoarthropathy and diabetic and healthy controls, and to determine the effect of the receptor activator of nuclear factor-kappaB ligand (RANKL) and its decoy receptor osteoprotegerin (OPG).
Methods Peripheral blood monocytes isolated from nine diabetic Charcot patients, eight diabetic control and eight healthy control participants were cultured in the presence of macrophage-colony stimulating factor (M-CSF) alone, M-CSF and RANKL, and also M-CSF and RANKL with excess concentrations of OPG. Osteoclast formation was assessed by expression of tartrate-resistant acid phosphatase on glass coverslips and resorption on dentine slices.
Results In cultures with M-CSF, there was a significant increase in osteoclast formation in Charcot patients compared with healthy and diabetic control participants ($p=0.008$). A significant increase in bone resorption was also seen in the former, compared with healthy and diabetic control participants ($p<0.0001$). The addition of RANKL to the cultures with M-CSF led to marked increase in osteoclastic resorption in Charcot (from 0.264±0.06% to 41.6±8.1%, $p<0.0001$) and diabetic control (0.000±0.00% to 14.2±16.5%, $p<0.0001$) patients, and also in healthy control participants (0.004±0.01% to 10.5±1.9%, $p<0.0001$). Although the addition of OPG to cultures with M-CSF and RANKL led to a marked reduction of resorption in Charcot patients (41.6±8.1% to 5.9±2.4%, $p=0.001$), this suppression was not as complete as in diabetic control patients (14.2±16.5% to 0.45±0.31%, $p=0.001$) and in healthy control participants (from 10.5±1.9% to 0.00±0.00%, $p<0.0001$).
Conclusions/interpretation These results indicate that RANKL-mediated osteoclastic resorption occurs in acute Charcot's osteoarthropathy. However, the incomplete inhibition of RANKL after addition of OPG also suggests the existence of a RANKL-independent pathway.

Keywords Charcot's osteoarthropathy · OPG · Osteoclasts · Osteolysis · RANKL · Resorption

Abbreviations

LIGHT	homologous to lymphotoxins exhibiting inducible expression and competing with herpes simplex virus glycoprotein D for herpes virus entry mediator (HVEM), a receptor expressed by T lymphocytes
MEM	minimum essential medium
M-CSF	macrophage-colony stimulating factor
OPG	osteoprotegerin
PBMCs	peripheral blood monocytes
RANK	receptor activator of nuclear factor-kappaB
RANKL	receptor activator of nuclear factor-kappaB ligand
sRANKL	soluble receptor activator of nuclear factor-kappaB ligand
TRAcP	tartrate-resistant acid phosphatase

G. Mabilleau · A. Sabokbar
Nuffield Department of Orthopaedic Surgery,
Botnar Research Centre, University of Oxford,
Oxford, UK

N. L. Petrova · M. E. Edmonds (✉)
Diabetic Foot Clinic,
King's College Hospital NHS Foundation Trust,
Denmark Hill,
London SE5 9RS, UK
e-mail: Michael.Edmonds@kch.nhs.uk

Introduction

Although Charcot's osteoarthropathy is characterised by increased local bone resorption [1], the exact cellular mechanisms contributing to the pathogenesis of this condition remain unresolved. Osteoclasts have been shown to be the principal cell type responsible for bone resorption [2]. These cells originate from the haemopoietic lineage and are known to undergo various stages of proliferation, fusion and differentiation before they are fully functionally active, mature osteoclasts. Recently, receptor activator of nuclear factor-kappaB (RANK) ligand (RANKL) has been identified as an essential mediator of osteoclast formation and activation [3]. RANKL is expressed on a variety of cell types such as bone forming osteoblasts, T lymphocytes, dendritic cells, endothelial cells and fibroblasts. RANKL mediates the process of osteoclastogenesis by binding to its RANK, which is expressed on mononuclear osteoclast precursors. The effects of RANKL–RANK interaction are physiologically counterbalanced by osteoprotegerin (OPG), which acts as a soluble receptor decoy for RANKL and blocks the interaction of RANKL with RANK. The ratio of RANKL to OPG has been suggested to regulate the extent of osteoclast formation and resorption. Therefore, any alteration in the RANKL/OPG ratio could be critical in the pathogenesis of osteolytic bone disorders [4].

Recently, Jeffcoate hypothesised that the RANK/RANKL/OPG pathway may play an important role in the osteolysis seen in acute Charcot's osteoarthropathy [5]. Using an in vitro technique to generate functional human osteoclasts from peripheral blood monocytes (PBMCs) [6] in the presence of macrophage-colony stimulating factor (M-CSF) [7] and soluble RANKL, it is possible to determine the cellular mechanisms involved in the process of osteoclast formation and resorption in physiological and pathological conditions. To our knowledge, this technique has not yet been studied in patients with Charcot's osteoarthropathy.

The aims of this study were: (1) to generate functional human osteoclasts in vitro from diabetic patients with acute Charcot's osteoarthropathy and from healthy and diabetic control participants; (2) to compare the extent of osteoclast formation and resorption; and (3) to determine the role of the RANK/RANKL/OPG pathway in osteoclastic activity in Charcot's osteoarthropathy.

Methods

Patients

We studied nine consecutive diabetic patients with recent onset of acute Charcot's osteoarthropathy (five men, four women; five type 1, four type 2 diabetes), eight diabetic patients with no previous history of Charcot's osteoarthropathy (five men, three women; four type 1, four type 2) and eight healthy control participants (five men, three women). Patients with acute Charcot's osteoarthropathy were matched for age and duration of diabetes with the diabetic control patients and for age with the healthy control participants. The mean age was similar between patients with Charcot's osteoarthropathy and diabetic control patients (53±2.8 versus 59±2.9 years [mean±SEM], $p=0.167$) as was the mean age between the former and healthy control participants (53±2.8 versus 47±2.7 years, $p=0.114$). The mean duration of diabetes was similar in both groups with diabetes (31±5.1 [Charcot patients] versus 27±4.6 years, $p=0.606$). Diabetes control as indicated by glycated Hb was also similar in the two diabetes groups (7.7±0.6 [Charcot's] versus 7.8±0.4%, $p=0.743$).

Diagnosis of Charcot's osteoarthropathy was made on the presentation of a hot swollen foot, with skin foot temperature 2°C greater than the corresponding site on the contralateral foot and with typical radiological changes of subluxation, dislocation or fragmentation of bone on standard foot radiographs [8]. All patients had intact feet and no evidence of foot infection or ulceration.

Ethical permission for this study was obtained from the King's College Hospital Research Ethics Committee and all participants gave written informed consent.

Isolation and culture of monocytes

Peripheral blood mononuclear cells were isolated as previously described [6]. Briefly, blood was diluted 1:1 in α-minimum essential medium (MEM; Invitrogen, Paisley, UK), layered over Histopaque and centrifuged (693 *g*) for 20 min. The interface layer was resuspended in MEM, then centrifuged (600 *g*) for a further 10 min. The resultant cells were resuspended in MEM with 10% heat-inactivated FCS and counted in a haemocytometer following lysis of erythrocytes by a 5% (vol./vol.) acetic acid solution.

To assess the extent of osteoclast formation and resorption, PBMCs were cultured on glass coverslips and dentine slices. Initially, 5×10^5 PBMCs were added to 6-mm diameter glass coverslips and 4-mm diameter dentine slices in MEM containing 100 UI/ml penicillin, 100 μg/ml streptomycin and 10% FCS (Gibco, Paisley, UK). After 2 h incubation, coverslips and dentine slices were vigorously rinsed in medium to remove non-adherent cells. The cultures were maintained in MEM/FCS under three different culture conditions: (1) human M-CSF (R&D Systems Europe, Abingdon, UK) alone at 25 ng/ml; (2) M-CSF plus 100 ng/ml human soluble RANKL (sRANKL; Peprotech, London, UK) (a concentration known to facilitate differentiation of osteoclast precursors to active bone-resorbing osteoclasts in vitro); and (3) M-CSF plus sRANKL plus 250 ng/ml human OPG (R&D Systems Europe).

Coverslips and dentine slices were cultured at 37°C in 5% CO_2 for 14 and 21 days respectively.

Osteoclast formation

After 14 days, the coverslips were examined histochemically for the expression of tartrate-resistant acid phosphatase (TRAcP), an osteoclast marker. Coverslips with newly formed osteoclasts were collected and rinsed in PBS buffer, fixed with formalin (10% [vol./vol.] in PBS buffer) for 10 min and rinsed in distilled water. TRAcP was histochemically revealed by a simultaneous coupling reaction using Naphtol AS-BI-phosphate as substrate and Fast violet B as the diazonium salt. The coverslips were incubated for 90 min at 37°C in a dark room, rinsed three times in distilled water and the residual activity was inhibited by 4% NaF (wt/wt) for 30 min. Coverslips were then rinsed in distilled water, counterstained with DAPI for 20 min and allowed to dry before mounting, using an aqueous medium. TRAcP-positive cells with more than three nuclei were identified as osteoclasts. The number of newly generated osteoclasts was assessed using a light microscope examination.

Osteoclast resorption

After 21 days, the dentine slices were removed from the culture wells, placed in NH_4OH (1 mol/l) for 30 min and sonicated for 5 min to remove any adherent cells. They were then rinsed in distilled water and stained with 0.5% (vol./vol.) toluidine blue prior to examination by light microscopy. The surface of each dentine slice was examined for evidence of lacunar resorption and the extent of eroded surface on each dentine slice was determined using image analysis and expressed as the percentage of surface area resorbed.

Statistical analyses

Data were expressed as a mean±SEM. Initially the difference within the three study groups (Charcot patients, healthy and diabetic controls) was assessed with the non-parametric Kruskall–Wallis test. Then the differences between Charcot and diabetic patients, and Charcot patients and healthy controls were assessed by the non-parametric Mann–Whitney *U* test. In each patient group, the differences between the various culture conditions were also assessed using the Mann–Whitney *U* test. Differences were considered significant at $p<0.05$.

Results

Osteoclast cultures in the presence of M-CSF

Osteoclast formation The mean number of newly formed TRAcP-positive multinucleated osteoclasts in the presence of M-CSF alone was significantly greater in the patients with acute Charcot's osteoarthropathy (48.6±18.2) than in diabetic (6.8±2.7) and healthy control participants (5.0±0.7) ($p=0.008$). The number of TRAcP-positive multinucleated osteoclasts formed in acute Charcot's osteoarthropathy was 7.2 and 9.7 times greater than those formed in diabetic ($p=0.010$) and healthy control groups ($p=0.003$), respectively.

Osteoclast resorption The newly formed osteoclasts exhibited increased functional activity as demonstrated by the extent of resorption on dentine slices, with percentage area resorption significantly elevated in the patients with acute Charcot's osteoarthropathy (0.264±0.06%) compared with diabetic (0.000±0.00%) and healthy control groups (0.004±0.01) ($p<0.0001$). The percentage of resorption was significantly greater in the Charcot patients than in the diabetic ($p=0.001$) and healthy control groups ($p=0.001$).

Osteoclast cultures in the presence of M-CSF and sRANKL

Osteoclast formation The addition of sRANKL led to an increase in the number of TRAcP-positive multinucleated osteoclasts in all three groups of patients. The mean number of these osteoclasts in patients with acute Charcot's osteoarthropathy was 96.0±21.6, which was significantly greater than that in the diabetic (56.5±11.5) and healthy (29.0±5.1) control groups ($p=0.010$; Fig. 1a,c,e). The number of TRAcP-positive multinucleated osteoclasts in the patients with acute Charcot's osteoarthropathy was 1.7 times higher than in diabetic control patients, but this finding did not reach significance ($p=0.105$). However, the number of these osteoclasts in the acute Charcot group was 3.3 times (and significantly) higher than in the healthy control group ($p=0.005$). When the number of cells in the cultures with M-CSF alone was compared with that after the addition of sRANKL, there was a significant increase in the diabetic control patients (from 6.8±2.7 to 56.5±11.5, $p=0.003$) and in the healthy participants (from 5.0±0.7 to 29.0±5.1, $p=0.002$), while the increase in the number of TRAcP-positive multinucleated osteoclasts in the acute Charcot group failed to reach significance (increase from 48.6±18.2 to 96.0±21.6, $p=0.059$; Fig. 2a).

Osteoclast resorption The percentage area resorption on dentine slices with M-CSF and sRANKL was significantly increased in the acute Charcot group (41.6±8.1%) compared with that in the diabetic (14.2±16.5%) and healthy control groups (10.5±1.9%; $p=0.005$). Resorption in the Charcot patients was 2.9 times higher than in diabetic control patients ($p=0.008$) and four times higher than in healthy participants ($p=0.005$; Fig. 1b,d,f). The addition of sRANKL to the cultures with M-CSF led to the

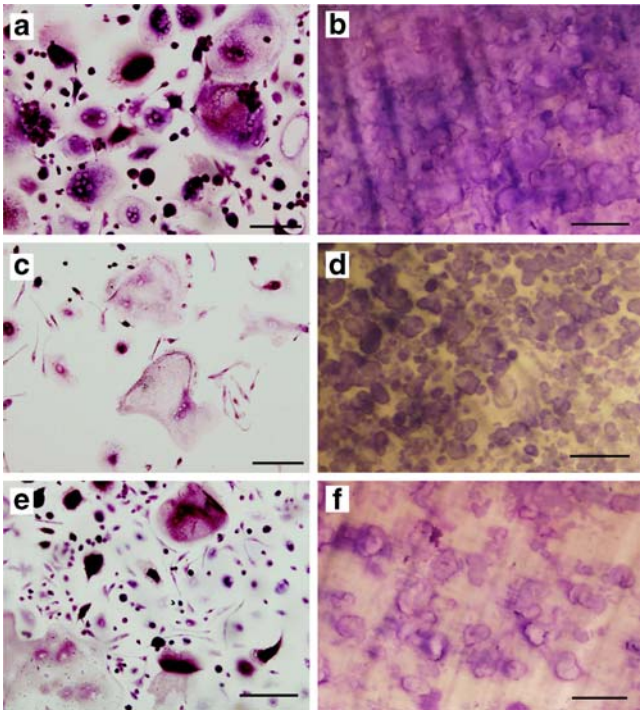

Fig. 1 Multinucleated TRAcP-positive cells were formed on glass coverslips (**a**, **c**, **e**) capable of lacunar resorption (**b**, **d**, **f**) after 14 and 21 days incubation, respectively, in the presence of 25 ng/ml human M-CSF and 100 ng/ml sRANKL. Newly formed osteoclasts were numerous and highly active in Charcot's patients (**a**, **b**) compared with diabetic (**c**, **d**) and healthy control (**e**, **f**) participants. Scale bars, 10 μm

following rises in the percentage area resorption when compared with M-CSF alone: Charcot's 0.264±0.06% to 41.6±8.1%, $p<0.0001$; diabetic control 0.000±0.00% to 14.2±16.5%, $p<0.0001$; healthy control 0.004±0.01% to 10.5±1.9%, $p<0.0001$ (Fig. 2b).

Osteoclast cultures in the presence of M-CSF, sRANKL and excess concentrations of OPG

Osteoclast formation The addition of excess concentrations of OPG led to a reduction in the number of TRAcP-positive multinucleated osteoclasts in the cultures with M-CSF, sRANKL and OPG in all the three groups of patients. However, after the addition of OPG, the number of TRAcP-positive multinucleated osteoclasts was still significantly increased in the Charcot group (54.4±17.6), as compared with diabetic (8.8±5.3) and healthy control participants (4.4±1.2; $p=0.003$). In the cultures with M-CSF, sRANKL and OPG, the number of TRAcP-positive multinucleated osteoclasts was greater in the Charcot patients than in the diabetic ($p=0.005$) and healthy control groups ($p=0.001$).

When OPG was added to the cultures with M-CSF and sRANKL, the reduction in the number of TRAcP-positive

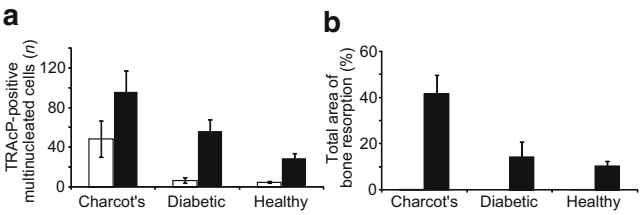

Fig. 2 **a** Quantitative comparison between the number (n) of TRAcP-positive cells formed in cultures with M-CSF alone (white bars) or with M-CSF and sRANKL (black bars) in patients with Charcot's osteoarthropathy and diabetic and healthy control participants. **b** Quantitative comparison between the percentage area resorption in the same cultures and patient groups. Statistical differences between the groups were determined using the Mann–Whitney U test, with significance as follows: **a** Charcot's $p=0.059$, diabetic control $p=0.003$, healthy control $p=0.002$; **b** Charcot's $p<0.0001$, diabetic control $p<0.0001$, healthy control $p<0.0001$

cells in Charcot patients was not significant (96.0±21.6 versus 54.4±17.6, $p=0.189$). OPG on the other hand significantly inhibited the number of TRAcP-positive cells in M-CSF and RANKL-mediated cultures from diabetic (reduced from 56.5±11.5 to 8.8±5.3, $p=0.005$) and healthy control participants (29.0±5.1 to 4.4±1.2, $p=0.003$; Fig. 3a).

Osteoclast resorption The addition of OPG led to a marked reduction of the percentage area resorption on dentine slices in Charcot patients (from 41.6±8.1% to 5.9±2.4%, $p=0.001$) and also in diabetic (14.2±16.5% to 0.45±0.31%, $p=0.001$) and healthy control (from 10.5±1.9% to 0.00±0.00%, $p<0.0001$) participants (Fig. 3b).

However, the percentage area resorption on the dentine slices was still greater in the cultures with M-CSF, RANKL and OPG from the patients with acute Charcot's osteoarthropathy (5.9±2.4%) than in those from diabetic (0.45±0.31%) and healthy control (0.00±0.00%) participants

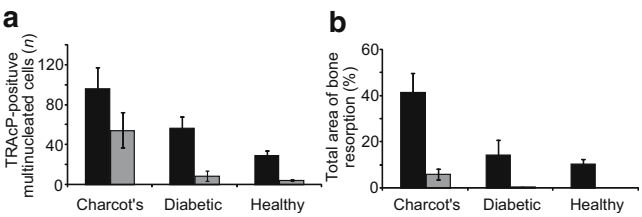

Fig. 3 **a** Comparison between the number (n) of TRAcP-positive cells formed in cultures with M-CSF and sRANKL (black bars) or with M-CSF, sRANKL and excess concentrations of OPG (250 ng/ml) (grey bars) in patients with Charcot's osteoarthropathy and diabetic and healthy control participants. **b** Comparison between the percentage area resorption in the same cultures and patient groups. Statistical differences between the groups were determined using the Mann–Whitney U test, with significance as follows: **a** Charcot's $p=0.189$, diabetic control $p=0.005$, healthy control $p=0.003$; **b** Charcot's $p=0.001$, diabetic control $p=0.001$, healthy control $p<0.0001$

(p=0.003). Resorption on the dentine slices was greater in the Charcot patients than in diabetic (p=0.005) and healthy control (p=0.003) groups.

Discussion

This study shows that monocytes from patients with acute Charcot's osteoarthropathy cultured in the presence of M-CSF alone were capable of differentiating into mature osteoclasts that exhibited increased resorption compared with diabetic and healthy control participants. Furthermore, osteoclasts generated after the addition of sRANKL were functionally more aggressive, exhibiting a considerable increase in the extent of resorbing activity in patients with acute Charcot's osteoarthropathy. This resorption was partially blocked by the addition of excess concentrations of OPG, a soluble receptor decoy for RANKL. This suggests that the increased osteoclastic activity in patients with acute Charcot's osteoarthropathy is mediated through both a RANKL-dependent and a RANKL-independent pathway.

Cultures from the patients with Charcot's osteoarthropathy showed increased osteoclast formation and resorption when cultured with M-CSF alone. Although M-CSF is an essential factor for proliferation, differentiation and survival of the monocyte-macrophage lineage [9, 10], it is not an osteoclastogenic factor and it is unusual to detect osteoclast formation and resorption in cultures with M-CSF, as was seen in the diabetic and healthy controls. This observation suggests that in acute Charcot's osteoarthropathy there may be increased levels of other circulating pro-inflammatory factors such as TNF-α [11, 12], IL-6 [13], IL-8 [14] and LIGHT (homologous to lymphotoxins exhibiting inducible expression and competing with herpes simplex virus glycoprotein D for herpes virus entry mediator [HVEM], a receptor expressed by T lymphocytes) [15], which have been previously shown to stimulate osteoclastogenesis independently of RANK/RANKL mechanisms. The concentrations of these circulating factors in diabetic and healthy control participants may not be sufficient to induce the formation and differentiation of active osteoclasts in the presence of M-CSF alone.

After the addition of sRANKL to M-CSF cultures, the newly formed osteoclasts exhibited markedly increased resorption in the patients with Charcot's osteoarthropathy, although the number of osteoclasts did not significantly increase in these patients compared with cultures with M-CSF alone. These observations may not be unique to Charcot's osteoarthropathy, and indeed similar observations have been reported in other conditions associated with increased bone resorption, such as rheumatoid arthritis where the addition of sRANKL resulted in a significant increase in lacunar resorption, but did not lead to a significant increase in the number of TRAcP-positive cells [16]. Overall, the observed extensive resorption in acute Charcot patients, in the presence of M-CSF and sRANKL, as compared with the diabetic or healthy control groups, may suggest that the osteoclast precursors circulating in acute Charcot patients are in a higher activated state and as such are more primed to becoming osteoclasts (mediated through RANKL) than those in the control groups.

In order to ascertain that RANKL was a major osteoclastic activator in patients with Charcot's osteoarthropathy, excess concentrations of OPG, the soluble receptor decoy to RANKL, were added to the cultures with M-CSF and RANKL. The rationale for this approach was that if osteoclastogenesis is mediated solely through RANK–RANKL interaction, addition of excess concentrations of OPG (as had been previously determined to be sufficient to block osteoclastogenesis through RANKL [15]) would completely abolish the process of osteoclast differentiation and activation. In the current study, although osteoclast formation and resorption in the diabetic and healthy control groups was completely blocked by the addition of OPG, the latter did not achieve total inhibition of osteoclast formation and resorption in patients with acute Charcot's osteoarthropathy. These results suggest that although RANKL-dependent pathways do play a significant role in the osteoclastic activity of Charcot's osteoarthropathy, an alternative pathway (other than RANK/RANKL) may also be involved. Osteoclastogenic mediators other than RANKL that have been reported to stimulate osteoclast differentiation independently of the RANKL pathway include TNF-α [11, 12], IL-6 [13], IL-8 [14] and LIGHT [15]. In acute Charcot's osteoarthropathy, it is possible that one or a combination of these factors may have initiated the circulating osteoclast precursors to be in a more 'primed' condition, a situation which as such could explain the observed resorption in Charcot monocyte cultures supplemented with M-CSF alone, without the exogenous addition of any osteoclastogenic mediators.

The osteolysis of Charcot's osteoarthropathy may be explained by our observation that osteoclast precursors from Charcot patients develop into mature osteoclasts that exhibit increased resorptive activity, especially in response to RANKL, unlike the increased resorption in response to bacterial infection, which is not mediated by RANKL [17]. Increased expression of RANKL has been previously demonstrated in pathological osteolysis associated with the development of various bone diseases [18] and a similar mechanism may contribute to osteolysis of Charcot's osteoarthropathy [5]. Furthermore, patients with Charcot's osteoarthropathy have severe neuropathy, which itself can also lead to increased expression of RANKL as a result of the loss of nerve-derived peptides known to antagonise its effect such as calcitonin gene-related peptide [5]. In

addition to the RANKL-dependent pathway, our results suggest that a RANKL-independent pathway, mediated by pro-inflammatory cytokines, may also be important. Indeed, Charcot's foot is characterised by excessive inflammation and proinflammatory cytokines have been implicated in its pathogenesis [19]. In support of this, a recent immunohistochemical analysis of bone samples isolated from Charcot's osteoarthropathy patients showed excessive osteoclastic activity in a microenvironment enriched with mediators of bone resorption (IL-1, IL-6 and TNF-α) [20]. Thus a RANKL-independent pathway, which is also known to play a role in other osteolytic disorders such as rheumatoid arthritis [21] and aseptic loosening [22], could contribute also to the pathogenesis of the Charcot's osteoarthropathy.

This study has indicated, for the first time that the RANKL-dependent pathway is important in the pathogenesis of Charcot's osteoarthropathy, thereby raising the possibility of the use of RANKL inhibition in the management of Charcot's foot. However, our observations also suggest that a RANKL-independent pathway may play a role, but further investigation is required to fully clarify the mechanism involved. If confirmed, specific pharmacological agents that counteract the RANKL-independent pathway, such as anti-TNF strategies, may be useful in the treatment of Charcot's osteoarthropathy. Whatever the relative importance of either pathway, this in vitro technique of generating human osteoclasts from PBMCs may allow specific characterisation of osteoclastic activity in each patient and could, in the future, lead to individually tailored anti-osteoclastic treatment for the patient with acute Charcot's osteoarthropathy.

Acknowledgements G. Mabilleau was supported by Furlong Charitable Trust. N. L. Petrova was supported by Diabetes UK Grant: BDA:05/0003025 and an EFSD/AstraZeneca Clinical Travel Fellowship.

Duality of interest The authors declare that there is no duality of interest associated with this manuscript.

References

1. Gough A, Abraha H, Li F et al (1997) Measurement of markers of osteoclast and osteoblast activity in patients with acute and chronic diabetic Charcot neuroarthropathy. Diabet Med 14:527–531
2. Teitelbaum SL (2000) Bone resoption by osteoclasts. Science 289:1504–1508
3. Yasuda H, Shima N, Nakagawa N et al (1998) Osteoclast differentiation factor is a ligand for osteoprotegerin/osteoclastogenesis-inhibitory factor and is identical to TRANCE/RANKL. Proc Natl Acad Sci U S A 95:3597–3602
4. Hofbauer LC, Schoppet M (2004) Clinical implications of the osteoprotegerin/ RANKL /RANK system for bone and vascular diseases. JAMA 292:490–495
5. Jeffcoate W (2004) Vascular calcification and osteolysis in diabetic neuropathy—is RANK-L the missing link? Diabetelogia 47:1488–1492
6. Sabokbar A, Athanasou NS (2003) Generating human osteoclasts from peripheral blood. Methods Mol Med 80:101–111
7. Fujikawa Y, Quinn JM, Sabokbar A, McGee JO, Athanasou NA (1996) The human osteoclast precursors circulate in the monocyte fraction. Endocrinology 137:4058–4060
8. Sanders LJ, Frykberg RG (2001) Charcot neuroarthropathy of the foot. In: Bowker JH, Phiefer MA (eds) Levin & O'Neal's the diabetic foot. 6th edn. Mosby, St Louis, pp 439–466
9. Flanagan AM, Lader CS (1998) Update on the biologic effects of monocyte-macrophage colony-stimulating factor. Curr Opin Hematol 5:181–185
10. Motoyoshi K (1998) Biological activities and clinical application of M-CSF. Int J Hematol 67:109–122
11. Kobayashi K, Takahashi N, Jimi E et al (2000) Tumor necrosis factor alpha stimulates osteoclast differentiation by mechanism independent of ODF/RANKL-RANK-interaction. J Exp Med 191: 257–286
12. Kudo O, Fujikawa Y, Itonaga I, Sabokbar A, Torisu T, Athanasou NA (2002) Proinflammatory cytokine (TNFalpha/IL-1alpha) induction of human osteoclast formation. J Pathol 198:220–227
13. Kudo O, Sabokbar A, Pocock A, Itonaga I, Fujikawa Y, Athanasou NA (2003) Interleukin-6 and interleukin-11 support human osteoclast formation by RANKL-independent mechanism. Bone 32:1–7
14. Bendre MS, Montague DC, Peery T, Akel NS, Gaddy D, Suva LJ (2003) Interleukin-8 stimulation of osteoclastogenesis and bone resorption is a mechanism for the increased osteolysis of metastatic bone disease. Bone 33:28–37
15. Edwards JR, Sun SG, Locklin R et al (2006) LIGHT (TNFSF14), a novel mediator of bone resorption, is elevated in rheumatoid arthritis. Arthritis Rheum 54:1451–1462
16. Hirayama T, Danks L, Sabokbar A, Athanasou NA (2002) Osteoclast formation and activity in the pathogenesis of osteoporosis in rheumatoid arthritis. Rheumatology 41:1232–1239
17. Zou W, Bar-Shavit Z (2002) Dual modulation of osteoclast differentiation by lipopolysaccharide. J Bone Miner Res 17:1211–1218
18. Grimaud E, Soubigou L, Couillaud S et al (2003) Receptor activator of nuclear factor kappaB ligand (RANKL)/osteoprotegerin (OPG) ratio is increased in severe osteolysis. Am J Pathol 163:2021–2031
19. Jeffcoate WJ, Game F, Cavanagh P (2005) The role of proinflammatory cytokines in the cause of neuropathic osteoarthropathy (acute Charcot foot) in diabetes. Lancet 366:2058–2061
20. Baumhauer JF, O'Keefe RJ, Schon LC, Pinzur MS (2006) Cytokine-induced osteoclastic bone resorption in Charcot arthropathy: an immunohistochemical study. Foot Ankle Int 27:797–800
21. Adamopoulos IE, Sabokbar A, Wordsworth BP, Carr A, Ferguson DJ, Athanasou NA (2006) Synovial fluid macrophages are capable of osteoclast formation and resorption. J Pathol 208:35–43
22. Sabokbar A, Kudo O, Athanasou NA (2003) Two distinct cellular mechanisms of osteoclast formation and bone resorption in periprosthetic osteolysis. J Orthop Res 21:73–80

Is There a Systemic Inflammatory Response in the Acute Charcot Foot?

NINA L. PETROVA, MD[1]
CAJE MONIZ, MD, FRCPATH[2]
DAVID A. ELIAS, MD, FRCR[3]
MURIEL BUXTON-THOMAS, MSC, FRCP[4]
MAUREEN BATES, MSC, DPODM[1]
MICHAEL E. EDMONDS, MD, FRCP[1]

Although patients with acute Charcot osteoarthropathy exhibit a marked local inflammatory response to trauma by the classical presentation of a red, hot swollen foot, the systemic acute phase response has not been fully investigated. The aim of this study was to measure the systemic serologic markers of inflammation in acute Charcot osteoarthropathy.

RESEARCH DESIGN AND METHODS — We studied 36 consecutive patients who presented to the Diabetic Foot Clinic over the last 5 years with a red, hot swollen foot and a skin temperature >2°C compared with the same site on the contralateral foot and who had no previous treatment. There was no evidence of any skin breakdown or ulceration. Foot skin temperatures were measured by Dermatemp 1001 (Exergen, Watertown, MA). The diagnosis of Charcot osteoarthropathy was confirmed in 25 cases by evidence of subluxation, dislocation, or fragmentation of bone on standard foot radiographs and in 11 cases by the presence of an increased focal uptake on the bony (third) phase of the triphasic Technetium-Diphosphonate bone scan (Tyco Healthcare) even though the radiographs at presentation were normal. In the patients with radiological abnormalities, the patterns of involvement were described using Sanders and Frykberg's classification (1). Four patients presented with pattern I (metatarsal-phalangeal joints), seven with pattern II (tarsometatarsal joints), four with pattern III (tarsal joints), one with pattern IV (ankle joint), and two with pattern V (calcaneum). Seven patients presented with multiple sites of involvement: six had a combination of patterns II and III, and one had patterns I and II. In the remaining 11 patients who presented with normal radiographs, there was increased focal uptake on the bony (third) phase of the triphasic Technetium Diphosphonate bone scan: 10 in the midfoot and 1 in the forefoot. These patients were similar to the Charcot foot stage 0 with normal radiograph and abnormal bone scan as described in Sella and Barrette's staging of Charcot osteoarthropathy (2).

Serum C-reactive protein (CRP), white cell count (WCC), erythrocyte sedimentation rate (ESR), Hb, and GHb were measured at presentation. Data on liver synthesis function including liver enzymes (aspartate transminase, alkaline phosphatase, and γ-glutamyl tranferase) and serum proteins (albumin and globulin) were also recorded. Renal function was assessed by serum creatinine levels.

Statistical analyses

Data are presented as median (25th–75th percentile). The limit for detection of the CRP assay was 5 mg/l, and therefore levels ≤5 mg/l were taken as 5 mg/l for the purpose of the analysis.

RESULTS — There were 21 type 1 (11 male and 10 female) and 15 type 2 (7 male and 8 female) diabetic patients. Median age was 51 years (41–62), and median duration of diabetes was 20 years (13–26.5). Skin foot temperature was 3.1°C (2.4–4.2) greater in the Charcot foot compared with the contralateral foot. Median CRP level was 5.8 mg/l (5–11) and ≤5 mg/l in 47.2% of patients presenting with acute Charcot osteoarthropathy. Median ESR was 21 mm/h (13–36); WCC was 7.0 10\S\9/l (5.8–8.1), reference range 4–11; GHb was 8.5% (7.3–10.3), reference range <6; and Hb was 13.1 g/dl (11.7–14.7). Patients had preserved synthesis liver function as indicated by normal liver enzymes (median aspartate transminase 25 units/l [19–29], reference range 10–50; alkaline phosphatase 105 units/l [76–136], reference range 30–130; γ-glutamyl tranferase 26 units/l [18–43], reference range 1–55) and normal protein synthesis (median serum albumin 44 g/l [40–46], reference range 35–50, and serum globulin 29 g/l [27–31], reference range 25–35). The median creatinine level was 88 μmol/l (79–109), reference range 45–120, and only one patient had renal failure and was on hemodyalisis treatment.

CONCLUSIONS — This report has shown that in the acute stage of Charcot osteoarthropathy, there is dissociation between the presence of local signs of inflammation, as demonstrated by increased skin temperature in the Charcot foot, and the lack of systemic response, as shown by a normal to slight increase in CRP levels, normal WCC, and mild increase in ESR. CRP is one of the well-established sensitive markers of inflammation widely used in clinical practice as a direct serological measure of acute phase response to injury and infection. The local inflammatory response seen in our patients may be related to increased expression of proinflammatory cytokines (3), but this did not lead to a classical systemic acute phase response. Lack of rise of CRP levels in our patients with acute Charcot osteoarthropathy cannot be related to abnormal hepatic synthesis, as both liver enzymes and albumin levels were within the reference range. Although there is evidence that CRP levels are markedly raised in patients with diabetic foot infection and osteomyelitis, some reports have suggested that it might be normal in patients with Charcot osteo-

From the [1]Diabetic Foot Clinic, King's College Hospital, London, U.K.; the [2]Department of Biochemistry, King's College Hospital, London, U.K.; the [3]Department of Diagnostic Radiology, King's College Hospital, London, U.K.; and the [4]Department of Nuclear Medicine, King's College Hospital, London, U.K.

Address correspondence and reprint requests to Dr. Nina Petrova, Diabetic Foot Clinic, King's College Hospital, Denmark Hill, London SE5 9RS. E-mail: petrovanl@yahoo.com.

Received for publication 20 October 2006 and accepted in revised form 31 December 2006.

Abbreviations: CRP; C-reactive protein; ESR, erythrocyte sedimentation rate; WCC, white cell count.

A table elsewhere in this issue shows conventional and Système International (SI) units and conversion factors for many substances.

DOI: 10.2337/dc06-2168

arthropathy (4,5). Indeed, in a small series of patients, serum CRP was significantly lower in patients with Charcot osteoarthropathy compared with patients with osteomyelitis (6). The WCC was normal in our patients with acute Charcot osteoarthropathy. Although the ESR was mildly raised in our patients, this was not related to anemia, as our patients had normal Hb levels. However, ESR has a high sensitivity but a low specificity, and there are many conditions that can lead to a rise in ESR in diabetic patients, including diabetic nephropathy per se. Thus, a moderate rise in ESR may not necessarily indicate the presence of acute Charcot osteoarthropathy (4).

Thus, there is dissociation between the local and systemic inflammatory response in acute Charcot osteoarthropathy. When patients present with a hot red foot, with no obvious skin breakdown and a CRP level that is normal or only slightly raised, acute Charcot osteoarthropathy should be firmly suspected.

Acknowledgments— N.L.P. was supported by Diabetes U.K. Grants BDA: RD 01/002284 and BDA: 05/0003025.

References

1. Frykberg RG, Sanders LJ: Charcot neuroarthropathy of the foot. In *Levin & O'Neal's The Diabetic Foot*. 6th ed. Bowker JH, Phiefer MA, Eds. St. Louis, Missouri, Mosby Press, 2001, p. 439–466
2. Sella EJ, Barrette C: Staging of Charcot neuroarthropathy along the medial column of the foot in the diabetic patient. *J Foot Ankle Surg* 38:34–40, 1998
3. Jeffcoate WJ, Game F, Cavanagh PR: The role of proinflammatory cytokines in the cause of neuropathic osteoarthropathy (acute Charcot foot) in diabetes. *Lancet* 366:2058–2061, 2005
4. Judge MS: Using serologic screening to identify and monitor at-risk Charcot patients. *Podiatry Today* 8:75–82, 2004
5. Pakarinen TK, Laine HJ, Honkonen SE, Peltonen J, Oksala H, Lahtela J: Charcot arthropathy of the diabetic foot: current concepts and review of 36 cases. *Scan J Surg* 1:195–201, 2002
6. Jude EB, Selby PL, Mawer EB, Burgess J, Boulton AJM: Inflammatory and bone turnover markers in Charcot arthropathy and osteomyelitis of the feet in diabetic patients (Abstract). *Diabetologia* 45 (Suppl. 2):A341–A342, 2002

Osteoporos Int (2014) 25:1197–1207
DOI 10.1007/s00198-013-2511-6

REVIEW

Neuropathy and the vascular-bone axis in diabetes: lessons from Charcot osteoarthropathy

N. L. Petrova · C. M. Shanahan

Received: 17 July 2013 / Accepted: 9 September 2013 / Published online: 3 October 2013

Abstract Emerging evidence from the last two decades has shown that vascular calcification (VC) is a regulated, cell-mediated process orchestrated by vascular smooth muscle cells (VSMCs) and that this process bears many similarities to bone mineralization. While many of the mechanisms driving VSMC calcification have been well established, it remains unclear what factors in specific disease states act to promote vascular calcification and in parallel, bone loss. Diabetes is a condition most commonly associated with VC and bone abnormalities. In this review, we describe how factors associated with the diabetic milieu impact on VSMCs, focusing on the role of oxidative stress, inflammation, impairment of the advanced glycation end product (AGE)/receptor for AGE system and, importantly, diabetic neuropathy. We also explore the link between bone and VC in diabetes with a specific emphasis on the receptor activator of nuclear factor κβ ligand/osteoprotegerin system. Finally, we describe what insights can be gleaned from studying Charcot osteoarthropathy, a rare complication of diabetic neuropathy, in which the occurrence of VC is frequent and where bone lysis is extreme.

Keywords Bone fracture · Charcot osteoarthropathy · Diabetes · Neuropathy · RANKL/OPG · Vascular calcification

N. L. Petrova
Diabetic Foot Clinic, King's College Hospital,
Denmark Hill, London SE5 9RS, UK

C. M. Shanahan (✉)
Cellular Signaling, Cardiovascular Division, James Black Centre,
King's College London, 125 Coldharbour Lane,
London SE5 9NU, UK
e-mail: cathy.shanahan@kcl.ac.uk

Introduction

Evidence emerging from the past 20 years has shown that vascular calcification (VC) is a major health problem, associated with increased cardiovascular morbidity and mortality. Calcification or biomineralization of arteries involves the deposition of hydroxyapatite (HA) in the extracellular matrix and occurs at two distinct sites within the vessel wall: the intima and the media [1]. Intimal calcification is commonly found in the aorta and coronary arteries, whereas medial calcification affects large-, medium- and small-sized arteries [2]. Intimal calcification is associated with lipid, macrophages and vascular smooth muscle cells (VSMCs) and occurs in the context of atherosclerosis, whereas medial calcification can exist independently of atherosclerosis and is associated with extracellular matrix components such as elastin and collagen and VSMCs [1]. HA deposition in the intima is often eccentric and is associated with luminal narrowing, plaque formation and rupture [3]. In contrast, medial calcification can occur throughout the vessel media and contributes to vascular stiffness, which in turn increases pulse–wave velocity to decrease diastolic blood pressure and increase systolic blood pressure [1].

It is now well-established that arterial calcification is a regulated, cell-mediated process orchestrated by VSMCs and that this process bears many similarities to bone mineralization [4]. Under normal conditions, VSMCs express potent inhibitors of calcification including matrix Gla protein and pyrophosphate and there are also powerful circulating inhibitors of HA formation such as fetuin A. In calcifying environments, expression or function of these inhibitory proteins is impaired [5]. In addition, VSMCs undergo phenotypic modulation and upregulate expression of a number of bone proteins including the master transcription factors Runx 2 and Msx2, as well as their downstream targets such as bone sialoprotein, osteocalcin and alkaline phosphatase (ALP) which act to further promote mineralization [6]. In particular,

ALP has been shown to degrade the potent calcification inhibitor pyrophosphate to promote VSMC calcification [7]. Concomitant with VSMC phenotypic change, cell death by apoptosis as well as matrix vesicle release, provide membranes and protein complexes that act as a nidus to nucleate mineral [8]. Importantly, many of the signals that promote VSMC osteo/chondrocytic change also have profound effects on bone mineralization leading to the suggestion that these processes not only share features in common, but may also be pathologically linked in some disease processes [4].

Whilst many of the mechanisms driving VSMC calcification have been well established, it remains unclear what factors in specific disease states act to promote vascular calcification and in parallel, bone loss. Diabetes is a condition most commonly associated with VC and bone abnormalities and with the global increase in the prevalence of diabetes, the burden of VC and its related adverse outcomes is also expected to rise (http://www.idf.org/diabetesatlas/5e/mortality). Indeed, VC is four times more common in diabetic patients compared with healthy subjects [9] and is associated with significant morbidity and mortality [10, 11]. It is a significant predictor of future fatal and nonfatal myocardial infarction, stroke and amputation [12] and is also a strong independent predictor of cardiovascular mortality in type 2 diabetes [13]. It is associated with the duration of diabetes, poor glycaemic control and nephropathy [10] but is often independent of chronic kidney disease [14], as it also occurs in subjects with preserved renal function [11], suggesting that diabetes itself can modulate calcification. Patients with diabetes are also at greater risk of developing osteoporosis and fragility fractures [15], and a link between VC and impaired bone health is now well established [16].

Many factors lead to the development of VC in diabetes, and drivers that require specific attention include oxidative stress, inflammation and derangement in the advanced glycation end product (AGE)/receptor for AGE (RAGE) system. Although these factors are common players in the pathogenesis of VC per se, in diabetes their importance is further emphasised by their association with the development of diabetic neuropathy, a common complication of diabetes, identified as the harbinger of VC [17]. Importantly, neuropathy not only modulates various pathways and mechanisms that cause calcification in diabetes [17] but also impacts on bone mineralization. The receptor activator of nuclear factor κβ ligand (RANKL)/osteoprotegerin (OPG) signalling pathway is of particular importance as these factors are key regulators of VC and bone loss potentially modulated by neuropathy, via the calcitonin-gene related protein (C-GRP) [18]. Disturbance of this pathway is significantly marked in Charcot osteoarthropathy, a rare complication of diabetes presenting with specific neuropathy, extensive local VC and severe osteolysis. However, the interactions between these pathologies have not been fully investigated.

To address this deficit, in this review, we describe how factors associated with the diabetic milieu impact on VSMCs to promote calcification and we also explore the link between bone and VC in diabetes with a specific emphasis on the RANKL/OPG system. Finally, we describe what lessons can be learnt from Charcot osteoarthropathy, where VC and extreme bone lysis occur concomitantly, in the context of neuropathy and inflammation.

Vascular calcification and neuropathy are linked in diabetes

Both intimal and medial artery calcification correlate with significant cardiovascular morbidity and are important predictors of cardiovascular mortality [1]. In diabetes, VC occurs at both anatomical sites and although either process may arise independently, a combination of intimal and medial calcification is frequently found [19]. Factors commonly associated with driving intimal calcification and atherosclerosis include oxidative stress, inflammation and accumulation of AGEs although these may also contribute to medial calcification. In contrast, neuropathy appears to be exclusively associated with medial calcification suggesting that the neuropathic environment has adverse effects on local VSMCs. However, both processes are likely to be interlinked as inflammation, oxidative stress and AGE/RAGE derangement can also lead to nerve impairment and hence neuropathy. Thus, there may be a vicious cycle of VSMC and nerve damage, which acts synergistically to further promote VC in the context of diabetic neuropathy (Fig. 1). How these factors potentially act to drive both VSMC and nerve damage are described below [17].

Oxidative stress

Oxidative stress plays a critical role in the pathobiology of VC [20] and has been identified as a key event in the pathogenesis of diabetic complications. Chronic hyperglycaemia leads to excessive free radical production and oxidative stress resulting in cellular injury and death. Increased oxidative stress occurs early in the onset of diabetes and is characterised by the presence of a decreased antioxidant capacity and an increased rate of lipoperoxidation [21] with clinical studies suggesting that this environment may be associated with the development of intimal calcification. For example, increased levels of oxidised low-density lipoprotein (LDL) immune complexes at baseline, in patients with type 1 diabetes, were associated with an increased risk of developing clinically significant coronary artery calcification, detected by computed tomography after a period of 11–20 years [22]. Atherosclerotic plaques contain high levels of oxysterols [23] which enhance VSMC calcification in vitro by inducing increased ALP activity and apoptosis [24]. Moreover, numerous studies have implicated reactive

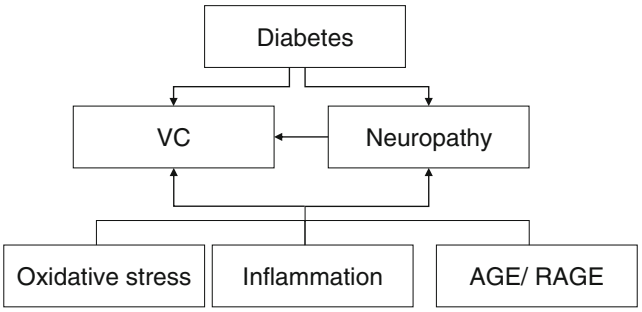

Fig. 1 Interaction between common risk factors for VC and neuropathy in diabetes. Diabetes is associated with VC and neuropathy and these two pathologies share common risk factors including oxidative stress, inflammation and AGE/RAGE derangement. Neuropathy is also linked with VC. It is possible that in diabetes, there may be a vicious cycle of parallel VSMC and nerve damage, which acts synergistically to further promote VC

oxygen species (ROS) in promoting the phenotypic switch of VSMCs from a contractile to an osteogenic phenotype, characterised by increased expression of the key osteogenic differentiation factor Runx2 [25]. In addition, hyperglycemia-induced oxidative stress is also associated with inflammation, another factor shown to promote VC in diabetes [26].

Inflammation

Inflammatory markers including acute-phase response proteins (C-reactive protein (CRP), haptogobin, fibrinogen, plasminogen activator inhibitor and serum amyloid A) as well as cytokines (tumour necrosis factor α (TNF-α) and interleukin-6) are raised in type 2 diabetes and correlate with calcification [27]. Raised inflammatory markers in patients with type 1 diabetes are also strongly associated with the progression of coronary artery calcification [28], while increased plasma levels of high sensitivity CRP and matrix GLA protein have been noted in patients with type 2 diabetes, suggesting that the process of VC may be paralleled by low-grade inflammation [29].

Raised levels of ROS and inflammatory cytokines in diabetes may link vascular and nerve damage. Chronic hyperglycaemia has been shown to promote endogenous TNF-α production by activated macrophages in microvascular and neural tissues, promoting increased microvascular permeability, hypercoagulation and associated nerve damage [30]. Hyperglycaemia-induced oxidative stress also leads to increased TNF-α expression in response to oxidised LDL, and evidence from pigs with streptozotocin-induced diabetes has shown increased expression of TNF-α and IL-6 in both the coronary media and adventitia, as a result of increased ROS production via augmented NAD(P)H oxidase activity [31]. Importantly, the proinflammatory cytokines TNF-α and IL-6 have been identified as key cytokines involved in promoting VC. These factors have been shown to promote VSMC osteogenic differentiation in vitro as blocking antibodies can inhibit TNF-α-induced ALP activity in human VSMCs. Upregulation of adventitial TNF-α production by activated monocytes and macrophages has also been shown to induce pro-calcific MSX-2 activity via the NF-kappaB pathway and paracrine Wnt signalling cascades leading to mural calcification and fibrosis via activation of mesenchymal progenitors in the arterial wall [32]. IL-6 can induce osteoblastic differentiation of VSMCs by increasing STAT3 phosphorylation and ALP activity [33] and in diabetes, IL-6 also triggers increased expression of heat shock proteins, thus potentiating bone morphogenic protein (BMP)2/4 action to promote VSMC osteogenic differentiation [34].

AGE/RAGE

A further signalling pathway that may be important in the pathogenesis of VC in diabetes is the AGE/RAGE system. Hyperglycaemia increases protein glycation and leads to formation of AGEs and tissue accumulation of fluorescent AGEs, detected by skin autofluorescence, is a significant predictor of cardiac mortality in diabetic patients [35]. Some of the biological effects of AGEs are modulated through the interaction with RAGE which activates signalling pathways leading to cellular dysfunction, organ damage and subsequently to complications. In diabetes, activation of AGEs/RAGE contributes to the acceleration of vascular inflammation as a result of enhanced inflammatory gene expression and proatherogenic responses in VSMCs [36].

Activation of RAGE plays a central role in the development of accelerated atherosclerosis in diabetes. A study in streptozotocin-induced diabetic RAGE (−/−)/apolipoprotein E (apoE−/−) double knockout mice clearly showed that RAGE activation has a central role in the formation and progression of atherosclerotic lesions, as the absence of RAGE was associated with significant attenuation of atherosclerotic plaque. The anti-atherosclerotic effects seen in these mice were associated with reduced expression of ROS and inflammatory cytokines, ultimately leading to reduced leukocyte recruitment [37]. Additional evidence from both animal and cell studies on the role of non-cross-linked and nonfluorescent Nε-carboxymethyl-lysine (CML), a major immunogen of AGEs, on the progression of atherosclerotic calcification, showed that the CML/RAGE axis induces apoptosis of macrophages, followed by osteogenic differentiation of VSMCs [38]. Furthermore, in vitro RAGE activation has been shown to induce osteogenic differentiation of VSMCs through Notch/MSX-2 induction, providing further evidence of its role in VC [39].

Diabetic neuropathy

Neuropathy is a common complication of diabetes and is an important risk factor for diabetic foot complications [40]. The first evidence to suggest the link between neuropathy and

calcified arteries came from clinical observations of diabetic foot patients [41] where it was noted that VC and bone loss often have a predominant peripheral distribution, similar to the distal "stocking" distribution of neuropathy. Calcified arteries can be identified on plain foot and ankle radiographs and recognised by the typical "pipe-stem or tramline" appearance of continuous parallel lines of calcification of foot and leg arteries [41]. This distal distribution suggests an interaction with peripheral diabetic neuropathy and indeed impaired vibration sensation, a clinical measure of neuropathy, has long been noted as a risk factor for VC [10]; more recently, a significant association between distal sensorimotor polyneuropathy and VC has been documented [9].

Studies focused on histological examination of the peripheral artery specimens from diabetic patients with neuropathy revealed medial calcification, characterised by the presence of calcified elastic fibres in the mildly affected arteries, to extensive calcium deposits and areas of true bone formation in the advanced lesions [19, 42]. Using immunohistochemisty and in situ hybridization, it was demonstrated that calcified vessels from diabetic patients showed diminished expression of matrix Gla-protein and osteonectin, key inhibitors of vascular calcification. Conversely, they showed increased expression of ALP, bone sialoprotein, bone Gla protein and collagen II—indicators of osteo/chondrogenesis [19].

Importantly, inflammation, oxidative stress and AGEs/RAGE disturbances are common players in the pathogenesis of both VC and neuropathy that impact on VSMCs and nerve fibres [43–45. Excess production of mitochondrial ROS and reactive nitrogen species is a pivotal step in hyperglycemia-induced nerve damage [46]. It is also the main cause of nerve damage in diabetic patients with good overall glucose control, as a result of short episodes of postprandial hyperglycaemia and increased ROS production [43]. Subclinical inflammation is also associated with the development of neuropathy in vivo [47] while in animal models, inactivation of TNF-α via either genetic inactivation or by neutralisation of the TNF-α protein using the monoclonal antibody infliximab, ameliorates diabetic neuropathy in mice [48]. Tissue accumulation of fluorescent AGEs, detected by skin autofluorescence, is associated with the severity of diabetic neuropathy [49] and accumulation of AGEs has been noted in peripheral nerves from diabetic rats and dogs [50]. Moreover, the absence of RAGE attenuates both structural and electrophysiological changes within the peripheral nerves in diabetic $RAGE^{-/-}$ mice [51]; it has been postulated that strategies targeting RAGE activation could be helpful to prevent both diabetic vascular complications and neuropathy.

Thus, the same factors and their complex interactions in "at risk" individuals modulate the occurrence and progression of both VC and nerve damage. However, an association does not always mean causation. While the same factors may drive both vascular and nerve damage concomitantly, it remains unknown whether loss of trophic factors, from damaged nerves in neuropathic tissues in diabetes, directly impacts on the vessel wall to drive VSMC-mediated calcification.

The impact of neuropathy on VC and bone in diabetes—the role of RANKL/OPG

Neuropathy may also provide a link between the vasculature and the skeletal system [18]. A high prevalence and coincidence of VC and cardiovascular disease in patients with osteoporosis has been well documented [52–54] and such an association has also been noted in patients with diabetes. Moreover, patients with both type 1 (due to underlying osteopenia) and type 2 diabetes (due to impaired bone quality and increased risk of falls) have increased osteoporotic fracture risk [15], while osteopenia in the diabetic lower limb is associated with peripheral nerve damage [55, 56].

The interaction between arteries and bone in diabetes is complex. However, one signalling pathway which could account for this association is the RANKL/OPG cytokine system [57, 58], which is also potentially modulated by neuropathy [18]. This cytokine system was initially linked with bone break down as RANKL, a cytokine from the TNF superfamily, has been described as a key regulator of osteoclast maturation and differentiation. RANKL binds to its target RANK, expressed on mononuclear osteoclastic precursors, induces NF-kβ signalling, resulting in NF-kβ translocation to the nucleus and drives osteoclastogenesis [59]. Apart from bone-forming osteoblasts, it has been shown that RANKL is expressed by a variety of cells including endothelial cells, T-cells, dendritic cells and fibroblasts. OPG, a soluble decoy receptor for RANKL, blocks the interaction between RANKL-RANK, thus acting as an antagonist for RANKL [59].

The first evidence to suggest the importance of the RANKL/OPG signalling pathway in the pathogenesis of calcification came from animal knockout studies. Mice lacking OPG develop arterial calcification of the aorta and renal arteries together with severe osteoporosis [60], and conversely transgenic mice overexpressing OPG develop osteopetrosis [61]. These important observations have led to a number of studies exploring this signalling pathway and its link with VC. There is evidence that calcified arteries of $OPG^{-/-}$ mice express RANKL and RANK, proteins not normally present in non-calcified arteries [62]. Similarly, a study in atherosclerotic human arteries has shown the presence of OPG and RANKL in advanced calcified lesions [63]. In vitro studies revealed that VSMCs incubated with RANKL, show a dose-dependent increase in calcification via RANKL/RANK interaction, associated with increased expression of BMP4 [64]. RANK activation leads to nuclear translocation of NF-kβ with involvement only of the alternative pathway with IKK-α activation, but not of the classical pathway of IKK-β. Furthermore, the process of

calcification was abolished by co-inhibition with OPG [64]. Immunohistochemistry of atherosclerotic tissue specimens revealed that OPG is deposited at sites of calcification [65], and this may be a protective mechanism to block RANKL-induced calcification. Paradoxically, OPG inhibits calcification of VSMCs induced by high calcium/phosphate treatment only in physiological concentrations, as its inhibitory effect is blunted at high concentrations [65]. This observation of a bi-phasic effect of its action on calcification supports the clinical findings of elevated serum OPG levels in patients with vascular disease and it has been suggested that this glycoprotein could serve as a marker of arterial vascular damage [65].

Similarly, in diabetes, serum OPG levels are raised [66], and significantly correlate with cardiovascular mortality [67]. In a 17-year prospective observational follow-up study in type 2 diabetes, elevated plasma OPG was a strong predictor of all-cause mortality, an effect which was independent of kidney function [68]. Furthermore, high serum OPG levels but not fibroblast growth factor 23 and 25-hydroxyvitamin D3 (modulators of VC in renal disease) were closely associated with the presence of arterial calcification in patients with type 2 diabetes [69]. Thus, in diabetes, there is a shift in classical factors known to modulate VC in chronic kidney disease, providing further evidence to support the notion that VC in diabetes is independent from progression of diabetic nephropathy [69].

Interestingly, it has been recently postulated that upregulated RANKL-mediated effects on arteries and bone could be triggered by the loss of nerve-derived peptides, e.g. calcitonin gene-related peptide (CGRP) [18]. The latter is a neuropeptide that acts as a neurotransmitter in small fibres (C-fibres) [70]. Local innervation plays a modulating role in bone growth, repair and remodelling. The terminal structure of the osseous CGRP-containing nerves directly contact osteoblasts, osteoclasts and the periosteal lining cells, and are a source of local CGRP, which can act as a local modulator of bone metabolism. CGRP increases osteoblastic cyclic adenosine monophosphate via acting on bone specific CGRP receptors [71] thus stimulating osteogenesis [72]. Osseous CGRP-containing fibres are also involved in pathologic events in bone. The density of CGRP fibres is increased near sites of post-fracture osteogenesis (healing callus) and is decreased at the stumps of non-union [73]. Evidence from bone marrow macrophage cultures has shown that CGRP inhibits RANKL-induced NF-κB activation, downregulates osteoclastic genes like tartarate-resistant acid phosphatase (TRAP) and cathepsin K, decreases the number of TRAP+ cells and RANKL-mediated bone resorption [74]. Interestingly, CGRP is also known as a potent vasodilatory peptide and an inhibitor of vascular hypertrophy. Loss of CGRP innervation in large vessels in rats contributes to age-related hypertrophy of VSMCs and intimal thickening [75]. However, whether it has any direct effects on VC has not been explored.

Thus, CGRP deficiency in diabetes may lead to impaired osteogenesis and delayed fracture healing, and also increased RANKL-mediated osteoclastic activity. It may also be responsible for enhanced RANKL-mediated calcification as calcified arteries and bone loss are frequently seen in patients with diabetic neuropathy. Although the full impact of neuropathy on vascular damage and bone loss has not been fully investigated, the magnitude of this interaction may be most dramatically illustrated in Charcot osteoarthropathy.

VC and bone destruction in Charcot osteoarthropathy are mediated via the RANKL/OPG signalling pathway

The association between diabetic neuropathy and VC extends to neuropathy-related complications including foot ulceration, osteomyelitis and Charcot osteoarthropathy. VC in peripheral arteries was reported in 54 % of patients presenting with uncomplicated foot ulcer and in 66 % of patients with osteomyelitis [76]. A condition in which VC is particularly common is Charcot osteoarthropathy (or Charcot foot) [76]; in some groups, VC has been observed in up to 90 % of cases [77]. This rare but devastating complication of diabetes requires specific attention as it links VC, neuropathy and bone destruction in diabetes and could provide novel insights into the interactions between these processes.

Although neuropathic joint disease has been associated with many conditions such as tabes dorsalis, syringomyelia, leprosy, hereditary sensory neuropathy and familial amyloid neuropathy, in the twenty-first century, Charcot foot is most frequently seen in patients with diabetes [77]. It has been reported that a prevalence of 1:680 of people with diabetes develop this condition [78]; however, more recent radiological analysis has shown the presence of Charcot joints on foot and ankle radiographs in up to 10 % of the patients with diabetes and neuropathy [79]. It commonly presents in the mid-foot with severe metatarsal/tarsal fracture/dislocation (Fig. 2) but also occurs in the forefoot and hind foot [77]. Rarely, in diabetes, the knee and the wrist can be affected [77]. Neuropathic joint disease is associated with enormous morbidity and disability [80]. The development of Charcot osteoarthropathy is preceded by trauma which subsequently leads to severe bone and joint destruction, foot deformity, ulceration and then sepsis and often amputation. It is also associated with significant mortality [81, 82], possibly related to the high prevalence of VC and extensive neuropathy, affecting not only the peripheral nervous system but also the autonomic nervous system [17].

The exact mechanisms which link neuropathy, VC and bone loss in Charcot osteoarthropathy are not fully understood but evidence from the last few years has highlighted the importance of RANKL/OPG. This signalling pathway is upregulated in patients with Charcot osteoarthropathy who exhibit elevated serum levels of RANKL, OPG and RANKL/OPG ratio [73],

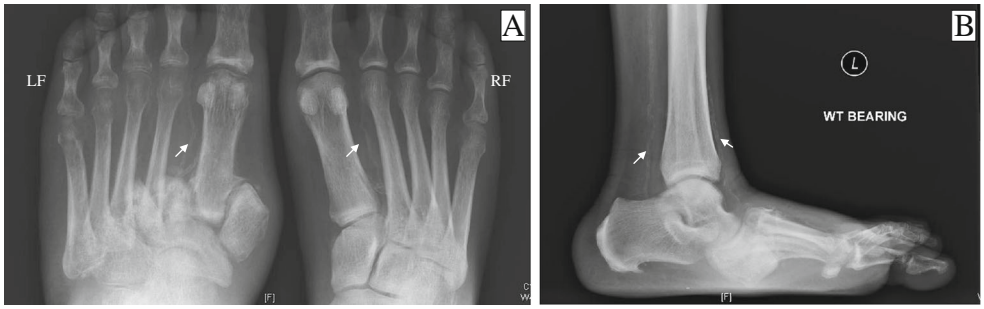

Fig. 2 Anterior–posterior foot radiograph (**a**) and lateral ankle radiograph (**b**) in a patient with left foot Charcot osteoarthropathy. Severe metatarsal-tarsal Lisfranc fracture/dislocation of the left mid-foot (**a**) with collapse of the medial arch and associated rocker-bottom foot deformity (**b**). Bilateral VC of the left and right dorsalis pedis arteries (**a**) and of the left posterior tibial and anterior tibial arteries (**b**) (*white arrows*)

with high serum OPG significantly associated with the presence of VC in foot and leg arteries in neuropathic patients [83].

In the vasculature histological examination of tibial peripheral artery specimens from Charcot patients, undergoing surgery identified positive RANKL staining in both medial and intimal calcified areas, which were not present in non-calcified areas or in specimens from control subjects [84]. Moreover, VSMCs from Charcot patients treated with RANKL show a greater capacity to mineralise and this increased osteoblastic differentiation was inhibited by OPG, confirming the role of RANKL in the process of calcification [84]. In bone, evidence from in vitro studies has shown that newly formed osteoclasts, derived from patients with Charcot osteoarthropathy, exhibit extensive resorbing activity in the presence of macrophage-colony stimulating factor (a survival factor) and RANKL, a response which is attenuated by OPG [85]. Thus, in the vessel wall, progenitor cells differentiate into osteoblast-like cells, depositing mineralised matrix, whereas in bone, the enhanced osteoclastic activation results in osteolysis and severe bone damage [86].

If RANKL and OPG are key players in both VC and bone loss in Charcot osteoarthropathy, what are the factors that activate this pathway? Importantly, evidence suggests that both neuropathy and inflammation may be causal.

Neuropathy and inflammation promote RANKL/OPG

The exact type of nerve damage in the pathogenesis of Charcot foot is not fully understood. However, a selective small fibre neuropathy has been noted [87] with a possible impairment of C-fibres and associated lack of CGRP. Whether CGRP modulates the vessel wall in diabetes is unknown; however, a small pilot immunohistological study has shown a trend towards reduced expression of CGRP in bone specimens from Charcot patients compared with controls [31]. The role of CGRP deficiency in the aetiology of Charcot osteorthropathy has not been fully proven; however, it is thought that deficiency of this neuropeptide may enhance the ratio of RANKL to OPG and thus promote VC and accelerate bone resorption [88]. Further work on the direct effects of CGRP on diabetic vessels and bone is now required.

A red hot inflamed foot is the classical clinical presentation of Charcot osteoarthropathy and uncontrolled inflammation has been shown to have deleterious effect on both vessels and bone. Indeed, VSMCs treated with Charcot serum showed increased capacity to mineralise suggesting that there are secreted mediators including proinflammatory cytokines, which can directly induce osteoblastic differentiation of VSMCs and promote calcification within the Charcot milieu [84]. Indeed, Charcot patients present with raised serum inflammatory markers (hsCRP, TNF-α and IL-6) as well as markers of bone resorption (C-terminal telopeptide of type I collage and alkaline phosphatase) when compared with controls [89]. Calcaneal bone mineral density of the affected foot is decreased when compared with the non-affected contralateral foot [90]. A further reduction in bone mineral density of the affected foot is noted in the natural history of the osteoarthropathy and this fall is closely associated with inflammation [91]. Recent in vitro studies on newly formed osteoclasts in patients with Charcot osteoarthropathy also suggest that inflammation modulates osteoclastic activity with a particular interaction between TNF-α, IL-6 and RANKL [92]. It is possible that in Charcot osteoarthropathy, TNF-α could promote bone resorption, as this pro-inflammatory cytokine not only induces RANKL expression but also enhances osteoclastogenesis in the presence of permissive levels of RANKL (Fig. 4) [93]. This is in agreement with a previous histological study of bone specimens from Charcot patients which has demonstrated that osteoclastic bone resorption is taking place in the presence of TNF-α, and IL-1β [94], cytokines also known to modulate VC [95].

All these observations provide firm evidence to support the recent hypothesis of the role of proinflammatory cytokines and RANKL activation in the pathogenesis of Charcot osteoarthropathy [96] and these could also promote VC. Questions that remain to be answered are why VC is common in diabetic neuropathy, whereas bone destruction leading to Charcot joints affects only a small subset of patients.

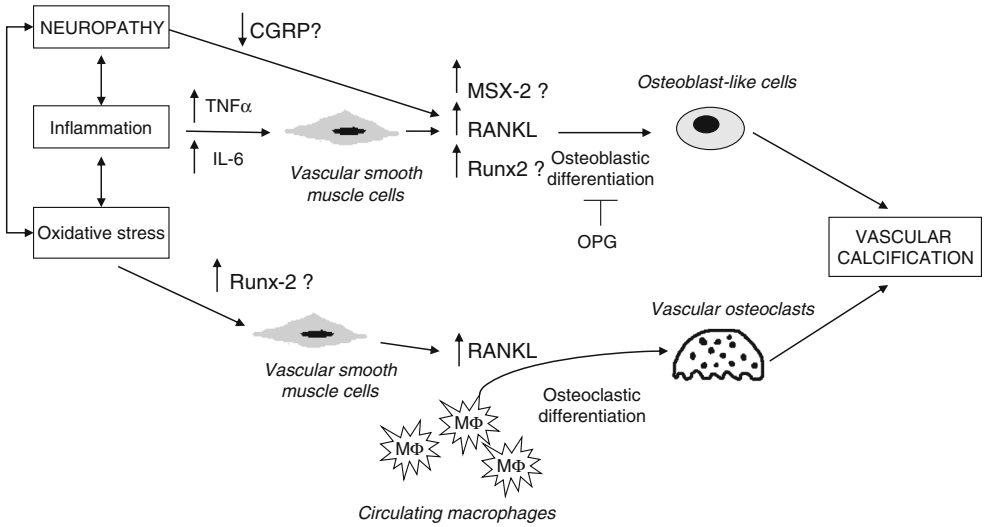

Fig. 3 The potential role of RANKL in the pathogenesis of VC in Charcot osteoarthropathy. In neuropathy, activation of VSMCs via lack of CGRP and inflammation associated with a rise in TNF-α and IL-6 could upregulate RANKL and possibly MSX-2 and Runx2 resulting in enhanced osteoblastic activity and formation of osteoblast-like cells. Upregulated Runx-2 in VSMCs in response to oxidative stress leads to enhanced RANKL expression due to direct promoter binding. RANKL attracts circulating microphages which differentiate into vascular osteoclasts. This results in mineralisation and true bone formation in the vessel wall ultimately leading to VC

One possible explanation is that there may be feedback mechanisms which elaborate RANKL signalling in both the vasculature and bone in the Charcot foot. For example, the osteogenic transcription factor Runx2, which is upregulated in the calcified vessel wall, is known to bind directly to the promoter region of RANKL and to promote its expression [97]. Increased RANKL in the vessel wall results in enhanced migration and differentiation of macrophages into osteoclast-like cells, ultimately leading to calcification and true bone formation in the affected arteries (Fig. 3) [98]. It is thought that these osteoclast-like cells may drive VC. It is plausible that in the context of Charcot foot, where there is great availability/differentiation of osteoclastic precursors [99], that VC is accelerated via this pathway. Moreover, in bone, trauma (with or without fracture), sets off an exaggerated inflammatory response with the release of proinflammatory cytokines and RANKL activation [96]. Fracture itself triggers a coordinated healing cytokine response with enhanced production of IL-1 and TNF-α [100]. Cytokine stimulation of the endothelium results in upregulation of receptors and adhesion molecules which in turn are capable of forming firm attachment with osteoclast precursors [94]. Furthermore, RANKL itself exhibits chemotactic properties towards human monocytes (osteoclastic precursors) [88]. Thus, local inflammation and enhanced RANKL expression may contribute to fracture and bone destruction as well as VC in Charcot osteoarthropathy (Fig. 4).

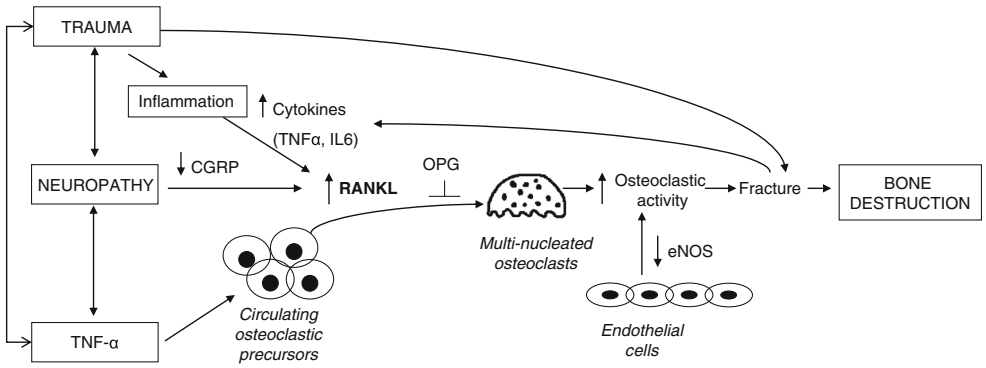

Fig. 4 The potential role of RANKL in bone destruction in Charcot osteoarthropathy. Nerve damage in diabetes is associated with loss of CGRP and increased RANKL-mediated osteoclastic activity. Trauma itself triggers an inflammatory response with a rise in TNF-α and IL-6, which modulates RANKL activation and osteoclastogenesis. TNF-α itself acts on osteoclast precursors and has a synergistic effect with RANKL on osteoclast activation. The increased local RANKL expression exhibits chemotactic properties towards circulating osteoclastic precursors resulting in increased osteoclastic activity, bone fracture and ultimately bone destruction. Reduced endothelial expression of nitric oxide synthase (eNOS) in diabetic neuropathy also contributes to this increased osteoclastic activity in the diabetic neuropathic foot

Although the interaction between VC, bone lysis and neuropathy in Charcot osteoarthropathy is highly probable, it has yet to be established why the frequently seen VC in diabetic peripheral neuropathy is bilateral, whereas the occurrence of Charcot joints is more commonly unilateral and is associated with the site of foot trauma and inflammation. Furthermore, RANKL itself has contrasting action on vessels and bone. In the vasculature, upregulated RANKL promotes both osteoclast differentiation of macrophages and osteoblast differentiation of progenitor cells (via binding with RANK expressed by VSMCs) [64, 98], whereas in bone, its effects are mainly limited to osteoclast regulation [86]. Furthermore, the temporal association between VC and bone destruction in Charcot osteoarthropaty is unknown. Although VC is frequently seen in diabetic neuropathy, only a subset of patients develops Charcot joints. Furthermore, it is not clear whether the local production of RANKL and cytokines in the vessels could increase osteoclastic activity and lead to destruction of bone through loss of mineral [86]. Alternatively, release of calcium and minerals could modulate the process of VC in Charcot osteoarthopathy, although evidence to support this hypothesis is sparse. A better understanding of the mechanisms and interaction of VC and bone could contribute to better management of this condition, as the current standard of treatment includes only casting immobilisation during the acute active stage of bone destruction [101]. Although recent studies have highlighted the importance of RANKL and inflammation in the pathogenesis of osteoclast activation and VC in Charcot osteoarthropathy, currently, there is no clinical experience with the use of therapies aimed to inhibit RANKL or TNF-α activation [101].

In addition, emerging evidence suggests that other potential vascular/bone pathways, mediated by neuropathy, may also be involved. Endothelial nitric oxide synthase (eNOS) is the enzyme that generates the vasoprotective molecule nitric oxide which acts to suppress osteoclast activity. In neuropathy, and particularly in Charcot osteoarthropathy, eNOS levels are significantly decreased suggesting endothelial dysfunction could also impact on bone loss [31].

In summary, these studies suggest that enhanced RANKL activity (via neuropathy, inflammation and oxidative stress), as well as other mechanisms, could modulate both VSMCs and osteoclasts and lead to VC and bone destruction. More research is now needed to establish whether VC in diabetic neuropathy identifies subjects "at risk" of developing Charcot osteoarthropathy, or alternatively could neuropathy-related bone destruction itself drive calcium deposition in diabetic arteries.

Conclusions

Bone and vessels are frequently damaged in diabetes and this damage could be modulated by neuropathy. Further studies of the complex relationship between VC and bone damage in the presence of neuropathy are now needed for a better understanding of the mechanisms whereby the diabetic milieu impacts on these processes. Charcot osteoarthropathy, a rare neuropathy-related complication in diabetes, is a useful model of VC and bone destruction, processes mediated via the RANKL/OPG signalling pathway and inflammatory modulators that now requires further investigation with the ultimate aim of devising therapeutics to ameliorate these interrelated and morbid conditions.

Acknowledgments We thank Professor Michael Edmonds for critical reading of the manuscript and useful comments.

Funding support The British Heart Foundation and Diabetes Research and Wellness Foundation supported this study.

Conflict of interests None

References

1. Proudfoot D, Shanahan CM (2001) Biology of calcification in vascular cells: intima versus media. Herz 26:245–251
2. London GM (2011) Arterial calcification: cardiovascular function and clinical outcome. Nefrologia 31:644–647
3. Maldonado N, Kelly-Arnold A, Vengrenyuk Y, Laudier D, Fallon JT, Virmani R, Cardoso L, Weinbaum S (2012) A mechanistic analysis of the role of microcalcifications in atherosclerotic plaque stability: potential implications for plaque rupture. Am J Physiol Heart Circ Physiol 303:H619–H628
4. Iyemere VP, Proudfoot D, Weissberg PL, Shanahan CM (2006) Vascular smooth muscle cell phenotypic plasticity and the regulation of vascular calcification. J Intern Med 260:192–210
5. Shanahan CM, Crouthamel MH, Kapustin A, Giachelli CM (2011) Arterial calcification in chronic kidney disease: key roles for calcium and phosphate. Circ Res 109:697–711
6. Tyson KL, Reynolds JL, McNair R, Zhang Q, Weissberg PL, Shanahan CM (2003) Osteo/chondrocytic transcription factors and their target genes exhibit distinct patterns of expression in human arterial calcification. Arterioscler Thromb Vasc Biol 23:489–494
7. Villa-Bellosta R, Wang X, Millan JL, Dubyak GR, O'Neill WC (2011) Extracellular pyrophosphate metabolism and calcification in vascular smooth muscle. Am J Physiol Heart Circ Physiol 301: H61–H68
8. Kapustin AN, Davies JD, Reynolds JL et al (2011) Calcium regulates key components of vascular smooth muscle cell-derived matrix vesicles to enhance mineralization. Circ Res 109:e1–e12
9. Moon J-S, Clark VM, Beabout JW, Swee RG, Dyck PJ (2011) A controlled study of medial arterial calcification of legs: implications for diabetic polyneuropathy. Arch Neurol 68:1290–1294
10. Everhart JE, Pettitt DJ, Knowler WC, Rose FA, Bennett PH (1988) Medial arterial calcification and its association with mortality and complications of diabetes. Diabetologia 31:16–23
11. Singh DK, Winocour P, Summerhayes B, Kaniyur S, Viljoen A, Sivakumar G, Farrington K (2012) Prevalence and progression of peripheral vascular calcification in type 2 diabetes subjects with preserved kidney function. Diabetes Res Clin Pract 97:158–165
12. Lehto S, Niskanen L, Suhonen M, Ronnemaa T, Laakso M (1996) Medial artery calcification. A neglected harbinger of cardiovascular complications in non-insulin-dependent diabetes mellitus. Arterioscler Thromb Vasc Biol 16:978–983

13. Niskanen L, Siitonen O, Suhonen M, Uusitupa MI (1994) Medial artery calcification predicts cardiovascular mortality in patients with NIDDM. Diabetes Care 17:1252–1256
14. Mehrotra R, Budoff M, Christenson P, Ipp E, Takasu J, Gupta A, Norris K, Adler S (2004) Determinants of coronary artery calcification in diabetics with and without nephropathy. Kidney Int 66:2022–2031
15. Hamann C, Kirschner S, Gunther K-P, Hofbauer LC (2012) Bone, sweet bone—osteoporotic fractures in diabetes mellitus. Nat Rev Endocrinol 8:297–305
16. Bandeira E, Neves AP, Costa C, Bandeira F (2012) Association between vascular calcification and osteoporosis in men with type 2 diabetes. J Clin Densitom 15:55–60
17. Jeffcoate WJ, Rasmussen LM, Hofbauer LC, Game FL (2009) Medial arterial calcification in diabetes and its relationship to neuropathy. Diabetologia 52:2478–2488
18. Jeffcoate W (2004) Vascular calcification and osteolysis in diabetic neuropathy-is RANK-L the missing link? Diabetologia 47:1488–1492
19. Shanahan CM, Cary NRB, Salisbury JR, Proudfoot D, Weissberg PL, Edmonds ME (1999) Medial localization of mineralization-regulating proteins in association with Monckeberg's sclerosis: evidence for smooth muscle cell-mediated vascular calcification. Circulation 100:2168–2176
20. Liu Y, Shanahan CM (2011) Signalling pathways and vascular calcification. Front Biosci 16:1302–1314
21. Marra G, Cotroneo P, Pitocco D, Manto A, Di Leo MAS, Ruotolo V, Caputo S, Giardina B, Ghirlanda G, Santini SA (2002) Early increase of oxidative stress and reduced antioxidant defenses in patients with uncomplicated type 1 diabetes: a case for gender difference. Diabetes Care 25:370–375
22. Lopes-Virella MF, Baker NL, Hunt KJ, Lachin J, Nathan D, Virella G, Group DER (2011) Oxidized LDL immune complexes and coronary artery calcification in type 1 diabetes. Atherosclerosis 214:462–467
23. Brown AJ, Jessup W (1999) Oxysterols and atherosclerosis. Atherosclerosis 142:1–28
24. Liu H, Yuan L, Xu S, Zhang T, Wang K (2004) Cholestane-3beta, 5alpha, 6beta-triol promotes vascular smooth muscle cells calcification. Life Sci 76:533–543
25. Byon CH, Javed A, Dai Q, Kappes JC, Clemens TL, Darley-Usmar VM, McDonald JM, Chen Y (2008) Oxidative stress induces vascular calcification through modulation of the osteogenic transcription factor runx2 by AKT signaling. J Biol Chem 283:15319–15327
26. Node K, Inoue T (2009) Postprandial hyperglycemia as an etiological factor in vascular failure. Cardiovasc 8:23
27. Donath MY, Shoelson SE (2011) Type 2 diabetes as an inflammatory disease. Nat Rev Immunol 11:98–107
28. Alman AC, Kinney GL, Tracy RP, Maahs DM, Hokansen JE, Rewere MJ, Snell-Bergeon JK (2013) Prospective association between inflammatory markers and progression of coronary artery calcification in adults with and without type1 diabetes. Diabetes Care 36(7):1967–1973
29. Thomsen SB, Rathcke CN, Zerahn B, Vestergaard H (2010) Increased levels of the calcification marker matrix gla protein and the inflammatory markers YKL-40 and CRP in patients with type 2 diabetes and ischemic heart disease. Cardiovasc 9:86
30. Satoh J, Yagihashi S, Toyota T (2003) The possible role of tumor necrosis factor-alpha in diabetic polyneuropathy. Exp Diabesity Res 4:65–71
31. La Fontaine J, Harkless LB, Sylvia VL, Carnes D, Heim-Hall J, Jude E (2008) Levels of endothelial nitric oxide synthase and calcitonin gene-related peptide in the Charcot foot: a pilot study. J Foot Ankle Surg 47:424–429
32. Thompson B, Towler DA (2012) Arterial calcification and bone physiology: role of the bone-vascular axis. Nat Rev Endocrinol 8:529–543
33. Abedin M, Lim J, Tang TB, Park D, Demer LL, Tintut Y (2006) N-3 fatty acids inhibit vascular calcification via the p38-mitogen-activated protein kinase and peroxisome proliferator-activated receptor-gamma pathways. Circ Res 98:727–729
34. Shao J-S, Cheng S-L, Sadhu J, Towler DA (2010) Inflammation and the osteogenic regulation of vascular calcification: a review and perspective. Hypertension 55:579–592
35. Lutgers HL, Graaff R, Links TP, Ubink-Veltmaat LJ, Bilo HJ, Gans RO, Smit AJ (2006) Skin autofluorescence as a noninvasive marker of vascular damage in patients with type 2 diabetes. Diabetes Care 29:2654–2659
36. Li S-l, Reddy MA, Cai Q, Meng L, Yuan H, Lanting L, Natarajan R (2006) Enhanced proatherogenic responses in macrophages and vascular smooth muscle cells derived from diabetic db/db mice. Diabetes 55:2611–2619
37. Soro-Paavonen A, Watson AMD, Li J et al (2008) Receptor for advanced glycation end products (RAGE) deficiency attenuates the development of atherosclerosis in diabetes. Diabetes 57:2461–2469
38. Wang Z, Jiang Y, Liu N, Ren L, Zhu Y, An Y, Chen D (2012) Advanced glycation end-product *N*-carboxymethyl-lysine accelerates progression of atherosclerotic calcification in diabetes. Atherosclerosis 221:387–396
39. Suga T, Iso T, Shimizu T, Tanaka T, Yamagishi S-i, Takeuchi M, Imaizumi T, Kurabayashi M (2011) Activation of receptor for advanced glycation end products induces osteogenic differentiation of vascular smooth muscle cells. J Atheroscler Thromb 18:670–683
40. Tesfaye S, Boulton AJM, Dyck PJ et al (2010) Diabetic neuropathies: update on definitions, diagnostic criteria, estimation of severity, and treatments. Diabetes Care 33:2285–2293
41. Edmonds ME, Morrison N, Laws JW, Watkins PJ (1982) Medial arterial calcification and diabetic neuropathy. Br Med J (Clin Res Ed) 284:928–930
42. Shanahan CM (2007) Inflammation ushers in calcification: a cycle of damage and protection? Circulation 116:2782–2785
43. Vincent AM, Russell JW, Low P, Feldman EL (2004) Oxidative stress in the pathogenesis of diabetic neuropathy. Endocr Rev 25:612–628
44. Yorek MA (2003) The role of oxidative stress in diabetic vascular and neural disease. Free Radic Res 37:471–480
45. Huijberts MSP, Schaper NC, Schalkwijk CG (2008) Advanced glycation end products and diabetic foot disease. Diabetes Metab Res Rev 24(Suppl 1):S19–S24
46. Figueroa-Romero C, Sadidi M, Feldman EL (2008) Mechanisms of disease: the oxidative stress theory of diabetic neuropathy. Rev Endocr Metab Disord 9:301–314
47. Herder C, Lankisch M, Ziegler D et al (2009) Subclinical inflammation and diabetic polyneuropathy: MONICA/KORA survey F3 (Augsburg, Germany). Diabetes Care 32:680–682
48. Yamakawa I, Kojima H, Terashima T et al (2011) Inactivation of TNF-α ameliorates diabetic neuropathy in mice. Am J Physiol Endocrinol Metab 301:E844–E852
49. Meerwaldt R, Links TP, Graaff R, Hoogenberg K, Lefrandt JD, Baynes JW, Gans ROB, Smit AJ (2005) Increased accumulation of skin advanced glycation end-products precedes and correlates with clinical manifestation of diabetic neuropathy. Diabetologia 48:1637–1644
50. Vlassara H, Brownlee M, Cerami A (1981) Nonenzymatic glycosylation of peripheral nerve protein in diabetes mellitus. Proc Natl Acad Sci U S A 78:5190–5192
51. Toth C, Rong LL, Yang C et al (2008) Receptor for advanced glycation end products (RAGEs) and experimental diabetic neuropathy. Diabetes 57:1002–1017
52. Hak AE, Pols HA, van Hemert AM, Hofman A, Witteman JC (2000) Progression of aortic calcification is associated with metacarpal bone loss during menopause: a population-based longitudinal study. Arterioscler Thromb Vasc Biol 20:1926–1931
53. Kado DM, Browner WS, Blackwell T, Gore R, Cummings SR (2000) Rate of bone loss is associated with mortality in older women: a prospective study. J Bone Miner Res 15:1974–1980

54. den Uyl D, Nurmohamed MT, van Tuyl LH, Raterman HG, Lems WF (2011) (Sub)clinical cardiovascular disease is associated with increased bone loss and fracture risk; a systematic review of the association between cardiovascular disease and osteoporosis. Arthritis Res Ther 13(1):R5
55. Young MJ, Marshall A, Adams JE, Selby PL, Boulton AJ (1995) Osteopenia, neurological dysfunction, and the development of Charcot neuroarthropathy. Diabetes Care 18:34–38
56. Rix M, Andreassen H, Eskildsen P (1999) Impact of peripheral neuropathy on bone density in patients with type 1 diabetes. Diabetes Care 22:827–831
57. Schoppet M, Preissner KT, Hofbauer LC (2002) RANK ligand and osteoprotegerin: paracrine regulators of bone metabolism and vascular function. Arterioscler Thromb Vasc Biol 22:549–553
58. Collin-Osdoby P (2004) Regulation of vascular calcification by osteoclast regulatory factors RANKL and osteoprotegerin. Circ Res 95:1046–1057
59. Boyce BF, Xing L (2008) Functions of RANKL/RANK/OPG in bone modeling and remodeling. Arch Biochem Biophys 473:139–146
60. Bucay N, Sarosi I, Dunstan CR et al (1998) Osteoprotegerin-deficient mice develop early onset osteoporosis and arterial calcification. Genes Dev 12:1260–1268
61. Simonet WS, Lacey DL, Dunstan CR et al (1997) Osteoprotegerin: a novel secreted protein involved in the regulation of bone density. Cell 89:309–319
62. Min H, Morony S, Sarosi I et al (2000) Osteoprotegerin reverses osteoporosis by inhibiting endosteal osteoclasts and prevents vascular calcification by blocking a process resembling osteoclastogenesis. J Exp Med 192:463–474
63. Dhore CR, Cleutjens JP, Lutgens E, Cleutjens KB, Geusens PP, Kitslaar PJ, Tordoir JH, Spronk HM, Vermeer C, Daemen MJ (2001) Differential expression of bone matrix regulatory proteins in human atherosclerotic plaques. Arterioscler Thromb Vasc Biol 21:1998–2003
64. Panizo S, Cardus A, Encinas M, Parisi E, Valcheva P, Lopez-Ongil S, Coll B, Fernandez E, Valdivielso JM (2009) RANKL increases vascular smooth muscle cell calcification through a RANK-BMP4-dependent pathway. Circ Res 104:1041–1048
65. Schoppet M, Kavurma MM, Hofbauer LC, Shanahan CM (2011) Crystallizing nanoparticles derived from vascular smooth muscle cells contain the calcification inhibitor osteoprotegerin. Biochem Biophys Res Commun 407:103–107
66. Browner WS, Lui LY, Cummings SR (2001) Associations of serum osteoprotegerin levels with diabetes, stroke, bone density, fractures, and mortality in elderly women. J Clin Endocrinol Metab 86:631–637
67. Anand DV, Lahiri A, Lim E, Hopkins D, Corder R (2006) The relationship between plasma osteoprotegerin levels and coronary artery calcification in uncomplicated type 2 diabetic subjects. J Am Coll Cardiol 47:1850–1857
68. Reinhard H, Lajer M, Gall M-A, Tarnow L, Parving H-H, Rasmussen LM, Rossing P (2010) Osteoprotegerin and mortality in type 2 diabetic patients. Diabetes Care 33:2561–2566
69. Aoki A, Murata M, Asano T et al (2013) Association of serum osteoprotegerin with vascular calcification in patients with type 2 diabetes. Cardiovasc 12:11
70. Pittenger G, Vinik A (2003) Nerve growth factor and diabetic neuropathy. Exp Diabesity Res 4:271–285
71. Bjurholm A, Kreicbergs A, Schultzberg M, Lerner UH (1992) Neuroendocrine regulation of cyclic AMP formation in osteoblastic cell lines (UMR-106-01, ROS 17/2.8, MC3T3-E1, and Saos-2) and primary bone cells. J Bone Miner Res 7:1011–1019
72. Bernard GW, Shih C (1990) The osteogenic stimulating effect of neuroactive calcitonin gene-related peptide. Peptides 11:625–632
73. Santavirta S, Konttinen YT, Nordstrom D, Makela A, Sorsa T, Hukkanen M, Rokkanen P (1992) Immunologic studies of nonunited fractures. Acta Orthop Scand 63:579–586
74. Wang L, Shi X, Zhao R, Halloran BP, Clark DJ, Jacobs CR, Kingery WS (2010) Calcitonin-gene-related peptide stimulates stromal cell osteogenic differentiation and inhibits RANKL induced NF-kappaB activation, osteoclastogenesis and bone resorption. Bone 46:1369–1379
75. Connat JL, Busseuil D, Gambert S et al (2001) Modification of the rat aortic wall during ageing; possible relation with decrease of peptidergic innervation. Anat Embryol (Berl) 204:455–468
76. Sharma A, Scammell BE, Fairbairn KJ, Seagrave MJ, Game FL, Jeffcoate WJ (2010) Prevalence of calcification in the pedal arteries in diabetes complicated by foot disease. Diabetes Care 33:e66
77. Petrova NL, Edmonds ME (2008) Charcot neuro-osteoarthropathy—current standards. Diabetes Metab Res Rev 24(Suppl 1):S58–S61
78. Sinha S, Munichoodappa CS, Kozak GP (1972) Neuro-arthropathy (Charcot joints) in diabetes mellitus (clinical study of 101 cases). Medicine (Baltimore) 51:191–210
79. Cavanagh PR, Young MJ, Adams JE, Vickers KL, Boulton AJ (1994) Radiographic abnormalities in the feet of patients with diabetic neuropathy. Diabetes Care 17:201–209
80. Sinacore DR, Withrington NC (1999) Recognition and management of acute neuropathic (Charcot) arthropathies of the foot and ankle. J Orthop Sports Phys Ther 29:736–746
81. van Baal J, Hubbard R, Game F, Jeffcoate W (2010) Mortality associated with acute Charcot foot and neuropathic foot ulceration. Diabetes Care 33:1086–1089
82. Gazis A, Pound N, Macfarlane R, Treece K, Game F, Jeffcoate W (2004) Mortality in patients with diabetic neuropathic osteoarthropathy (Charcot foot). Diabet Med 21:1243–1246
83. Edmonds MEKBA, Saldana Chaparro R, Dew T, Stock S, Moniz C, Petrova NL (2009) Serum levels of osteoprotegerin are raised in diabetic peripheral neuropathy and are significantly correlated with peripheral arterial calcification. Diabetologia 52:S97
84. Ndip A, Williams A, Jude EB, Serracino-Inglott F, Richardson S, Smyth JV, Boulton AJM, Alexander MY (2011) The RANKL/RANK/OPG signaling pathway mediates medial arterial calcification in diabetic Charcot neuroarthropathy. Diabetes 60:2187–2196
85. Mabilleau G, Petrova NL, Edmonds ME, Sabokbar A (2008) Increased osteoclastic activity in acute Charcot's osteoarthropathy: the role of receptor activator of nuclear factor-kappaB ligand. Diabetologia 51:1035–1040
86. Alexander MY (2009) RANKL links arterial calcification with osteolysis. Circ Res 104:1032–1034
87. Stevens MJ, Edmonds ME, Foster AV, Watkins PJ (1992) Selective neuropathy and preserved vascular responses in the diabetic Charcot foot. Diabetologia 35:148–154
88. Rogers LC, Frykberg RG, Armstrong DG et al (2011) The Charcot foot in diabetes. Diabetes Care 34:2123–2129
89. Edmonds M, Dew T, Musto R, Thomson S, Sherwood R, Moniz C, Petrova NL (2008) Serum proinflammatory cytokines TNF-alpha and IL-6 are raised in acute Charcot osteoarthropathy and correlate with a marker of bone resorption. Diabetologia 51(Suppl 1):S510
90. Petrova NL, Foster AVM, Edmonds ME (2005) Calcaneal bone mineral density in patients with Charcot neuropathic osteoarthropathy: differences between type 1 and type 2 diabetes. Diabet Med 22:756–761
91. Petrova NL, Edmonds ME (2010) A prospective study of calcaneal bone mineral density in acute Charcot osteoarthropathy. Diabetes Care 33:2254–2256
92. Petrova NL, Shanahan C, Edmonds M (2011) The proinflammatory cytokines TNF-α and IL-6 modulate RANKL-mediated osteoclastic resorption in vitro in patients with acute Charcot osteoarthropathy. Diabetologia 54(Suppl 1):S11
93. Lam J, Takeshita S, Barker JE, Kanagawa O, Ross FP, Teitelbaum SL (2000) TNF-alpha induces osteoclastogenesis by direct stimulation of macrophages exposed to permissive levels of RANK ligand. J Clin Investig 106:1481–1488

94. Baumhauer JF, O′Keefe RJ, Schon LC, Pinzur MS (2006) Cytokine-induced osteoclastic bone resorption in charcot arthropathy: an immunohistochemical study. Foot Ankle Int 27: 797–800
95. Al-Aly Z (2007) Medial vascular calcification in diabetes mellitus and chronic kidney disease: the role of inflammation. Cardiovasc Hematol Disord Drug Targets 7:1–6
96. Jeffcoate WJ, Game F, Cavanagh PR (2005) The role of proinflammatory cytokines in the cause of neuropathic osteoarthropathy (acute Charcot foot) in diabetes. Lancet 366: 2058–2061
97. Sun YBC, Yuan K, Chen J, Mao X, Heath JM, Javed A, Zhang K, Anderson PG, Chen Y (2012) Smooth muscle cell-specific runx2 deficiency inhibits vascular calcification. Circ Res 111:543–552
98. Byon CH, Sun Y, Chen J et al (2011) Runx2-upregulated receptor activator of nuclear factor kB ligand in calcifying smooth muscle cells promotes migration and osteoclastic differentiation of macrophages. Arterioscler Thromb Vasc Biol 31:1387–1396
99. Mabilleau G, Petrova N, Edmonds ME, Sabokbar A (2011) Number of circulating CD14-positive cells and the serum levels of TNF-α are raised in acute charcot foot. Diabetes Care 34:e33
100. Kon T, Cho TJ, Aizawa T, Yamazaki M, Nooh N, Graves D, Gerstenfeld LC, Einhorn TA (2001) Expression of osteoprotegerin, receptor activator of NF-kappaB ligand (osteoprotegerin ligand) and related proinflammatory cytokines during fracture healing. J Bone Miner Res 16:1004–1014
101. Petrova NL, Edmonds M (2013) Medical management of Charcot arthropathy. Diab Obes Met 15:193–197

review article

Diabetes, Obesity and Metabolism 2012.

REVIEW ARTICLE

Medical management of Charcot arthropathy

N. L. Petrova & M. E. Edmonds

Diabetic Foot Clinic, King's College Hospital, London, UK

Charcot arthropathy is a major complication of diabetes and it poses management challenges to health care professionals. Early diagnosis and timely intervention are essential for improved outlook of these patients. Casting therapy has been accepted as the mainstay treatment of the acute Charcot foot, although there are still controversies regarding its duration, the choice of removable and non-removable device and weight-bearing casts vs. non-weight-bearing casts. Two groups of antiresorptive therapies have been evaluated in the treatment of the acute Charcot foot, bisphosphonates (intravenous and oral) and calcitonin. These therapies have clearly shown a reduction of bone turnover, although, they have not shown a significant effect on temperature reduction. Current evidence to support their use is weak. An anabolic agent to speed up clinical resolution and fracture healing may be helpful and a clinical trial to evaluate the possible benefit of 1–84 recombinant human parathyroid hormone on fracture healing in the acute Charcot foot is in progress. This paper summarises the current approach to medical management of acute Charcot arthropathy with specific emphasis on casting and pharmacological therapy. Emerging new studies of the pathogenesis of this condition are also discussed.

Keywords: bisphosphonates, calcitonin, casting therapy, Charcot arthropathy, receptor activator of nuclear factor $\kappa\beta$ ligand (RANKL), TNF-α

Date submitted 4 May 2012; date of first decision 6 June 2012; date of final acceptance 28 July 2012

Charcot neuropathic arthropathy, commonly referred as the Charcot foot, is a rare but devastating complication of type 1 and type 2 diabetes [1]. It presents without warning and can rapidly lead to severe bone and joint destruction resulting in horrendous foot deformity [2]. Predisposing factors are somatic and autonomic neuropathy, osteopenia and renal impairment [3]. It classically presents as unilateral redness and swelling of the foot. These initial signs may be underestimated by the patient because of the co-existing peripheral neuropathy and only 30% report pain or discomfort at presentation [4]. Trauma is an important trigger and has been reported by 22–53% of the patients [2,5]. It commonly presents in the mid-foot but also occurs in the forefoot and hind-foot. Rarely, in diabetes, the knee and the wrist can also be affected by Charcot arthropathy [6–8].

It is extremely important to have a high index of suspicion. This should be followed by a rapid diagnosis and early intervention, and with such a modern approach, many Charcot feet can now be healed and deformity prevented [3].

Medical Management

The medical management of Charcot arthropathy includes casting therapy and treatment with bisphosphonates and calcitonin.

Casting Therapy

Casting therapy is considered as the mainstay in Charcot foot management [9]. It offloads the foot, reduces mechanical forces, oedema and inflammation, redistributes the plantar pressure, limits bone and joint destruction and arrests the progression of deformity [2]. Its overall aim is to maintain a plantigrade foot which can then allow weight-bearing in a shoe or brace. In patients with suspected Charcot feet, instant offloading can arrest the development of the osteoarthropathy. A favourable outcome has been reported in patients in whom casting was initiated early compared with patients with delayed presentation [10]. Only 1 out of 11 index patients developed extended foot fractures and severe deformity in contrast to the 12 out of 13 control patients in whom a late diagnosis has been made [10]. These patients were treated with casting late in the course of the disease, in contrast to the remaining 11 patients in whom offloading was started immediately [10].

Although casting has been accepted as the gold standard treatment for acute Charcot arthropathy, there are still three controversies associated with it. Firstly, the duration of casting therapy, secondly the use of non-removable or removable casts and thirdly should patients be weight-bearing or not.

Duration of Casting Therapy. Duration of casting therapy can vary from an average of 9 weeks to a median of 11 months according to different studies (Table 1). The response to casting therapy is usually monitored by clinical assessment of reduction of redness and swelling of the foot and by reduction of skin foot temperature difference measured by infrared thermometry [15].

The response of Charcot arthropathy to casting therapy has been evaluated by quantitative assessment of activity by bone scanning and skin foot temperatures. There was a strong correlation between temperature difference and the ratio of isotope uptake of the affected and non-affected foot ($r = 0.90$, $p < 0.00001$) [16]. More recently, the role of dynamic MRI in

Correspondence to: Dr Nina L. Petrova, Diabetic Foot Clinic, King's College Hospital, Denmark Hill, London SE5 9RS, UK.
E-mail: petrovanl@yahoo.com

Table 1. Duration of casting therapy in patients treated for acute Charcot arthropathy

Study	Patients/Charcot feet	Duration of casting
Pinzur et al. [11]	10 patients	Average 9.2 weeks (range 8–16 weeks)
De Souza [12]	27 patients/34 feet	Average 14 weeks (range 4–20 weeks)
Armstrong et al. [4]	55 patients	Average 18.5 ± 10.6 weeks (range 4–56 weeks)
Game et al. [13]	219 patients	Median 10 months (range 2–29 months)
Bates et al. [14]	46 patients	Median 11 months (range 8–17 months)

the follow-up of 40 patients treated with casting therapy for acute Charcot arthropathy has been investigated. All patients underwent clinical and MRI follow-up at 3 monthly intervals and there was a strong correlation between clinical and MRI findings in the healing of bony lesions [17].

Removable vs. Non-removable Cast. Although the superiority of non-removable to removable casting has not been evaluated in a randomised controlled study, it is generally accepted that the non-removable cast is the gold standard therapy for Charcot arthropathy. Interestingly, an audit of the current practice, patterns in the initial management of Charcot arthropathy in the United States indicated that total contact casting was the first choice of management in only 49% of cases [18], whereas in the UK, non-removable casts at any one point of time were used only in 34% of the cases [13]. However, this UK web-based survey of the management of acute Charcot arthropathy clearly confirmed a superior outcome and shorter time to resolution in non-removable vs. removable casts [13].

Although there are different modifications of a total contact cast and no one method of its application has been universally accepted, the general rule is that casts should be checked regularly and replaced as necessary [19]. Furthermore, patients should be instructed to monitor their blood glucose levels and body temperature and to check casts for any stains or cracks daily and report immediately if concerned about any cast-related complications (cast rubs, ulcers and infection).

Weight-bearing or Non-weight-bearing Casts. There is no clear evidence as to whether non-weight-bearing cast immobilisation is superior to a weight-bearing one. In a recent study, 27 patients were treated with total contact cast for Charcot arthropathy and were allowed to bear weight as tolerated and no deleterious effect from weight-bearing was reported [12]. Strict non-weight-bearing on the affected foot leads to increased mechanical forces of the contralateral non-affected foot and indeed development of contralateral Charcot arthropathy has been reported in up to 40% of patients [2]. When instituting offloading therapy in a patient, it is important to consider patient's comorbidities and risk of falls. It may be advisable to use crutches for supported walking and/or wheelchair to reduce pressure on both feet and prevent contralateral involvement [20].

Progression from Casts to Footwear

Patients should be changed from cast to shoes when the foot skin temperature difference is less than 2 °C [4]. Casting immobilisation should be followed by a gradual rehabilitation from cast treatment to suitable footwear. When the patient comes out of the cast there will be wasting of the calf muscles and joint stiffness. It is important to be aware of the dangers of reactivating the bony destruction phase by excessive rapid mobilisation or protracted weight bearing in the early stages of rehabilitation. Too rapid mobilisation can be disastrous, resulting in further bone and joint damage and can lead to prolonged casting treatment. Extremely careful rehabilitation should be the rule, beginning with just a few short steps in the new footwear. At this stage patients should be provided with removable bivalve casts or cast walkers which they should wear the majority of time whilst they are gradually rehabilitating into footwear. In patients with hind foot involvement, an alternative to a removable cast or a removable bivalve cast is the Charcot restraint orthotic walker (CROW), which can aid the transition from cast to an ankle–foot orthosis (AFO) with bespoke footwear [3]. This is a bespoke bivalved total-contact device which externally fixates the ankle. The added extra internal padding cushions the vulnerable medial malleolar area and thus prevents ulceration and accommodates deformity. It is used after swelling is controlled and progressive destruction has been halted by total-contact casting.

In the rehabilitation phase, the patient should be instructed to look for swelling, redness and warmth of the foot and encouraged to seek urgent advice as soon as possible to rule out relapse. If there is no increase in warmth, swelling and redness then the patient can walk a few more steps the next day, and very carefully build up to a reasonable amount of walking. Finally, the patient may progress to bespoke footwear with moulded insoles. The transition from cast to shoes is a crucial element of the treatment and this should be performed on an individual approach. Patients need close observation to detect any relapse which will be evident from further swelling and heat in the foot and in one series of patients, relapse was detected in 30% of the cases [14].

In the chronic stable stage, deformity needs to be accommodated, supported or corrected. Patients with Charcot foot deformity should be followed up promptly to prevent secondary ulceration, the risk of which is fourfold higher when compared with the overall risk of foot ulcers in diabetic feet [20].

Pharmacological Management

Current therapies in the treatment of the Charcot foot aim to correct the imbalance between bone resorption and bone formation. There is firm evidence that Charcot arthropathy is associated with increased osteoclastic activity [21] and antiresorptive therapies have been used with some success. Two groups of therapies have been evaluated in the treatment of the acute Charcot foot consisting of bisphosphonates (intravenous and oral) and calcitonin (Table 2), [22–25].

These therapies have clearly demonstrated a reduction of bone turnover. However, they have not shown a significant effect on temperature reduction between the active treatment

Table 2. Antiresorptive therapies in acute Charcot osteoarthropathy

	Bisphosphonates			
Active substance	Pamidronate	Zolendronate	Alendronate	Calcitonin
Study design	Double blind randomised control trial	Double blind randomised controlled trial	Randomised controlled trial	Randomised controlled trial
Subject number	39 21 active/18 placebo	39 18 active/17 placebo	20 11 active/9 controls	32 16 active/16 controls
InterventionActive/ control group	90 mg pamidronate in normal saline/placebo (normal saline)	4 mg zolendronic acid/placebo	70 mg alendronate/9 control subjects	Salmon calcitonin 200 IU + calcium supplementation/calcium supplementation
Route of administration	i.v./i.v.	i.v./i.v.	Oral once a week/nil	nasal spray + oral/oral
Duration of intervention	Single dose infusion for 4 h	Three infusions in 1 month intervals	6 months – weekly	6 months – daily
Reduction in skin foot temperatures	Non-significant active vs. placebo	N/A	Non-significant active vs. control	Non-significant active vs. control
Reduction in bone turnover	Significant active vs. placebo	N/A	Significant active vs. control	Significant active vs. control
Reduction in symptoms	Significant active vs. placebo	N/A	Significant active vs. control	N/A
Median total immobilisation time	N/A	Significant placebo vs. active	N/A	N/A

N/A, not available.

group and the control group [22,23,25]. Also the benefit of these therapies on fracture healing and resolution of the arthropathy is unknown, as none of these studies reported data on radiological follow-up.

With regard to the time to clinical resolution, patients treated with zolendronic acid required significantly longer immobilisation compared with the placebo group (Table 2), [24]. This is in agreement with recent data, which reported that the median time to resolution in those who received any form of bisphosphonates was greater compared with individuals who did not [13].

Although some authors consider bisphosphonates as useful adjuncts to standard management [26], a recent systematic review of the treatment of acute Charcot arthropathy with bisphosphonates has reported that the evidence to support their use is weak [27] and indeed these therapies have not been approved in the United States by the Food and Drug Administration for use in patients with Charcot arthropathy [28]. It is possible that the window of opportunity to administer these antiresorptive therapies is limited and there may be no definite benefit in patients who have already developed extensive fractures and bone fragmentation at presentation.

Another way to improve bone remodelling is to use an anabolic agent, as it may speed up clinical resolution and fracture healing and an initial pilot study in acute Charcot osteoarthropathy has evaluated the effect of human parathyroid hormone on fracture healing in patients with Charcot osteoarthropathy. Although this pilot observation has shown more rapid fracture consolidation, faster oedema control and temperature stabilisation, and earlier return to weight bearing [29], larger studies are needed to confirm the possible role of anabolic agents in the treatment of Charcot foot. At present, a double-blind, randomised, control study in patients with acute Charcot arthopathy to evaluate the possible benefit of 1–84 recombinant human parathyroid hormone on fracture healing is in progress [30].

Future Therapies

Recently, considerable progress has been made with our understanding of the pathogenesis of this difficult condition. It is a bone and joint destruction, associated with increased osteoclastic activity and uncontrolled inflammation [31]. Advances in cellular biology have helped to elucidate the mechanisms of increased osteoclastic activity in acute Charcot arthropathy. The recently discovered receptor activator of nuclear factor $\kappa\beta$ ligand (RANKL), a cytokine from the tumour necrosis factor (TNF)-ligand superfamily, has been identified as a key factor for osteoclast differentiation and regulation [32]. Using an *in vitro* technique to generate functional human osteoclasts from peripheral blood monocytes [33,34], it has been shown that newly formed osteoclasts from patients with acute Charcot arthopathy exhibit an increased response to RANKL in comparison with osteoclasts from diabetic patients and healthy subjects [35]. Furthermore, this response is modulated by the proinflammatory cytokine TNF-α, [36]. This is in agreement with the recent hypothesis that the proinflammatory cytokines play an important role in the inflammatory osteolysis of Charcot arthropathy [31]. Moreover, a further study has shown increased expression of TNF-α by activated monocytes and increased serum levels of TNF-α in patients with active Charcot arthropathy compared with diabetic control patients [37]. Thus, there is an

interaction between inflammation and bone resorption. These observations are important because they lead to possible novel therapies with new pharmacological agents to inhibit RANKL or TNF-α mediated osteoclastic activity and thus improve the overall management of this condition.

Conclusions

Offloading and casting therapy remain the main medical therapy of acute Charcot arthropathy. Recent studies have highlighted the superiority of a non-removable cast to removable devices. The overall benefit of the antiresorptive therapies on healing remains unclear and the benefit of anabolic therapy with parathyroid hormone is yet to be established. Emerging new studies in cellular biology may lead to improved understanding of the mechanisms of pathological bone and joint destruction in Charcot arthropathy and may provide a scientific basis for new interventions to improve the outlook of these patients.

Conflict of Interest

The authors have equally contributed to the design, data collection, analysis and writing the manuscript. Both authors have no competing interests.

References

1. Petrova NL, Foster AV, Edmonds ME. Differences in presentation of Charcot osteoarthropathy in type 1 compared with type 2 diabetes. Diabet Med 2004; **22**: 1235–1236.
2. Sanders LJ, Frykberg RG. Charcot neuroarthropathy of the foot. In: Bowker JH, Phiefer MA, eds. Levin & O'Neal's The Diabetic Foot. 6 edn. St Louis: Mosby Press, 2001; 439–466.
3. Petrova NL, Edmonds ME. Charcot osteoarthropathy-current standards. Diabetes Metab Res Rev 2008; **24**(Suppl. 1): S58–61.
4. Armstrong DG, Todd WF, Lavery LA, Harkless LB, Bushman TR. The natural history of acute Charcot's arthropathy in a diabetic foot specialty clinic. Diabet Med 1997; **14**: 357–363.
5. Pinzur MS. Benchmark analysis of diabetic patients with neuropathic (Charcot) foot deformity. Foot Ankle Int 1999; **20**: 564–567.
6. Lambert AP, Close CF. Charcot neuroarthropathy of the knee in type 1 diabetes: treatment with total knee arthroplasty. Diabet Med 2002; **19**: 338–341.
7. Lambert AP, Close CF. Charcot neuroarthropathy of the wrist in type 1 diabetes. Diabetes Care 2005; **28**: 984–985.
8. Wilmot EG, Jadoon KA, Olczak SA. Charcot's neuroarthropathy of the wrist in type 2 diabetes. Pract Diab Int 2008; **25**: 263.
9. Jude EB, Boulton AJM. Medical treatment of Charcot arthopathy. J Am Podiatr Med Assoc 2002; **92**: 381–383.
10. Chantelau E, Richter A, Ghassem-Zadeh N, Poll LW. "Silent" bone stress injuries in the feet of diabetic patients with polyneuropathy: a report on 12 cases. Arch Orthop Trauma Surg 2007; **127**: 171–177.
11. Pinzur MS, Lio T, Posner M. Treatment of Eichenholtz stage I Charcot foot arthropathy with a weight-bearing total contact cast. Foot Ankle Int 2006; **27**: 324–329.
12. De Souza LJ. Charcot arthropathy and immobilization in a weigh-bearing total contact cast. J Bone Joint Surg Am 2008; **90**: 754–759.
13. Game FL, Catlow R, Jones GR et al. Audit of acute Charcot's disease in the UK: the CDUK study. Diabetologia 2012; **55**: 862.
14. Bates M, Petrova NL, Edmonds ME. How long does it take to progress from cast to shoes in the management of Charcot osteoarthropathy? Diabet Med 2006; **23**(Suppl. 2): 1–30.
15. Armstrong DG, Lavery LA. Monitoring healing of acute Charcot's arthropathy with infrared thermometry. J Rehabil Res Dev 1997; **34**: 317–321.
16. McGill M, Molyneaux L, Bolton T, Ioannou K, Uren R, Yue DK. Response of Charcot's arthropathy to contact casting: assessment by quantitative techniques. Diabetologia 2000; **43**: 482–484.
17. Zampa V, Bargellini I, Rizzo L et al. Role of dynamic MRI in the follow-up of acute Charcot foot in patients with diabetes mellitus. Skeletal Radiol 2011; **40**: 991–999.
18. Pinzur MS, Shields N, Trepman E, Dawson P, Evans A. Current practice patterns in the treatment of Charcot foot. Foot Ankle Int 2000; **21**: 916–920.
19. Rogers LC, Frykberg RG, Armstrong DG et al. The Charcot foot in diabetes. Diabetes Care 2011; **34**: 2123–2129.
20. Larsen K, Fabrin J, Holstein P. Incidence and management of ulcers in diabetic Charcot feet. J Wound Care 2001; **10**: 323–328.
21. Gough A, Abraha H, Li F et al. Measurement of markers of osteoclast and osteoblast activity in patients with acute and chronic diabetic Charcot neuroarthropathy. Diabet Med 1997; **14**: 527–531.
22. Jude E, Selby PL, Burgess J et al. Biphosphonates in the treatment of Charcot neuroarthropathy: a double-blind randomised controlled trial. Diabetologia 2001; **44**: 2032–2037.
23. Pakarinen TK, Laine HJ, Maenpaa H, Mattil P, Lahtela J. The effect of Zolendronic acid on the clinical resoltution of Charcot neuroarthropathy: a pilot randomized controlled trial. Diabetes Care 2011; **34**: 1514–1516.
24. Pitocco D, Ruotolo V, Caputo S et al. Six-month treatment with alendronate in acute Charcot neuroarthropathy: a randomized controlled trial. Diabetes Care 2005; **28**: 1214–1215.
25. Bem R, Jirkovska A, Fejfarova V, Skibova J, Jude EB. Intranasal calcitonin in the treatment of acute Charcot neuroosteoarthropathy. Diabetes Care 2006; **29**: 1392–1394.
26. Smith C, Kumar S, Causby R. The effectiveness of non-surgical interventions in the treatment of Charcot foot. Int J Evid Based Healthc 2007; **5**: 437–449.
27. Richard JL, Almastri M, Schudiner S. Treatment of acute Charcot foot with bisphosphonates: a systemic review of the literature. Diabetologia 2012; **55**: 1258–1264.
28. Wuckich D, Sung W. Charcot arthropathy of the foot and ankle: modern concepts and management review. J Diabetes Complications 2009; **23**: 409–426.
29. Brosky T, Recknor C, Grant S. The effect of teriparatide [human parathyroid hormone (1–34)] therapy on fracture healing in Charcot neuroarthropathy of lower extremity. Osteoporos Int 2005; **16**(Suppl. 4): S44.
30. EU Clinical Trials Register. Available from URL: http://www.clinicaltrialsregister.eu/ctr-search?query=2009-016873-13+.
31. Jeffcoate W, Game F, Cavanagh P. The role of proinflammatory cytokines in the cause of neuropathic osteoarthropathy (acute Charcot foot) in diabetes. Lancet 2005; **366**: 2058–2061.
32. Yasuda H, Shima N, Nakagawa N et al. Osteoclast differentiation factor is a ligand for osteoprotegerin/ osteoclastogenesis – inhibitory factor and is identical to TRANCE/RANKL. Proc Natl Acad Sci U S A 1998; **95**: 3697–3602.
33. Sabokbar A, Athanasou NS. Generating human osteoclasts from peripheral blood. Methods Mol Med 2003; **80**: 101–111.

34. Fujikawa Y, Quinn JM, Sabokbar A, McGee JO, Athanasou NA. The human osteoclast precursors circulate in the monocyte fraction. Endocrinology 1996; **137**: 4058–4060.

35. Mabilleau G, Petrova NL, Edmonds ME, Sabokbar A. Increased osteolcastic activity in acute Charcot's osteoarthropathy: the role of receptor activator of nuclear factor kappa β ligand. Diabetologia 2008; **51**: 1035–1040.

36. Petrova NL, Shanahan C, Edmonds ME. The proinflammatory cytokine TNF-α modulates RANKL-mediated osteoclastic resorption *in vitro* in patients with acute Charcot osteoarthropathy. Diabet Med 2012; **29**: 13.

37. Uccioli L, Sinistro A, Almerighi C et al. Proinflammatory modulation of the surface and cytokine phenotype of monocytes in patients with acute Charcot foot. Diabetes Care 2010; **33**: 350–355.

DIABETES/METABOLISM RESEARCH AND REVIEWS
Diabetes Metab Res Rev 2008; **24**(Suppl 1): S58–S61.
Published online in Wiley InterScience (www.interscience.wiley.com) **DOI:** 10.1002/dmrr.846

REVIEW ARTICLE

Charcot neuro-osteoarthropathy – current standards

N. L. Petrova
M. E. Edmonds*

Diabetic Foot Clinic, King's College Hospital, Denmark Hill, London, UK

*Correspondence to:
M. E. Edmonds, Diabetic Foot Clinic, King's College Hospital, Denmark Hill, London SE5 9RS, UK. E-mail: Michael.Edmonds@kch.nhs.uk

Summary

It is extremely important to have a high index of suspicion for Charcot neuro-osteoarthropathy (CN) and to encourage early presentation of the patient. This should be followed by a rapid diagnosis and early intervention, and with such a modern approach many CN can now be healed and deformity prevented. CN can be divided into two phases: acute active phase and chronic stable phase.

The acute active phase includes those patients presenting early with normal X-ray and those presenting later with deformity and radiological changes of CN. The acute phase is characterized by unilateral erythema and oedema. The foot is at least 2 °C hotter than the contralateral foot.

Patients should have initially an X-ray examination which, at this time, may be normal. We then proceed to two investigations: initially a technetium diphosphonate bone scan, which will detect early evidence of bone damage and also locate the site of this damage. If the result of the bone scan is positive, we would proceed to magnetic resonance imaging (MRI) examination, which would describe in more detail the nature of the bony damage.

The aim of treatment is immobilization in a plaster cast until there is no longer evidence on X-ray of continuing bone destruction, and the foot temperature is within 2 °C of the contralateral foot. An alternative treatment is a prefabricated walking cast, such as the Aircast. A randomized controlled study of a single 90 mg pamidronate infusion has shown a significant reduction of the markers of bone turnover and skin temperature in treated, compared with control subjects although the fall in skin temperature was similar in both groups. There was a similar finding in a recent study with alendronate. Calcitonin has also been used in the acute stage and there was a more rapid transition to the stable chronic phase in the treated group compared with controls.

In the chronic stable phase, the foot is no longer warm and red. There may still be oedema but the difference in skin temperature between the feet is usually less than 2 °C. The X-ray shows fracture healing, sclerosis and bone remodelling. The patient must now be rehabilitated and gradually moved from cast treatment to suitable footwear. The patient needs close observation to detect any relapse, which will be evident from further swelling and heat in the foot. Careful rehabilitation is always necessary after a long period in a cast.

Keywords Charcot neuro-osteoarthropathy; fracture; skin foot temperature; casting; orthotics

Introduction

Charcot neuro-osteoarthropathy (CN) is a major complication of diabetes. It often presents without warning and can rapidly deteriorate into severe and irreversible foot deformity leading then to ulceration and amputation [1].

Received: 9 October 2007
Revised: 19 December 2007
Accepted: 28 January 2008

Prognosis of this condition is poor and mortality is high [2]. Although neuropathic joint disease has been associated with many conditions such as tabes dorsalis, syringomyelia, leprosy, hereditary sensory neuropathy and familial amyloid neuropathy, it is now most commonly seen in patients with diabetes. This article will describe the incidence, predisposition and presentation of CN and then discuss the current standards of management in the two main stages of this condition, namely, the acute active stage and the chronic inactive stable stage.

Incidence

Sinha *et al* cited a prevalence of 1 : 680 of people with diabetes developing this condition [3]. Evidence of radiological changes associated with the CN has been reported in up to 10% of patients with diabetes and neuropathy [4]. More recently, a difference in the presentation of CN between type 1 and type 2 diabetes has been noted. Patients with type 1 diabetes present at a younger age and have longer duration of diabetes compared with type 2 diabetes [5]. A relative preponderance of type 1 diabetes compared with type 2 diabetes has also been recorded.

Predisposition

The predisposing factors are somatic and autonomic neuropathy, osteopenia and renal impairment. There is evidence that a small fibre neuropathy predisposes to the CN [6], although other work has shown both small and large fibre neuropathy to be important [7]. Underlying osteopenia has been reported in type 1 but not in type 2 diabetes [8]. A relationship between diabetic nephropathy, renal replacement therapy and the development of the CN has been noted. Diabetic patients who have had a renal transplant have a high risk of fracture at the ankle and the foot [9]. Trauma is an important factor in the pathogenesis and was found to be present in 22–53% of the cases [10,11]. CN may also follow injudicious mobilization after surgery, a period of bed rest or casting.

Presentation

It is an acute osteoarthropathy with bone and joint destruction. About 30% of patients complain of pain or discomfort [10]. It commonly presents in the mid-foot but also occurs in the forefoot and hind foot. The prognosis for the hind foot is much more serious with the high risk of instability of the ankle and the necessity for a major amputation. Rarely, in diabetes, the knee can also be affected by CN.

It is extremely important to have a high index of suspicion and to encourage early presentation of the patient. This should be followed by a rapid diagnosis and early intervention, and with such a modern approach many CN can now be healed and deformity prevented.

Differential diagnosis of Charcot osteoarthropathy

It is important to differentiate between the red, hot, swollen appearance of CN and the red, hot swollen cellulitic foot. Cellulitis is more likely in the presence of an ulcer that may show typical signs of infection. Infection severe enough to cause generalized redness, warmth and swelling will usually cause local signs such as discolouration of the bed of the wound, and discharge from the ulcer. The swelling of CN responds more rapidly to elevation than does that of the infected foot. Interestingly, there is dissociation between the presence of local signs of inflammation and the lack of systemic response. Recent study has shown that C-reactive protein was within the normal range in almost 50% of patients of the patients presenting with acute CN and only moderately elevated in the remainder [12]. Indeed, in a small series of patients, serum C-reactive protein was significantly lower in patients with CN compared with patients with osteomyelitis [13].

Gout and deep vein thrombosis may also masquerade as CN but can be excluded by measurement of serum uric acid (which is usually raised in gout) and duplex vein scan.

Current standards of management

CN can be divided into two phases: the acute active stage and the chronic inactive stage.

Acute active stage

The acute phase is characterized by unilateral erythema and oedema. The foot is at least 2 °C hotter than the contralateral foot and the difference may be as great as 10 °C. This may be measured with an infrared skin thermometer [14].

According to the presence of radiological abnormality, the acute active stage may be divided into early acute stage and advanced acute stage. Patients may present early in the acute active phase with normal X-ray or later when there may be already existing deformity and radiological changes of CN. Normal radiograph at presentation does not rule out CN and it is important to carry out further imaging investigations to reveal underlying abnormality. Initially a technetium diphosphonate bone scan will detect early evidence of bone damage showing increased focal uptake on the bony (third) phase. This stage has been recently described as stage 0 with normal radiograph and abnormal bone scan in Sella and Barrette's staging of CN [15]. Magnetic resonance imaging (MRI) may describe in more detail the nature of the bony damage

DOI: 10.1002/dmrr

and MRI abnormalities at this early stage of CN include sub-chondral bone marrow oedema with or without microfracture [16,17].

Offloading at this stage is important and could arrest progression to overt changes and indeed a pilot study has reported a resolution of bone marrow oedema and healing of microfractures after casting treatment [18]. Initially the foot is immobilized in a non-weight bearing plaster cast. The cast is checked after 1 week, and replaced if it has become loose due to reduction of oedema. It should be regularly checked and replaced as necessary. The patient should use crutches and be encouraged to avoid weight bearing on the affected side. However, we recognize that in many cases it is difficult to be completely non-weight bearing because the patient has multiple comorbidities including loss of proprioception, postural hypotension, high body mass index and, in some cases, neuropathy of the upper limbs, all of which can make it difficult for him to use crutches. Furthermore, a wheelchair existence is often impractical in many home environments. Also, total immobility has disadvantages in itself with loss of muscle tone, reduction in bone density and loss of body fitness. The casting is continued until the swelling has resolved and the temperature of the affected foot is within 2 °C of the contralateral foot. An alternative treatment is a prefabricated walking cast, such as the Aircast. A moulded insole should replace the standard insole provided with the cast by the manufacturer. The hindfoot CN is probably best treated in a total contact cast.

If diagnosis is not made at this early stage of CN or patients present late, the osteoarthropathy progresses to the advanced acute stage. Extensive bone damage is incurred leading to joint sub-luxation and dislocation with subsequent deformity. These changes can develop very rapidly. Foot radiographs reveal the extensive damage and changes at this stage include bone fractures and joint sub-luxations or dislocations [1]. Treatment at this stage is also with a cast immobilization until there is no longer evidence on X-ray of continuing bone destruction and the foot temperature is within 2 °C of the contralateral foot.

Chronic stable stage

Conservative treatment

The foot is no longer warm and red. The oedema may persist but the difference in skin temperature between the feet is usually less than 2 °C. The X-ray shows fracture healing, sclerosis and bone remodelling. Although some studies have reported an average time of casting of 18 weeks [10], some patients may need a cast for over a year. Indeed, a recent study of 46 patients with acute CN treated with offloading, reported a median duration of casting treatment of 11 months. Patients need close observation to detect any relapse, which will be evident from further swelling and heat in the foot and in the same series of patients relapse was detected in 30% of them and total duration of casting treatment required was 20 months [19]. This is a crucial stage in the treatment. The patient must now be rehabilitated and gradually moved from cast treatment to suitable footwear. When the patient comes out of the cast there will be wasting of the calf muscles and joint stiffness. The physiotherapist must be aware of the dangers of reactivating the bony destruction phase by excessively rapid mobilization or protracted weight bearing in the early stages of rehabilitation. Too rapid mobilization can be disastrous, resulting in further bone and joint damage. Extremely careful rehabilitation should be the rule, beginning with just a few short steps in the new footwear. The patient rests for the remaining of the day and monitors the foot. If there is no increase in warmth, swelling and redness then he can walk a few more steps the next day, and very carefully build up to a reasonable amount of walking. Finally, the patient may progress to bespoke footwear with moulded insoles.

Treatment in the chronic stage will be described for the forefoot, mid-foot and hind foot.

Forefoot

This usually stabilizes without bony deformity but patients may need moulded insoles in bespoke shoes.

Mid-foot

When the mid-foot has stabilized, the patient can now progress from a total-contact cast to a bivalved cast or Aircast walker fitted with a cradled moulded insole. The rockerbottom foot with plantar bony prominence is a site of very high pressure. Regular reduction of callus can prevent ulceration. If ulceration does occur, an ostectomy may be needed. If stabilization cannot be achieved by conservative means, then it is possible to carry out operative procedures in the mid-foot.

Hindfoot

Hindfoot CN may be difficult to stabilize. An attempt may be made with total-contact casting. The cast may have been used during the acute phases, to reduce oedema and halt progressive bony changes and deformity. Continued use of the cast will help to achieve stability of the hindfoot. Alternatively, a Charcot restraint orthotic walker (CROW) may be used, followed by an ankle–foot orthosis (AFO) with bespoke footwear.

The CROW

This is a bespoke bivalved total-contact device that externally fixates the ankle. Extra internal padding has been added to cushion the vulnerable medial malleolar area. The yellow corrugations contain ethyl vinyl acetate (EVA) to strengthen the device without increasing the bulk. All internal metal rivets have extra padding. The rigid, durable outer shell is constructed out of polypropylene and is lined with EVA. There is a bespoke moulded insole to accommodate any existing deformity and to redistribute plantar pressures. A rockerbottom,

DOI: 10.1002/dmrr

crepe sole is attached to facilitate roll-off during walking. It is used after swelling is controlled and progressive destruction halted by total-contact casting.

The ankle–foot orthosis (AFO)

The AFO is a device used to stabilize the foot and ankle. There are two main forms of AFO, the traditional conventional metal and leather calliper and the newer thermoplastic types, which are more cosmetic.

Surgical treatment

Although non-operative treatment with use of total contact cast followed by an appropriate bracing and footwear is considered to be the gold standard treatment for CN, surgical treatment is essential when conservative treatment fails. Operative treatment is indicated for chronic recurrent ulcerations and joint instability when patients present with unstable or displaced fracture-dislocations. Surgical intervention includes open reductions and internal fixation and at times combined with external fixation [20]. It can be 'symptomatic' such as exostotomy in cases complicated by chronic recurrent ulceration associated with osseous prominence in the Charcot deformed foot, or incision and drainage in the infected CN. Alternatively it can aim to address biomechanical problems and currently surgical reconstruction for CN includes open reduction with internal or external fixation, dorsiflectory osteotomies of the metatarsals, intra-medullary rodding and arthrodesis of the damaged joints [21]. In a series of 28 patients with CN dislocation external fixation with bone stimulation has been used with no further breakdown after surgery [21]. Early experience with using specific Taylor spatial external fixation system has also been reported [22].

Conclusion

We have described the natural history of the CN. A full understanding of the progression of events is necessary in order to make an early diagnosis and institute active treatment. There should be a high index of suspicion for the CN so as to intervene early and prevent the progression to Charcot deformity.

Conflict of interest

The authors have no conflicts of interest.

References

1. Sanders LJ, Frykberg RG. Charcot neuroarthropathy of the foot. In Levin ME, O'Neal LW, Bowker JH, Pfeifer MA (eds). *The Diabetic Foot* (6th edn), vol. 21. Mosby: St Louis, MO, 2001; 439–465.
2. Gazis A, Pound N, Macfarlane R, Treece K, Game F, Jeffcoate W. Mortality in patients with diabetic neuropathic osteoarthropathy (Charcot foot). *Diabet Med* 2004; **21**: 1243–1246.
3. Sinha S, Munichoodappa CS, Kozak GP. Neuroarthropathy (Charcot joints) in diabetes mellitus. *Medicine* 1972; **51**: 191–210.
4. Cavanagh PR, Young MJ, Adams JE, Vickers KL, Boulton AJ. Radiographic abnormalities in the feet of patients with diabetic neuropathy. *Diabetes Care* 1994; **17**: 201–209.
5. Petrova NL, Foster AVM, Edmonds ME. Difference in presentation of Charcot osteoarthropathy in type 1 compared with type 2 diabetes. *Diabetes care* 2004; **27**: 1235–1236.
6. Stevens MJ, Edmonds ME, Foster AVM, *et al*. Selective neuropathy and preserved vascular responses in the diabetic Charcot foot. *Diabetologia* 1992; **35**: 148–154.
7. Young MJ, Marshall A, Adams JE, *et al*. Osteopenia, neurological dysfunction, and the development of Charcot neuroarthropathy. *Diabetes Care* 1995; **18**: 34–38.
8. Petrova NL, Foster AVM, Edmonds ME. Calcaneal bone mineral density in patients with Charcot neuropathic osteoarthropathy-differences between type 1 and type 2 diabetes. *Diabet Med* 2005; **22**: 756–761.
9. Thompson RC, Havel P, Goetz F. Presumed neuropathic skeletal disease in diabetic kidney transplant recipients. *J Am Med Assn* 1983; **249**: 1317–1319.
10. Armstrong DG, Todd WF, Lavery LA, *et al*. The natural history of acute Charcot's arthropathy in a diabetic foot specialty clinic. *Diabet Med* 1997; **14**: 357–363.
11. Pinzur MS. Benchmark analysis of diabetic patients with neuropathic (Charcot) foot deformity. *Foot Ankle Int* 1999; **20**: 564–567.
12. Petrova NL, Moniz C, Elias DA, Buxton-Thomas M, Bates M, Edmonds ME. Is there a systemic inflammatory response in the acute Charcot foot? *Diabetes Care* 2007; **30**: 997–998.
13. Jude EB, Selby PL, Mawer EB, Burgess J, Boulton AJM. Inflammatory and bone turnover markers in Charcot arthropathy and osteomyelitis of the feet in diabetic patients. *Diabetologia* 2002; **45**(Suppl. 2): A341 (1056).
14. Armstrong DG, Lavery LA. Monitoring healing of acute Charcot's arthropathy with infrared dermal thermometry. *J Rehabil Res Dev* 1997; **34**: 317–321.
15. Sella EJ, Barrette C. Staging of Charcot neuroarthropathy along the medial column of the foot in the diabetic patient. *J Foot Ankle Surg* 1998; **38**: 34–40.
16. Edmonds ME, Petrova NL, Elias DA. The earliest magnetic resonance imaging sign of mid-foot Charcot osteoarthropathy is oedema of subchondral (subarticular) bone marrow which needs prompt therapeutic offloading. *Diabet Med* 2005; **22**(Suppl. 2): 93–P272.
17. Chantelau E, Poll LW. Evaluation of the diabetic charcot foot by MR imaging or plain radiography–an observational study. *Exp Clin Endocrinol Diabetes* 2006; **114**: 428–431.
18. Edmonds ME, Petrova NL, Edmonds AE, Elias DA. What happens to the initial bone marrow oedema in the natural history of Charcot osteoarthropathy? *Diabetologia* 2006; **49**(Suppl. 1): 684 (1126).
19. Bates M, Petrova NL, Edmonds ME. How long does it take to progress from cast to shoes in the management of Charcot osteoarthropathy? *Diabet Med* 2006; **23**(Suppl. 2): 27–A100.
20. Schon LC, Marks RM. The management of neuroarthropathic fracture-dislocations in the diabetic patient. *Orthop Clin North Am* 1995; **26**: 375–392.
21. Wang JC, Le Aw, Tsukuda RK. A new technique for Charcot's foot reconstruction. *JAMPA* 2002; **92**: 429–436.
22. Roukis TS, Zgonis T. The management of acute Charcot fracture-dislocations with the Taylor's spatial external fixation system. *Clin Podiatr Med Surg* 2006; **23**: 467–483.

DOI: 10.1002/dmrr